UNIVERSITY OF SOUTHAMPTON

FACULTY OF MEDICINE, HEALTH & LIFE SCIENCES

School of Medicine

Signalling by Wnt/β-catenin in Human Bronchial Epithelial Cells

by

Mark Dominic Steel

MA MB BS MRCP

Thesis for the degree of Doctor of Philosophy

June 2006

UNIVERSITY OF SOUTHAMPTON

ABSTRACT

FACULTY OF MEDICINE, HEALTH & LIFE SCIENCES
SCHOOL OF MEDICINE

Doctor of Philosophy

SIGNALLING BY WNT/β-CATENIN IN HUMAN BRONCHIAL EPITHELIAL CELLS

by Mark Dominic Steel

The embryonic Wnt/β-catenin ('canonical') pathway has been implicated in epithelial regeneration. To investigate the role of Wnt signal transduction in the airways, I characterised the expression of key pathway components in human bronchial epithelial (HBE) cells and studied the influence of cell density on pathway activity, using subconfluent cells in log-phase growth as a simple model of repairing epithelium. Primary HBE cells and H292 bronchial epithelial cells were found to express TCF-4 and -3, with variable low-level expression of TCF-1 and LEF-1, transcription factors that are regulated by β-catenin. The cells also had the potential to respond to Wnt signals through expression of members of the Frizzled receptor family, including FZD-5 and -6. In confluent H292 cells, 20mM lithium and 25% v/v Wnt-3a conditioned medium induced 4.5-fold ($p=0.008$) and 1.4-fold ($p=0.006$) increases in TOPflash activity, respectively. Under conditions of reduced cell density, TOPflash activity increased 1.8-fold ($p=0.002$) in association with increased nuclear localisation of hypophosphorylated (transcriptionally active) β-catenin and increased cell proliferation. This up-regulation in reporter activity occurred independently of EGF receptor activation and could not be recapitulated by use of low-calcium medium to disrupt cadherin-mediated cell-cell adhesion, but was associated with changes in FZD6 gene expression. I conclude that reactivation of this embryonic pathway might play a role in bronchial epithelial regeneration, and that modulation of Fzd6 receptors may regulate Wnt signalling at confluence. Recognising that chronic inflammatory disorders of the airways involve epithelial damage and repair, I speculate that altered Wnt signalling might contribute to disease pathogenesis or progression.

LIST OF CONTENTS

LIST OF FIGURES

LIST OF TABLES

ACKNOWLEDGEMENTS

Supervisors

Dr Jane Collins.

Professor Donna Davies.

Professor Stephen Holgate.

Laboratory support

Dr Sarah Puddicombe and members of the Brooke laboratory.

Miss Kate Hayes.

Dr Susan Wilson and members of the Histochemistry Research Unit.

Dr Anton Page and Mr Roger Alston of the Biomedical Imaging Unit.

Dr John Holloway.

Dr Mark Dixon.

Helpful discussions

Dr Peter Lackie.

Dr Ian Hiles and Dr Carmel Hogan of GlaxoSmithKline.

Gifts

Dr Hans Clevers of the University Medical Centre Utrecht, The Netherlands, for the ABC antibody used in preliminary experiments.

Dr Robert Kypta of the MRC Laboratory for Molecular Cell Biology, University College London, for the SW480 cells.

Clinical support

Professor Ratko Djukanovic.

Drs Rory O'Donnell, Paul Beckett, Matthew Thornber & other clinical research fellows.

Miss Meredith O'Donnell.

Mrs Linda Jackson and Mrs Paula Pearson.

The research nurses.

The Wellcome Trust Clinical Research Facility.

General support

Mr Frank Anderson.

The secretarial staff of RCMB.

Funding

The Medical Research Council (UK): Clinical Training Fellowship G84/5708.

And finally

This thesis is dedicated to Rachel and Imogen.

ABBREVIATIONS

7-AAD (7-aminoactinomycin D); ABC ('active'/hypophosphorylated β-catenin); Akt (protein kinase B); ALI (air-liquid interface); AMPS (ammonium persulphate); ANOVA (analysis of variance); APC/Apc (adenomatous polyposis coli); *arm* (*armadillo*); ATCC (American Type Culture Collection).

BEBM (bronchial epithelium basal medium); BEGM (bronchial epithelium growth medium); bFGF (basic fibroblast growth factor); BSA (bovine serum albumin).

CamKII (Ca^{2+}-calmodulin-dependent protein kinase II); CBP (CREB-binding protein); CK-1α (casein kinase-1α); CM (conditioned medium); CRD (cysteine-rich domain).

DAB (3,3'-diaminobenzidine); DAG (diacyl glycerol); DKK/Dkk (Dickkopf); DLR (dual-luciferase reporter); DMEM (Dulbecco's modified Eagle's medium); DMSO (dimethyl sulphoxide); dNTP (deoxynucleoside triphosphates); DSLB (denaturing sample lysis buffer); DVL/Dvl/Dsh (dishevelled).

EDTA (Ethylenediaminetetraacetic acid); EGF (epidermal growth factor); EMTU (epithelial-mesenchymal trophic unit).

FBS (foetal bovine serum); FGF (fibroblast growth factor); FITC (fluorescein isothiocyanate); Frat (frequently rearranged in advanced T-cell lymphomas); FZD/Fzd/Fz (frizzled).

GBP (Gsk-3 binding protein); GMA (glycolmethacrylate); Gsk-3β (glycogen synthase kinase-3β).

HBE (human bronchial epithelial); HBSS (Hanks balanced salt solution); HDAC (histone deacetylase); HGF (hepatocyte growth factor; scatter factor); HMG (high mobility group); HRP (horseradish peroxidase).

IAA (isoamylalcohol); ICAT (inhibitor of β-catenin and Tcf-4); IGF-II (insulin-like growth factor-II); ILK (integrin-linked kinase); IP_3 (inositol 1,4,5-trisphosphate); ITS (insulin, transferrin and sodium selenite).

JNK (c-Jun NH(2)-terminal kinase).

LB (loading buffer); LEF-1/Lef-1 (lymphoid enhancing factor-1); Lrp (low-density lipoprotein receptor-related protein).

M-MLV RT (Moloney murine leukaemia virus Reverse Transcriptase); MMP (matrix metalloproteinase); MRC (Medical Research Council).

NHLBI (National Heart, Lung and Blood Institute); NLK (NEMO-like kinase); NSCLC (non-small cell lung cancer).

PAGE (polyacrylamide gel electrophoresis); PBC (pan-β-catenin); PBS (phosphate-buffered saline); PCP (planar cell polarity); PCR (polymerase chain reaction); PI3K (phosphatidylinositol 3-kinase); PKB (protein kinase B); PKC (protein kinase C); PLC (phospholipase C); PLL (poly-L-lysine); PMSF (phenylmethyl-sulfonyl fluoride).

qPCR (quantitative polymerase chain reaction).

REIC (reduced expression in immortalised cells); RPA (RNase protection assay); RTK (receptor tyrosine kinase); RT-PCR (reverse transcription-polymerase chain reaction).

SAB (streptavidin/biotin); SAEC (small airway epithelial cells); SARP (secreted apoptosis-related proteins); SCLC (small cell lung cancer); SDS (sodium dodecylsulphate); S.E.M. (standard error of the mean); SFRP/Sfrp (secreted frizzled-related protein); Shh (sonic hedgehog); SMG (submucosal gland); SMOH (smoothened).

TAK-1 (TGFβ activated kinase-1); TBE (Tris-borate EDTA); TBS (Tris-buffered saline); TEMED (N,N,N',N'-tetramethylethylenediamine); TGF-β (transforming growth factor-β); TCF/Tcf (T-cell factor); TLE (transducin-like enhancer of split); 7TMS (seven transmembrane spanning); β-TRCP (β-transducin repeat-containing protein).

wg (*wingless*); WHO (World Health Organisation).

CHAPTER 1

INTRODUCTION

There is accumulating evidence that bronchial epithelial repair plays an important role in the pathogenesis of chronic inflammatory disorders of the airways. In asthma, the bronchial epithelium appears to be abnormally susceptible to oxidant-induced apoptosis (Bucchieri et al., 2002), with selective shedding of columnar cells and failure to proliferate as part of the normal repair response (Demoly et al., 1994). As a consequence, the asthmatic epithelium is persistently stressed and activated, releasing cytokines and growth factors that drive both chronic airways inflammation and airway wall remodelling (Holgate et al., 1999). Therefore, investigating the processes that regulate epithelial repair could provide new insights into diseases of the airway. In this respect, recent interest has focused on the role played by reactivation of embryonic signalling pathways (Beachy et al., 2004; Watkins et al., 2003).

In mammalian lung development, reciprocal paracrine signals between epithelial and mesenchymal cells orchestrate the process of branching morphogenesis (Chuang and McMahon, 2003; Shannon and Hyatt, 2004). A number of morphogenetic proteins have been identified in fetal lung, including members of the Wnt family (Chuang and McMahon, 2003; Shannon and Hyatt, 2004). Wnts are secreted, lipid-modified, short-range signalling proteins that act in both autocrine and paracrine modes to influence individual cell fate (Brandon et al., 2000; Moon et al., 1997; Nelson and Nusse, 2004; Wilson et al., 2001), and are thought to provide spatial information required for tissue modelling (Christian, 2000; Hecht and Kemler, 2000). The best characterised of the Wnt signalling pathways is the so-called 'canonical' pathway, a key component in which is β-catenin (Behrens et al., 1996; Miller et al., 1999). In human fetal lung, a role for the canonical Wnt pathway in branching morphogenesis has been suggested by the localisation of β-catenin to the nuclear compartment of epithelial cells as they invade surrounding mesenchyme (Eberhart and Argani, 2001).

β-catenin is a 92kD intracellular protein with dual function; it plays a fundamental role in cell-cell adhesion, linking classical cadherins to the actin cytoskeleton (Aberle et al., 1996; Ozawa et al., 1989), and also regulates gene expression through direct interaction with members of the T-cell factor/Lymphoid enhancing factor-1 (Tcf/Lef-1) family of transcription factors (Behrens et al., 1996; Miller et al., 1999). In the absence of a Wnt signal, β-catenin is normally maintained at low levels within the cytosolic compartment by the glycogen synthase kinase-3β/adenomatous polyposis coli/axin (Gsk-3β/Apc/axin) destruction complex; Gsk-3β sequentially phosphorylates specific serine/threonine residues in the N-terminal region of β-catenin, thereby identifying it for degradation via the ubiquitin pathway (Behrens et al., 1998; Liu et al., 2002; Polakis, 2002). Under such conditions, Tcf/Lef-1 members function as transcriptional repressors through association with co-repressors, including those of the transducin-like enhancer of split (TLE) family (Brantjes et al., 2001). However, when Wnts interact with members of the Frizzled (Fzd) receptor family, the destruction complex is inactivated. This allows β-catenin to accumulate within the cytosol and translocate into the nuclear compartment, where it can bind to Tcf/Lef-1 members, lift transcriptional repression, and activate the transcription of target genes (Miller et al., 1999) (Figure 1.1). The importance of transcriptional repression is highlighted by the observation that mutations in the APC gene or N-terminal region of β-catenin (β-cateninΔN) are associated with several human cancers (Li et al., 2002a).

Evidence suggests that the Wnt/β-catenin pathway also plays an important role in adult tissue homeostasis (Beachy et al., 2004). Thus, transient nuclear localisation of β-catenin has been observed in human colorectal epithelial cells during the regenerative phase following radiation-induced injury (Hardy et al., 2002) and human endometrial cells during the mid/late-proliferative and early secretory phases of the menstrual cycle (Nei et al., 1999), strongly suggesting a role in epithelial regeneration. Furthermore, target genes identified in human colorectal cancer cells include those involved in cell migration (*MMP7*, *CD44*) (Crawford et al., 1999; Wielenga et al., 1999) and proliferation (*cyclin-D1*, *c-myc*) (He et al., 1998; Shtutman et al., 1999), both key steps in epithelial restitution (Dupuit et al., 2000; Shimizu et al., 1994). Given these observations, I chose to investigate the possibility that

reactivation of this embryonic signalling pathway might play an important role in *bronchial* epithelial regeneration following injury.

1.1 The discovery of Wnt

In 1982, whilst investigating loci of retroviral *int*egration in the murine genome, Nusse and Varmus first identified *int-1* as a candidate proto-oncogene, activated by the mouse mammary tumour virus (Nusse and Varmus, 1982). Five years later, the *wingless* (*wg*) gene, required for normal segment polarity in the fruit-fly (*Drosophila melanogaster*) embryo, was reported to be the homolog of mouse *int-1*, providing a link between oncogenesis and normal embryonic development (Rijsewijk et al., 1987). Within a decade of its discovery, degenerate PCR analyses had identified several *int-1* related genes, highly conserved across diverse species. Resulting confusion in nomenclature led to its revision, and so the *Wnt* (*wingless* and *int*) gene family was formally introduced in 1991 (Nusse et al., 1991). By this time, Papkoff *et al* had identified the *int-1* gene product as a secreted glycoprotein (Papkoff et al., 1987; Papkoff, 1989)., tightly bound to proteoglycans of the cell surface and extracellular matrix (Papkoff and Schryver, 1990), and thought to be involved in autocrine and short-range paracrine signalling, determining cell fate and embryonic patterning (Nusse and Varmus, 1992).

Various bioassays have played a key role in our understanding of Wnt signalling pathways and function. McMahon and Moon were the first to report that microinjection of Wnt-1 RNA into early frog (*Xenopus laevis*) embryos induced body axis duplication, with formation of two heads (McMahon and Moon, 1989). Subsequent studies discovered that the exact same phenotype could also be induced by ectopic Wnt-2 (Landesman and Sokol, 1997), -3a (Wolda and Moon, 1992), -8a (Christian et al., 1991) or -8b (Cui et al., 1995). In contrast, axis duplication was not induced by ectopic Wnt-4 (Du et al., 1995) or -5a (Moon et al., 1993), but complex malformations resulted from altered cell migration within embryonic tissues. Consequently, this developmental bioassay led to the classification of Wnts into two functional groups, namely Wnt-1 (class-1) and Wnt-5a (class-5a), suggesting the existence of two or more distinct Wnt signalling pathways (Moon et al., 1993).

An important non-developmental bioassay has been the response of mouse mammary epithelial (C58MG) cells when stimulated with Wnts, *in vitro*. Since isolation of biologically active Wnt proteins has proved problematic, C57MG cells have been stimulated by transfection with DNA encoding specific *Wnt* genes (autocrine assay), or by co-culture with Wnt expressing fibroblasts (paracrine assay). Either way, cellular transformation, characterised by elongated cell morphology in association with shedding of cell clusters into culture medium, has been observed with Wnt-1 (Jue et al., 1992), -2, -3a and -7a, but not Wnt-4 or -5a (Wong et al., 1994). Importantly, those Wnts identified as class-1 in *Xenopus* are the same as those identified as transforming in C57MG cells, whereas class-5a Wnts are non-transforming. This finding further supported the concept of distinct Wnt signalling pathways.

1.2 The canonical Wnt/β-catenin signalling pathway

In 1989, Ozawa and Kemler discovered three proteins associated with the cytoplasmic domain of the epithelial cell-cell adhesion molecule uvomorulin (E-cadherin), and named them as α-, β- and γ-catenin (Ozawa et al., 1989). Two years later, the *β-catenin* gene was identified as the homolog of *armadillo* (*arm*) in *Drosophila* (McCrea et al., 1991). By this time, phenotypic analysis of *Drosophila* mutants with abnormal body segmentation had implicated *arm* as a segment polarity gene and component of the *wingless* signalling pathway (Riggleman et al., 1990), suggesting β-catenin to be downstream of Wnt-1 in vertebrates. Initially, it was thought that β-catenin transduced class-1 Wnt signals by increasing cadherin-mediated intercellular adhesion (Hinck et al., 1994). However, in 1995, observed nuclear accumulation of ectopic β-catenin in association with *Xenopus* axis duplication led Funayama and Gumbiner to propose that β-catenin might signal by regulating gene expression (Funayama et al., 1995). The following year, Molenaar and Clevers reported direct binding of β-catenin to the N-terminus of XTcf-3, the *Xenopus* homolog of mammalian T cell factor (Tcf) and lymphocyte enhancer-binding factor-1 (Lef-1), members of the high mobility group (HMG) box family of transcription factors (Molenaar et al., 1996). Furthermore, by demonstrating that induction of axis duplication by microinjected β-catenin could be suppressed in

Xenopus embryos expressing XTcf-3ΔN, a dominant-negative XTcf-3 mutant with N-terminal deletion, Molenaar and Clevers provided evidence to support a 'canonical' Wnt/β-catenin (*wg/arm*) signalling pathway, with regulation of gene expression as the final step (Molenaar et al., 1996).

1.2.1 The β-catenin destruction complex

In 1994, Hinck and Papkoff first observed the accumulation of β-catenin within the cytosol of Wnt-1 stimulated cells (Hinck et al., 1994). The same response was later shown to occur in C57MG cells stimulated with other transforming Wnts (Shimizu et al., 1997). Interested in the link between the adenomatous polyposis coli (APC) gene and human colorectal cancer, Munemitsu and Polakis reported negative regulation of cytosolic β-catenin levels by APC protein, in 1995 (Munemitsu et al., 1995). In human colorectal cancer (SW480) cells containing a loss-of-function APC mutation, they observed that unusually high levels of cytosolic β-catenin could be markedly reduced by transfecting cells with wild-type APC. Thus, constitutive activation of the canonical pathway became implicated in colorectal oncogenesis. In the years following this discovery, much research has focused on the mechanism by which APC functions. Evidence suggests that APC binds directly to axin and glycogen synthase kinase-3β (GSK-3β) to form a 'destruction complex', within which APC and axin appear to serve as scaffolding proteins, binding β-catenin for presentation to GSK-3β (Miller et al., 1999).

In the absence of a Wnt signal, GSK-3β phosphorylates specific serine/threonine residues within the N-terminal region of β-catenin, thereby promoting its rapid degradation (Miller et al., 1999). Liu *et al* (Liu et al., 2002) recently published data suggesting that *in vivo* phosphorylation of β-catenin by GSK-3β occurs in a sequential manner, with residue T41 preceding S37, then S33. However, prior to this, β-catenin appears to require 'priming' through initial phosphorylation at residue S45 by casein kinase-1α (CK-1α), a protein that is ubiquitously expressed, appears constitutively active, and binds directly to axin (Liu et al., 2002). Only when all four (S45, T41, S37 and S33) residues are phosphorylated can β-transducin repeat-containing protein (β-TRCP) ubiquinate β-catenin (Liu et al., 2002), thereby directing

it to the proteosome (Orford et al., 1997). In this way, the signalling pool of uncomplexed β-catenin in the cytosolic compartment is normally maintained at low levels (Figure 1.1).

In the presence of a class-1 Wnt signal, the constitutive activity of GSK-3β is inhibited (Cook et al., 1996). As a consequence, decreased degradation allows steady-state levels of cytosolic β-catenin to rise, allowing translocation to the nucleus and interaction with Tcf/Lef-1 transcription factors (Miller et al., 1999). Consistent with this, Willert and Nusse found that cyclohexamide, a protein synthesis inhibitor, could block both the accumulation of β-catenin and up-regulated expression of target genes induced by Wnt-3a, suggesting class-1 wnt signal transduction to be dependent on *de novo* synthesis of β-catenin (Willert et al., 2002). Importantly, Staal and Clevers observed increased levels of hypophosphorylated (non-phosphorylated T41 and S37) β-catenin associated with activation of a Tcf/Lef-1 reporter construct in Wnt-1 stimulated human embryonic kidney (293T) cells (Staal et al., 2002). Furthermore, despite accumulation of total β-catenin, pharmacological inhibition of proteosome-mediated proteolysis neither increased levels of hypophosphorylated β-catenin nor activated the Tcf/Lef-1 reporter, suggesting hypophosphorylated β-catenin to be the transcriptionally active signalling fraction (Staal et al., 2002).

The mechanism by which class-1 Wnts inhibit GSK-3β activity is complex and remains unclear. Genetic studies in *Drosophila* initially identified *frizzled-2* (*Dfz2*) (Bhanot et al., 1996), *arrow* (Wehrli et al., 2000) and *dishevelled* (Siegfried et al., 1994) as genes encoding key proteins required for *wingless* signal transduction upstream of *zeste-white 3* (*zw3*), the *Drosophila* homologue of GSK-3β. Frizzleds (Fzd/Fz) comprise a family of seven transmembrane spanning (7TMS) proteins, first identified as Wnt/wg receptors in 1996 (Bhanot et al., 1996; Yang-Snyder et al., 1996). The *arrow* gene encodes a single-pass transmembrane protein, homologous to mammalian low-density lipoprotein receptor-related protein-5 (Lrp-5) and Lrp-6 (Wehrli et al., 2000). Evidence suggests that Lrp-5/6 serves as a co-receptor, associating with Fzd in a Wnt-dependent manner (Mao et al., 2001; Tamai et al., 2000). The resulting Wnt receptor complex promotes direct binding of axin to the cytoplasmic domain of Lrp-5/6 (Mao et al., 2001; Tamai et al., 2000), possibly giving

rise to the observed dissociation of GSK-3β from axin in response to Wnt-1 stimulation (Li et al., 1999). An alternative, non-mutually exclusive mechanism for destabilising the destruction complex might involve recruitment by dishevelled (Dvl/dsh) of Frat-1 (frequently rearranged in advanced T-cell lymphomas-1) and Frat-2, mammalian homologues of GSK-3 binding protein (GBP) and positive regulators of β-catenin (Li et al., 1999; Saitoh et al., 2001d). However, modelling of Wnt signal transduction is further complicated by the increasing number of proteins shown to associate with Dvl and members of the destruction complex (visit http://www.stanford.edu/~rnusse/wntwindow.html). These include kinases and phosphatases that probably account for the observed hyperphosphorylation of Dvl (Lee et al., 1999) and hypophosphorylation of axin/APC (Miller et al., 1999) induced by class-1 Wnts. Since the affinity of the destruction complex for β-catenin appears to be dependent on axin/APC phosphorylation status, the relative activities of these kinases and phosphatases may also modulate the ability of GSK-3β to access and phosphorylate β-catenin (Miller et al., 1999). Whether Wnt signals directly alter the intrinsic kinase activity of GSK-3β *per se* remains a subject for debate.

1.2.2 Tcf/Lef-1 mediated transcription

When Molenaar and Clevers first reported direct binding of β-catenin to the N-terminus of XTcf-3, they observed that this interaction was a necessary step before XTcf-3 could activate a Tcf/Lef-1 reporter construct (Molenaar et al., 1996). Indeed, evidence now suggests that all members of the Tcf/Lef-1 family function as transcriptional repressors in the absence of active β-catenin (Brantjes et al., 2001). In this respect, studies have implicated several co-repressors, including Groucho in *Drosophila* (Cavallo et al., 1998). Murine homologues of Groucho comprise a family of Groucho-related genes, termed *Grg-1*, *-2*, *-3*, *-4* and *-5*, the latter encoding a truncated variant. Groucho homologues in man are transducin-like enhancer of split-1 (TLE-1), -2, -3 and -4, and the truncated variant known as amino-terminal enhancer of split (hAES). Brantjes and Clevers have shown that Grg/TLE can bind all known mammalian Tcf/Lef-1 members, repressing transcription equipotently (Brantjes et al., 2001). Evidence suggests that Grg/TLE mediate repression through interaction with histone deacetylase-1 (HDAC), causing chromatin to condense (Brantjes et al., 2001).

However, truncated Grg-5/hAES fail to bind HDAC and may act as de-repressors, perhaps modulating repression by other Grg/TLE members (Brantjes et al., 2001). Binding of β-catenin to Tcf/Lef-1 appears to lead to recruitment of several co-activators, including CREB-binding protein (CBP) (Takemaru and Moon, 2000). By functionally antagonising HDAC, the histone acetylase activity of CBP is thought to lift Grg/TLE-mediated repression, allowing Tcf/Lef-1 to actively transcribe target genes (van Noort and Clevers, 2002).

Given the link between constitutive activation of Tcf/Lef-1 transcription factors and both oncogenesis and teratogenesis, it is perhaps not surprising that negative regulatory mechanisms have evolved to operate on the canonical pathway at multiple levels in the absence of a Wnt signal (Figure 1.1). In addition to the destruction complex and transcriptional co-repressors outlined above, evidence suggests that cytoplasmic factors inhibit nuclear import of β-catenin (Fagotto et al., 1998), and ICAT (inhibitor of β-catenin and Tcf-4) interferes with β-catenin/Tcf-4 binding (Tago et al., 2000). Together, these mechanisms appear to provide tight regulation of genes involved in cell proliferation, survival, differentiation and migration (Table 1.1).

1.3 Non-canonical Wnt signalling pathways

In 1997, Shimizu *et al* (Shimizu et al., 1997) published data to show that, in contrast to transforming Wnts, non-transforming Wnts do not induce accumulation of β-catenin within the cytosol of C57MG cells, suggesting class-5a Wnts signal independently of β-catenin via one or more 'non-canonical' pathways. That same year, Slusarski and Moon reported that, unlike class-1 Wnts, Wnt-5a could induce release of Ca^{2+} from intracellular stores in Zebrafish (*Danio rerio*) embryos through activation of the inositol signalling pathway in a G-protein-dependent manner (Slusarski et al., 1997a; Slusarski et al., 1997b). These observations have led to the concept of a Wnt/Ca^{2+} signalling pathway (Kuhl et al., 2000a; Miller et al., 1999), with associated activation of protein kinase C (PKC) (Sheldahl et al., 1999) (Figure 1.2). Importantly, Wnt-5a has been shown to functionally antagonise the activity of class-1 Wnts in both *Xenopus* embryos (Torres et al., 1996) and C57MG cells (Olson and Gibo, 1998), and evidence from Kuhl and Moon suggests that cross-talk from the

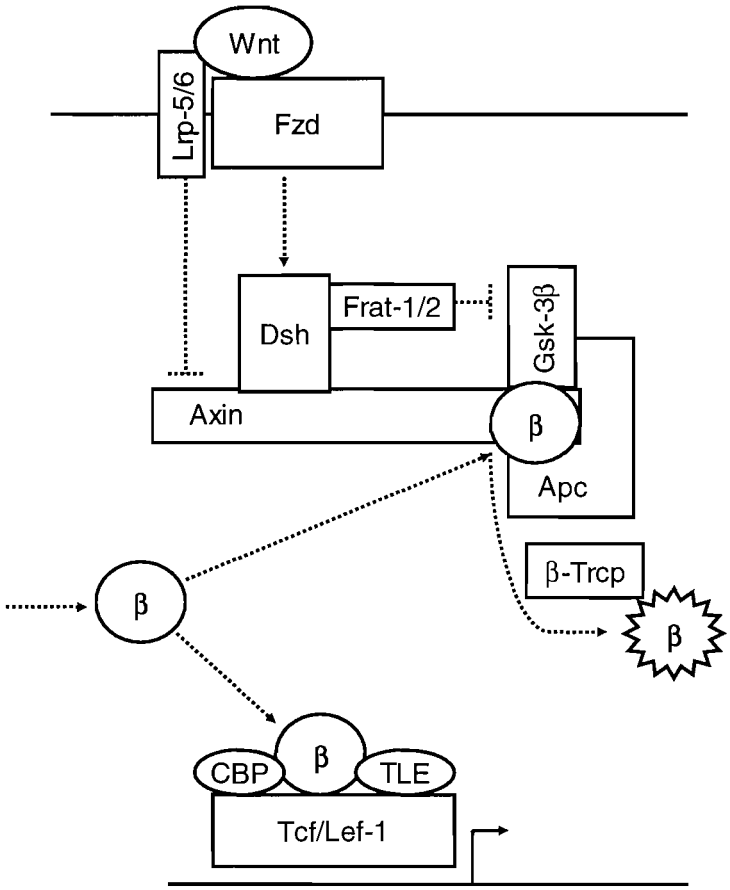

Figure 1.1: The canonical Wnt/β-catenin signalling pathway.

See text for details. β (β-catenin); Fzd (frizzled); Lrp-5/6 (low-density lipoprotein receptor-related protein-5/6); Dsh (dishevelled); Frat-1/2 (frequently rearranged in advanced T-cell lymphomas-1/2); Gsk-3β (glycogen synthase kinase-3β); Apc (adenomatous polyposis coli protein); β-Trcp (β-transducin repeat-containing protein); CBP (CREB-binding protein); TLE (transducin-like enhancer of split).

Wnt/Ca^{2+} pathway negatively regulates Wnt/β-catenin signalling at two levels (Kuhl et al., 2001). At one level, Ca^{2+}-calmodulin-dependent protein kinase II (CamKII), activated by a rise in levels of intracellular Ca^{2+}, appears to block Tcf/Lef-1 mediated transcription downstream of β-catenin (Kuhl et al., 2001). This finding is consistent with observations made by Ishitani *et al* (Ishitani et al., 1999) in which TGFβ activated kinase-1 (TAK-1), downstream of CamKII, activates NEMO-like kinase

Target gene	Cell type	References
Proliferation		
c-myc	colon cancer	[86]
cyclin-D1	colon cancer	[243][262]
PPAR-δ	colon cancer	[85]
Survival		
Survivin	colon cancer	[302]
Stress response		
c-jun	colon cancer	[149]
fra-1	colon cancer	[149]
uPAR	colon cancer	[149]
IL-8	hepatocytes	[140]
(De)differentiation		
ZO-1*	colon cancer	[149]
ID2	colon cancer	[216]
MSX-1/2	teratocarcinoma	[287]
REST/NRSF	teratocarcinoma	[287]
Migration		
CD44	colon cancer	[286]
MMP-7	colon cancer	[14][41]
MMP-26	A549 lung cancer	[151]
Negative feedback		
Axin-2 (Axil, Conductin)	colon cancer	[108][148][297]
β-TRCP	teratocarcinoma	[287]
TCF-1†	colon cancer	[217]
TLE	teratocarcinoma	[287]
Positive feedback		
FZD-7	teratocarcinoma	[287]
LEF-1	colon cancer	[97]
Miscellaneous		
Claudin-1	colon cancer	[164]

Table 1.1: Target genes for Tcf/Lef-1 identified in man.

*Down-regulated expression; †β-catenin insensitive isoforms.

(NLK), thereby phosphorylating Tcf/Lef-1 transcription factors and inhibiting their interaction with β-catenin. The second level of negative regulation is thought to involve inhibition of class-1 Wnt signal transduction by PKC-mediated phosphorylation of Dvl (Kuhl et al., 2001). However, other groups have reported canonical pathway activation to be dependent on (Cook et al., 1996) or augmented by (Chen et al., 2000) PKC, and it may be that the influence of PKC on signalling by β-catenin is cell context dependent.

During vertebrate gastrulation, formation of the body axis results from co-ordinate cell migration, termed convergent extension movements, a process dependent on cadherin-mediated cell-cell adhesion (Kuhl and Wedlich, 1996). Studies have shown increased intercellular adhesion and enhanced convergent extension movements in *Xenopus* embryos expressing ectopic class-1 Wnts, with opposing effects induced by class-5a Wnts (Du et al., 1995; Torres et al., 1996). These observations support the hypothesis that class-1 and -5a Wnts differentially regulate convergent extension movements via their influence on cell adhesion. However, recent evidence from Kuhl and Moon suggests that normal body axis formation is also dependent on Tcf/Lef-1 mediated transcription, and that negative regulation of Wnt/β-catenin signalling by the Wnt/Ca^{2+} pathway might play an important role in orchestrating this morphogenetic process (Kuhl et al., 2001).

Planar cell polarity (PCP), otherwise known as tissue polarity, is a term employed by developmental biologists to describe the coherent alignment of epithelial cells in body parts of *Drosophila*. Genetic studies initially identified *frizzled-1* (*fz*) (Vinson and Adler, 1987) and *dsh* (Theisen et al., 1994) as PCP genes, with mutations giving rise to phenotypes characterised by misalignment of trichomes (hairs) on the wings, bristles on the legs and thorax, or ommatidia (photoreceptors) in the eyes (Shulman et al., 1998). In 1998, Boutros *et al* (Boutros et al., 1998) published data suggesting c-Jun NH(2)-terminal kinase (JNK) to be downstream of dsh in the PCP pathway (Figure 1.2). More recently, JNK has also been implicated in the regulation of convergent extension movements in *Xenopus* embryos (Yamanaka et al., 2002). However, whereas Wnt-5a activates JNK in *Xenopus* (Yamanaka et al., 2002), the role of wg/wnt in *Drosophila* PCP remains controversial. Thus, at least in vertebrate

development, canonical Wnt/β-catenin and non-canonical Wnt/Ca^{2+} and Wnt/JNK pathways appear to orchestrate embryonic cell migration and tissue morphogenesis.

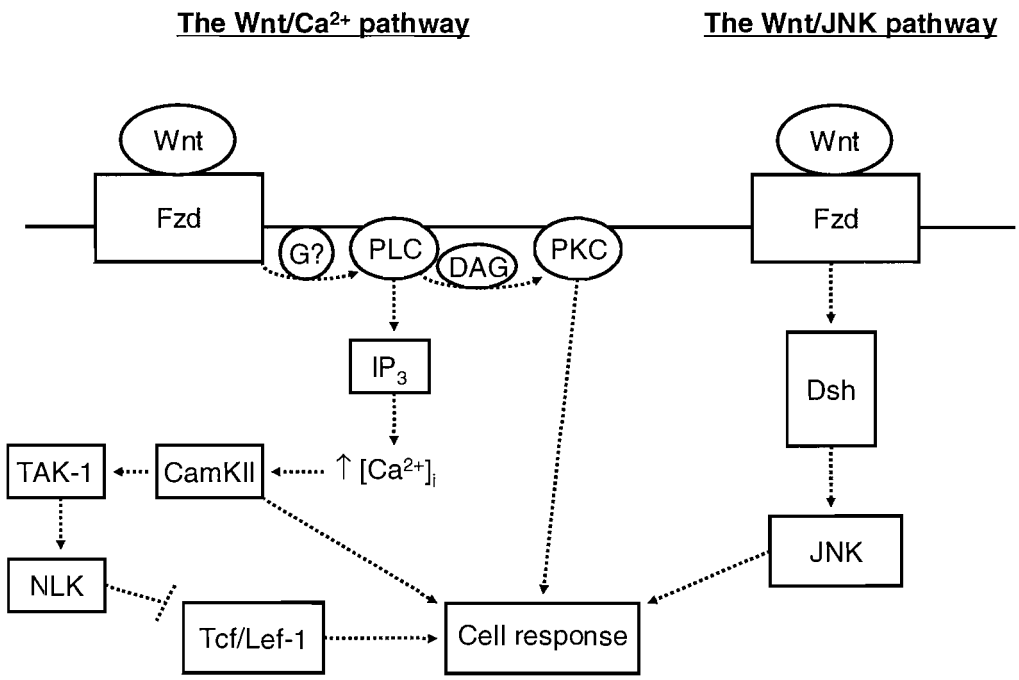

Figure 1.2: Non-canonical Wnt signalling pathways.

See text for details. Fzd (frizzled); G (G-protein); PLC (phospholipase C); DAG (diacyl glycerol); PKC (protein kinase C); IP_3 (inositol 1,4,5-trisphosphate); $[Ca^{2+}]_i$ (intracellular ionised calcium); CamKII (Ca^{2+}-calmodulin-dependent protein kinase II); TAK-1 (TGFβ activated kinase-1); NLK (NEMO-like kinase); Dsh (dishevelled); JNK (c-Jun NH(2)-terminal kinase).

1.3.1 Wnt signal specificity

The mechanism governing Wnt signal specificity remains a fundamental question in the field of Wnt research. Observed induction of axis duplication in *Xenopus* embryos by Wnt-5a co-expressed with human frizzled-5 (He et al., 1997) has questioned the signal specificity of Wnt proteins and cast doubt on the validity of the Wnt-1/-5a classification. Instead, this suggests that signal specificity is governed by the Wnt

receptor itself, and baseline responses to ectopically expressed *frizzled* genes alone has led to their provisional classification into those that activate the Wnt/β-catenin pathway (e.g. human frizzled-5) and those that activate the Wnt/Ca^{2+} pathway (e.g. human frizzled-1, -3 and -6) (Kuhl et al., 2000b). However, human frizzled-1 has also been shown to transduce a canonical signal through interaction with Wnt-1, -2, -3 or -3a, but not -5a despite evidence of it binding (Gazit et al., 1999). Thus, individual frizzled receptors might be capable of transducing either canonical or non-canonical signals, depending on the Wnt involved. Although not every Wnt binds every frizzled, there is evidence to suggest a fair degree of receptor promiscuity and functional redundancy, the significance of which remains to be determined (Dale, 1998).

More recently, interest in the mechanism of Wnt signal specificity has focused on Lrp-5/6 co-receptor function. Studies have shown induction of *Xenopus* axis duplication by ectopic Lrp-6 and blockade of class-1, but not class-5a, Wnt signals by a dominant-negative Lrp-6 construct (Semenov et al., 2001; Tamai et al., 2000). The same selective action has also been observed with Lrp-5 (Mao et al., 2001), suggesting requirement of Lrp-5/6 by the Wnt/fzd complex when transducing canonical, but not non-canonical, signals. By co-expressing Lrp-6 with human frizzled-5 fused to either a class-1 or -5a Wnt, Holmen *et al* (Holmen et al., 2002) reported strong activation of a Tcf/Lef-1 reporter in 293T cells. Importantly, using a range of mouse frizzleds, the potency of the fusion protein to transduce a canonical signal was found to be dependent not on the Wnt but on the frizzled involved. Interestingly, in this context, Lrp-5 appeared less potent than Lrp-6 (Holmen et al., 2002). Evidence would therefore suggest that Wnt signal specificity resides with the frizzled receptor and not with any intrinsic property of the Wnt itself. By binding to frizzled, Wnt simply serves to recruit Lrp-5/6 in a frizzled-dependent manner, with formation of a heterotrimeric complex leading to activation of the canonical pathway. In this model, the Wnt-1/5a classification can be explained by class-5a Wnts having relatively high affinity for the cysteine-rich domain (CRD) of frizzleds that have low affinity for Lrp-5/6.

Since 1996, two families of secreted Wnt antagonist have been identified, namely the secreted frizzled-related proteins (Sfrp) and Dickkopf (Dkk) proteins. Members of the Sfrp family possess the CRD without the seven transmembrane segments (7TMS) of Fzd, are not splice variants of fzd genes, and appear to operate by directly binding specific Wnts in the extracellular space (Wodarz and Nusse, 1998). In this way, Sfrp may function to inhibit activation of either the canonical or non-canonical pathways by interfering with Wnt/Fzd interactions. In contrast, evidence suggests that Dkk-1 selectively blocks canonical signalling through direct interaction with Lrp-5/6, thereby preventing formation of the Wnt/Fzd/Lrp-5/6 heterotrimeric complex (Semenov et al., 2001; Zorn, 2001). Interestingly, whereas Dkk-1 and -4 prevent class-1 Wnt induced axis duplication in *Xenopus* embryos, Dkk-2 and Dkk-3 do not (Krupnik et al., 1999). Furthermore, Dkk-2 appears to facilitate canonical signal transduction through synergistic interaction with Lrp-5/6 (Li et al., 2002b; Wu et al., 2000). Thus, Sfrp and Dkk proteins might function to modulate Wnt signalling and Wnt signal specificity.

1.4 Growth factor and cell adhesion cross-talk with the canonical pathway

The receptor tyrosine kinase (RTK) family serves an array of growth factors that activate multiple signalling cascades, including the phosphatidylinositol 3-kinase/protein kinase B (PI3K/PKB) pathway. Some published reports suggest that class-1 Wnt induced activation of Tcf/Lef-1 mediated transcription may be *enhanced* by growth factor co-stimulation, with growth factor alone having no detectable effect. Consistent with this, ectopic PKB (Akt) has been shown to increase activation of a Tcf/Lef-1 reporter by Wnt-1 in Swiss mouse embryo (NIH3T3) fibroblasts (Yuan et al., 1999). Similarly, using lithium as a non-competitive inhibitor of GSK-3β and mimicker of class-1 Wnts, co-stimulation with either insulin-like growth factor-I (IGF-I) (Playford et al., 2000) or epidermal growth factor (EGF) (Chen et al., 2000) has been shown to enhance Tcf/Lef-1 reporter activity in human embryonic kidney (HEK 293) cells. However, there are also reports of growth factors independently stabilising β-catenin and transiently activating Tcf/Lef-1 mediated transcription in certain cell types. For example, activation of the canonical pathway has been observed in C57MG cells stimulated with hepatocyte growth factor (HGF, scatter

factor) (Papkoff and Aikawa, 1998), and in rat bladder cancer (NBT-II) cells stimulated with IGF-II (Morali et al., 2001). In the context of epithelial repair, the EGF receptor (ErbB1) plays a central role by promoting all phases of epithelial restitution, including cell migration, proliferation and differentiation (Davies et al., 1999). Indeed, up-regulated ErbB1 expression is a response to epithelial injury observed in the human airway (Puddicombe et al., 2000). Intriguingly, the EGF receptor has been shown to activate Tcf/Lef-1 transcription factors in murine dermal fibroblasts (Cheon et al., 2004), non-transformed human mammary epithelial (MCF-10A) cells (Graham and Asthagiri, 2004) and human tumour cells (Lu and Hunter, 2004), possibly providing an essential co-signal required for passage through the G1/S checkpoint of the cell cycle (Graham and Asthagiri, 2004). Thus, it is tempting to speculate that co-operative signalling between Wnt/β-catenin and the EGF receptor might play an important role in the proliferative response of the bronchial epithelium following injury.

The mechanisms by which Tcf/Lef-1 transcription factors are activated by members of the RTK family remain unclear. One possibility is that growth factors stabilise β-catenin by inhibiting the GSK-3β/Apc/axin destruction complex (Cheon et al., 2004; Papkoff and Aikawa, 1998). Indeed, PKB can inhibit GSK-3β by phosphorylating its serine-9 (Ser9) residue (Fang et al., 2000). However, studies have shown that although insulin inhibits GSK-3β by this means, it does not induce a detectable change in cytosolic levels of β-catenin or Tcf/Lef-1 mediated transcription (Ding et al., 2000). Furthermore, activation of the canonical pathway by Wnt-1 occurred in the absence of Ser9 phosphorylation (Ding et al., 2000). Hence, signalling specificity would appear to reflect distinct mechanisms by which class-1 Wnts and PKB inhibit GSK-3β. Whereas PKB phosphorylates Ser9, class-1 Wnts selectively prevent phosphorylation of β-catenin by modifying the scaffolding of the GSK-3β/axin/APC destruction complex. In this model, transient phosphorylation of Ser9 by PKB may not allow sufficient time for GSK-3β to significantly alter the fate of β-catenin.

Negative regulation of Tcf/Lef-1 mediated transcription by TAK-1/NLK (Ishitani et al., 1999) has previously been mentioned as an event downstream of CamKII in the Wnt/Ca^{2+} pathway. However, TAK-1 was originally named because of its activation

by transforming growth factor-β (TGF-β). This pleiotropic cytokine operates through a receptor with serine/threonine kinase activity, and has been shown to *inhibit* the ectopic β-catenin-induced activation of a Tcf/Lef-1 reporter in chick embryonic chondrocytes (Dong et al., 2005). In contrast, TGF-β has also been shown to *activate* Tcf/Lef-1 mediated transcription independently of β-catenin, and act synergistically with class-1 Wnts, by inducing direct binding of Smad-3 and -4 to Tcf/Lef-1 in 293T and HepG2 cells (Labbe et al., 2000; Letamendia et al., 2001; Nishita et al., 2000). Thus, TGF-β might influence cell fate during the process of epithelial repair by modulating Tcf/Lef-1 transcriptional activity downstream of both Wnt/β-catenin and the EGF receptor.

In addition to the regulation of cadherin-based intercellular adhesion by Wnts (Du et al., 1995; Hinck et al., 1994; Torres et al., 1996), modulation of the canonical pathway by cell-cell and cell-matrix adhesive mechanisms have also been proposed. Adherens junctions comprise cadherin/β-catenin complexes linked to the actin cytoskeleton via α-catenin (Aberle et al., 1996). Studies have shown that the induction of axis duplication in *Xenopus* embryos by ectopic β-catenin can be blocked by exogenous C-cadherin (Fagotto et al., 1996) or α-catenin (Sehgal et al., 1997). Furthermore, ectopic E-cadherin (Gottardi et al., 2001) or α-catenin (Giannini et al., 2000) reduces Tcf/Lef-1 mediated transcription in SW480 cells. These observations suggest that classical cadherins and α-catenin compete with Tcf/Lef-1 transcription factors for direct binding to the *armadillo*-like (*arm*) repeat domain of β-catenin, thereby modifying the kinetics of the uncomplexed, transcriptionally active pool (Huber and Weis, 2001; Stockinger et al., 2001; von Kries et al., 2000). Thus, when cell-cell contacts are disrupted as a consequence of epithelial injury, reduced competition from classical cadherins and α-catenin might allow cells to be more responsive to canonical Wnt signals. Furthermore, the EGF receptor might *indirectly* influence canonical Wnt signalling by liberating transcriptionally active β-catenin from the membrane compartment through destabilisation and down-regulation of adherens junctions (Al Moustafa et al., 2002; Eger et al., 2000; Hoschuetzky et al., 1994; Muller et al., 1999; Shiozaki et al., 1995; Takahashi et al., 1997; Tsukatani et al., 1997).

Finally, integrin-linked kinase (ILK) is a serine/threonine kinase, the activity of which is regulated by cell-matrix interactions through direct binding to the cytoplasmic domains of β_1-, β_2- and β_3-integrins. In rat intestinal epithelial (IEC-18) cells, ectopic ILK has been shown to activate the canonical pathway (Novak et al., 1998) via the PI3K/PKB cascade (Delcommenne et al., 1998). However, transient inhibition of GSK-3β by endogenous ILK may not necessarily give rise to activation of Tcf/Lef-1 mediated transcription. The above interactions are summarised in Figure 1.3.

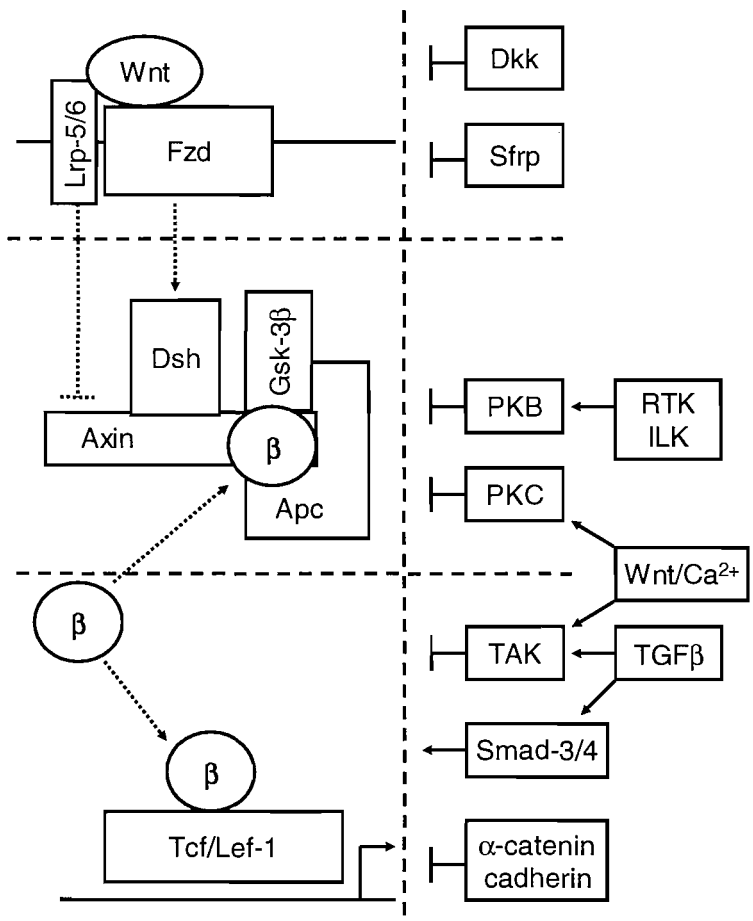

Figure 1.3: Cross-talk with the canonical Wnt pathway.

See text for details. β (β-catenin); Fzd (frizzled); Lrp-5/6 (low-density lipoprotein receptor-related protein-5/6); Dsh (dishevelled); Gsk-3β (glycogen synthase kinase-3β); Apc (adenomatous polyposis coli protein); Dkk (Dickkopf protein); Sfrp (secreted frizzled-related protein); RTK (receptor tyrosine kinase); ILK (integrin-linked kinase); PKB (protein kinase B); PKC (protein kinase C); TGFβ (transforming growth factor-β); TAK-1 (TGFβ activated kinase-1).

1.5 Wnt signalling and embryonic lung development

Wnts appear to signal across several cell diameters, functioning as morphogens during embryonic development similar to members of the Sonic Hedgehog (Shh) and bone morphogenetic protein (Bmp) families (Christian, 2000). Overlapping concentration gradients of Wnts, SFRP and DKK across fields of cells help orchestrate differential gene expression, determining individual cell phenotype in time and space (Christian, 2000). Since my interest is in respiratory disease, in particular bronchial asthma, further discussion will tend to focus on what is currently known about Wnt signalling in mammalian and human lung.

Mammalian lung morphogenesis involves invasion by epithelium into surrounding mesenchyme, a process dependent on reciprocal paracrine signalling between epithelial and underlying mesenchymal cells (Perl and Whitsett, 1999). Following creation of the primitive lung bud from the embryonic foregut, branching morphogenesis gives rise to formation of the respiratory tree (Perl and Whitsett, 1999). Paracrine signals thought to be involved within the epithelial-mesenchymal trophic unit (EMTU) include Wnts, Shh, Bmp-4, and members of the EGF, TGF-β, fibroblast growth factor (FGF) and platelet-derived growth factor (PDGF) families (Perl and Whitsett, 1999). In mouse embryonic lung, *in situ* hybridisation analysis has identified expression of WNT-2 (Bellusci et al., 1996) and -2b (-13) (Zakin et al., 1998) confined to mesenchymal cells around sites of branch formation. In contrast, WNT-7b RNA appears restricted to the airway epithelium, whereas genes encoding WNT-11 and SFRP-1, -2 and -4 are expressed by both epithelial and mesenchymal cells (Tebar et al., 2001; Weidenfeld et al., 2002). *In situ* hybridisation and immunohistochemical analysis has also identified message and protein for β-catenin, Lef-1, Tcf-1, Tcf-3 and Tcf-4 in both airway epithelial and underlying mesenchymal cells, suggesting involvement of the *canonical* Wnt signalling pathway in lung morphogenesis (Tebar et al., 2001). Furthermore, as a surrogate marker for Tcf/Lef-1 activation, nuclear β-catenin is frequently observed in both cell types at sites of mesenchymal invasion, becoming less prominent in mesenchymal cells as lung development progresses (Tebar et al., 2001). Interestingly, RNA encoding LEF-1 and TCF-1 is not detected in mouse lung tissue at one day post-partum, possibly reflecting

a role for these transcription factors in the establishment of pulmonary architecture by birth, rather than its maintenance throughout life (Oosterwegel et al., 1993). However, in ferret trachea, evidence suggests that Lef-1 plays a key role in submucosal gland (SMG) morphogenesis at least during the neonatal period. Surface tracheal epithelial cells expressing LEF-1 RNA have been shown to condense shortly before invading mesenchyme, initially giving rise to an SMG bud (Duan et al., 1998). During subsequent SMG formation, LEF-1 expression is predominantly observed in epithelial cells at the tips of invading fronts (Duan et al., 1998). Loss of LEF-1, using antisense RNA, blocks SMG morphogenesis in a ferret trachea xenograft model (Duan et al., 1999). However, ectopic LEF-1 does not induce SMG formation in either a human bronchial xenograft model or transgenic mouse (Duan et al., 1999). These data suggest that Lef-1 defines a subset of surface airway epithelial progenitor cells involved in the initiation and propagation of SMG development, but that factors other than Lef-1 are also required. Although it is reasonable to postulate a canonical Wnt signal being such a factor, this hypothesis has been questioned by Ritchie *et al* (Ritchie et al., 2001), who failed to detect nuclear β-catenin in neonatal ferret tracheal epithelium, either by immunohistochemistry or laser confocal microscopy. However, Ritchie analysed frozen sections and did not appear to be aware of the report by Munné *et al* (Munne et al., 1999) in which freezing of positive control tissues and cells induced loss of nuclear β-catenin staining with the widely used (pan-)β-catenin antibody (clone 14; BD Biosciences).

1.5.1 Wnt signalling and lung development in man

Table 1.2 shows known genes encoding major elements of the Wnt signalling pathway in man. Nomenclature can appear confusing, and alternative names for certain human Wnt-related genes are shown in Table 1.3. Based on a review of the literature, Table 1.4 summarises what is currently known about WNT, FZD, LRP, DVL, FRAT, TCF/LEF-1, SFRP and DKK gene expression in human foetal lung. References in Table 1.4 generally refer to studies in which WNT-related genes have been cloned and characterised, with northern blot analysis of several human tissues. Since lung tissue is comprised of more than forty cell types, such studies provide no indication of which cells express which genes. However, expression of genes

WNT	WNT-1, -2, -2B, -3, -3A, -4, -5A, -5B, -6, -7A, -7B, -8A, -8B, -9A, -9B, -10A, -10B, -11, -16
FZD	FZD-1, -2, -3 ($8p_{21}$), -4, -5, -6, -7, -8, -9 ($7q_{11}$), -10
LRP	LRP-5, -6
DVL	DVL-1, -2, -3
FRAT	FRAT-1, -2
TCF/LEF-1	TCF-1, -3, -4, LEF-1
SFRP	SFRP-1, -2, -4, -5, FRZB
DKK	DKK-1, -2, -3, -4

Table 1.2: Known WNT-related genes in man.

FZD (frizzled); LRP (low-density lipoprotein receptor-related protein); DVL (dishevelled); FRAT (frequently rearranged in advanced T-cell lymphomas); SFRP (secreted frizzled-related protein); DKK (Dickkopf protein).

encoding WNT-2 (Levay-Young and Navre, 1992) and -5a (Clark et al., 1993), and SFRP-1 (Finch et al., 1997) have been reported in human foetal lung fibroblasts, *in vitro*. In addition, *in situ* hybridisation has demonstrated the expression of WNT-11 RNA to be restricted to mesenchymal cells, becoming localised to epithelial branch points as lung formation progresses (Lako et al., 1998). Finally, evidence in support of a role for canonical Wnt signalling in human foetal lung development comes from studies that have shown nuclear β-catenin in airway epithelial cells as they invade surrounding mesenchyme during the process of branching morphogenesis (Eberhart and Argani, 2001; Nakatani et al., 2002). In contrast, no nuclear β-catenin was detected in lung tissue from a deceased 18 month old child (Eberhart and Argani, 2001).

	Alternative nomenclature
WNT-1	INT-1
WNT-2	IRP (INT-1 related protein)
WNT-2B	WNT-13
WNT-9A	WNT-14
WNT-9B	WNT-15
WNT-15	WNT-14B
FZD-9 ($7q_{11}$)	FZD-3 ($7q_{11}$); *not* FZD-3 ($8p_{21}$)
LRP-5	LR-3, LRP-7
FRAT-1	GBP
TCF-1	TCF-7
TCF-3	TCF-7L1
TCF-4	TCF-7L2
LEF-1	TCF-1α
SFRP-1	FRP, FRP-1, SARP-2, FRZA
SFRP-2	FRP-2, SARP-1, SDF-5
SFRP-4	FRPAP, FRPHE
SFRP-5	SARP-3
FRZB	SFRP-3, Fritz
DKK-3	REIC

Table 1.3: Alternative nomenclature for WNT-related genes in man.

LRP (low-density lipoprotein receptor-related protein); FRAT (frequently rearranged in advanced T-cell lymphomas); SFRP (secreted frizzled-related protein); DKK (Dickkopf protein).

	Detected?	Technique	Cell source	References
WNT-1	ND	-	-	-
WNT-2	yes	NB	tissue, fibroblasts	[112][139][278]
WNT-2B	yes	NB	tissue	[114]
WNT-3	no	NB	tissue	[113]
WNT-3A	no	NB	tissue	[222]
WNT-4	ND	-	-	-
WNT-5A	yes	PCR	neonatal tissue, fibroblasts	[36]
WNT-5B	yes	NB	tissue	[220]
WNT-6	no	NB	tissue	[120]

	Detected?	Technique	Cell source	References
WNT-7A	yes	PCR	tissue	[101]
WNT-7B	yes	NB	tissue	[118]
WNT-8A	no	NB	tissue	[221]
WNT-8B	yes	PCR	tissue	[225]
WNT-10A	yes	NB	tissue	[120]
WNT-10B	ND	-	-	-
WNT-11	yes	NB, ISH	tissue, mesenchymal cells	[117][132]
WNT-14	yes	NB	tissue	[222]
WNT-15	no	NB	tissue	[119]
WNT-16	ND	-	-	-
FZD-1	yes	NB	tissue	[219]
FZD-2	yes	NB	tissue	[219][303]
FZD-3	ND	-	-	-
FZD-4	yes	NB	tissue	[116]
FZD-5	yes	NB	tissue	[220]
FZD-6	yes	NB	tissue	[265]
FZD-7	yes	NB	tissue	[219]
FZD-8	yes	NB	tissue	[221]
FZD-9	no	PCR	tissue	[279]
FZD-10	yes	NB	tissue	[121]
LRP-5	yes	NB	tissue	[54]
LRP-6	ND	-	-	-
DVL-1	yes	NB	tissue	[206]
DVL-2	yes	WB	tissue	[230]
DVL-3	yes	NB	tissue	[206]
FRAT-1	yes	DB	tissue	[71]
FRAT-2	yes	DB	tissue	[71]
TCF-1	ND	-	-	-
LEF-1	ND	-	-	-
TCF-3	ND	-	-	-
TCF-4	ND	-	-	-
SFRP-1	yes	NB	tissue, fibroblasts	[70]
SFRP-2	ND	-	-	-
FRZB	no	ISH	tissue	[92]
SFRP-4	ND	-	-	-
SFRP-5	ND	-	-	-
DKK-1	no	NB	tissue	[69]
DKK-2	ND	-	-	-
DKK-3	ND	-	-	-
DKK-4	ND	-	-	-

Table 1.4: WNT-related gene expression in human foetal lung.

ND (not done or reported); NB (northern blot); DB (mRNA dot blot); PCR (polymerase chain reaction); ISH (*in situ* hybridisation); WB (western blot); FZD (frizzled); LRP (low-density lipoprotein receptor-related protein); DVL (dishevelled); FRAT (frequently rearranged in advanced T-cell lymphomas); SFRP (secreted frizzled-related protein); DKK (Dickkopf protein).

1.6 Wnt signalling and cancer

It is estimated that 85% of all colorectal cancers contain loss-of-function APC mutations (Miyoshi et al., 1992), giving rise to abnormally high levels of cytosolic β-catenin (Munemitsu et al., 1995) and constitutive activation of Tcf-4 (Korinek et al., 1997). Of the remaining 15% of colorectal cancers with wild-type APC, point mutations have been found in the N-terminal region of β-catenin (β-cateninΔN), involving one or more of the four residues (S45, T41, S37 and S33) normally phosphorylated by GSK-3β (Morin et al., 1997). As a consequence, β-cateninΔN escapes degradation and constitutive Tcf-4 activation occurs (Morin et al., 1997). Furthermore, gain-of-function β-cateninΔN mutations are associated with several other human cancers, including malignant melanoma and cancers of the liver, prostate, ovary and uterus (Morin, 1999). However, the precise relationship between canonical pathway activation and cancer pathogenesis remains to be elucidated.

1.6.1 The functional consequence of Tcf/Lef-1 activation

Consistent with known target genes of Tcf/Lef-1 (Table 1.1), functional studies suggest that canonical Wnt signalling plays an important role in the regulation of cell proliferation, survival, differentiation and migration. In human colon cancer cells, ectopically expressed dominant-negative Tcf-4 induces G0/G1 cell cycle arrest (Mariadason et al., 2001; Tetsu and McCormick, 1999), promotion of a more differentiated colonic epithelial phenotype (Mariadason et al., 2001; Naishiro et al., 2001), and increased susceptibility to chemotherapeutic drug-induced apoptosis (Chen et al., 2001). Conversely, in normal mammalian colonic epithelial cells, ectopic β-cateninΔN induces 1) cell dedifferentiation, with loss of apico-basal polarity, 2) cell immortalisation, characterised by an unlimited proliferative potential and escape from senescence, and 3) cell transformation, defined as loss of both contact inhibited growth and anoikis (apoptosis induced by loss of cell anchorage with cells in suspension) (Naishiro et al., 2001; Wagenaar et al., 2001). These observations have led to the hypothesis that constitutive Tcf-4 activation is an early event in colorectal cancer pathogenesis, giving rise to a pre-malignant phenotype similar to that of a *dysregulated* adult stem-cell. Whereas pluripotent adult stem-cells account for

approximately 0.5-2.0% of the epithelial cell population in normal colonic crypts, *the stem-cell theory of cancer* suggests an abnormal expansion in number of immortalised cells, leading to pre-malignant polyp formation whilst increasing the risk of acquiring secondary mutations required for invasiveness and malignant progression (Taipale and Beachy, 2001).

Mesenchymal invasion by epithelial cells during submucosal gland (SMG) morphogenesis suggests an association between Lef-1 activation and cell migration (Duan et al., 1998). In colorectal cancer (DLD-1) cells with a loss-of-function APC mutation, ectopic Lef-1 induces epithelial-mesenchymal transition (EMT), characterised by loss of apico-basal polarity and destabilisation of cadherin-mediated cell junctions prior to cell migration and invasion of extracellular matrix (Kim et al., 2002). EMT can also be induced in approximately 5% of normal human corneal epithelial (HCE) or canine kidney epithelial (MDCK) cells when transfected with LEF-1 and co-cultured with Wnt-1 secreting fibroblasts (Kim et al., 2002). Furthermore, in contrast to low migrating malignant melanoma cells or normal melanocytes, highly migrating melanoma cells express LEF-1 and migratory activity can be inhibited by using a dominant-negative Lef-1 (Murakami et al., 2001). Importantly, the LEF-1 gene has itself been shown to be a target of the canonical pathway in colon cancer cells, providing a potential positive-feedback loop which may contribute to the invasive/malignant phenotype (Hovanes et al., 2001).

In vitro functional studies have focused primarily on cells in which canonical pathway activation is either constitutive or ectopically manipulated. However, transgenic mice have helped provide some insight into *physiologically regulated* Tcf/Lef-1 function, *in vivo*. Indeed, canonical Wnt signalling has been implicated in adult mammalian tissue homeostasis, including that of the intestinal crypt (Korinek et al., 1998) and hair follicle (DasGupta and Fuchs, 1999). Following development, follicles proceed through cycles of active hair growth (anagen) and rest (telogen). Part way along each follicle, a compartment known as the 'bulge' is thought to contain a population of adult stem-cells, expressing Tcf-3. Asymmetric stem-cell division gives rise to transit amplifying cells that migrate up the follicle, lose Tcf-3 expression, and adopt the fate of epidermal keratinocytes. However, around the time of transition from telogen to anagen, a proportion of transit amplifying cells migrate down the

follicle, switch from expressing Tcf-3 to Lef-1, and differentiate into matrix cells, a subset of which go on to form the hair shaft. Although the mechanism responsible for switching Tcf-3 to Lef-1 in matrix cells remains unclear, observed induction of LEF-1 gene expression by Bmp-4 during tooth and hair follicle development may be of relevance (Kratochwil et al., 1996).

Studies using transgenic mice harbouring a Tcf/Lef-1 reporter (TOPGAL) suggest that activation of the canonical pathway in adult stem-cells occurs only transiently, around the time of transition from telogen to anagen (DasGupta and Fuchs, 1999). In addition, TOPGAL activity was detected in those matrix cells destined to form the hair shaft. Surprisingly, sequential sections demonstrated TOPGAL-positive cells to be Ki67-negative, and Ki67-positive transit amplifying cells to be TOPGAL-negative, indicating lack of association between Tcf/Lef-1 activation and cell proliferation (DasGupta and Fuchs, 1999). These observations have led to a model of hair cycling in which physiological activation of Tcf-3 regulates asymmetric stem-cell division, promoting generation of transit amplifying cells that adopt the fate of matrix cells, rather than epidermal keratinocytes (DasGupta and Fuchs, 1999). Subsequent Lef-1 activation, induces the expression of hair-specific keratin genes, promoting terminal differentiation of matrix cells and their incorporation into the hair shaft (DasGupta and Fuchs, 1999; Merrill et al., 2001). This model is consistent with observed inhibition of hair cycling and growth in transgenic mice expressing dominant-negative β-catenin (Huelsken et al., 2001), and with frequent hair matrix tumour (pilomatricomas) occurrence in transgenic mice expressing β-cateninΔN (Gat et al., 1998). Interestingly, the latter mice also exhibit extensive squamous metaplasia and keratinisation in various other epithelia, including that of the salivary and mammary glands (Gounari et al., 2002).

In transgenic Tcf-4 knockout mice, death occurs within 24 hours of birth and is associated with a single histological abnormality, i.e. the intestinal epithelium appears damaged, yet consists entirely of differentiated enterocytes with no sign of a rapid-cycling (Ki67-positive) transit amplifying cell population (Korinek et al., 1998). Based on the assumption that slow-cycling adult stem-cells were no longer present, this observation led to the suggestion that physiological Tcf-4 activation plays an

important role in mammalian intestinal crypt homeostasis, possibly helping to *maintain* the adult stem-cell compartment (Korinek et al., 1998). However, given the current lack of a specific marker for adult stem-cells (Booth and Potten, 2000) and the apparent role played by canonical signalling in mammalian hair cycling, an alternative interpretation is that physiological activation of Tcf-4 functions to regulate asymmetric stem-cell division, with abnormal intestinal epithelium resulting from a block in production of transit amplifying cells, as opposed to a loss of the adult stem-cell compartment. The absence of other organ abnormality on histological survey may reflect functional redundancy within the Tcf/Lef-1 family.

In summary, the functional consequence of Tcf/Lef-1 activation is complex and appears dependent on multiple factors, including cell type, pattern of Tcf/Lef-1 expression, canonical Wnt signal strength, and whether activation is regulated or constitutive. Although the importance of epithelial-mesenchymal interactions is well recognised in both intestinal crypt and hair follicle homeostasis, putative canonical Wnts remain to be identified.

1.6.2 Wnt signalling and lung cancer in man

Human lung cancer has traditionally been classified into two main groups based on histology and cell behaviour. Small cell lung cancer (SCLC) carries a poorer prognosis, tending to grow rapidly and metastasize early. Non-small cell lung cancers (NSCLC) comprise a heterogeneous group of histological types, including squamous, adeno, and large cell carcinomas. In contrast to malignant disease of the colon, functional mutations involving APC or β-catenin appear to be relatively rare in lung cancer. In two separate studies, screening a total of 137 lung cancers, no APC mutations were identified (Cooper et al., 1996; Wada et al., 1997). In three additional studies, screening a total of 352 lung cancers (123 SCLC and 229 NSCLC), mutations in β-catenin affecting S45, T41, S37 or S33 were identified in only 5 cases, all of which were NSCLC, with 4 being adenocarcinomas (Shigemitsu et al., 2001; Sunaga et al., 2001; Ueda et al., 2001). However, these findings neither confirm nor exclude the possibility that constitutive activation of the canonical Wnt pathway might play an important role in the pathogenesis of human lung malignancy.

Despite the absence of published data describing the pattern of Tcf/Lef-1 expression in normal adult human and neoplastic airway epithelium, nuclear β-catenin has been used as a surrogate marker of Tcf/Lef-1 activation. Although the majority of immunohistochemical studies have focused on membranous β-catenin expression in NSCLC, reporting inverse relationships with local tumour invasion, regional metastasis and overall prognosis (Bremnes et al., 2002), a few studies have specifically investigated the prevalence of nuclear β-catenin using non-frozen sections. In 229 cases of NSCLC, Pirinen *et al* (Pirinen et al., 2001) observed nuclear β-catenin in 7%, demonstrating a positive correlation with Ki67 expression and negative correlation with membranous β-catenin staining. Hommura *et al* (Hommura et al., 2002) also observed a direct correlation with Ki67 expression, but grouped cytosolic &/or nuclear β-catenin together, stating a combined frequency in excess of 80% in 217 cases of NSCLC. Finally, Nakatani *et al* (Nakatani et al., 2002) investigated a rare subset of NSCLC, termed 'foetal lung' adenocarcinoma (FLAC), characterised by morules (solid, spherical cell clusters) and complex glandular histology reminiscent of developing foetal lung. Nuclear β-catenin was evident in all 11 cases of low-grade FLAC, 2 out of 8 cases (25%) of high-grade FLAC, and 1 out of 24 cases (4%) of conventional primary lung adenocarcinoma (Nakatani et al., 2002). However, better evidence in support of constitutive Tcf/Lef-1 activation comes with use of a reporter construct. From a panel of 15 lung cancer cell lines (SCLC and NSCLC), only A427 adenocarcinoma cells activated a Tcf/Lef-1 reporter to levels comparable with those detected in colorectal cancer cells harbouring a canonical Wnt pathway mutation (Sunaga et al., 2001). Indeed, A427 cells were themselves shown to contain a mutation in β-catenin affecting T41 (Sunaga et al., 2001). Taken together, these data suggest that constitutive activation of the canonical Wnt pathway is an infrequent event in NSCLC pathogenesis.

Tsuji *et al* (Tsuji et al., 2000) cloned and characterised one of several genes frequently down-regulated in both immortalised and tumour-derived cell lines. This gene was initially termed REIC (reduced expression in immortalised cells), but later found to be DKK-3 (Tsuji et al., 2000). Expression of DKK-3 RNA appears to vary during cell cycle progression in normal human foetal (KMS-6) fibroblasts, with

lowest level expression coinciding with transition from G1 to S-phase (Tsuji et al., 2001). Furthermore, ectopic DKK-3 induces growth inhibition in human osteosarcoma (Saos-2) cells without detectable increase in apoptosis (Tsuji et al., 2001). In 57 cases of resected NSCLC, expression of DKK-3 RNA was significantly reduced in 63% when compared with adjacent normal lung tissue (Nozaki et al., 2001). This was particularly notable for squamous cell and poorly differentiated adenocarcinomas, and suggests a role for Dkk-3 both in normal cell cycle control and cell transformation.

Finally, in the process of cloning and characterising several WNT-related genes, northern blot analyses have detected expression of WNT-7B and FZD-1, -2, -4, -5, -6, -7, -8 and -10 in A549 lung adenocarcinoma cells (Kirikoshi et al., 1999; Kirikoshi et al., 2001b; Koike et al., 1999; Sagara et al., 1998; Saitoh et al., 2001a; Saitoh et al., 2001b; Tokuhara et al., 1998). In addition, WNT-2 and -10B RNA has been identified in other lung cancer cell lines (Hardiman et al., 1997; Levay-Young and Navre, 1992). In resected lung, expression of WNT-7A appears reduced in both SCLC and NSCLC when compared with adjacent 'normal' tissue, and this is reflected in lung cancer cell lines when compared with primary 'normal' bronchial epithelial cells from heavy smokers (Calvo et al., 2000). In contrast, amounts of WNT-2 (Katoh, 2001a) and WNT-5A (Iozzo et al., 1995) RNA appear to be increased in lung cancer tissue, though their cellular source has not been identified. However, the functional significance of these genes in the pathogenesis of human lung cancer remains unclear.

1.7 Wnt signalling in adult tissue homeostasis and non-malignant disease

Given the history of *Wnt-1* gene discovery, it is perhaps not surprising that research to date has focused primarily on embryonic development and cancer. However, with physiological Tcf/Lef-1 activation implicated in maintaining &/or regulating adult stem-cells &/or transit amplifying cells, attention has turned to the possible role played by Wnt signalling pathways in adult tissue homeostasis (Beachy et al., 2004). Consistent with this hypothesis, animal models have shown up-regulated WNT gene expression in early response to acute injury, suggesting a replay of embryonic morphogenetic signalling events as part of the process of adult tissue regeneration. In a rat femur fracture model of bone healing, Hadjiargyrou *et al* (Hadjiargyrou et al.,

2002) observed increased expression of WNT-5A and rat FZD, along with known target genes of the canonical pathway. In addition, Surendran *et al* (Surendran et al., 2002) reported up-regulated WNT-4 gene expression from 48 hours following acute renal tubular obstruction and pressure-induced epithelial injury in mice. The collecting duct epithelium was shown to be the initial source of WNT-4 RNA, by *in situ* hybridisation (Surendran et al., 2002). Finally, in surgically incised mouse skin, Labus *et al* (Labus et al., 1998) also observed WNT-4 gene induction from 2 to 30 hours post-wounding, with no detectable WNT-1, -3A or -7B RNA. Since onset of expression preceded inflammatory cell infiltration, resident skin cells were thought to be involved. *In vitro* studies using confluent primary fibroblasts from neonatal mouse skin revealed synergistic WNT-4 gene induction in response to scrape-wounding and fibrin degradation product stimulation (Labus et al., 1998).

Investigating essentially the same *in vivo* model of acute skin wounding and repair in transgenic mice expressing TOPGAL, Cheon *et al* (Cheon et al., 2002) observed transient Tcf/Lef-1 activation, from day 8 to 14, in Ki67-positive dermal fibroblasts at the site of injury. Furthermore, in transgenic mice expressing β-cateninΔN, cutaneous wound healing was associated with excessive fibroblast proliferation and increased collagen deposition, leading to hypertrophic (keloid) scar formation (Cheon et al., 2002). Interestingly, in the mouse model of pressure-induced epithelial injury reported by Surendran *et al* (Surendran et al., 2002), failure to relieve renal tubular obstruction led to induction of WNT-4 gene expression in α-smooth muscle actin-positive fibroblasts, secreting matrix collagen. In this case, peak levels of WNT-4 RNA were detected in fibrotic lesions surrounding collecting ducts between 10 and 14 days post-obstruction. Importantly, these lesions could be reproduced within 3 days of introducing WNT-4 expressing fibroblasts into normal murine kidneys, but not if control fibroblasts were used. Surprisingly, *in vitro* studies found increased steady-state levels of cytosolic β-catenin in fibroblasts stimulated with Wnt-4, suggesting activation of the canonical pathway (Surendran et al., 2002).

Taken together, these data are consistent with a model of repair in which acute tissue injury leads to early induction of WNT gene expression in damaged epithelial and mesenchymal cells. As a consequence, paracrine and autocrine activation of the

canonical pathway in (myo)fibroblasts gives rise to a pro-fibrogenic phenotype that is normally transient. However, if injury is repeated or sustained, persistent WNT(-4) gene expression prolongs autocrine activation of (myo)fibroblasts, leading to their excessive proliferation and increased collagen deposition. In addition, the model suggests potential co-operation between Wnts and TGF-β in this fibroproliferative process through synergistic activation of Tcf/Lef-1 (Labbe et al., 2000; Letamendia et al., 2001; Nishita et al., 2000). Although Cheon *et al* (Cheon et al., 2002) only detected canonical pathway activation in dermal fibroblasts, transient activation in other cell types may have been missed between days 2 and 8 post-injury. Furthermore, the model employed was of acute injury and repair, and was therefore not designed to investigate Tcf/Lef-1 activation in the context of chronic repair and tissue remodelling.

A few studies have sought evidence for canonical Wnt pathway activation in non-malignant adult human tissues. Eberhart *et al* (Eberhart and Argani, 2001) conducted a near-full body survey of a 44 year-old male who had died with pneumonia. Nuclear β-catenin was observed in neurones and astrocytes of the brain, glomerulosa cells of the adrenal gland, and epithelial cells of the renal tubules and pancreatic acini. In addition, positive staining was evident in endothelial cells of capillaries, in keeping with the postulated role of canonical Wnt signalling in angiogenesis (Wright et al., 1999). Importantly, transient nuclear localisation of β-catenin has been observed in human colorectal epithelial cells during the regenerative phase following radiation-induced injury (Hardy et al., 2002) and human endometrial cells during the mid/late-proliferative and early secretory phases of the menstrual cycle (Nei et al., 1999), strongly suggesting a role in epithelial regeneration.

1.7.1 Wnt signalling and non-malignant disease in man

If Wnt signalling is involved in adult tissue homeostasis, then abnormal loss of Wnt signal strength might play a role in the development of human diseases associated with increased apoptosis (Thompson, 1995). Indeed, attenuated canonical signalling has been implicated in degenerative conditions such as Alzheimer's disease (Mudher and Lovestone, 2002), retinitis pigmentosa (Jones et al., 2000a; Jones et al., 2000b)

and heart failure (Schumann et al., 2000). Historically, members of the SFRP family were termed secreted apoptosis-related proteins (SARP), because they appear to modulate the apoptotic susceptibility of cells through regulation of the canonical pathway (Melkonyan et al., 1997). In retinitis pigmentosa (RP), characterised by progressive loss of photoreceptors, Jones *et al* (Jones et al., 2000a; Jones et al., 2000b) observed up-regulated expression of SFRP-1, -2, -3 (FRZB) and -5 RNA in RP retinas compared with controls. Similarly, in failing hearts associated with cardiomyocyte apoptosis, Schumann *et al* (Schumann et al., 2000) reported higher levels of SFRP-3 and -4 gene expression when compared with controls. *In situ* hybridisation demonstrated that cardiomyocytes were themselves the source of SFRP-3 and -4, and lower levels of Triton X-100 soluble β-catenin tended to be found in failing heart tissue (Schumann et al., 2000).

There is also evidence to suggest that altered Wnt signalling might contribute to a pro-inflammatory phenotype in mesenchymal cells. In association with high levels of interleukin-6 (IL-6), -8 and -15 RNA, Sen *et al* (Sen et al., 2000) observed up-regulated WNT-5A and FZD-5 gene expression in activated fibroblast-like synoviocytes (FLS) from patients with rheumatoid arthritis. In addition, ectopic WNT-5A induced similar activation of normal FLS (Sen et al., 2000). Furthermore, inhibition of Wnt-5a/Fzd-5 signalling using either antisense WNT-5A, a dominant-negative WNT-5A construct or a Fzd-5 blocking antibody, diminished expression of pro-inflammatory cytokines in activated FLS (Sen et al., 2001). Whether Wnt-5a/Fzd-5 interactions activate the canonical or non-canonical pathway in this cell type remains unclear. However, Wnt-1 stimulation of rat pheochromocytoma (PC12) cells has been shown to induce activation of the pro-inflammatory transcription factor, NF-κB, through inhibition of GSK-3β (Bournat et al., 2000).

1.8 Wnt signalling in adult human lung

Based on a review of the literature, Table 1.5 summarises what is currently known about WNT, FZD, LRP, DVL, FRAT, GSK-3β, APC, TCF/LEF-1, SFRP and DKK gene expression in adult human lung. Despite reported expression of several WNT and all but one FZD genes in normal tissue samples, surprisingly little is known about

their cellular localisation or functional roles. Similarly, very few studies have sought evidence for canonical Wnt pathway activation in non-malignant adult human lung tissue. The majority of reports on β-catenin staining in non-frozen sections have been done in the context of lung cancer research. Of these, only a minority have specifically commented on the pattern of β-catenin expression in 'normal' portions of surgically resected lung. For example, Pirinen *et al* (Pirinen et al., 2001), Hommura *et al* (Hommura et al., 2002) and Carayol *et al* (Carayol et al., 2002b) all report a basolateral membranous pattern of staining for β-catenin in columnar cells with no sign of nuclear localisation in non-malignant regions of airway epithelium. The 1998 abstract by Bullock *et al* (Bullock et al., 1998) represents the only report of β-catenin staining in non-frozen sections of non-malignant diseased lung. In this study, endobronchial biopsies and resected lung specimens from subjects and patients with asthma, chronic obstructive pulmonary disease (COPD), pulmonary fibrosis and sarcoidosis were investigated. Although areas of bronchial and alveolar epithelial damage were associated with increased expression of α-, β- and γ-catenin, and E-cadherin in all subject/patient groups, the abstract provides no indication of whether nuclear β-catenin was present or not (Bullock et al., 1998). However, Nakatani *et al* (Nakatani et al., 2002) observed nuclear β-catenin in reactive type II pneumocytes in the vicinity of tumour growth. Furthermore, in the near-full body survey of a 44 year-old male who had died with pneumonia, Eberhart *et al* (Eberhart and Argani, 2001) also identified nuclear β-catenin in 20-49% of reactive pneumocytes, in addition to occasional chondrocytes of bronchial cartilage. These *in vivo* data suggest a role for canonical Wnt pathway activation in the regulation of type II pneumocytes responding to alveolar injury.

	Detected?	**Technique**	**Cell source**	**References**
WNT-1	ND	-	-	-
WNT-2	yes	NB	tissue	[112][278]
WNT-2B	yes	NB	tissue	[114]
WNT-3	no	NB	tissue	[113]
WNT-3A	yes	NB	tissue	[222]
WNT-4	ND	-	-	-
WNT-5A	yes	NB	tissue	[105]
WNT-5B	no	NB	tissue	[220]
WNT-6	no	NB	tissue	[120]

	Detected?	Technique	Cell source	References
WNT-7A	yes	PCR	tissue, epithelial cells	[23]
WNT-7B	yes	NB	tissue	[118]
WNT-8A	no	NB	tissue	[221]
WNT-8B	no	NB	tissue	[225]
WNT-10A	no	NB	tissue	[120]
WNT-10B	yes	NB, AGC	tissue, fibroblasts + IL-13	[83][135]
WNT-11	no	NB	tissue	[117]
WNT-14	yes	NB	tissue	[222]
WNT-15	no	NB	tissue	[119]
WNT-16	yes	PCR	tissue	[68]
FZD-1	yes	NB, PCR	tissue	[219][227]
FZD-2	yes	NB, PCR	tissue	[303]
FZD-3	yes	PCR	tissue	[227]
FZD-4	yes	NB, PCR	tissue	[116][227]
FZD-5	yes	NB	tissue	[220]
FZD-6	yes	NB, PCR	tissue	[227][265]
FZD-7	yes	PCR	tissue	[227]
FZD-8	yes	NB	tissue	[221]
FZD-9	no	NB, PCR	tissue	[227][279]
FZD-10	yes	NB, PCR	tissue	[121][227]
LRP-5	yes	NB	tissue	[54][89]
LRP-6	yes	NB	tissue	[19]
DVL-1	yes	NB	tissue	[206]
DVL-2	ND	-	-	-
DVL-3	yes	NB	tissue	[206]
FRAT-1	yes	DB	tissue	[71]
FRAT-2	yes	DB	tissue	[71]
GSK-3β	yes	PCR, WB	tissue	[134]
APC	yes	PCR, IHC	tissue, bronchial epithelium	[162][274]
TCF-1	ND	-	-	-
LEF-1	ND	-	-	-
TCF-3	yes	IHC	not specified	[4]
TCF-4	no	IHC	-	[4]
	yes	IF, IP	small airway epithelial cells	[24]
SFRP-1	no	NB	tissue	[70][159]
	yes	mRNA	tissue (emphysematous lung)	[102]
SFRP-2	no	NB	tissue	[159]
FRZB	ND	-	-	-
SFRP-4	ND	-	-	-
SFRP-5	no	NB	tissue	[159]
DKK-1	no	NB	tissue	[125]
DKK-2	yes	NB	tissue	[125]
DKK-3	yes	NB	tissue	[125][267]
DKK-4	yes	PCR	tissue	[125]

Table 1.5: WNT-related gene expression in adult human lung.

ND (not done or reported); NB (northern blot); DB (mRNA dot blot); AGC (Affymetrix GeneChip array); PCR (polymerase chain reaction); ISH (*in situ* hybridisation); WB (western blot); IP (immunoprecipitation); IF (immunofluorescent microscopy); IHC (immunohistochemistry); FZD (frizzled); LRP (low-density lipoprotein receptor-related protein); DVL (dishevelled); FRAT (frequently rearranged in advanced T-cell lymphomas); SFRP (secreted frizzled-related protein); DKK (Dickkopf protein).

Using commercially available normal human primary small airway epithelial cells (SAEC), Carayol *et al* (Carayol et al., 2002a) observed down-regulated expression of both E-cadherin and β-catenin following 48 hours stimulation with 50ng/ml TNF-α, *in vitro*. This was associated with a redistribution of β-catenin from the cell membrane to the cytosol. However, following 24 hours stimulation with TNF-α, addition of 10^{-7}M dexamethasone induced transient nuclear localisation of β-catenin at 6 hours, with reversal of the effects of TNF-α and return to membranous staining by 24 hours (48 hours from the onset of the experiment). The same response was also observed in cultured human bronchial epithelial (HBE) cells from 'normal' portions of surgically resected lung (Carayol et al., 2002a). Subsequent studies in SAEC appear to show dexamethasone-induced nuclear translocation of Tcf-4 and increased β-catenin/Tcf-4 complex formation, associated with a 3 to 5-fold increase in cell proliferation and 50% reduction in apoptosis (Carayol et al., 2002b). Interestingly, an immunohistochemical survey of normal adult human tissues by Barker *et al* (Barker et al., 1999) failed to detect Tcf-4 protein expression in 'lung' but did appear to detect Tcf-3, although cell types involved were not stated. With the exception of screening lung cancer cell lines for evidence of constitutive canonical pathway activation (Sunaga et al., 2001), no studies have employed a Tcf/Lef-1 reporter to investigate the ability of cells from adult human lung to transduce a canonical Wnt signal.

1.8.1 Wnt signalling and non-malignant lung disease

To date, only three research groups from around the world have published data with a clear interest in Wnt signalling pathways and non-malignant human lung disease. In all cases, the focus has been on chronic airways disease, including bronchial asthma, emphysema, chronic bronchitis and cystic fibrosis. Work by Carayol *et al* (Carayol et al., 2002b; Carayol et al., 2002a) has already been mentioned. They have investigated the *in vitro* response of normal SAEC (and HBE cells) to pro-inflammatory TNF-α and anti-inflammatory dexamethasone, and appear to be suggesting a model in which corticosteroid therapy promotes airway epithelial restitution in asthma through activation of the β-catenin signalling pathway. However, based on current evidence, the relationship between dexamethasone-induced cell proliferation/survival and β-catenin/Tcf-4 complex formation remains an *association* of unclear significance.

Furthermore, the hypothesis that *canonical Wnt signalling plays a role in regeneration of the adult human airway epithelium* has yet to be directly tested.

The second research group has also already been mentioned. Duan and Engelhardt are interested in the role of Lef-1 in submucosal gland (SMG) morphogenesis, especially since SMG hypertrophy and hyperplasia are important features of airway wall remodelling in chronic hypersecretory lung diseases, such as asthma, chronic bronchitis and cystic fibrosis (Duan et al., 1998). In normal human lung, SMGs are confined to cartilaginous airways (trachea and bronchi) at approximately 3 glands per mm^2 (Engelhardt et al., 1995). SMG hyperplasia, with associated extension into chronically diseased bronchiolar airways, suggests retention of SMG progenitor cells into adult life. Consistent with this hypothesis, Engelhardt *et al* (Engelhardt et al., 1995) observed SMG formation by adult human bronchial epithelial cells reconstituted into a xenograft model of the airway wall. However, the pattern of Tcf/Lef-1 expression in adult human lung remains undetermined, and evidence in support of canonical Wnt pathway activation in SMG morphogenesis is currently lacking.

The third group have published abstracts implicating altered Wnt signalling in the pathogenesis of emphysema. Imai and D'Armiento identified SFRP-1 as a gene up-regulated in surgically resected emphysematous lung, but not detected in 'normal' control tissue (Imai and D'Armiento, 2000). SFRP-1 RNA could also be induced in mouse lung exposed to cigarette smoke (Imai and D'Armiento, 2002). Consistent with the observed correlation between emphysema severity and the apoptotic index of resected lung tissue, ectopic SFRP-1 increased oxidant (H_2O_2) stress-induced apoptosis in SAEC, pulmonary vascular endothelial cells and normal human lung fibroblasts (NHLF), *in vitro* (Imai and D'Armiento, 2002; Mercer et al., 2002). This was associated with a reduction in cellular levels of β-catenin, but had no apparent effect on rates of cell proliferation (Mercer et al., 2002). In addition, ectopic SFRP-1 induced up-regulated expression of matrix metalloproteinase-1 (MMP-1) in NHLF and MMP-2 in both NHLF and SAEC (Mercer et al., 2002). Like SFRP-1, MMP-1 is also up-regulated in emphysematous lung and not detected in control tissue (Imai et al., 2001). Furthermore, transgenic mice expressing MMP-1 develop emphysema

(D'Armiento et al., 1992). This group would appear to be suggesting a model for emphysema in which induction of SFRP-1 gene expression by cigarette smoke exposure in genetically susceptible individuals interferes with canonical Wnt signalling, leading to increased MMP release and oxidant-induced apoptosis in resident cells of the distal airway.

1.9 Summary

Bronchial epithelial repair plays an important role in the pathogenesis of chronic inflammatory disorders of the airways, such as asthma and chronic bronchitis. Therefore, investigating the processes that regulate epithelial repair could provide new insights into these conditions. Wnts are a highly conserved family of short-range signalling proteins that play a fundamental role in cell fate determination and tissue patterning during embryonic development. Through β-catenin-mediated activation of Tcf/Lef-1 transcription factors, the canonical pathway targets genes involved in cell proliferation, survival, differentiation and migration, and cross-talks with signals downstream of growth factors and cell adhesion mechanisms. In mammalian foetal lung, reciprocal paracrine signalling within the epithelial-mesenchymal trophic unit orchestrates branching morphogenesis and submucosal gland development, and Wnts are thought to play key roles in both these processes. In addition, Wnts have been implicated in adult tissue homeostasis, possibly helping to maintain &/or regulate adult stem-cell &/or transit amplifying cell populations. In this respect, reactivation of Wnt signalling pathways during adult tissue regeneration may represent a replay of embryonic morphogenetic signalling events. Furthermore, dysregulated canonical signalling has been suggested in the pathogenesis of several cancers and non-malignant human diseases, the latter associated with increased apoptosis, chronic inflammation and tissue remodelling. However, despite reports that many WNT-related genes are expressed in adult human lung tissue, very little is known about which cells are involved and their functional significance remains undetermined.

1.9.1 Hypothesis

Given the above, it is postulated that ***reactivation of the canonical Wnt signalling pathway plays a role in human bronchial epithelial regeneration following injury***, and that ***altered canonical signalling contributes to the pathogenesis of chronic airways disease***. Based on this, the following sub-hypotheses were tested:

1. ***Adult human bronchial epithelial (HBE) cells express key components of the Wnt/β-catenin signalling pathway*** (chapter 3 and 5).

2. ***HBE cells are capable of transducing a canonical Wnt signal*** (chapters 4 and 5).

3. ***Regulation of the Wnt/β-catenin signalling pathway plays a role in bronchial epithelial repair*** (chapters 6 and 7).

CHAPTER 2

MATERIALS and METHODS

2.1 Materials

2.1.1 Cell cultures

H292 human pulmonary mucoepidermoid carcinoma cells, L Wnt-3a cells and parental L-cells (murine fibroblasts) were supplied by the American Type Culture Collection (ATCC). SW480 human colorectal adenocarcinoma cells were kindly provided by Dr. RM Kypta (University College London). RPMI 1640 medium, Hanks Balanced Salt Solution (HBSS), Dulbecco's modified Eagle's medium (DMEM), LHC-9 medium, foetal bovine serum (FBS), L-glutamine, penicillin, streptomycin, collagen, 10x Trypsin-EDTA and plasticware were supplied by Invitrogen, Paisley, UK. 24-well Costar transwell plates were supplied by Corning Costar, High Wycombe, UK. UltraCULTURE medium was supplied by BioWhittaker, Wokingham, UK. Bronchial Epithelium Basal Medium (BEBM) and SingleQuot supplements required to make Bronchial Epithelium Growth Medium (BEGM) were supplied by Clonetics, San Diego, CA, USA. ITS (insulin, transferrin and sodium selenite) supplement, bovine serum albumin (BSA), retinoic acid, dimethyl sulphoxide (DMSO), lithium chloride (LiCl), calcium chloride ($CaCl_2$), magnesium sulphate (Mg_2SO_4), Trypan Blue and a Haemacytometer were supplied by Sigma-Aldrich, Poole, UK. G418 antibiotic was supplied by BD Biosciences, Oxford, UK. 0.22μm Millex-GV filters were supplied by Millipore, Watford, UK. Recombinant human epidermal growth factor (EGF) was supplied by PeproTech, London, UK. Tyrphostin (AG1478) was supplied by Biomol, Hamburg, Germany.

x2 ALI (air-liquid interface) medium comprised BEBM supplemented with 3μg/ml bovine serum albumin (BSA) and BEGM SingleQuots of 8μl/ml bovine pituitary extract (BPE), and 2μl/ml each of insulin, hydrocortisone, transferrin, tri-iodothyronine, epinephrine and human epidermal growth factor (EGF); x2 ALI

medium was stored at +4°C for up to 7 days. When ready for use, x1 ALI medium was made by mixing x2 ALI medium with an equivalent volume of DMEM containing 2µl/ml of $5x10^{-5}$M retinoic acid in DMSO; retinoic acid was added to DMEM when ready to use, and precautions were taken to avoid exposing it to light.

2.1.2 RNA extraction

TRIzol Reagent was supplied by Invitrogen, Paisley, UK. Chloroform, isopropyl alcohol (isopropanol) and ethanol were supplied by Sigma-Aldrich, Poole, UK. DNase1, 10x DNase buffer and DNase Inactivator were supplied by Ambion, Huntingdon, UK. Quartz capillaries were supplied by Amersham Biosciences, Little Chalfont, UK. A GeneQuant spectrophotometer was supplied by Biochrom, Cambridge, UK.

2.1.3 Agarose gel electrophoresis

HighStrength Analytical Grade agarose, a Sub-Cell GT electrophoresis tank, Power Pac 300 transformer, gel plates and combs were supplied by Bio-Rad, Hemel Hempstead, UK. Ethidium bromide, 1x Tris-borate EDTA (TBE) and RNaseZAP were supplied by Sigma-Aldrich, Poole, UK. Vistra green and DNA molecular weight markers were supplied by Amersham Biosciences, Little Chalfont, UK. Gene Genius Bio Imaging System and GeneSnap software were supplied by Syngene, Cambridge, UK. A FluorImager 595 was supplied by Molecular Dynamics, Sunnyvale, CA, USA.

2.1.4 RNase protection assays (RPA)

The RiboQuant Human Frizzled (hFZD) Multi-Probe Template Set and Human Control RNA-2 were supplied by BD Biosciences, Oxford, UK. MAXIscript T7 and RPA III Ribonuclease Protection Assay kits were supplied by Ambion, Huntingdon, UK. [α^{32}P] UTP was supplied by Amersham Biosciences, Little Chalfont, UK. Ethylenediaminetetraacetic acid (EDTA), phenol, chloroform, isoamylalcohol (IAA), ammonium acetate (NH_4OAc), ethanol, 10x Tris-borate EDTA (TBE), urea, ammonium persulphate (AMPS) and N,N,N',N'-tetramethylethylenediamine

(TEMED) were supplied by Sigma-Aldrich, Poole, UK. Pellet paint was supplied by Merck Biosciences, Nottingham, UK. A TopCount-NXT Microplate Scintillation Counter was supplied by Packard Bioscience Company, USA. Polyacrylamide gel mould plates (Sequi-Gen GT Sequencing Cell) and a gel dryer (model 583) were supplied by Bio-Rad, Hemel Hempstead, UK. Repelcote VS was supplied by BDH, Poole, UK. Accugel 19:1 was supplied by National Diagnostics, Hull, UK. A Phosphor Screen and cassette, a Storm 860 PhosphorImager and FragmeNT Analysis software were supplied by Molecular Dynamics, Sunnyvale, CA, USA

2.1.5 Reverse transcription-polymerase chain reaction (RT-PCR)

PrimerSelect (Lasergene5) software was supplied by DNASTAR, Madison, WI, USA. Random hexamers, and forward (sense) and reverse (anti-sense) primers were supplied by MWG-Biotech, Milton Keynes, UK. JumpStart Taq DNA Polymerase, 10x PCR buffer II, magnesium chloride ($MgCl_2$), Tris-HCl and EDTA were suppled by Sigma-Aldrich, Poole, UK. 1x TE Buffer comprised 10mM Tris-HCl (pH 8.0), and 1mM EDTA. Deoxynucleoside triphosphates (dNTP) were supplied by Invitrogen, Paisley, UK. Moloney murine leukaemia virus Reverse Transcriptase (M-MLV RT), 5x RT buffer and primers for the β-actin gene were supplied by Promega, Southampton, UK. A PTC-225 Peltier Thermal Cycler was supplied by Bio-Rad, Hemel Hempstead, UK.

2.1.6 DNA sequencing

MinElute PCR Purification Kits and DyeEx Spin Columns were supplied by Qiagen, Crawley, UK. Ethanol was supplied by Sigma-Aldrich, Poole, UK. Forward (sense) and reverse (anti-sense) primers were supplied by MWG-Biotech, Milton Keynes, UK. ABI Prism BigDye Terminator Cycle Sequencing Ready Reaction Kits v3.0, a GeneAmp PCR System 9700 and an ABI Prism 377 DNA Analyzer were supplied by Applied Biosystems, Brackley, UK. Chromas v1.45 software (Conor McCarthy, Griffith University, Queensland, Australia) was available on-line as freeware. MegAlign (Lasergene5) software was supplied by DNASTAR, Madison, WI, USA.

2.1.7 Quantitative real-time RT-PCR (qPCR; TaqMan)

Primer Express software was supplied by Applied Biosystems, Warrington, UK. Forward (sense) and reverse (anti-sense) primers and FAM probes were supplied by MWG-Biotech, Milton Keynes, UK. Primers and FAM probe for 18S rRNA, and 2x PCR master mix were supplied by Eurogentec, Seraing, Belgium. SYBR Green dye was supplied by Invitrogen, Paisley, UK. 96-well thermal cycling plates, optically clear seals, fluorescein calibration dye, an iCycler iQ machine and iCycler iQ Optical system software version 3.0a were supplied by Bio-Rad, Hemel Hempstead, UK.

2.1.8 Western blot analysis

Tris, Tris-HCl, sodium dodecylsulphate (SDS), methanol, acrylamide, bis-acrylamide, ammonium persulphate (AMPS), 5µl N,N,N',N'-tetramethylethylenediamine (TEMED), propanol, glycine, hydrochloric acid (HCl), glycerol, 2-mercaptoethanol, bromophenol blue, Tween 20, phosphate-buffered saline (PBS) and mouse IgG_{2a} isotype control antibody (M-9144) were suppled by Sigma-Aldrich, Poole, UK. Complete Mini Protease Inhibitor Cocktail tablets were supplied by Boehringer Mannheim, Mannheim, Germany. A Mini-PROTEAN 3 electrophoresis module, Mini Trans-Blot electrophorectic transfer module and Bio-Rad Power Pack 300 were supplied by Bio-Rad, Hemel Hempstead, UK. Full Range Rainbow recombinant protein molecular weight markers, Hybond C nitrocellulose membranes and the enhanced chemiluminescence (ECL Plus) detection system were supplied by Amersham Biosciences, Little Chalfont, UK. Tcf-4 antibody (clone 6H5-3; IgG_{2a}) was supplied by Upstate Biotechnology, Lake Placid, NY, USA. Horseradish peroxidase (HRP) conjugated rabbit anti-mouse IgG (P0260) was supplied by DakoCytomation, Ely, UK. A GeneGnome chemiluminescence imaging system and GeneSnap software were supplied by Syngene, Cambridge, UK.

1x Denaturing Sample Lysis Buffer (DSLB) comprised 10mM Tris-HCl (pH 7.4), and 1% w/v SDS; 40µl/ml Complete Mini Protease Inhibitor Cocktail solution was added prior to the application of DSLB. 7.5% separation gel stock solution comprised 22.5ml 30% w/v acrylamide/bis-acrylamide 50:1, 22.5ml 1.5M Tris-HCl (pH 8.8),

44.6ml distilled H_2O and 0.45ml 20% w/v SDS. Stacking gel stock solution comprised 12.5ml 30% w/v acrylamide/bis-acrylamide 50:1, 25ml 0.5M Tris-HCl (pH6.8), 62ml distilled H_2O and 0.5ml 20% w/v SDS. Running Buffer comprised 0.025M Tris, 0.192M glycine, 0.1% w/v SDS, pH 8.3 with HCl. 5x Loading Buffer (LB) comprised 0.3125M Tris-HCl (pH 6.8), 50% v/v glycerol, 25% v/v 2-mercaptoethanol, 10% w/v SDS and 0.01% v/v bromophenol blue. Transfer Buffer comprised 25mM Tris, 192mM glycine and 20% v/v methanol, pH 8.0-8.3. Wash Buffer comprised 0.5% v/v Tween 20 in PBS, pH 7.4. Blocking Buffer comprised 5% w/v milk powder in Wash Buffer, filtered through Whatman N° 1 filter paper before addition of 40µl/ml Complete Mini Protease Inhibitor Cocktail solution.

2.1.9 TCF/Lef-1 reporter (TOPflash) assays

TOPflash and FOPflash reporter constructs were supplied by Upstate Biotechnology, Lake Placid, NY, USA. The pRL-TK plasmid, Dual-Luciferase Reporter (DLR) Assay System and disposable polypropylene luminometer tubes were supplied by Promega, Southampton, UK. The pEGFP-C1 plasmid was supplied by BD Biosciences, Oxford, UK. Epicurian Coli SURE (Stop Unwanted Rearrangement Events) 2 Supercompetent Cells were supplied by Stratagene, La Jolla, CA, USA. LB (Luria Bertani) Agar, LB Broth, ampicillin and ethanol were supplied by Sigma-Aldrich, Poole, UK. EndoFree Plasmid Maxi Kits and Effectene Transfection Reagent Kits were supplied by Qiagen, Crawley, UK. Quartz capillaries were supplied by Amersham Biosciences, Little Chalfont, UK. A GeneQuant spectrophotometer was supplied by Biochrom, Cambridge, UK. BamHI restriction endonuclease and 10X Buffer B were supplied by Boehringer Mannheim, Germany.

2.1.10 Glycolmethacrylate (GMA) processing

Acetone, methyl benzoate, poly-L-lysine (PLL) and glass microscope slides were supplied by Merck Biosciences, Nottingham, UK. Phenylmethyl-sulfonyl fluoride (PMSF), idioacetamide and ammonia were supplied by Sigma-Aldrich, Poole, UK. GMA solution A, GMA solution B and benzoyl peroxide were supplied by Park

Scientific, Northampton, UK. A Jung Supercut 2065 ultramicrotome was supplied by Leica Microsystems, Milton Keynes, UK.

2.1.11 Immunostaining

(Pan-)β-catenin antibody (PBC; clone 15; IgG_1) was supplied by BD Biosciences, Oxford, UK. Hypophosphorylated ('active') β-catenin antibody (ABC; clone 8E7; $IgG_{1\kappa}$) was supplied by Upstate Biotechnology, Lake Placid, NY, USA. E-cadherin antibody (clone HECD-1; IgG_1) was supplied by R&D Systems, Abingdon, UK. Ki67 antibody (clone MIB-1; IgG_1), Fluorescein Isothiocyanate (FITC) conjugated rabbit anti-mouse IgG (F0261), and biotinylated rabbit anti-mouse IgG F(ab)2 (E0413) were supplied by DakoCytomation, Ely, UK. Mouse IgG_1 isotype control antibody (M-9269), paraformaldehyde, phosphate-buffered saline (PBS), ammonium chloride (NH_4Cl), Triton X-100, bovine serum albumin (BSA), 7-aminoactinomycin D (7-AAD), sodium azide and hydrogen peroxide were supplied by Sigma-Aldrich, Poole, UK. 8-well Nunc Lab-Tek II glass chamber slides, foetal bovine serum (FBS) and Dulbecco's Modified Eagle Medium (DMEM) were supplied by Invitrogen, Paisley, UK. Acetone, sodium chloride, Tris and hydrochloric acid (HCl) was supplied by Merck Biosciences, Nottingham, UK. Mowiol was supplied by Harlow Chemical, Harlow, UK. Citifluor was supplied by Citifluor, London, UK. Liquid DAB (3,3'-diaminobenzidine) Substrate Packs and Mayer's haematoxylin were supplied by BioGenex, Wokingham, UK. Crystal Mount was supplied by Biomedia, Foster City, CA, USA. Dibutyl phthalate containing xylene (DPX) was supplied by BDH, Poole, UK. An Axioskop 2 microscope, AxioCam digital camera and KS400 software were supplied by Carl Zeiss, Welwyn Garden City, UK. A confocal laser scanning microscope (Model CLSM SP2) was supplied by Leica Microsystems, Milton Keynes, UK.

Tris-buffered saline (TBS) comprised 80g sodium chloride, 6.05g Tris, 38ml 1M HCl and distilled water to a total volume of 10 litres, pH 7.6. Tris-HCl comprised 12ml 0.2M Tris, 19ml 0.1M HCl and 19ml distilled water, pH 7.6. Blocking Medium comprised 10% v/v FBS and 1% w/v BSA in DMEM.

2.2 Ethical approval and subject consent

All studies using samples obtained from human volunteers conformed to the Declaration of Helsinki, and were approved by the Southampton Joint University and Hospitals Ethics Committee. Written informed consent was obtained from each subject.

2.3 Phenotyping volunteer subjects

Adult volunteer subjects, aged 18-56 years, were phenotyped according to their medical history, skin prick tests to common aeroallergens, and histamine bronchial provocation test. Subjects were then categorised into one of the following groups:

- Normal, non-atopic, life-long non-smoker.
- Mild persistent atopic asthma (ventolin-only); non-smoker.
- Moderate persistent atopic asthma (on inhaled corticosteroid); non-smoker.
- Current smokers with chronic bronchitis; non-atopic ± fixed airflow obstruction.

Categorisation of established asthma into mild and moderate persistent disease was based on definitions outlined by the combined WHO/NHLBI working group of 1995. The diagnosis of chronic bronchitis was based on the MRC definition of smoking-related cough productive of sputum on most days of three or more consecutive months in each of two or more consecutive years. All patients were examined and had no significant co-morbid conditions.

2.3.1 Skin prick testing

The atopic status of each subject was based on the result of skin prick testing to common aeroallergens. These included house dust mite (*Dermatophagoides pteronyssinus* and *D. farinae*), cat and dog hair, feathers, grass and tree pollens, and fungal allergens (*Aspergillus fumigatus* and *Candida albicans*) (ALK-Abelló, Hungerford, UK). Allergen was introduced into the epidermis over the flexor surface of the forearm using sterile microlancets. Histamine was used as a positive control

and sterile saline as a negative control. After 15 minutes, the size of each wheal was measured in 2-dimensions. Wheals greater than 2 x 2 mm were considered positive, provided the negative control remained negative. Subjects were classified as atopic if they reacted positively to one or more allergens, and were asked to refrain from taking antihistamines to prevent a false-negative result.

2.3.2 Histamine bronchial provocation test

Bronchial responsiveness refers to a change in airway calibre in response to a variety of non-specific physical or chemical stimuli. An exaggerated bronchoconstrictor response is termed bronchial hyperresponsiveness (BHR). The histamine bronchial provocation test is widely used to provide a measure of bronchial responsiveness, expressed as the concentration of histamine required to produce a 20% fall in FEV_1 (forced expiratory volume in 1 second), termed the PC_{20}. The threshold used to define BHR is arbitrary, but non-cumulative values of 8mg/ml or less are generally employed. When defined this way using histamine, BHR is said to have 97% sensitivity and 71% specificity for physician-diagnosed asthma (Cockcroft et al., 1977). Absence of BHR therefore questions the diagnosis of asthma, and 'asthmatic' subjects without BHR were excluded. Similarly, non-asthmatic subjects with BHR were also excluded. Prior to measurement of histamine PC_{20}, subjects were asked to avoid use of their short- and long-acting bronchodilators for at least 6 and 12 hours, respectively. FEV_1 was measured using a dry wedge spirometer (Vitalograph, Buckingham, UK). Subjects with baseline FEV_1 less than 70% predicted had their challenge deferred. The nebuliser (Medicaid, Pagham, UK) was driven by 8L/min compressed air, producing particles of less than 5μm diameter at a delivery rate of 0.25-0.50ml/min. Using a nose clip, the subject was initially asked to forcibly inhale 5 breaths of nebulised 0.9% sodium chloride (normal saline), each from functional residual capacity (FRC) to total lung capacity (TLC). Measurements of FEV_1 were then made at 1 and 3 minutes, and the challenge aborted if FEV_1 fell by more than 10% with saline. Otherwise, the procedure was repeated using nebulised histamine, starting at 0.03mg/ml with doubling concentrations until either a fall in FEV_1 of $\geq$ 20% from the post-saline measurement occured or 16mg/ml histamine was reached.

Subjects remained under observation until FEV_1 had recovered to baseline levels, usually requiring two puffs of salbutamol from a metered-dose inhaler (MDI).

2.4 Fibreoptic bronchoscopy and collection of samples

Research fibreoptic bronchoscopy was undertaken in accordance with departmental guidelines. Subjects were free of respiratory tract infection for at least four weeks, and had to be nil by mouth for at least four hours before starting the procedure. All subjects had their FEV_1 measured both pre- and post-nebulised salbutamol 2.5mg plus ipratropium bromide 500μg. The post-nebulised FEV_1 had to be greater than 60% predicted for the subjects age, height and sex before bronchoscopy could commence. Intravenous access was established and atropine 600μg iv administered. Supplemental oxygen was routinely delivered via nasal cannulae, and pulse oximetry (Pulsox-7; Minolta, Tokyo, Japan) monitored throughout the procedure. The bronchoscopist was assisted by a nurse. In addition, a second nurse and doctor were present to act as advocates for the subject. Midazolam 1-5mg iv was offered to relax the subject if necessary. The oropharynx and larynx were anaesthetised with 10% xylocaine spray plus 4% topical lignocaine before the fibreoptic bronchoscope (XT20; Olympus, Tokyo, Japan) was passed between the vocal cords into the trachea. 1% topical lignocaine was then used to anaesthetise the lower airway of one lung before samples were taken. The maximum total dose of topical anaesthetic allowed was 300mg. Up to six endobronchial biopsies were obtained from sub-segmental carinae using alligator forceps, and primary human bronchial epithelial (HBE) cells were collected using a sheathed nylon cytology brush in up to four sub-segmental bronchi. Biopsies were immediately fixed in ice-cooled acetone (Merck Biosciences, Nottingham, UK) for glycolmethacrylate (GMA) processing. Cells brushed from the central airways were initially collected in sterile phosphate-buffered saline (PBS; Invitrogen, Paisley, UK). Following completion of the bronchoscopy, an equal volume of RPMI 1640 medium (Invitrogen) supplemented with 20% foetal bovine serum (FBS; Invitrogen) was added to the primary cell suspension before centrifuging the sample at 150xg for 5 minutes prior to establishing HBE cell cultures. Subjects remained under observation for at least 3 hours post-procedure. Measurements of FEV_1 and vital signs were documented, along with the return of safe swallowing.

Following review made by the bronchoscopist, the subject was allowed to leave the department with contact telephone numbers and advice. A final check by phone was made the following morning.

2.5 Epithelial cell cultures

Unless otherwise stated, serum-free Bronchial Epithelium Growth Medium (BEGM; Clonetics, San Diego, CA, USA) comprised Bronchial Epithelium Basal Medium (BEBM) supplemented with 52μg/ml bovine pituitary extract (BPE), 5μg/ml insulin, 10μg/ml transferrin, 0.1ng/ml retinoic acid, 0.5ng/ml human epidermal growth factor (EGF), 0.5μg/ml epinephrine, 0.5μg/ml hydrocortisone, 6.5ng/ml tri-iodothyronine, 1μg/ml gentamicin sulphate and amphotericin B (GA-100). Growth factor-free BEBM was supplemented with 1% v/v ITS (10μg/ml insulin, 5.5μg/ml transferrin and 5μg/ml sodium selenite; Sigma-Aldrich, Poole, UK) and 1% v/v bovine serum albumin (BSA; Sigma-Aldrich). Standard RPMI 1640 medium (Invitrogen, Paisley, UK) was supplemented with 10% heat-inactivated foetal bovine serum (FBS; Invitrogen) and 2mM L-glutamine (Invitrogen). Serum-free UltraCULTURE medium (BioWhittaker, Wokingham, UK) was supplemented with 2mM L-glutamine (Invitrogen). For low Ca^{2+} experiments, serum-free LHC-9 (Laboratory of Human Carcinogenesis-9) medium (Invitrogen) was used supplemented with 2mM L-glutamine (Invitrogen) ± 0.424mM $CaCl_2$ (Sigma-Aldrich) and 0.407mM Mg_2SO_4 (Sigma-Aldrich). In addition, all culture media were supplemented with 50IU/ml penicillin and 50μg/ml streptomycin (Invitrogen) to reduce the risk of bacterial and fungal infections. All cell culture techniques were performed in MDH Microflow Class II Biological safety cabinets, and cells were incubated at 37°C in a 5% CO_2 humidified atmosphere in Heraeus incubators. All Nunc plasticware (Invitrogen) had the Nunclon Δ surface.

2.5.1 Primary human bronchial epithelial (HBE) cell cultures

HBE cell cultures were established by seeding cells brushed from the proximal airways of volunteer subjects into vented Nunc tissue culture flasks containing serum-free BEGM. Primary cells were grown on collagen (Invitrogen), and fed with fresh

medium every 2 days. When the monolayer was near-confluent, cells were washed with Ca^{2+}- and Mg^{2+}-free Hanks Balanced Salt Solution (HBSS; Invitrogen) and trypsinized for 5 minutes at 37°C with 10x Trypsin-EDTA (Invitrogen) diluted 1 in 10 with HBSS. Following detachment of adherent cells from the plastic culture surface, Trypsin was neutralised by addition of standard RPMI 1640 medium and cells were centrifuged at 150xg for 5 minutes. The supernatant was discarded and the cell pellet re-suspended with fresh culture medium. Cell count and cell viability were assessed using Trypan Blue (Sigma-Aldrich) and a Haemacytometer (Sigma-Aldrich) before seeding cells onto new plasticware. Cells were used for experimentation at passage 2 (P2) or P3.

2.5.2 Epithelial cell line cultures

H292 human pulmonary mucoepidermoid carcinoma cells (ATCC) and SW480 human colorectal adenocarcinoma cells (Dr. RM Kypta, University College London) were grown in vented Nunc tissue culture flasks. Cells were maintained in standard RPMI 1640 medium, and fed with fresh medium every 1-2 days. When the monolayer was near-confluent, cells were trypsinized, counted and seeded as described in Section 2.5.1.

2.6 Wnt-3a containing conditioned medium

Confluent L Wnt-3a cells (ATCC; CRL-2647) were split 1:10 and seeded into 175cm^2 vented Nunc tissue culture flasks (Invitrogen, Paisley, UK) containing 30ml Dulbecco's modified Eagle's medium (DMEM; Invitrogen) supplemented with 10% heat-inactivated foetal bovine serum (FBS; Invitrogen), 2mM L-glutamine (Invitrogen), 50IU/ml penicillin and 50µg/ml streptomycin (Invitrogen), without G418 (BD Biosciences, Oxford, UK), and incubated for 4 days. The medium was removed, centrifuged at 1,000g for 10min and filtered through a 0.22µm Millex-GV filter (Millipore, Watford, UK). Cells were cultured a further 3 days in 30ml of fresh supplemented DMEM to generate a second batch of conditioned medium that was combined with the first to make the Wnt-3a conditioned medium. As a control, conditioned medium from parental L-cells (ATCC; CRL-2648) was produced in the

same way. Although this is *mouse* Wnt-3a, homology with its human counterpart is close enough for it to be biologically active in human cells (Hino et al., 2003; Liu et al., 2003).

2.7 Air-liquid interface (ALI) cultures

At passage 2 (P2), primary human bronchial epithelial (HBE) cells were seeded into the inserts (apical chamber) of 24-well Costar transwell plates (Corning Costar, High Wycombe, UK) at 1 x 10^5 viable HBE cells per well in 150µl Bronchial Epithelium Growth Medium (BEGM; Clonetics, San Diego, CA, USA); the basal chamber contained 500µl BEGM. Within each insert, cells were grown on collagen-coated, microporous, polycarbonate membranes, and culture medium was changed every 48 hours. When 100% confluent, cells were brought to the air-liquid interface by removing medium from the apical chamber and replacing BEGM in the basal chamber with 300µl/well ALI medium (see Section 2.1.1). ALI medium was replaced daily, with care taken to remove any medium from the apical chamber that had leaked across the transwell. From day 7 at the air-liquid interface, mucous production became evident, and this was removed by washing cells with 150µl/well Dulbecco's modified Eagle's medium (DMEM; Invitrogen, Paisley, UK). On days 7, 14 and 21 at the air-liquid interface, the epithelium was carefully cut from the insert on its polycarbonate membrane, and fixed in ice-cooled acetone (Merck Biosciences, Nottingham, UK), supplemented with 2mM phenylmethyl-sulfonyl fluoride (PMSF; Sigma-Aldrich, Poole, UK) and 20mM idioacetamide (Sigma-Aldrich), ready for glycolmethacrylate (GMA) processing.

2.8 RNA extraction

Extraction and isolation of RNA from cultured cell monolayer was achieved using TRIzol Reagent (Invitrogen, Paisley, UK) in accordance with the manufacturer's instructions. Following addition of TRIzol at a volume based on surface area of the culture dish (1ml per $10cm^2$), cells were lysed and harvested by scraping. Lysates were homogenised by passing the sample several times through a pipette. Samples

were then stored in RNase-free eppendorf tubes at -80°C until time for RNA isolation.

2.8.1 RNA isolation

Cell lysates in TRIzol were incubated at room temperature for 5 minutes to allow complete dissociation of nucleoprotein complexes. Chloroform (Sigma-Aldrich, Poole, UK) was added at 200µl per 1ml TRIzol before vigorous shaking by hand for 15 seconds. The sample was then incubated at room temperature for a further 5 minutes before centrifugation at 12,000xg for 15 minutes at 4°C. This achieved sample separation into an upper colourless aqueous phase containing RNA, and a lower red phenol-chloroform phase containing DNA and protein. The RNA-containing aqueous phase was transferred into a new RNase-free eppendorf tube with care being taken not to disturb the interphase. RNA was precipitated by gentle mixing with isopropyl alcohol (isopropanol; Sigma-Aldrich) at 500µl per 1ml TRIzol followed by incubation at room temperature for 15 minutes. The sample was then centrifuged at 12,000xg for 30 minutes at 4°C, and the supernatant carefully discarded to leave the RNA pellet. This was gently washed by addition of 75% v/v ethanol (Sigma-Aldrich) at 1ml per 1ml TRIzol, followed by centrifugation at 7,500xg for 5 minutes at 4°C and removal of the supernatant. The RNA pellet was allowed to partially air-dry for 5-10 minutes before re-suspension in RNase-free ultra-high quality (UHQ) water or DNase treatment. In the former case, RNA was fully dissolved by gentle pipetting and incubation at 55-60°C for 10 minutes. Re-dissolved RNA was then stored at -80°C for later use.

2.8.2 DNase treatment of extracted RNA

Following RNA isolation from TRIzol, DNase treatment was undertaken in order to remove contaminating genomic DNA from the sample. Immediately after partial air-drying of the RNA pellet, the sample was re-suspended in a master mix comprising 17µL RNase-free UHQ water, 2µL 10x DNase buffer and 1µL DNase1 (Ambion, Huntingdon, UK), and incubated for 60 minutes at 37°C. 5µL DNase Inactivator (Ambion) was then added and the sample incubated for 2 minutes at room

temperature before pulse spinning to pellet the slurry. The RNA sample was then stored at -80°C. When aliquots of RNA were later taken for analysis, care was taken to avoid carry over of DNase Inactivator slurry.

2.8.3 RNA degradation check and quantification

When handling RNA, precautions were taken to prevent RNase contamination. RNA concentration and purity was checked by measurement of absorbance at 260nm (A_{260}) and 280nm (A_{280}) using quartz capillaries (Amersham Biosciences, Little Chalfont, UK) and a GeneQuant spectrophotometer (Biochrom, Cambridge, UK). 1% agarose gel electrophoresis (see method below) was used to confirm the concentration of RNA and also check for RNA degradation. 2µl (100-500ng) RNA sample was mixed with 5µl 1x RNA gel loading buffer prior to gel loading. Figure 2.1 shows a representative gel with bands representing 18S and 28S ribosomal RNA stained with ethidium bromide (Sigma-Aldrich). The discrete nature of these two bands for each sample indicates that the RNA has not degraded.

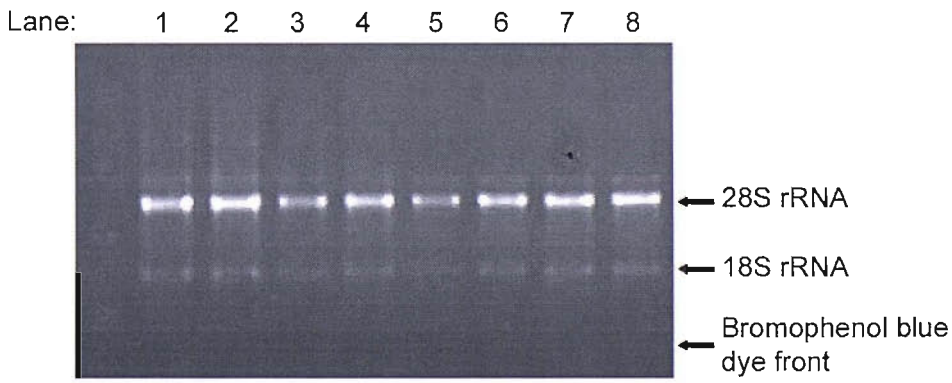

Figure 2.1: Representitive agarose gel for RNA quantification and degradation check.

2.9 Agarose gel electrophoresis

To make a 1% agarose gel, 1g of HighStrength Analytical Grade agarose (Bio-Rad, Hemel Hempstead, UK) was dissolved in 100ml 1x Tris-borate EDTA (TBE; Sigma-

Aldrich, Poole, UK) by heating to near-boiling point in a microwave oven. The 1% agarose solution was allowed to cool to 55-60°C before addition and mixing of ethidium bromide (Sigma-Aldrich) to a final concentration of 0.5µg/ml. The solution was then poured onto a pre-cleaned gel plate (Bio-Rad) with masking tape at each end. A comb was inserted, and the gel was allowed to set over 30-45 minutes at room temperature. The masking tape was removed and the gel plate immersed in a Sub-Cell GT electrophoresis tank (Bio-Rad) containing 1x TBE before careful removal of the comb. Prior to gel loading, RNA or DNA samples were mixed with 2-5µl 1x RNA or DNA gel loading buffer, respectively. To reduce the risk of RNA degradation during the process of electrophoresis, a dedicated RNA tank pre-cleaned with RNaseZAP (Sigma-Aldrich) was used, and care was taken to avoid RNase contamination. The electrophoresis tank was attached to a Power Pac 300 transformer (Bio-Rad) such that nucleic acid could migrate through the gel from the cathode (negative, black) to the anode (positive, red). 80-100mA constant current was applied across the gel until the bromophenol blue dye front had reached the desired point. Intercalation of ethidium bromide between nucleotide bases allowed bands of nucleic acid to be detected by fluorescence under ultraviolet (UV) light. Bands were imaged using the Gene Genius Bio Imaging System (Syngene, Cambridge, UK) and captured using GeneSnap software (Syngene). To image bands of DNA using the more sensitive Vistra Green (Amersham Biosciences, Little Chalfont, UK) detection system, RT-PCR products were resolved along a 1% agarose gel without addition of ethidium bromide. The gel was then stained using 0.01% v/v Vistra Green in 1x TBE for 30 minutes on a rotary shaker, and washed for 10 minutes with 1x TBE. Intercalation of Vistra Green between nucleotide bases allowed detection of DNA by fluorescence following laser excitation at 532nm using a FluorImager 595 (Molecular Dynamics, Sunnyvale, CA, USA).

2.10 RNase protection assays (RPA)

2.10.1 Basic principle

The RiboQuant Human Frizzled (hFZD) Multi-Probe Template Set (BD Biosciences, Oxford, UK) comprises DNA templates containing the T7 promoter. This kit was

Gene template	Alternative name	Unprotected probe size (bp)	Protected probe size (bp)
fritz	FRZB (SFRP3)	435	406
SARP1	SFRP2	380	351
SARP2	SFRP1	345	316
smoothened	SMOH	312	283
frz1/FZD2	FZD2	282	253
frizzled 3	FZD3 Accession N°: AA436403	255	226
FZD3	FZD9 Accession N°: U82169	231	202
frizzled 5	FZD5	210	181
frizzled 6	FZD6	192	163
L32	-	141	112
GAPDH	-	126	97

Table 2.1: The Human Frizzled Multi-Probe Set (BD Biosciences).

used in conjunction with MAXIscript T7 and RPA III Ribonuclease Protection Assay kits (Ambion, Huntingdon, UK) to investigate Frizzled (FZD) and secreted Frizzled-related protein (SFRP) gene expression. RPA allows detection of non-amplified RNA. In principle, radiolabelled anti-sense RNA probes are synthesised with a flanking region. Probes that hybridise with sample RNA are then protected from RNase digest. However, the flanking region of protected probes does not hybridise and remains susceptible to RNase digest, thus reducing probe size by a predictable amount. Following RNase inactivation, RNA is denatured into single strands that can then be resolved by polyacrylamide gel electrophoresis (PAGE) and detected using a phosphoimager. Using full-length probes (containing the flanking region) of known nucleotide size as a reference ladder, the identity of bands formed by protected probes can be determined based on their calculated and predicted nucleotide size. Since RPA does not involve signal amplification, band intensity of the protected probe remains linearly related to the amount of complementary RNA in the sample. However,

comparison of expression between independent experiments requires normalisation of band intensity to that of one or more internal control genes, because radioactivity of the probe will decay over time. The eleven templates of the Human Fizzled Multi-Probe Set are listed in Table 2.1 with predicted nucleotide size of full-length and protected probes. GAPDH and L32 ribosomal protein are internal controls.

2.10.2 Protocol

MAXIscript T7 and RPA III Ribonuclease Protection Assay kits (Ambion) were used in accordance with manufacturer's instructions. To synthesize radiolabelled anti-sense RNA probes, the following reagents were mixed in an eppendorf tube and incubated for 60 minutes at 37°C: 7µl nuclease-free water, 1µl RiboQuant Multi-Probe DNA (BD Biosciences), 2µl 10x Transcription Buffer, 1µl 10mM ATP, 1µl 10mM CTP, 1µl 10mM GTP, 5µl 20µCi/µl [α^{32}P] UTP (Amersham Biosciences, Little Chalfont, UK) and 2µl (30U) T7 RNA Polymerase and Ribonuclease Inhibitor. 1µl (2U) DNase I was then added and the mix incubated a further 15 minutes at 37°C to allow digestion of DNA templates. DNase was then inactivated by addition of 1µl 0.5M ethylenediaminetetraacetic acid (EDTA; Sigma-Aldrich, Poole, UK), pH7.6. Following addition of 80µl nuclease-free water, steps were next taken to extract the probes from the mixture. 100µl phenol/chloroform/isoamylalcohol (50µl phenol, 48µl chloroform, 2µl IAA; Sigma-Aldrich) was added and mixed before centrifugation at high-speed in a Micro Centaur Microfuge for 5 minutes at room temperature. The supernatant was transferred to a new eppendorf for re-extraction with 100µl chloroform/IAA (50:1; Sigma-Aldrich) and further centrifugation at high-speed in the Microfuge for 5 minutes at room temperature. Again, the supernatant was transferred to a new eppendorf tube before addition of 1µl pellet paint (Merck Biosciences, Nottingham, UK) and precipitation of probe RNA with 10µl (1/10 vol) 5M ammonium acetate (NH_4OAc) and 275µl (2.5 vols) ethanol (Sigma-Aldrich). This was facilitated by incubation for 30 minutes at -80°C, before centrifugation at 13,000xg for 20 minutes at 4°C. Supernatant was carefully discarded and the pellet washed with 1ml ice cold 70% v/v ethanol (Sigma-Aldrich). Supernatant was again

carefully discarded and the pellet air-dried for 5-10 minutes before re-suspension in 50µl RPA III Hybridization Solution. Cherenkov scintillation counts were measured on duplicate 1µl aliquots using a TopCount-NXT Microplate Scintillation Counter (Packard Bioscience Company, USA), and the mean count calculated. A further 1µl aliquot was diluted in 200µl nuclease-free water and stored for later use as a full-length probe reference ladder. Remaining stock probe solution was diluted with RPA III Hybridization Solution to 3.5 x 10^5 Cherenkov counts per µl.

Sample RNA, dissolved in nuclease-free water, was prepared by aliquoting 5-20µg into a thermal cycling tube, and freezing it before drying it completely in a vacuum evaporator centrifuge for 30-60 minutes with no heat. Sample RNA was then re-suspended in 8µL RPA III Hybridization Solution before addition of 2µL diluted probe. Hybridization was achieved by initial incubation for 2-3 minutes at 95°C followed by 12-16 hours at 56°C. 15 minutes prior to RNase treatment, the sample was incubated at 37°C. 100µL 1:1000 RNase A/T1 Mix in RNase Digestion Buffer III was then added to the RNA/probe sample before incubation for 45 minutes at 30°C. RNase was then inactivated, and protected probe precipitated, by addition of 190µl Inactivation/Precipitation III/ethanol/Yeast tRNA (150µl Inactivation/Precipitation III, 38µl ethanol, 2µl Yeast tRNA) and incubation for 30 minutes at -20°C. Following centrifugation at 13,000xg for 30 minutes at 4°C, supernatant was carefully discarded and the probe containing pellet washed with 100µl ice cold 90% ethanol (Sigma-Aldrich). Supernatant was then aspirated and the pellet air-dried for 5-10 minutes before re-suspension in 5µl Gel Loading Buffer II. Of the 201µl dilute full-length probe to be used as a reference ladder, a 1.5µl aliquot was added to 5µl Gel Loading Buffer II. Human Control RNA-2 (BD Biosciences) was used as a positive control. Yeast tRNA (Ambion) ± RNase was used as a negative control, i.e. check of RNase integrity. Absence of bands in the Yeast tRNA minus RNase (RNase Digestion Buffer III without RNase A/T1 Mix) would suggest loss of probe during the precipitation step that followed RNase treatment. Standard precautions were taken when working with radioactive material. These included use of lead screens in a dedicated 'hot' lab, wearing of radiation dose monitoring badges and rings, and regular surveillance of the bench and pipettes for radioactive

contamination. Radioactive material was stored and disposed of in accordance with university health and safety regulations.

2.10.3 Polyacrylamide gel electrophoresis (PAGE) and imaging quantification

Dedicated polyacrylamide gel mould plates (Sequi-Gen GT Sequencing Cell; Bio-Rad, Hemel Hempstead, UK) were cleaned with ethanol (Sigma-Aldrich), siliconised (Repelcote VS; BDH, Poole, UK), and assembled with 0.4mm spacers. A 5% acrylamide/8M Urea/1x Tris-borate EDTA (TBE) solution was prepared as follows: 4.66ml 40% acrylamide/bis-acrylamide 19:1 (Accugel 19:1; National Diagnostics, Hull, UK), 3.73ml 10x TBE (Sigma-Aldrich), 17.91g Urea (Sigma-Aldrich), RNase-free water to a total volume of 37.3ml. To promote polymerization and gel formation, a solution of 225µl 10% w/v ammonium persulphate (AMPS; Sigma-Aldrich) and 30µl N,N,N',N'-tetramethylethylenediamine (TEMED; Sigma-Aldrich) was added, and the mix immediately poured into the gel mould, ensuring no air bubbles. A comb was inserted, and the gel left to set over 40 minutes at room temperature. The gel was then immersed in 0.5x TBE, the comb removed and wells flushed, before pre-running it for 1-2 hours at 40 watts constant power until the gel had heated to 50°C. Wells were flushed once again to remove urea, before loading with reference (full-length), sample (RNase treated) and control probes, pre-heating to 95°C for 3-5 minutes and quenched on ice. 50 watts constant power was applied across the gel until the bromophenol blue dye front had travelled approximately 30cm. The gel mould was dismantled and the gel carefully transferred onto filter paper before transfer to a gel dryer (model 583; Bio-Rad) for 60 minutes at 80°C. The gel was then placed against a pre-light bleached Phosphor Screen in a cassette (Molecular Dynamics, Sunnyvale, CA, USA) and left for 3 days at -20°C before scanning on a Storm 860 PhosphorImager (Molecular Dynamics). FragmeNT Analysis software (Molecular Dynamics) was used to identify protected probe bands, based on size relative to full length reference probe bands, and quantify band intensity.

2.11 Reverse transcription-polymerase chain reaction (RT-PCR)

2.11.1 Primer design for RT-PCR

In designing forward (sense) and reverse (anti-sense) primers for RT-PCR, the cDNA sequence for the human gene of interest was copied in FASTA format from LocusLink in the Online Mendelian Inheritance in Man (OMIM) database (www.ncbi.nlm.nih.gov). The coding sequence (CDS), and 5'- and 3'-untranslated regions (UTR) were marked. Interspersed repeats and low complexity regions were identified and masked using RepeatMasker (http://repeatmasker.genome.washington.edu/cgi-bin/RepeatMasker). Using the Basic Local Alignment Search Tool (BLAST) in LocusLink, intron/exon boundaries within the cDNA sequence were identified, along with sequence homologies within the human genome. The masked cDNA sequence was then imported into PrimerSelect software (Lasergene5; DNASTAR, Madison, WI, USA). Parameters were initially set for a high stringency search, and potential primer sets were scored and ranked. Forward and reverse primers flanking at least one intron (untranslated intervening sequence) were chosen such that PCR products arising from genomic DNA could be easily differentiated from products arising from amplified cDNA. In addition, one member of each primer pair was chosen to span an intron-exon boundary, thereby reducing the chance of exponential genomic DNA amplification. To avoid primers with extensive sequence homology outside the gene of interest, a standard nucleotide-nucleotide BLAST [blastn] was performed in LocusLink before final selection. Forward and reverse primer sequences were sent to MWG-Biotech (Milton Keynes, UK) who returned each synthesised primer in lyophilised form. These were re-suspended in 1x TE Buffer (10mM Tris-HCl, pH 8.0, 1mM EDTA; Sigma-Aldrich, Poole, UK) to make a stock solution of 100pmol/µl (100µM). Further dilution in RNase-free UHQ water allowed working aliquots of 10pmol/µl (10µM) to be stored at -80°C for later use.

2.11.2 Reverse transcription (RT)

The reverse transcription step converts sample RNA to complementary DNA (cDNA), allowing subsequent polymerase chain reaction (PCR) by DNA (Taq) polymerase. 1µg sample RNA was added to 1µl of 3µg/ml (3pg) random hexamer (MWG Biotech) and 1µl of 10mM deoxynucleoside triphosphates (dNTP; Invitrogen, Paisley, UK), with addition of UHQ water to a total volume of 10µL. The mix was incubated for 5 minutes at 80°C before snap cooling on ice to anneal random hexamers to the sample RNA. A master mix comprising 5.5µl UHQ water, 4µl 5x RT buffer and 0.5µl (100U) Moloney murine leukaemia virus Reverse Transcriptase (M-MLV RT; Promega, Southampton, UK) was then added to the sample RNA mix before incubation for 60 minutes at 37°C followed by 10 minutes at 70°C to denature the enzyme. RT-minus controls had UHQ water in place of Reverse Transcriptase in this reaction. Samples were stored at -80°C for later use.

2.11.3 Polymerase chain reaction (PCR)

PCR allows exponential amplification of select cDNA within a sample depending on forward and reverse primers employed. The polymerase chain reaction consists of repeated cycles of a three step process. The first step involves *denaturation* of cDNA into single strands by heating to 94°C for 20 seconds. The second step involves the *annealing* of forward and reverse primers to sense and anti-sense DNA by lowering the temperature for 30 seconds. The final step involves DNA (Taq) polymerase mediated *extension* from each primer along the DNA template with the temperature increased to 72°C for optimal Taq function. The duration of this latter phase may vary depending on predicted product size, but 40-60 seconds is generally adequate time for synthesis of products less than 1000 base pairs.

In each 25µl thermocycling reaction, 1µl (50ng) sample cDNA template was added to the wall of the thermal cycling tube along with 0.5µl each of 10µM (5pmol) forward and reverse primer (MWG Biotech). For negative controls, RT-minus sample or UHQ water was used in place of cDNA. A master mix comprising 18.25µl UHQ water, 2.5µl 10x PCR buffer II (Sigma-Aldrich), 1.5µl 25mM magnesium chloride (1.5mM

$MgCl_2$; Sigma-Aldrich), 0.5µl 10mM dNTP (Invitrogen) and 0.25µl of 2.5U/µl JumpStart Taq DNA Polymerase (Sigma-Aldrich) was added to the bottom the thermal cycling tube before it was pulse spun and immediately placed in a PTC-225 Peltier Thermal Cycler (Bio-Rad, Hemel Hempstead, UK) pre-heated at 94°C for a 'hot start', designed to minimise the risk of initial mis-priming. After 2 minutes, PCR was commenced in accordance with the above pre-programmed cycle parameters, including the annealing temperature, time allowed for extension, and number of cycles. In principle, the chance of mis-priming can be reduced by increasing the annealing temperature &/or decreasing the Mg^{2+} concentration. However, increasing PCR specificity in this was may occur at the expense of reaction efficiency, and a balance may have to be found when optimising conditions for each primer pair. Raising the number of PCR cycles may increase sensitivity, but this will be limited by consumption of dNTP with each cycle, especially if PCR specificity is sub-optimal. In addition, decline in Taq Polymerase activity over time at high temperature may influence both PCR efficiency and sensitivity. A primer pair for the β-actin gene (Promega) was used as an internal positive control for RT-PCR. Absence of a positive control band would suggest sample RNA degradation, failed RT step, or failed PCR. In addition, two negative controls were employed. The first was a RT-minus control in which Reverse Transcriptase was excluded from the reverse transcription step, pre-PCR. In this case, failure to synthesise cDNA should lead to absence of detectable PCR product unless genomic DNA is amplified. The second negative control comprised the primer pair for β-actin (Promega) with addition of UHQ water instead of sample cDNA. Presence of detectable PCR product in this reaction would suggest amplification of contaminating DNA.

2.11.4 Agarose gel electrophoresis

RT-PCR products were resolved by 1.5% agarose gel electophoresis. The gel was loaded with 5-7µl PCR product mixed with 2µl 1x DNA gel loading buffer. The gel was also loaded with 1-3µl DNA molecular weight markers (Amersham Biosciences, Little Chalfont, UK) mixed with 2µl 1x DNA gel loading buffer.

2.12 DNA sequencing

Prior to sequencing RT-PCR products, primers and dNTPs were removed from dsDNA amplicons using the MinElute PCR Purification Kit (Qiagen, Crawley, UK) in accordance with the manufacturer's instructions. From each PCR reaction, 20µl of product was added to 100µl Buffer PB, and the mix applied to a MinElute resin column before centrifugation at 10,000xg for 1 minute at room temperature. The flow-through, containing primers and dNTPs, was discarded. To wash the dsDNA amplicons, 750µl ethanol-containing Buffer PE was applied to the MinElute column before repeat centrifugation at 10,000xg for 1 minute. Again, the flow-through was discarded, and the MinElute column spun an additional minute to remove all remaining ethanol. Eluant containing dsDNA amplicons was obtained by application of 10µl Buffer EB (10mM Tris-HCl, pH 8.5) and centrifugation at 10,000xg for 1 minute. Sequencing of purified RT-PCR products was achieved using the ABI Prism BigDye Terminator Cycle Sequencing Ready Reaction Kit v3.0 (Applied Biosystems, Brackley, UK) in accordance with the manufacturer's instructions. The following were mixed in a thermal cycling tube on ice: 8µL Terminator Ready Reaction Mix (dye terminators, dNTP, AmpliTaq DNA polymerase, $MgCl_2$, buffer), 500ng sample DNA, 3.2pmol primer (forward *or* reverse) and nuclease-free water to a final volume of 20µL. The tube was then placed in a GeneAmp PCR System 9700 (Applied Biosystems) programmed for 25 cycles of the following three step process: *denaturation* at 96°C for 10 seconds, *annealing* at 50°C for 5 seconds, and *extension* at 60°C for 4 minutes. Extension products were then stored at +4°C until removal of excess dye terminators. The DNA template pGEM-3Zf(+) included in the kit was employed as a positive control. Extension products were purified using DyeEx Spin Columns (Qiagen) in accordance with the manufacturer's instructions. The aim was to remove unincorporated dye terminators prior to polyacrylamide gel electrophoresis (PAGE), thereby improving the signal-to-noise ratio. A ready-to-use spin column was gently vortexed to re-suspend the resin. Equilibration buffer was removed by centrifugation at 750xg for 3 minutes, before careful application of extension products to the gel bed. Eluant containing purified extension products was obtained following centrifugation at 750xg for a further 3 minutes, and allowed to dry before storage in the dark at -20°C. Extension products then were sent to Dr Mark Dixon's

laboratory (Bolderwood, University of Southampton) to be resolved by PAGE on an ABI Prism 377 DNA Analyzer (Applied Biosystems). The quality of the sequence signal was inspected using Chromas v1.45 software (Conor McCarthy, Griffith University, Queensland, Australia), and alignment with reference sequence achieved using MegAlign software (Lasergene5; DNASTAR, Madison, WI, USA).

2.13 Quantitative real-time RT-PCR (qPCR; TaqMan)

Quantitative PCR involves simultaneous thermocycling and real-time detection of PCR products using either SYBR Green double-stranded DNA (dsDNA) binding dye or the fluorogenic 5'-nuclease assay (TaqMan). SYBR Green fluoresces when bound to dsDNA, but fluorescence is drastically reduced when dsDNA denatures to single-stranded DNA. Since SYBR Green fluorescence is proportional to the amount of dsDNA, a real-time net increase in fluorescence can be detected toward the end of the *extension* step of each thermocycle. This method of amplicon detection is remarkably sensitive, but may lack specificity. Confidence in the latter may be improved by checking the amplicon's peak melt temperature (T_M), an indicator of amplicon size, against that predicted.

The fluorogenic 5'-nuclease assay employs an oligonucleotide probe with 5'-reporter dye (e.g. 6-carboxy-fluorescein, i.e. FAM) and 3'-quencher dye (e.g. 6'-carboxy-N,N,N',N'-tetramethyl-rhodamine, i.e. TAMRA) attached (see Figure 2.2). When intact, flourescence from the reporter dye of the probe is quenched. During the *annealing* step of PCR, the probe binds to the target cDNA of interest, between the forward and reverse primer sites. During the *extension* step, the probe is cleaved by the 5'-nuclease activity of Taq DNA polymerase, separating the reporter dye from the quencher dye, thereby allowing the reporter dye to emit its characteristic fluorescence. Once again, since the amount of cleaved probe is proportional to the amount of dsDNA, a real-time net increase in fluorescence can be detected toward the end of the *extension* step of each thermocycle. PCR probes improve qPCR specificity, but may reduce the sensitivity of amplicon detection, when compared with the SYBR Green assay.

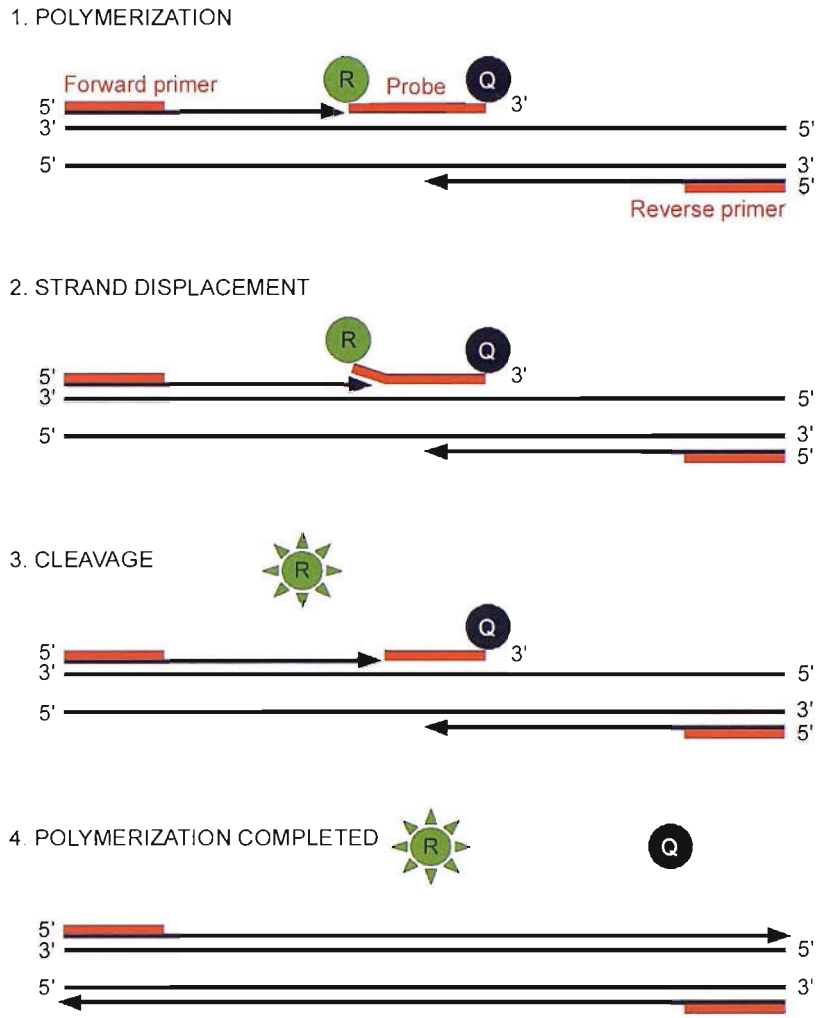

Figure 2.2: The fluorogenic 5'-nuclease assay for quantitative PCR.

During polymerization, the 5'-nuclease activity of Taq DNA polymerase displaces and cleaves the probe, liberating the reporter dye (R) from the influence of the quencher (Q) dye.

2.13.1 Primer and probe design for qPCR

Forward and reverse primers for *cyclin-D1*, *MMP7*, *IL-8* (Table 4.1) and FZD6 (Table 7.1) were designed by Dr Rob Powell (University of Southampton) using Primer Express software (Applied Biosystems, Brackley, UK). Criteria used in qPCR primer design included primer lengths of 18-22 base pairs, an amplicon length of 100-150 base pairs, a maximum melt temperature (T_M) difference between primer pairs no greater than 3°C, and a mean primer T_M of 68 ± 2°C. A FAM probe was also designed for *cyclin-D1* and *IL-8*, whereas the SYBR Green dye assay was used for *MMP7* and

FZD6. Primer and probe sequences were sent to MWG-Biotech (Milton Keynes, UK) who returned them synthesised in lyophilised form. These were re-suspended in 1x TE Buffer (10mM Tris-HCl, pH 8.0, 1mM EDTA; Sigma-Aldrich, Poole, UK) to make a stock solution of 100pmol/µl (100µM), stored at -80°C for later use. Commercially available primers and FAM probe were employed for 18S rRNA (Eurogentec, Seraing, Belgium).

2.13.2 qPCR protocol

In each 12.5µl thermocycling reaction, 5µl (25ng) sample cDNA template, pre-diluted 1:10 with UHQ water, was added to 7.5µl master master mix (MMM) placed on the wall of each well of a 96-well thermal cycling plate (Bio-Rad, Hemel Hempstead, UK). For reactions using a FAM probe, MMM comprised 0.15µl each of 100µM (15pmol) forward and reverse primer, 6.25pmol of FAM probe, and 6.5µl 2x PCR master mix (Eurogentec), containing Taq DNA Polymerase and dNTP. For reactions using the SYBR Green dye assay, MMM comprised 0.15µl each of 100µM (15pmol) forward and reverse primer, 0.7µl UHQ water, 6.5µl 2x PCR master mix (Eurogentec), 0.06µl of 1:100 SYBR Green (Invitrogen, Paisley, UK) and 0.12µl of 1mM fluorescein calibration dye (Bio-Rad). After applying an optically clear seal (Bio-Rad), the 96-well plate was pulse spun and placed in an iCycler iQ machine (Bio-Rad), allowing simultaneous thermocycling and real-time detection of PCR products. The PCR protocol began with a 95°C 'hot start' for 8 minutes, followed by 50 cycles of *denaturation* (95°C for 15 seconds) and *annealing/extension* (60°C for 60 seconds). When using the SYBR Green dye assay, SYBR melt curve analysis was performed in order to assess the quality of the signal and identify the peak melt temperature (T_M), an indicator of amplicon size. All samples were measured in triplicate. RT-minus samples and UHQ water were used as negative controls in place of sample cDNA template.

2.13.3 The $\Delta\Delta C_T$ method of gene quantification

By setting the threshold for fluorescence emission baseline just above background levels, iCycler iQ Optical system software version 3.0a (Bio-Rad) was used to

determine the threshold cycle (C_T value) for each reaction. Relative gene expression levels were calculated using the comparative C_T ($\Delta\Delta C_T$) method of quantification with 1µl 18S rRNA primer and FAM probe mix (Eurogentec) as the normalising control. The $\Delta\Delta C_T$ method of gene quantification assumes that the functioning of a primer pair within a PCR reaction approximates to 100% efficiency. Therefore, the primer pair used to investigate each gene of interest had to be validated by constructing a standard curve based on the amplification of 2-fold serial dilutions of template cDNA (5-8 different concentrations). Log_{10}[RNA concentration] was plotted against mean C_T value for each dilution on x and y axes, respectively, and a straight line drawn according to best fit. Primer sets were deemed suitable for the $\Delta\Delta C_T$ method of gene quantification if the gradient (m) of the slope, derived from the formula y=mx+c, was between -3.2 and -3.5, and the R^2 value for the best line fit from the data points was >0.95. This process of validation was performed by Dr Rob Powell (University of Southampton), and all primer sets met these criteria. The amount of target gene, normalised to 18S rRNA (the endogenous reference gene) and relative to a calibrator, was calculated from the equation:

$$2^{-\Delta\Delta C_T}$$

Where:

- $\Delta\Delta C_T = \Delta C_T$ (sample) – ΔC_T (calibrator)
- ΔC_T (sample or calibrator) = C_T (target gene) – mean C_T (18S rRNA)

Outlying C_T values were excluded from analysis, and ΔC_T (calibrator) was arbitrarily taken as the lowest ΔC_T (sample) on the 96-well plate.

2.14 Western blot (WB) analysis

Cells were cultured on 6-well Nunc plates (Invitrogen, Paisley, UK) and harvested by scraping in 200µl/well Denaturing Sample Lysis Buffer (DSLB) containing protease inhibitors (see Section 2.1.8), pre-heated to 95°C for 10 minutes. Lysates were placed in eppendorf tubes, vortexed for 15 seconds, and heated to 95°C for 5 minutes. Samples were then sonicated for 15 seconds, clarified by centrifugation at 16,000xg for 10 minutes, and stored at -80°C until time for western blot analysis.

2.14.1 SDS PAGE

The protein components of cell lysates in DSLB were resolved by sodium dodecylsulphate (SDS) polyacrylamide gel electrophoresis (PAGE), using a Mini-PROTEAN 3 electrophoresis module (Bio-Rad, Hemel Hempstead, UK) and 1mm thick 7.5% polyacrylamide gels. Glass gel mould plates were cleaned with 10% w/v SDS, rinsed with methanol and allowed to dry before assembly. A 7.5% polyacrylamide separation gel was prepared by addition of 33µl 10% w/v ammonium persulphate (AMPS; Sigma-Aldrich, Poole, UK) and 5µl N,N,N',N'-tetramethylethylenediamine (TEMED; Sigma-Aldrich) to 10ml 7.5% separation gel stock solution (see Section 2.1.8), and the mix immediately poured into the gel mould, ensuring no air bubbles. To achieve polymerisation, the mix was overlayed with 3mm propanol (Sigma-Aldrich) in order to exclude oxygen, and left for 45 minutes to set. The polymerised separation gel was rinsed with distilled H_2O, and excess water removed by blotting with filter paper. A stacking gel was prepared by addition of 16.7µl 10% w/v AMPS and 3.8µl TEMED to 5ml stacking gel stock solution (see Section 2.1.8), and the mix immediately poured above the polyacrylamide separation gel, again ensuring no air bubbles. A 10-tooth comb was inserted, and the gel left for 40 minutes to set. The Mini-PROTEAN 3 electrophoresis module was then assembled, before immersing the gel in pre-chilled Running Buffer (see Section 2.1.8) and removing the comb. Prior to loading each sample onto the gel using a pipette with fine gel loading tip, 24µl of cell lysate in DSLB was mixed with 6µl of 5x Loading Buffer (LB; see Section 2.1.8) and heated to 95°C for 5 minutes. One lane was loaded with 10µl Full Range Rainbow recombinant protein molecular weight markers (Amersham Biosciences, Little Chalfont, UK). A Bio-Rad Power Pack 300 was used to apply 30V across the gel for 10 minutes, followed by 130V until the bromophenol blue dye front reached the end of the separation gel (approximately 1 hour). The gel mould was then dismantled and the stacking gel cut away, ready for Western blotting.

2.14.2 Western blotting

Resolved proteins were transferred from the polyacrylamide gel to an equivalent sized Hybond C nitrocellulose membrane (Amersham Biosciences) using a Mini Trans-Blot electrophorectic transfer module (Bio-Rad). Prior to assembly of the transfer cassette, the gel and nitrocellulose membrane were pre-soaked in pre-chilled Transfer Buffer (see Section 2.1.8) for 15 minutes. The transfer cassette was assembled in Transfer buffer such that the gel and nitrocellulose membrane were sandwiched between two pieces of Whatman 3MM filter paper, followed by two Scotch-Brite pads, ensuring no air bubbles. The cassette was then inserted into the Mini Tans-Blot tank containing Transfer Buffer with the nitrocellulose membrane placed nearest the anode (positive charge). Electrophoretic transfer was achieved at 80V constant voltage for 3 hours with current limited to 300mA using an internal ice block, two external chill blocks, a magnetic flea and stirrer. The blotted nitrocellulose membrane was then removed, air dried on a piece of dry filter paper for 5 minutes, and stored wrapped in clingfilm at +4°C for up to 2 weeks, ready for immunodetection.

2.14.3 Immunodetection

Immunodetection of Tcf-4 protein on the nitrocellulose blot was achieved using the enhanced chemiluminescence (ECL Plus) detection system (Amersham Biosciences). The nitrocellulose membrane was initially rehydrated in Wash Buffer (see Section 2.1.8) for 10 minutes, prior to application of Blocking Buffer (see Section 2.1.8) for 1 hour. Following a wash with Wash Buffer, the membrane was incubated for 90 minutes with 2µg/ml Tcf-4 antibody (clone 6H5-3; IgG_{2a}; Upstate Biotechnology, Lake Placid, NY, USA). The membrane was then washed with Wash Buffer before 60 minute incubation with horseradish peroxidase (HRP) conjugated rabbit anti-mouse IgG (P0260; DakoCytomation, Ely, UK) at a titre of 1:4000 in Wash Buffer. The membrane was then washed with Wash Buffer prior to application of ECL Plus reagent for 5 minutes in accordance with the manufacturer's instructions, ensuring no air bubbles. Following removal of excess ECL Plus reagent, the nitrocellulose blot was carefully wrapped with a single layer of clingfilm before examination using a GeneGnome chemiluminescence imaging system (Syngene, Cambridge, UK) and

GeneSnap software (Syngene). A mouse IgG_{2a} isotype control antibody (Sigma-Aldrich; M-9144) was employed as a check for non-specific staining. All incubation and washing steps employed a rota-shaker.

2.15 Tcf/Lef-1 reporter (TOPflash) assays

2.15.1 Basic principle

TOPflash (Upstate Biotechnology, Lake Placid, NY, USA) is a Tcf/Lef-1 OPtimised reporter plasmid comprising two sets (with the second set in reverse orientation) of three copies of the Tcf/Lef-1 consensus recognition sequence (5'-AGATCAAAGGG-3') (van Noort and Clevers, 2002) upstream of the *Herpes simplex virus* (HSV) thymidine kinase (TK) promoter and firefly (*Photinus pyralis*) luciferase gene (Figure 2.3). Transfection of TOPflash into cells allows investigation of Tcf/Lef-1 activity by measurement of firefly luciferase production. To control for cellular influences on TOPflash activity outside the Tcf/Lef-1 consensus recognition sites, a control population of cells is transfected with FOPflash (Upstate Biotechnology). This differs from TOPflash in that Tcf/Lef-1 binding sites are mutated (5'-AGGCCAAAGGG-3')

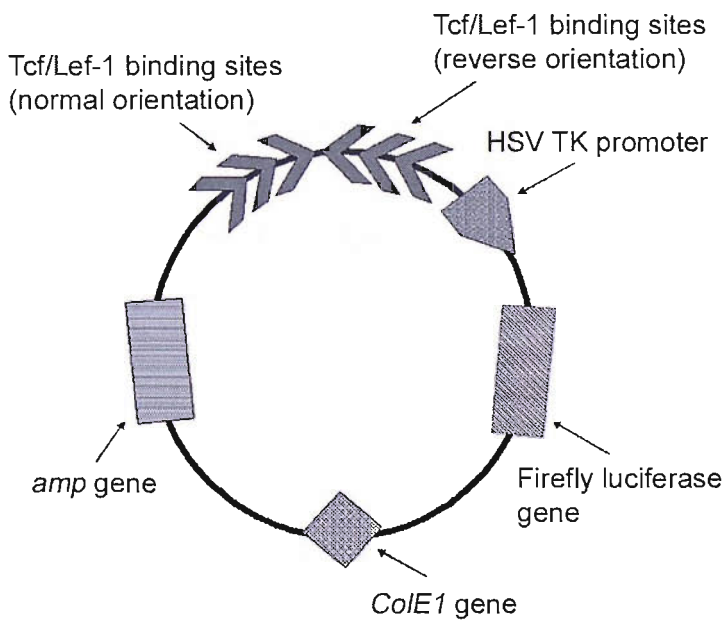

Figure 2.3: The TOPflash reporter construct.

and are no longer recognised. To control for differences in transfection efficiency between TOPflash and FOPflash, each reporter is co-transfected with a constitutively active pRL-TK plasmid (Promega, Southampton, UK), comprising the HSV TK promoter upstream of the sea pansy (*Renilla reniformis*) luciferase gene. After normalising firely luciferase production to that of *Renilla*, the ratio of TOPflash-to-FOPflash provides a measure of *relative* Tcf/Lef-1 activity.

2.15.2 Expanding stocks of TOPflash, FOPflash and pRT-TK plasmids

Each stock of plasmid was expanded by transformation and culture of Epicurian Coli SURE (Stop Unwanted Rearrangement Events) 2 Supercompetent Cells (Stratagene, La Jolla, CA, USA) using a protocol based on the manufacturer's instructions. Cells were thawed on ice and gently mixed before transferring 25µl cell suspension to a pre-chilled thermal cycling tube. 0.5-50ng plasmid DNA was added and gently swirled before incubation for 30 minutes on ice. The tube was heat-pulsed at 42°C for 30 seconds before further incubation on ice for 2 minutes. Tube contents were then spread onto a petri dish with LB Agar (Sigma-Aldrich, Poole, UK) containing 50µg/ml ampicillin (Sigma-Aldrich), before overnight incubation at 37°C to select transformed cells; TOPflash, FOPflash and pRL-TK plasmids all contain the ampicillin-resistance (*amp*) gene. A single colony was picked to inoculate a 10ml starter culture of LB Broth (Sigma-Aldrich) containing 50µg/ml ampicillin. This was placed in a shaking incubator at 37°C and 300rpm for 6-8 hours. The starter culture was then added to 200ml LB Broth containing 50µg/ml ampicillin for overnight incubation at 37°C and 300rpm. TOPflash, FOPflash and pRL-TK all contain the *ColE1* gene, making them high-copy vectors.

2.15.3 Plasmid purification

Stocks of TOPflash, FOPflash and pRL-TK plasmids, expanded in competent cells, were purified using an EndoFree Plasmid Maxi Kit (Qiagen, Crawley, UK) in accordance with the manufacturer's instructions. 100ml suspended transformed cell culture was centrifuged at 6000xg for 15 minutes at 4°C and the supernatant discarded. The bacterial pellet was re-suspended in 10ml Buffer P1 (50mM Tris-HCl,

pH 8.0, 10mM EDTA, 100µg/ml RNase A) before addition of 10ml Lysis Buffer P2 (200mM NaOH, 1% w/v SDS) and incubation for 5 minutes at room temperature. Genomic DNA, proteins and cell debris were then removed by passage through a QIAfilter Maxi Cartridge following their precipitation by addition of 10ml chilled Neutralization Buffer P3 (3M potassium acetate, pH 5.5). 2.5m Buffer ER was mixed with the filtered lysate before incubation for 30 minutes on ice. The filtered lysate was then run along a Qiagen-tip 500 resin column pre-equilibrated with 10ml Buffer QBT (750mM NaCl, 50mM MOPS, pH 7.0, 15% v/v isopropanol, 0.15% v/v Triton X-100). Plasmid DNA binds to the resin of the column and was washed with 30ml Buffer QC (1M NaCl, 50mM MOPS, pH 7.0, 15% v/v isopropanol). Plasmid DNA was then eluted with 15ml Buffer QN (1.6M NaCl, 50mM MOPS, pH 7.0, 15% v/v isopropanol) and collected in a 30ml endotoxin-free tube, before precipitation by addition of 10.5ml isopropanol at room temperature. Following centrifugation at ≥ 15,000xg for 30 minutes at 4°C, the supernatant was carefully discarded and the plasmid DNA pellet washed with 5ml endotoxin-free 70% v/v ethanol (Sigma-Aldrich) to remove precipitated salt and replace less volatile isopropanol. After further centrifugation at ≥ 15,000xg for 10 minutes at 4°C, the supernatant was again carefully discarded and the pellet air-dried for 5-10 minutes before re-dissolving plasmid DNA in 200µl endotoxin-free buffer TE (10mM Tris-HCl, pH 8.0, 1mM EDTA).

2.15.4 Plasmid DNA quantification and agarose gel analysis

Double stranded DNA concentration and purity was checked by measurement of absorbance at 260nm (A_{260}) and 280nm (A_{280}) using quartz capillaries (Amersham Biosciences, Little Chalfont, UK) and a GeneQuant spectrophotometer (Biochrom, Cambridge, UK). To check for DNA degradation, samples of TOPflash and FOPflash were resolved on a 1% agarose gel. Both vectors have a single site recognised by the BamHI restriction endonuclease (Boehringer Mannheim, Germany), and this was used to cut and linearise each plasmid in a 20µl reaction comprising 2µl 10x Buffer B (Boehringer Mannheim), 15.5µl UHQ water, 2µl (0.2µg) plasmid DNA and 0.5µl (5U) BamHI, incubated for 45 minutes at 37°C. Cut and uncut samples were loaded. Figure 2.4 shows the result of the degradation check. A single discrete band for

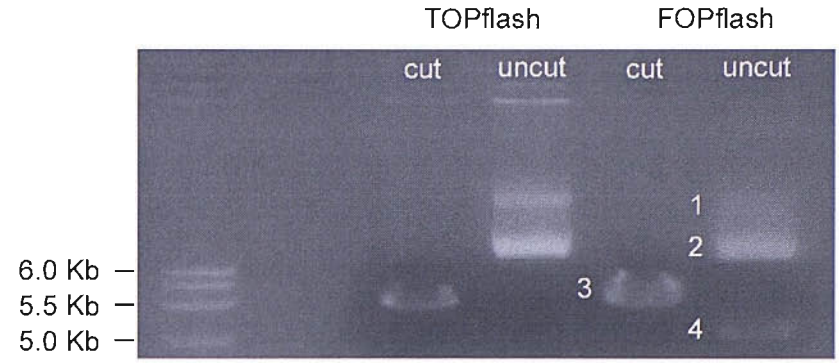

Figure 2.4: Degradation check for TOPflash and FOPflash.

Double-stranded plasmid DNA resolved as a band of predicted size (~5.5 Kb) on a 1% agarose gel (3) after it had been cut and linearised by a BamHI digest. By comparison, uncut circular plasmid resolved into three distinct bands corresponding to covalently closed (relaxed; 2), nicked (open circular; 1) and supercoiled (4) states.

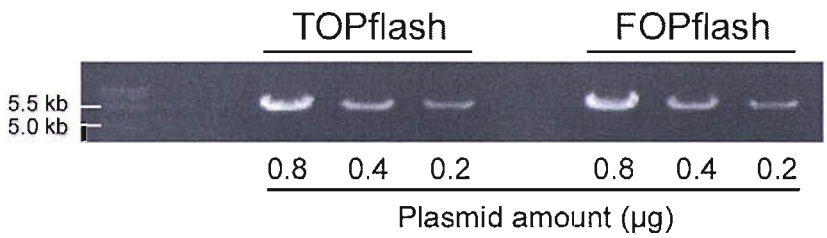

Figure 2.5: Quantification of TOPflash & FOPflash by agarose gel electrophoresis.

The relative concentration of TOPflash and FOPflash DNA was initially assessed using a GeneQuant spectrophotometer. Measurements were confirmed by resolving these constructs on a 1% agarose gel, after the plasmids had been cut and linearised using the BamH1 restriction endonuclease.

TOPflash and FOPflash that have been cut indicates that plasmid DNA has not degraded and is of predicted size (~5.5kb). Up to three discrete bands may be observed for uncut plasmid, corresponding to nicked, covalently closed and supercoiled DNA. Relative TOPflash and FOPflash concentrations were also confirmed by agarose gel analysis (Figure 2.5).

2.15.5 Sequencing TOPflash and FOPflash

The integrity of the three wild-type and mutated Tcf/Lef-1 consensus recognition sites in TOPflash and FOPflash, respectively, was confirmed by sequencing of plasmid DNA using the ABI Prism BigDye Terminator Cycle Sequencing Ready Reaction Kit (see Section 2.12). The sense (5'-ACGGTCACAGCTTGTCTGTA-3') and anti-sense (5'-CCGACTG CATCTGCGTGTTC-3') primers used were 80-90 bases away from the Tcf/Lef-1 consensus recognition sites, and were designed by Dr Jane Collins and synthesized by MWG-Biotech (Milton Keynes, UK).

2.15.6 Transient cell transfection

Transfection refers to the introduction of nucleic acids into eukaryotic cells, and is equivalent to the process of transformation in prokaryotic bacteria. Transient transfection of H292 and SW480 cells was achieved in accordance with the manufacturer's instructions using Effectene Transfection Reagent (Qiagen), a non-liposomal lipid formulation. Cells were seeded in 6-well Nunc plates (Invitrogen, Paisley, UK) at 5 x 10^5 (high-density) or 5 x 10^4 (low-density) cells per well, and incubated for 24 hours in 2ml per well standard RPMI 1640 medium (Invitrogen). Culture medium was then replaced with 1.6ml per well fresh standard RPMI 1640 medium before preparation of plasmid DNA. For each well, 0.79μg TOPflash or FOPflash was mixed with 0.01μg pRL-TK (minimum DNA contration 0.1μg/μl). Buffer EC (Effectene Transfection Reagent kit; Qiagen) was added to a total volume of 100μl, before addition of 6.4μl Enhancer (Effectene Transfection Reagent kit; Qiagen) and incubation for 5 minutes at room temperature. 8μl Effectene Transfection Reagent (1:10 ratio of DNA to Effectene) was then added, followed by further incubation for 10 minutes at room temperature, allowing complex formation to occur. Following addition of 0.6ml standard RPMI 1640 culture medium, transfection complexes were applied drop-wise to cells in the well. After incubation for 7 hours, cells were washed with 2ml serum-free UltraCULTURE medium (BioWhittaker, Wokingham, UK) ready for experimentation. For each measurement of relative Tcf/Lef-1 activity, duplicate TOPflash and FOPflash wells were employed. The optimal amount of plasmid DNA and ratio of DNA to Effectene Reagent used for

transfection were initially identified by transfecting H292 cells with the pEGFP-C1 vector (BD Biosciences, Oxford, UK). This plasmid contains the *Cytomegalovirus* (CMV) promoter upstream of the Green Fluorescent Protein (GFP) gene, and allowed estimates of transfection efficiency by direct inspection using a fluorescence microscope. Fluorescence Activated Cell Sorting (FACS) analysis, kindly performed by Miss Kate Hayes (University of Southampton), indicated 32.75% transfection efficiency in H292 cells using this protocol. Importantly, attempts by Dr Robert Powell (University of Southampton) to transfect primary human bronchial epithelial (HBE) cells using Effectene Reagent, or other lipid formulations, proved unsuccessful. Indeed, successful transfection of HBE cells could only be achieved using adenoviral constructs.

2.15.7 Cell harvesting and dual luciferase assays

Sequential measurement of the amounts of firefly and *Renilla* luciferase in each well of cells was achieved using the Dual-Luciferase Reporter (DLR) Assay System (Promega, Southampton, UK) in accordance with the manufacturer's instructions. The luciferase family of enzymes catalyse reactions resulting in the generation of light (Figure 2.6), the amount of which can be measured using a luminometer. Cells in each well were actively lysed and harvested by scraping following addition of 250µl 1x Passive Lysis Buffer (PLB), and stored at -20°C until time for dual luciferase assays. Each cell lysate was then thawed and allowed to reach room

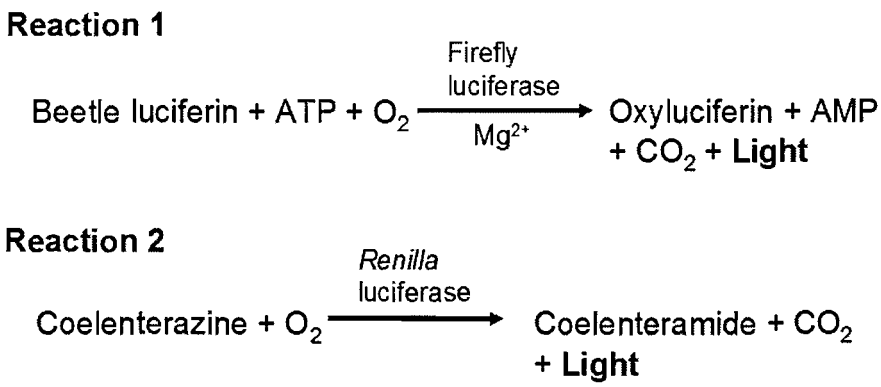

Figure 2.6: Dual luciferase assay reactions.

temperature. 50µl Luciferase Assay Reagent II (LAR II) was placed in the bottom of a disposable polypropylene luminometer tube (Promega) before careful addition of 10µl cell lysate. The resulting 'glow-type' luminescent signal from firefly luciferase activity was immediately measured in a luminometer (model TD-20/20; Turner Designs) pre-programmed to summate the amount of emitted light over a 10 second period, following an initial 2 second pre-measurement delay. The 'glow-type' luminescent signal from *Renilla* luciferase activity was next measured following addition of 50µl Stop & Glo Reagent. Importantly, Stop & Glo Reagent has been designed to simultaneously quench firefly luciferase activity and initiate the *Renilla* luciferase reaction. Furthermore, both 'glow-type' signals decay slowly over the periods of measurement, and the relationship between the amount of luciferase and light emitted is linear. Background light emission was measured from LAR II plus 1x PLB without sample ± Stop & Glo Reagent, and mean values subtracted from sample firefly and *Renilla* luciferase measurements. Corrected TOPflash and FOPflash firely luciferase values were then normalised to their respective internal pRL-TK controls before calculating the mean of duplicate measurements. The ratio of TOPflash-to-FOPflash was then used as a measure of *relative* Tcf/Lef-1 activity.

2.16 Immunofluorescent staining of cells *in vitro*

2.16.1 Fixation

Cells were cultured on 8-well Nunc Lab-Tek II glass chamber slides (Invitrogen, Paisley, UK) and were washed with pre-chilled unsupplemented RPMI 1640 medium (Invitrogen) before removal of the polystyrene chamber. Cells were then immediately fixed in pre-chilled acetone (Merck Biosciences, Nottingham, UK) for 10 minutes at -20°C, air-dried for 15 minutes, and stored for up to 2 weeks at -20°C wrapped in aluminium foil, prior to staining. Cells stained using the (pan-)β-catenin antibody (BD Biosciences, Oxford, UK) were fixed with 4% paraformaldehyde (Sigma-Aldrich, Poole, UK) in phosphate-buffered saline (PBS; Sigma-Aldrich) for 20 minutes at room temperature. Cells were then washed with PBS for 5 minutes, prior to application of 50mM ammonium chloride (NH_4Cl; Sigma-Aldrich) in PBS for 10 minutes at room temperature; NH_4Cl stabilises protein cross-linking by

paraformaldehyde. Cells were washed again for 5 minutes with PBS, then permeabilsed with 0.5% v/v Triton X-100 (Sigma-Aldrich) in PBS for 10 minutes at room temperature. Cells were stored for up to 2 weeks at +4°C in 1% sodium azide (Sigma-Aldrich), or washed with PBS prior to staining.

2.16.2 Immunostaining

Cells were initially rehydrated with Tris-buffered saline (TBS; see Section 2.1.11) for 10 minutes at room temperature, prior to application of Blocking Medium (see Section 2.1.11) for 30 minutes. Following drainage, cells were incubated for 2 hours with primary mouse monoclonal antibody at the optimal concentration (Table 2.2); the ABC antibody was applied for one hour rather two. Cells were then washed with TBS before 60 minute incubation with Fluorescein Isothiocyanate (FITC) conjugated rabbit anti-mouse IgG (F0261; DakoCytomation, Ely, UK) at a titre of 1:100 in 3% BSA/TBS. Cells were washed with TBS prior to counterstaining nuclei with 1μg/ml 7-aminoactinomycin D (7-AAD; Sigma-Aldrich) for 10 minutes. Following a final wash with TBS, slides were mounted with Mowiol (Harlow Chemical, Harlow, UK) containing 0.1% citifluor (Citifluor, London, UK), and left overnight at +4°C to allow

Antibody	Concentration used (μg/ml)
(Pan-)β-catenin (PBC; clone 14; IgG_1) BD Biosciences, Oxford, UK	2.5
Hypophosphorylated ('active') β-catenin (ABC; clone 8E7; IgG_1) Upstate Biotechnology, Lake Placid, NY, USA	4.3
E-cadherin (clone HECD-1; IgG_1) R&D Systems, Abingdon, UK	2.5
Ki67 (clone MIB-1; IgG_1) DakoCytomation, Ely, UK	7.0
Mouse IgG_1 isotype control (M-9269) Sigma-Aldrich, Poole, UK	

Table 2.2: Primary antibodies employed for immunofluorescent staining.

the mountant to set before examination using a confocal laser scanning microscope (model CLSM SP2; Leica Microsystems, Milton Keynes, UK). Isotype controls were employed as a check for non-specific staining. Precautions were taken to avoid photo-bleaching of FITC and 7-AAD. Images from the red (7-AAD), green (FITC) and phase-contrast channels of the confocal laser scanning microscope were layered and processed using Adobe Photoshop v5.5 software.

2.16.3 Semi-quantitative image analysis

At least three random fields of view were taken when quantifying the percentage nuclear staining by hypophosphorylated ('active') β-catenin (ABC), or the percentage of H292 or primary human bronchial epithelial (HBE) cells expressing Ki67. Counts of total and Ki67-positive cells were performed manually. To quantify the percentage nuclear ABC staining, Adobe Photoshop v5.5 software was used to create a 'mask' from the red (7-AAD) channel such that only nuclear ABC could be visualised when layered over the green (FITC) channel. The histogram function in Adobe Photoshop v5.5 was then used to summate the number of pixels in the green channel with an intensity level ranging from 50 to 255. The denominator (*total* number of 'nuclear' pixels) was then derived by layering the 'mask' onto a white background and measuring the number of pixels in the luminosity channel with an intensity of 255. In co-culture experiments, L-cell nuclei were excluded from the analysis.

2.17 Immunohistochemistry and immunocytochemistry

2.17.1 Glycolmethacrylate (GMA) processing

Endobronchial and colorectal cancer biopsies (anonymised bowel resection specimens), and air-liquid interface (ALI) cultures, were fixed in ice-cooled acetone (Merck Biosciences, Nottingham, UK), supplemented with 2mM phenylmethyl-sulfonyl fluoride (PMSF; Sigma-Aldrich, Poole, UK) and 20mM idioacetamide (Sigma-Aldrich) to inhibit protease activity, and left overnight at -20°C. The following day, biopsies were transferred to fresh acetone followed by methyl benzoate (Merck Biosciences), each for 15 minutes at room temperature. Tissue was then infiltrated with 5% methyl benzoate in GMA solution A (Park Scientific,

Northampton, UK) for 6 hours at 4°C, with changing of the GMA solution every 2 hours. Biopsies were embedded in GMA resin (10ml GMA solution A, 250µl GMA solution B, 45mg benzoyl peroxide; Park Scientific) that was allowed to polymerise overnight at +4°C. Blocks were stored in air-tight containers at -20°C until sectioned.

2.17.2 Sectioning of GMA-embedded material

2µm thick tissue sections were cut using a Jung Supercut 2065 ultramicrotome (Leica Microsystems, Milton Keynes, UK), and allowed to float on 0.2% v/v ammonia water (Sigma-Aldrich) for 60-90 seconds. Sections were then picked onto 0.01% w/v poly-L-lysine (PLL) coated glass microscope slides (Merck Biosciences) and allowed to dry over 1-2 hours at room temperature. Slides were stored wrapped in aluminium foil at -20°C for up to 2 weeks until stained.

2.17.3 Immunostaining

Endogenous peroxidase was inhibited with a mix of 0.1% sodium azide (Sigma-Aldrich) and 0.3% hydrogen peroxide (Sigma-Aldrich), applied for 30 minutes at room temperature. Sections were then washed with Tris-buffered saline (TBS; see Section 2.1.11). Blocking Medium (see Section 2.1.11) was next applied for 30 minutes. Following drainage, sections were incubated overnight at room temperature with primary mouse monoclonal antibody at the optimal concentration (Table 2.3). After washing with TBS, biotinylated rabbit anti-mouse IgG F(ab)2 (E0413; DakoCytomation, Ely, UK) was applied at a titre of 1:300 in 3% BSA/TBS for 2 hours. After washing with TBS, secondary antibody detection was achieved using the Liquid DAB (3,3'-diaminobenzidine) Substrate Pack (BioGenex, Wokingham, UK). Tris-HCl containing 1:200 Streptavidin-Biotin complexes was applied for 2 hours before washing with TBS. DAB solution was then applied for 10 minutes, before washing in running tap water for 5 minutes. Sections were counterstained with Mayer's haematoxylin (BioGenex) for 2 minutes, and allowed to 'blue' in running tap water for 5 minutes. Slides were drained and Crystal Mount (Biomedia, Foster City, CA, USA) applied before baking at 80°C for 10 minutes. When the slides were cool and completely dry, sections were mounted with Dibutyl phthalate containing xylene

(DPX; BDH, Poole, UK). Isotype controls were employed to check for non-specific staining. Images were captured using an Axioskop 2 microscope (Carl Zeiss, Welwyn Garden City, UK), AxioCam digital camera (Carl Zeiss) and KS400 software (Carl Zeiss).

Antibody	Concentration used (µg/ml)
(Pan-)β-catenin (PBC; clone 14; IgG_1) BD Biosciences, Oxford, UK	0.3125
Hypophosphorylated ('active') β-catenin (ABC; clone 8E7; IgG_1) Upstate Biotechnology, Lake Placid, NY, USA	4.3
Mouse IgG_1 isotype control (M-9269) Sigma-Aldrich, Poole, UK	

Table 2.3: Primary antibodies employed for immunostaining.

2.18 Statistical analysis

Parametric data are presented as mean ± standard error of the mean (S.E.M.), with at least three independent experiments performed. For comparison of TOPflash reporter activity between H292 and SW480 cells (chapter 3), and semi-quantitative image analysis of the percentage nuclear staining by hypophosphorylated ('active') β-catenin (ABC), or percentage of cells expressing Ki67, statistical significance was assessed using the unpaired Student's T-test. All quantitative RT-PCR (qPCR; TaqMan) and remaining TOPflash data were analysed using the paired Student's T-test, comparing stimulated and control H292 cell populations. In addition, qPCR and TOPflash time-responses were assessed using one-way Analysis of Variance (ANOVA). Data from RNase protection assays (RPA) involving primary human bronchial epithelial (HBE) cells were treated as non-parametric and presented as median + interquartile range. At least four independent experiments were performed, and statistical significance assessed using the (unpaired) Mann-Whitney U test. All

statistical tests were processed using SPSS v10.1 software for Windows, and statistical significance set at $p < 0.05$.

CHAPTER 3

IDENTIFICATION OF THE CANONICAL WNT SIGNAL TRANSDUCTION PATHWAY IN ADULT HUMAN AIRWAY EPITHELIAL CELLS

3.1 Aims of the study

Bronchial epithelial repair plays an important role in the pathogenesis of chronic inflammatory disorders of the airways, such as asthma (Holgate et al., 1999) and smoking-related chronic bronchitis (O'Donnell et al., 2004; Richter et al., 2002). Therefore, investigating the processes that regulate epithelial repair could provide new insights into these conditions. Postulating that ***reactivation of the canonical Wnt signalling pathway plays a role in human bronchial epithelial regeneration following injury***, the aims of this study were to test the sub-hypothesis that ***adult human bronchial epithelial (HBE) cells express key components of the Wnt/β-catenin signalling pathway***, using *in vitro* cultures of primary HBE cells obtained from volunteer subjects by fibreoptic bronchoscopy.

Evidence suggests that nuclear signalling by β-catenin requires expression of one or more members of the Tcf/Lef-1 family of transcription factors (Molenaar et al., 1996; van Noort and Clevers, 2002). Therefore, expression of these transcription factors was investigated at the mRNA and protein level using reverse transcription-polymerase chain reaction (RT-PCR) and Western blot analysis. The current model of canonical Wnt signalling suggests translocation of β-catenin into the nuclear compartment of cells to be a prerequisite for pathway activation (Miller et al., 1999). Thus, evidence of nuclear localisation of β-catenin has been widely used in the literature as a surrogate marker for canonical Wnt signalling activity. Therefore, the cellular expression and localisation of β-catenin was investigated by laser confocal microscopy. Finally, to investigate Tcf/Lef-1 transcriptional activity, cells were transiently transfected with a Tcf/Lef-1 OPtimised reporter plasmid (TOPflash) comprising three copies of the Tcf/Lef-1 consensus recognition sequence (5'-AGATCAAAGGG-3') (van Noort and Clevers, 2002) upstream of the *Herpes*

simplex virus (HSV) thymidine kinase (TK) promoter and firefly (*Photinus pyralis*) luciferase gene.

3.2 Methods and results

3.2.1 H292 and primary HBE cells express TCF/LEF-1 transcription factors

For analysis of TCF/LEF-1 gene expression, $55cm^2$ Nunc petri dishes were seeded with 3×10^6 H292 or SW480 cells in 8ml standard RPMI 1640 medium, incubated for 32 hours, and then serum-starved for 18 hours in UltraCULTURE medium. Cells were lysed with 5.5ml TRIzol Reagent per petri dish before RNA extraction and DNase treatment to remove contaminating DNA (see Section 2.8). RNA was reverse transcribed to cDNA prior to 35 cycles PCR with forward and reverse primers designed for TCF/LEF-1 family members (Table 3.1 and Figure 3.1) using PrimerSelect (Lasergene5) software (see Section 2.11). Each cycle consisted of a *denaturation* step (94°C for 20 seconds), followed by an *annealing* step (58°C for 30 seconds) and an *extension* step (72°C for 60 seconds); the Mg^{2+} concentration was 1.5mM. Amplicons were resolved by 1.5% agarose gel electrophoresis, and products

Gene (Accession N°)	**Primer sequences** (**F**orward and **R**everse)	**Exon**	**Product size** (base pairs)
LEF-1 (NM_016269.1)	**F:** 5'-ACCCATCCCGAGACATCAAATAA-3' **R:** 5'-CCAGGAGGACCGGGAATCATA-3'	3-4 7	375
TCF-1 (NM_201634.1)	**F:** 5'-CTTAAGGAGAGCGCTGCCATCAAC-3' **R:** 5'-TTATCTGCACGGACCACACCAATC-3'	6 9-10	276
TCF-3 (NM_031283.1)	**F:** 5'-GGCCTCAGGACAGCGCGTTCTTTA-3' **R:** 5'-CAGGCTGGACATCGAGGCGTTCAT-3'	3 7-8	530
TCF-4 (NM_030756.1)	**F:** 5'-TAGGCGCCAACGACGAACTGATTT-3' **R:** 5'-GGAACCTGGACACGGAAGCATTGA-3'	1 7-8	777

Table 3.1: RT-PCR primers for detecting TCF/LEF-1 family members.
Forward (sense) and reverse (anti-sense) primers were designed using PrimerSelect (Lasergene5) software. One primer in each primer pair was designed to span an intron-exon boundary, thereby reducing the chance of amplifying genomic DNA. The optimal annealing temperature was 58°C, and the optimal Mg^{2+} concentration was 1.5mM.

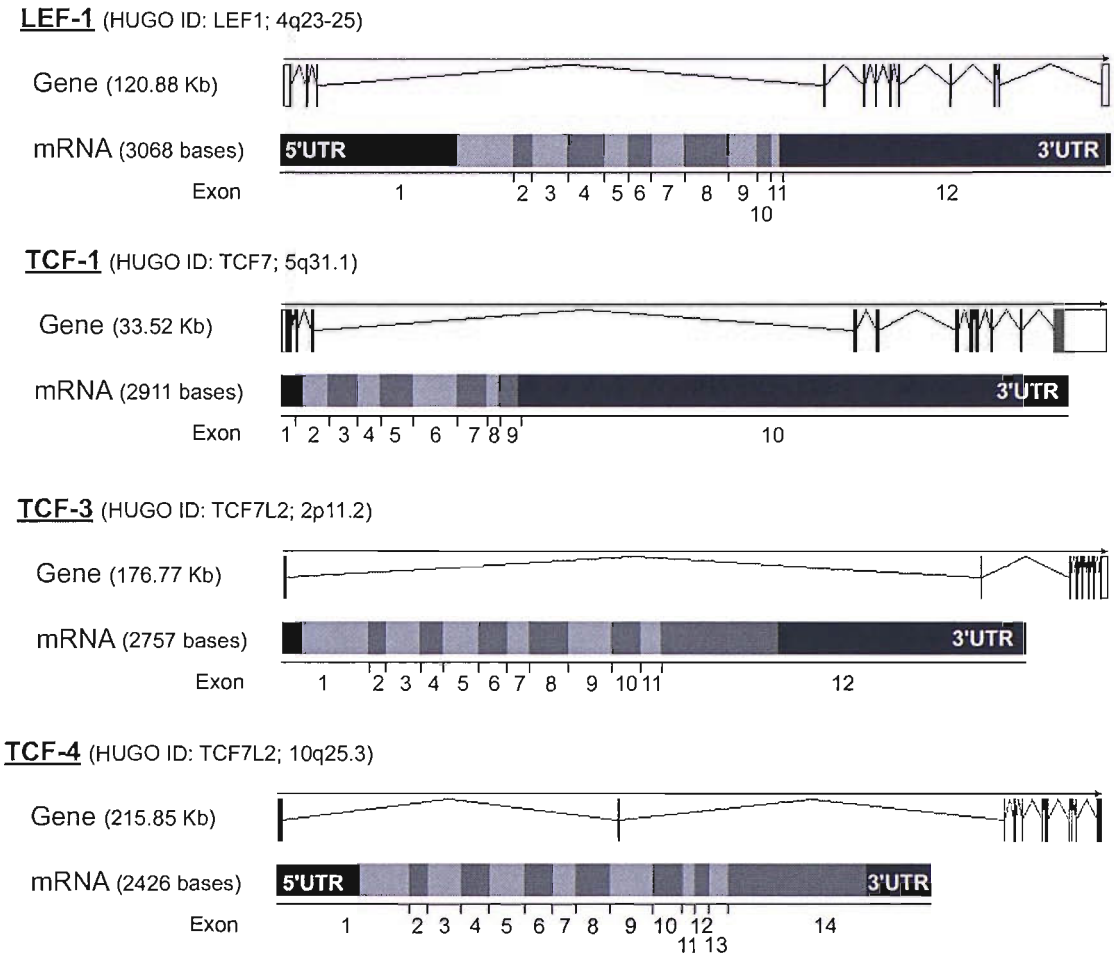

Figure 3.1: TCF/LEF-1 genes and mRNA.

The Ensembl database was interrogated for genomic and mRNA sequences encoding each member of the TCF/LEF-1 family. Introns and exons were identified along with the coding sequence and untranslated regions (UTR).

detected using ethidium bromide and the Gene Genius Bio Imaging System (Syngene, Cambridge, UK). Commercially available primers for β-actin (Promega, Southampton, UK) were used as a positive control. The SW480 colorectal cancer cells express all four Tcf/Lef-1 family members (Brantjes et al., 2001), and were therefore also used as a positive control. At the time of harvesting, SW480 cells were 60-70% confluent and H292 cells were >90% confluent. Three independent experiments were performed per cell type.

Figure 3.2 shows a representative agarose gel in which amplicons of predicted size are seen for each member of the TCF/LEF-1 family in SW480 cells. A second, smaller DNA product is also observed for LEF-1, and larger product observed for

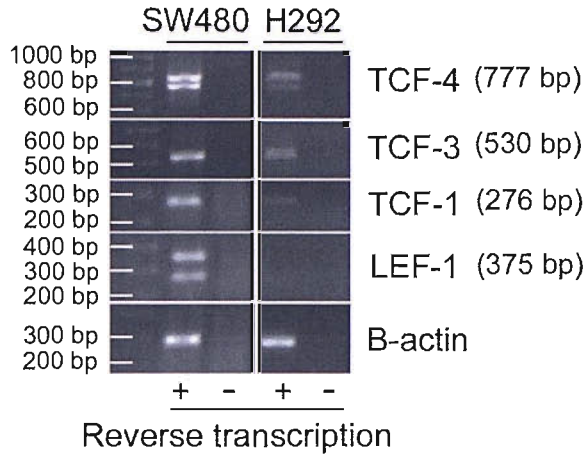

Figure 3.2: Expression of TCF/LEF-1 mRNA in H292 cells.

RNA was extracted from confluent H292 bronchial epithelial cells in serum-free basal medium. RT-PCR (35 cycles) was used to amplify cDNA encoding members of the TCF/LEF-1 family, and amplicons were resolved by 1.5% agarose gel electrophoresis. β-actin and SW480 colorectal carcinoma cells were used as positive controls. RT-minus negative controls were also included. In H292 cells, bands of predicted size were observed for TCF-4 and -3, with low-level expression of TCF-1 and no detectable message for LEF-1. A second, smaller band was observed for LEF-1 and larger band observed for TCF-4; these were later shown to represent splice variants (see Figure 3.5).

TCF-4. Importantly, no bands are detected in the RT-minus control, indicating that amplicons were derived from amplified RNA and not genomic DNA. Furthermore, the absence of DNA fragments for β-actin in the RT-minus control excludes sample contamination. In H292 cells, amplicons of predicted size are seen for TCF-4 and -3, with low-level expression of TCF-1 and no detectable message for LEF-1.

In parallel experiments, primary HBE cell cultures were established by seeding cells brushed from the proximal airways of mild persistent asthmatic and normal volunteer subjects. At passage 2 (P2), 5 x 10^5 viable HBE cells from each subject were seeded onto collagen-coated 55cm^2 Nunc petri dishes containing 8ml BEGM. Cells were incubated and culture medium changed every 48 hours. When near-confluent, BEGM was replaced with growth factor-free BEBM. Cells were then lysed with 5.5ml TRIzol Reagent per petri dish prior to RNA extraction, DNase treatment and analysis by RT-PCR. Figure 3.3 shows a representative agarose gel with samples from three mild persistent asthmatic and three normal control subjects. Bands of predicted size are shown for TCF-4 and -3, with low-level expression of LEF-1, and no detectable

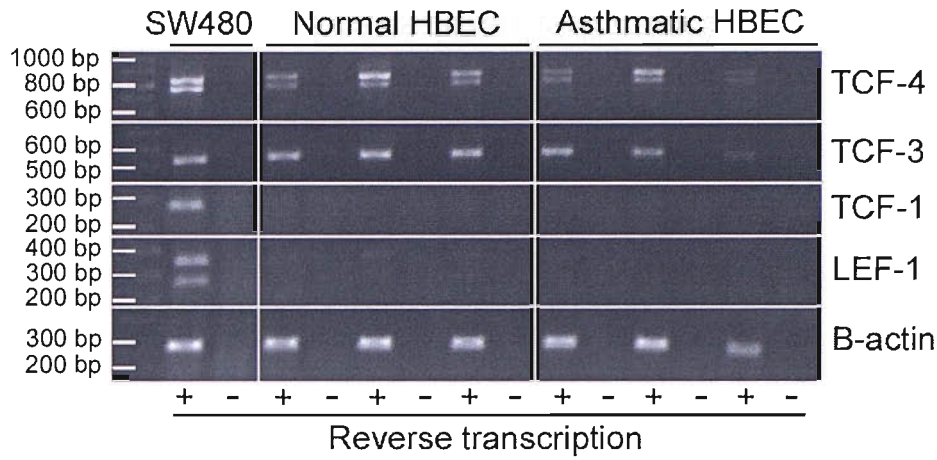

Figure 3.3: Expression of TCF/LEF-1 mRNA in normal and asthmatic HBE cells.

RNA was extracted from cultured primary human bronchial epithelial (HBE) cells at confluence in serum-free basal medium. RT-PCR (35 cycles) was used to amplify cDNA encoding members of the TCF/LEF-1 family, and amplicons were resolved by 1.5% agarose gel electrophoresis. β-actin and SW480 colorectal carcinoma cells were used as positive controls. RT-minus negative controls were also included. In a representative gel from three mild persistent asthmatic and three normal control subjects, bands of predicted size are shown for TCF-4 and -3, with low-level expression of LEF-1, and no detectable message for TCF-1. A second, smaller band is seen for LEF-1 and larger band observed for TCF-4. These represent splice variants (see Figure 3.5).

message for TCF-1. An additional DNA product is again observed for TCF-4, with no detection of fragments in the RT-minus controls. No difference in the pattern of TCF/LEF-1 gene expression was identified between the asthmatic and control groups.

To check for low-level expression of LEF-1 in H292 cells and TCF-1 in primary HBE cells, RT-PCR products were resolved by 1.5% agarose gel electrophoresis and bands detected using vistra green (Amersham Biosciences, Little Chalfont, UK) and laser light, a more sensitive detection system than ethidium bromide. The LEF-1 DNA product of predicted size was not detected in H292 cells, but low-level expression of the smaller LEF-1 PCR product was seen. In samples from three mild persistent asthmatic and three normal control subjects, variable, low-level expression of TCF-1 and LEF-1 was observed. No products were detected in the RT-minus controls (Figure 3.4).

For sequencing of TCF/LEF-1 RT-PCR products, dsDNA amplicons were purified using the MinElute PCR Purification Kit (Qiagen, Crawley, UK), and the ABI Prism

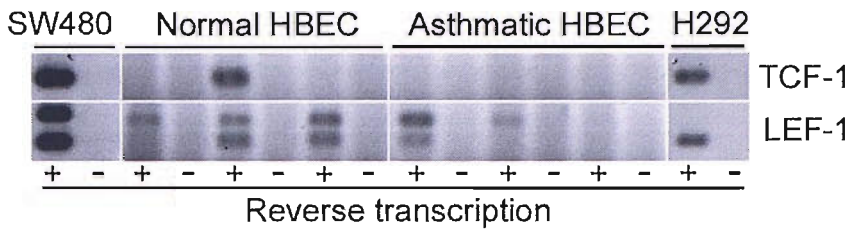

Figure 3.4: Expression of TCF-1 & LEF-1 mRNA in H292 and HBE cells.

RNA was extracted from confluent H292 and primary human bronchial epithelial (HBE) cells in serum-free basal medium. RT-PCR (35 cycles) was used to amplify cDNA encoding TCF-1 and LEF-1, and amplicons were resolved by 1.5% agarose gel electrophoresis. Bands were detected using vistra green, a more sensitive detection system than ethidium bromide. SW480 colorectal carcinoma cells were used as a positive control. RT-minus negative controls were also included. In a representative gel from three mild persistent asthmatic and three normal control subjects, variable low-level expression of TCF-1 and LEF-1 can be seen.

BigDye Terminator Cycle Sequencing Ready Reaction Kit v3.0 (Applied Biosystems, Brackley, UK) employed (see Section 2.12). Extension products were then purified using DyeEx Spin Columns (Qiagen), and resolved by polyacrylamide gel electrophoresis on an ABI Prism 377 DNA Analyzer (Applied Biosystems). The quality of the sequence signal was inspected using Chromas v1.45 software, and alignment with reference sequence achieved using MegAlign (Lasergene5) software. Prior to sequencing, amplicons corresponding to the upper and lower bands observed for LEF-1 and TCF-4 were resolved by 1% agarose gel electrophoresis, individually picked using sterile pipette tips, added to separate 20µl aliquots of nuclease-free water, and reamplified by 20 cycles PCR. Sequences for RT-PCR products corresponding to TCF-1, TCF-3, and upper and lower products for LEF-1 were established using the appropriate forward primer in Table 3.1. However, tendency for the sequence signal to degenerate beyond 400bp from the primer site meant that additional reverse primers were required in order to establish the sequences of the upper and lower products isolated using the primers for TCF-4; these additional reverse primers (5'-GCACCACTGGCACTTTGTTAGA-3' and 5'-CATTGCTGTACGTGATAAGAGG-3') were designed using PrimerSelect (Lasergene5) software. Sequencing confirmed all RT-PCR products of predicted size to be members of the TCF/LEF-1 family (sequences in Section 10.1). Interestingly, the lower LEF-1 band was found to correspond to a splice variant (isoform) with exon 6 (84 bp) deleted. Furthermore, the lower TCF-4 product (777 bp) corresponds to

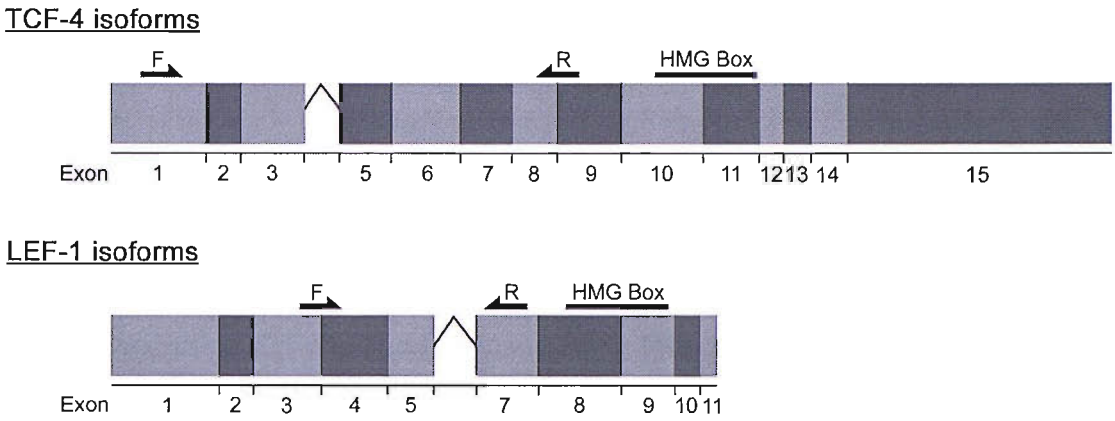

Figure 3.5: Expression of TCF-4 & LEF-1 isoforms in H292 and HBE cells.

Upper and lower bands observed for LEF-1 and TCF-4 RT-PCR were resolved by 1.5% agarose gel electrophoresis, reamplified by PCR (20 cycles), and sequenced using the ABI Prism BigDye Terminator Cycle Sequencing Ready Reaction Kit along with forward (F) or reverse (R) primers. The lower LEF-1 band in figures 3.2, 3.3 and 3.4 corresponds to a splice variant with exon 6 (84 bp) deleted. The lower TCF-4 band (777 bp) in figures 3.2 and 3.3 corresponds to Vega gene TCFL2-003, the sequence of which was used to design the primers for RT-PCR. The upper TCF-4 band (846 bp) has an additional 69 bp corresponding to exon 4 in Vega genes TCFL2-002 and TCFL2-004; thus, the lower TCF-4 band is a splice variant with exon 4 (69 bp) deleted.

Vega gene TCFL2-003, the sequence of which was used to design the primers for RT-PCR. The upper TCF-4 amplicon (846 bp) has an additional 69 bp corresponding to exon 4 in Vega genes TCFL2-002 and TCFL2-004. Thus, the lower TCF-4 band is a splice variant with exon 4 (69 bp) deleted (Figure 3.5).

3.2.2 H292 and primary HBE cells express Tcf-4 protein

Western blot analysis was next used to investigate Tcf-4 protein expression, but owing to the unavailability of specific antibodies, analysis of Tcf-1, Tcf-3 and Lef-1 protein was not possible at this time. 6-well Nunc plates were seeded with 5 x 10^5 H292 cells per well in 2ml standard RPMI 1640 medium, incubated for 30 hours, and then placed in serum-free UltraCULTURE medium for 18 hours. When harvested, H292 cells were >80% confluent. Three independent experiments were performed. In parallel experiments, primary HBE cell cultures were established from three normal volunteer subjects. At passage 2 (P2), collagen-coated 6-well Nunc plates were seeded with 1 x 10^5 viable HBE cells per well in 2ml BEGM. Cells were incubated

and culture medium changed every 48 hours. When confluent, BEGM was replaced with growth factor-free BEBM for 18 hours before harvesting. Cell lysates were obtained by scraping in 200µl/well of Denaturing Sample Lysis Buffer (DSLB), and processed as described in Section 2.14. Proteins were resolved on a 7.5% sodium dodecylsulphate (SDS) polyacrylamide gel and transferred to a Hybond C nitrocellulose membrane. Immunodetection of Tcf-4 protein on the nitrocellulose blot was achieved using Tcf-4 antibody (clone 6H5-3; IgG_{2a}; Upstate Biotechnology, USA), horseradish peroxidase (HRP) conjugated rabbit anti-mouse IgG (P0260; DakoCytomation, Ely, UK), and the enhanced chemiluminescence (ECL Plus) detection system (Amersham Biosciences). Proteins were imaged using a GeneGnome chemiluminescence imaging system and GeneSnap software (Syngene). A mouse IgG_{2a} isotype control antibody (M-9144; Sigma-Aldrich, Poole, UK) was employed as a check for non-specific staining. In keeping with the RT-PCR data, bands of predicted size for Tcf-4 protein (66 kD) were observed in both H292 and primary HBE cells, not evident in the isotype control. A second band of between 50 and 66 kD was also detected with both anti-Tcf-4 and the isotype control, indicating it to be non-specific staining with a relative molecular mass consistent with albumin (Figure 3.6).

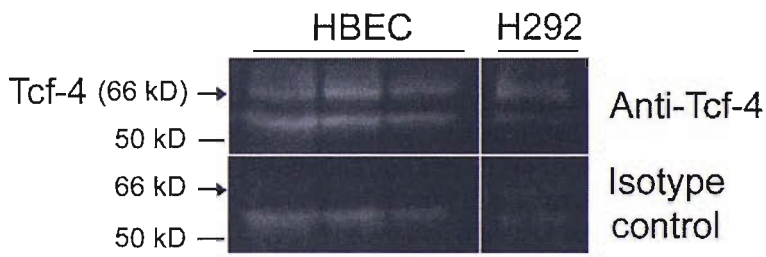

Figure 3.6: Expression of Tcf-4 protein in H292 and HBE cells.

H292 and HBE cell cultures from three healthy volunteer subjects were grown to confluence, lysed into SDS sample buffer, and analysed by SDS-PAGE and Western blotting with a nitrocellulose membrane and anti-Tcf-4 monoclonal antibody or isotype control. Both HBE and H292 cells expressed a band of predicted size for Tcf-4 protein (66 kD) not evident in the isotype control. A lower band was also observed with a relative molecular mass consistent with that for albumin.

3.2.3 H292 and primary HBE cells exhibit nuclear localisation of β-catenin

In addition to using a pan-β-catenin antibody to investigate the cellular expression and localisation of β-catenin by laser confocal microscopy, a second monoclonal antibody was employed to assess the hypophosphorylated (non-phosphorylated T41 and S37) pool of β-catenin, thought to represent the transcriptionally active fraction (Staal et al., 2002; van Noort et al., 2002). 8-well Nunc Lab-Tek II glass chamber slides were seeded with 1.5 x 10^5 H292 or SW480 cells per chamber in 500μl standard RPMI 1640 medium. Cells were incubated for 54 hours with culture medium changed at 24 hours, and then placed in serum-free UltraCULTURE medium for 18 hours. Cells were fixed in pre-chilled acetone for 10 minutes at -20°C, and then air-dried for 15 minutes. Alternatively, they were fixed at room temperature with 4% paraformaldehyde in phosphate-buffered saline (PBS) for 20 minutes, stabilised with 50mM ammonium chloride (NH_4Cl) in PBS for 10 minutes, and then permeabilised with 0.5% v/v Triton X-100. When fixed, H292 cells were >80% confluent. Cells were immunostained using either pan-β-catenin (PBC; clone 14; BD Biosciences, Oxford, UK) or hypophosphorylated ('active') β-catenin (ABC; clone 8E7; Upstate Biotechnology, USA) monoclonal antibodies, followed by FITC conjugated rabbit anti-mouse IgG (F0261; DakoCytomation), as described in Section 2.16.2. Nuclei of H292 cells were counterstained with 7-aminoactinomycin D (7-AAD; Sigma-Aldrich). The SW480 colorectal cancer cells contain a known APC gene mutation, leading to nuclear localisation of β-catenin (Munne et al., 1999) and high constitutive activation of Tcf/Lef-1 transcription factors (Korinek et al., 1997), and were therefore used as a positive control. When fixed in acetone at -20°C, intense nuclear localisation of FITC (green) labelled β-catenin was seen using the ABC antibody, but not when using the PBC antibody. In contrast, nuclear epitopes were preserved when the PBC antibody was applied to cells fixed in 4% paraformaldehyde and permeabilised with Triton X-100. In all preparations, diffuse cytosolic staining was observed and membranous staining was absent (Figure 3.7). Importantly, staining was absent in the isotype controls. Thus, fixation with 4% paraformaldehyde at room temperature was employed when using the PBC antibody.

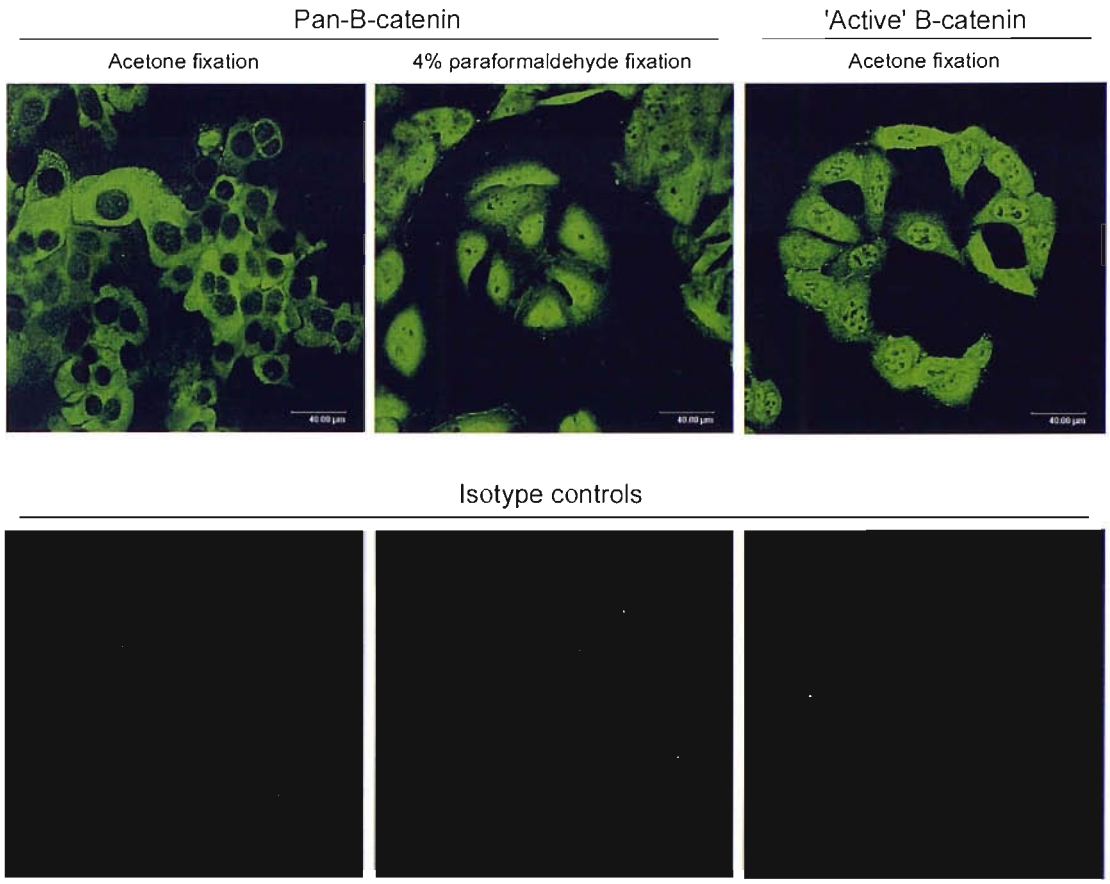

Figure 3.7: Confocal images of β-catenin expression in SW480 cells.

SW480 colorectal carcinoma cells were used as a positive control for immunofluorescent localisation of FITC (green) labelled β-catenin by laser confocal microscopy. With cultured cells fixed in acetone at -20°C, intense nuclear localisation of β-catenin was seen using the anti-hypophosphorylated ('active') β-catenin (ABC) monoclonal antibody, but not when using the anti-pan-β-catenin (PBC) monoclonal antibody (clone 14; BD Biosciences, Oxford, UK). In contrast, nuclear epitopes were preserved when the PBC monoclonal antibody was applied to cells fixed with 4% paraformaldehyde and permeabilised with Triton X-100 at room temperature. In all preparations, diffuse cytosolic staining was observed, but membranous staining was absent. Nuclei were not counterstained with 7-AAD. The isotype controls were negative.

Figure 3.8 shows a representative confocal image of confluent H292 cells in serum-free basal medium fixed in 4% paraformaldehyde, permeabilised with Triton X-100, and stained with FITC-labelled PBC antibody. Nuclei are counterstained with 7-AAD (red). In contrast with SW480 cells, the pattern of PBC expression is predominantly membranous, but yellow co-localisation of FITC and 7-AAD is also present (arrowed), indicating nuclear localisation of β-catenin. The isotype control shows no significant staining. The same pattern of β-catenin expression was also observed

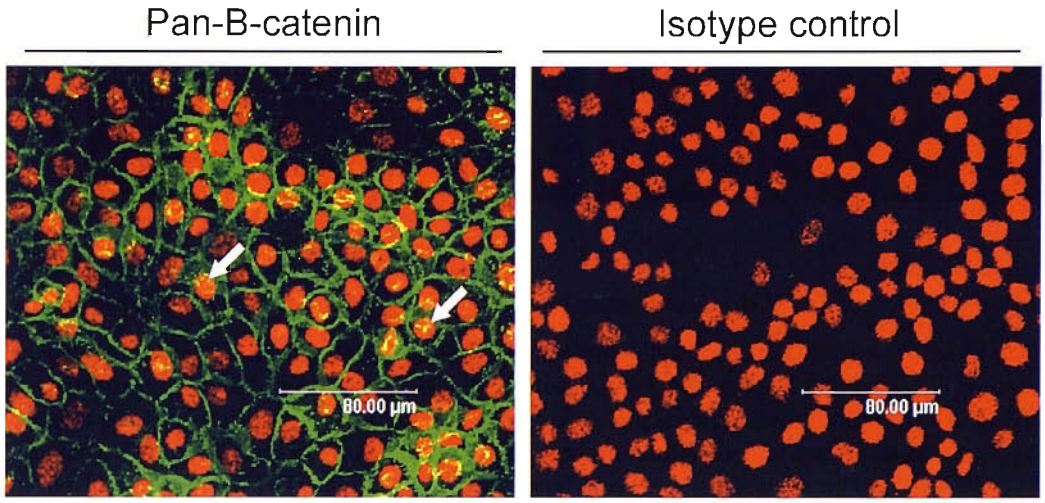

Figure 3.8: Confocal image of pan-β-catenin expression in H292 cells.

Confluent H292 bronchial epithelial cells in serum-free basal medium were fixed with 4% paraformaldehyde, permeabilised with Triton X-100, and stained using FITC (green) labelled anti-pan-β-catenin (PBC) monoclonal antibody. Nuclei were counterstained using 7-AAD (red). The pattern of PBC expression was predominantly membranous. In addition, yellow co-localisation of FITC and 7-AAD (arrowed) suggests nuclear localisation of PBC. The isotype control was negative.

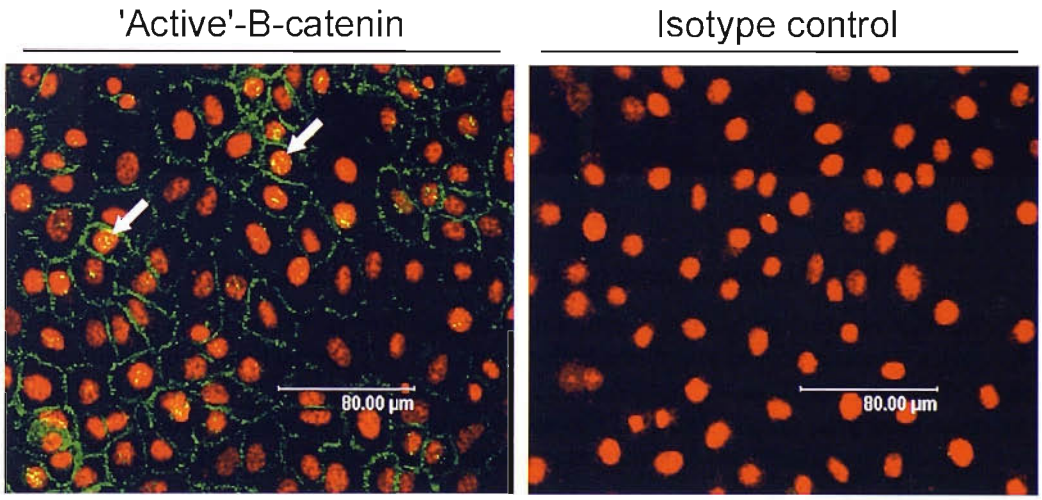

Figure 3.9: Confocal image of 'active' β-catenin expression in H292 cells.

Confluent H292 bronchial epithelial cells in serum-free basal medium were fixed with acetone and stained using FITC (green) labelled anti-hypophosphorylated ('active') β-catenin (ABC) monoclonal antibody. Nuclei were counterstained using 7-AAD (red). In addition to membranous staining, yellow co-localisation of FITC and 7-AAD (arrowed) suggests nuclear localisation of ABC. The isotype control was negative.

using the ABC antibody, indicating nuclear localisation of hypophosphorylated (transcriptionally active) β-catenin (Figure 3.9).

In parallel experiments, primary HBE cell cultures were established from normal volunteer subjects. At passage 2 (P2), collagen-coated 8-well Nunc Lab-Tek II glass chamber slides were seeded with 5 x 10^4 viable HBE cells per chamber in 500μl BEGM. Cells were incubated and culture medium changed every 48 hours. When confluent, BEGM was replaced with growth factor-free BEBM for 18 hours, prior to fixation and immunostaining for β-catenin. Figure 3.10 shows the pattern of PBC expression to be predominantly membranous with evidence of diffuse cytosolic staining and minimal nuclear localisation. However, in addition to exhibiting membranous staining, yellow co-localisation of FITC and 7-AAD was more readily evident with the ABC antibody, indicating nuclear localisation of transcriptionally active β-catenin (Figure 3.11).

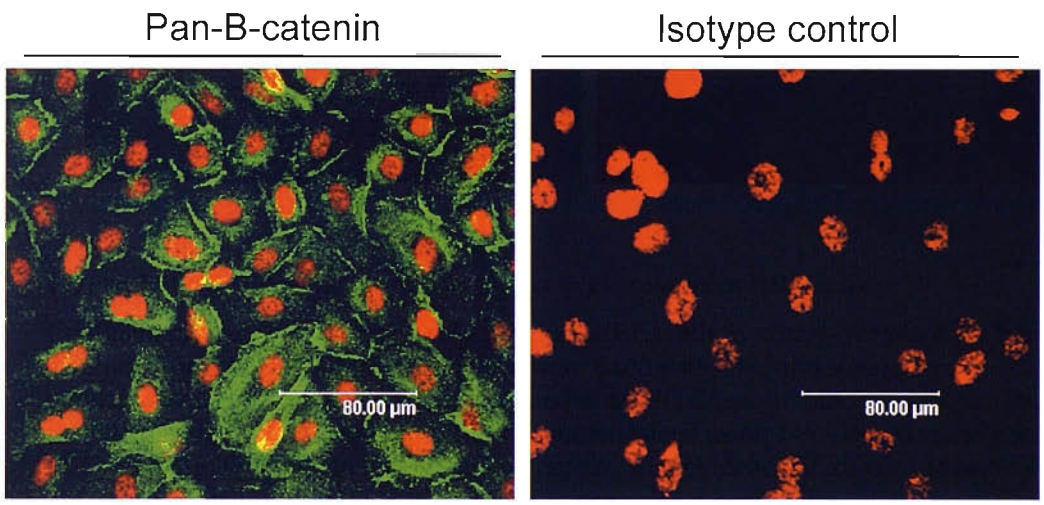

Figure 3.10: Confocal image of pan-β-catenin expression in HBE cells.

Confluent primary human bronchial epithelial (HBE) cells in serum-free basal medium, obtained from healthy volunteer subjects, were fixed with 4% paraformaldehyde, permeabilised with Triton X-100, and stained using FITC (green) labelled anti-pan-β-catenin (PBC) monoclonal antibody. Nuclei were counterstained using 7-AAD (red). The pattern of PBC expression was predominantly membranous, with evidence of diffuse cytosolic staining, and minimal nuclear localisation. The isotype control was negative.

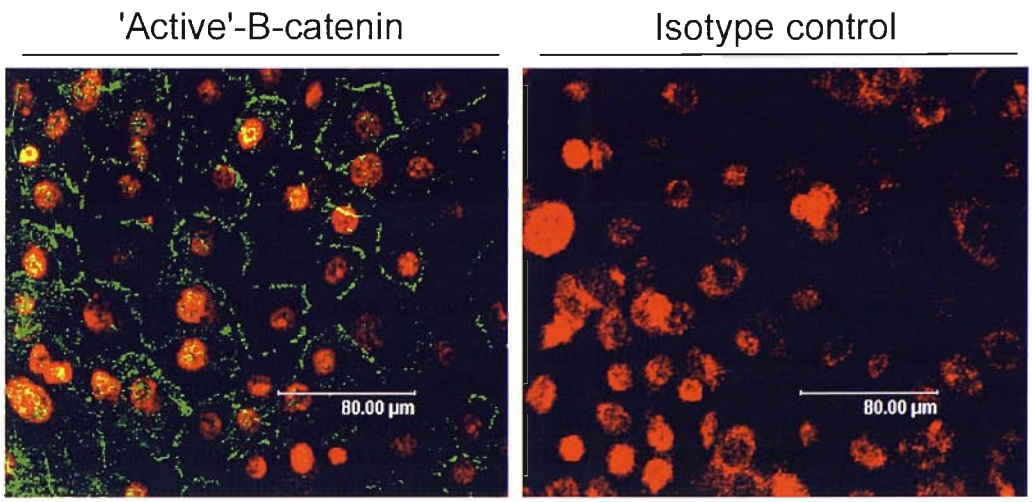

Figure 3.11: Confocal image of 'active' β-catenin expression in HBE cells.

Confluent primary human bronchial epithelial (HBE) cells in serum-free basal medium, obtained from healthy volunteer subjects, were fixed with acetone and stained using FITC (green) labelled anti-hypophosphorylated ('active') β-catenin (ABC) monoclonal antibody. Nuclei were counterstained using 7-AAD (red). Yellow co-localisation of FITC and 7-AAD was evident, indicating nuclear localisation of ABC. In addition, ABC localised to membranous cell-cell contacts. The isotype control was negative.

3.2.4 Confluent H292 cells exhibit low constitutive activation of a Tcf/Lef-1 reporter

The TOPflash reporter was used to investigate baseline Tcf/Lef-1 transcriptional activity in human bronchial epithelial cells. However, adequate transient transfection of primary HBE cells proved elusive, leading to cautious reliance on the immortalised human bronchial epithelial tumour (H292) cell line. 6-well Nunc dishes were seeded with 5 x 10^5 H292 or SW480 cells per well in 2ml standard RPMI 1640 medium, incubated for 24 hours, and then transiently transfected with 0.79µg TOPflash or FOPflash (Upstate Biotechnology, USA) per well, mixed with 0.01µg pRL-TK plasmid (Promega), using Effectene Transfection Reagent (Qiagen) at a 1:10 DNA:Effectene ratio (see Section 2.15.6). In each experiment, duplicate TOPflash and FOPflash wells were employed. Cells were incubated for 7 hours, before serum-starvation in UltraCULTURE medium for 18 hours. Cells were then actively lysed and harvested in 250µl per well 1x Passive Lysis Buffer (PLB), and The Dual-Luciferase Reporter (DLR) Assay System (Promega) used to measure the amounts of

firefly and *Renilla* luciferase in each sample (see Section 2.15.7). Background light emission was measured from LAR II with 1x PLB without sample ± Stop & Glo Reagent, and mean values subtracted from sample firefly and *Renilla* luciferase measurements. Corrected TOPflash and FOPflash firely luciferase values were then normalised to their respective internal pRL-TK controls before calculating the mean of duplicate samples. For comparison between H292 (n=6) and SW480 (n=3) cells, data are presented as mean TOPflash:FOPflash ratio ± standard error of the mean (S.E.M.), and statistical significance assessed using the unpaired Student's T-test. When harvested, SW480 cells were 60-70% confluent, and H292 cells were >80% confluent. A 17.5-fold increase in TOPflash activity above FOPflash control was seen in SW480 cells, indicating high constitutive activation of the canonical Wnt pathway. In contrast, low constitutive activation was observed in confluent H292 cells under serum-free conditions, with a mean ratio of TOPflash over FOPflash equalling two (Figure 3.12).

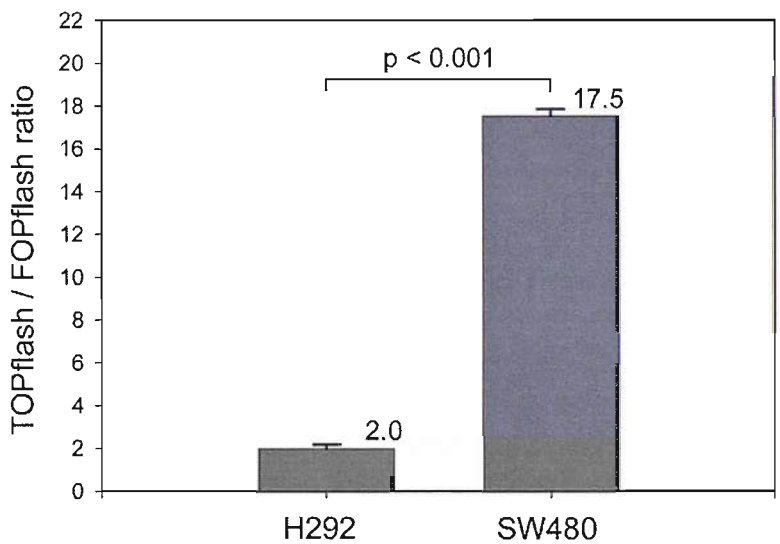

Figure 3.12: TOPflash reporter activity in H292 and SW480 cells at baseline.

SW480 colorectal carcinoma (n=3) and H292 bronchial epithelial (n=6) cells were transiently transfected with TOPflash or FOPflash reporters for assessment of Tcf/Lef-1 transcriptional activity under serum-free conditions. H292 cells were >80% confluent in all experiments. Data are expressed as mean ± S.E.M and were analysed using the unpaired Student's T-test. High constitutive activation of the TOPflash reporter was detected in SW480 cells. In contrast, low constitutive activation of TOPflash was observed in H292 cells.

3.3 Discussion

Evidence suggests that nuclear signalling by β-catenin requires expression of one or more members of the Tcf/Lef-1 family of transcription factors (Molenaar et al., 1996; van Noort and Clevers, 2002). I have shown that H292 and primary HBE cells both express mRNA encoding Tcf-4 and -3, with variable low-level expression of TCF-1 and LEF-1. This pattern of expression is similar to that reported in murine lung tissue, in which loss of detectable mRNA for TCF-1 and LEF-1 occurs from day one post-partum (Oosterwegel et al., 1993), possibly reflecting a role for these transcription factors in the establishment of pulmonary architecture, rather than in its maintenance throughout postnatal life. However, Lef-1 has also been implicated in postnatal submucosal gland development (Duan et al., 1998; Duan et al., 1999), and the degree of functional redundancy within the Tcf/Lef-1 family remains unclear. Consistent with reports of multiple isoforms for TCF-4 (Duval et al., 2000) and LEF-1 (Hovanes et al., 2001), I detected splice variants with deletions of exon 4 (69 bp) in TCF-4 and exon 6 (84 bp) in LEF-1. However, neither of these exons encodes the β-catenin nor HMG DNA binding domains, and their functional significance remains to be determined. Importantly, the pattern of TCF/LEF-1 expression appears similar between H292 and primary HBE cells, and no difference was identified between asthmatic and healthy control groups. In keeping with my RT-PCR data, I detected expression of Tcf-4 protein in both H292 and primary HBE cells, in contrast to the lack of expression reported by Barker *et al* (Barker et al., 1999) in immunostained sections of adult human lung.

I have also shown that confluent H292 and primary HBE cells under serum-free conditions exhibit nuclear localisation of β-catenin, consistent with canonical Wnt pathway activity. Furthermore, this observation was made using a monoclonal antibody (ABC) that recognises the hypophosphorylated (non-phosphorylated T41 and S37) form of β-catenin, thought to represent the transcriptionally active fraction (Staal et al., 2002; van Noort et al., 2002). However, levels of nuclear β-catenin were relatively low, and the pattern of expression was predominantly membranous. Although consistent with involvement of β-catenin in the formation of cadherin-

mediated intercellular adherens junctions (Aberle et al., 1996; Ozawa et al., 1989), membranous staining by the ABC antibody was an interesting and novel observation, raising the possibility that adherens junctions might serve as a reservoir for the transcriptionally active fraction of β-catenin in these cells. In contrast, SW480 colorectal cancer cells exhibit a fibroblastoid phenotype with relatively high levels of nuclear β-catenin and absent membranous staining (Munne et al., 1999), consistent with their APC gene mutation (Korinek et al., 1997) and lack of classical cadherin expression (Gottardi et al., 2001). Importantly, nuclear staining was lost when the pan-β-catenin antibody (clone 14) was used on SW480 cells fixed in acetone at -20°C. Indeed, using the same antibody, Munné *et al* (Munne et al., 1999) observed nuclear β-catenin in formalin-fixed cytospins of SW480 cells, but not in samples stored and sectioned at -80°C. With similar findings in frozen sections of colorectal cancer tissue, the authors concluded that freezing might somehow mask specific epitopes on β-catenin in the nuclear compartment (Munne et al., 1999). This appears not to be an issue with the ABC antibody, where staining was unaffected by the fixation method employed.

My data show that adult HBE cells express members of the TCF/LEF-1 family of transcription factors and exhibit nuclear localisation of β-catenin. Although these findings support my hypothesis, they do not measure signalling by an intact canonical Wnt pathway. For this reason, I used the TOPflash construct to investigate Tcf/Lef-1 transcriptional activity. However, I was unable to achieve adequate transient transfection of primary HBE cells, and so employed TOPflash-containing H292 cells instead. Indeed, there have been no reports of Tcf/Lef-1 reporter use in primary human airway epithelial cells in the literature to date. In the absence of a Wnt stimulus or canonical pathway mutation, several mechanisms have evolved that normally repress transcription by Tcf/Lef-1 (Nusse, 1999). These include negative regulation of cytosolic β-catenin by the Gsk-3β/Apc/axin destruction complex (Behrens et al., 1998; Liu et al., 2002), and association of Tcf/Lef-1 with co-repressors of the transducin-like enhancer of split (TLE) family (Brantjes et al., 2001). Consistent with reports by Korinek *et al* (Korinek et al., 1997), I observed *high* constitutive activation of the β-catenin signalling pathway in SW480 cells, indicating that my TOPflash reporter was functionally intact. In contrast, and in keeping with

my confocal data, I observed *low* constitutive activation of the TOPflash reporter in confluent H292 cells under serum-free conditions, consistent with reports of wild-type β-catenin in this cell type (Ueda et al., 2001). These findings suggest that β-catenin/Tcf/Lef-1 complexes are tightly controlled in H292 cells, and that these cells do not contain Wnt pathway mutations. Thus, TOPflash-containing H292 cells may provide a useful model for investigating factors that might regulate β-catenin mediated Tcf/Lef-1 transcriptional activity in adult human bronchial epithelial cells.

CHAPTER 4

LITHIUM-INDUCED ACTIVATION OF THE CANONICAL WNT SIGNAL TRANSDUCTION PATHWAY IN ADULT HUMAN AIRWAY EPITHELIAL CELLS

4.1 Aims of the study

In chapter 3, my data suggested that Tcf/Lef-1 transcriptional activity is tightly controlled in confluent adult human bronchial epithelial (HBE) cells devoid of exogenous growth factors under serum-free conditions. However, these experiments do not confirm the existence of an intact canonical Wnt pathway. Therefore, the aims of this study were to test the hypothesis that ***HBE cells are capable of transducing a canonical Wnt signal, leading to up-regulation of Tcf/Lef-1 transcriptional activity***.

In the absence of a Wnt signal, Tcf/Lef-1 transcriptional activity is normally repressed through negative regulation of cytosolic β-catenin by the Gsk-3β/Apc/axin destruction complex (Behrens et al., 1998; Liu et al., 2002) and by binding of repressor proteins of the transducin-like enhancer of split (TLE) family (Brantjes et al., 2001). However, class-1 Wnt-induced inactivation of the destruction complex allows β-catenin to accumulate within the cytosol and translocate into the nuclear compartment where it can bind to Tcf/Lef-1, functionally antagonise TLE-mediated repression, and activate the transcription of target genes (Miller et al., 1999; Brantjes et al., 2001; Takemaru and Moon, 2000; van Noort and Clevers, 2002). Lithium mimics class-1 Wnt activity by acting as a non-competitive inhibitor of Gsk-3β, and has been widely employed as an exogenous activator of the canonical pathway (Coghlan et al., 2000; Phiel and Klein, 2001). Therefore, evidence of lithium-induced nuclear localisation of β-catenin and activation of Tcf/Lef-1 transcription factors was sought using laser confocal microscopy and TOPflash-containing H292 cells. In addition, quantitative PCR (qPCR) was used to investigate lithium-induced changes in *cyclin-D1*, *MMP7* (*matrilysin*) and *IL-8* gene expression, identified in other human cell types as target genes of β-catenin/Tcf/Lef-1 transcriptional activation involved in

cell proliferation, migration and stress responses (Brabletz et al., 1999; Crawford et al., 1999; Levy et al., 2002; Shtutman et al., 1999; Tetsu and McCormick, 1999).

4.2 Methods and results

4.2.1 Lithium induces nuclear localisation of β-catenin in H292 and primary HBE cells

To investigate the cellular expression and localisation of β-catenin in response to lithium stimulation, 8-well Nunc Lab-Tek II glass chamber slides were seeded with 1.5 x 10^5 H292 cells per chamber in 500μl standard RPMI 1640 medium. Cells were incubated for 54 hours with culture medium changed at 24 hours, and then placed in serum-free UltraCULTURE medium ± 20mM lithium chloride (LiCl) for 16 hours. Cells were fixed and immunostained using either pan-β-catenin (PBC; clone 14; BD Biosciences, Oxford, UK) or hypophosphorylated ('active') β-catenin (ABC; clone 8E7; Upstate Biotechnology, USA) monoclonal antibodies, and slides examined by laser confocal microscopy (see Section 2.16). As previously observed (Section 3.2.3), the pattern of PBC expression in H292 cells (>80% confluent) was predominantly membranous. However, lithium stimulation enhanced the yellow co-localisation of FITC-labelled PBC and 7-AAD, indicating a lithium-induced increase in nuclear localisation of β-catenin (Figure 4.1). Furthermore, the same pattern of β-catenin expression was also observed using the ABC antibody, indicating a lithium-induced increase in nuclear localisation of hypophosphorylated (transcriptionally active) β-catenin (Figure 4.2). This observation was confirmed by semi-quantitative analysis (see Section 2.16.3) of percentage nuclear staining by ABC on random fields of view (n=3) from confocal images of H292 cells stimulated ± LiCl. Data are presented as mean % nuclear ABC staining ± standard error of the mean (S.E.M.), with statistical significance assessed using the unpaired Student's T-test. Percentage nuclear ABC staining significantly increased from 28 ± 3% to 46 ± 5% in response to lithium stimulation (Figure 4.3).

In parallel experiments, primary HBE cell cultures were established by seeding cells brushed from the proximal airways of normal volunteer subjects. At passage 2 (P2),

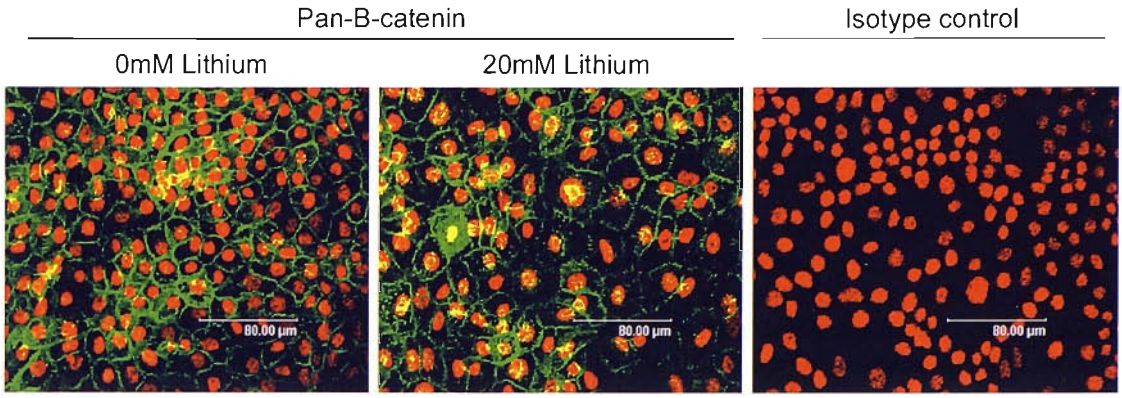

Figure 4.1: Confocal images of PBC expression in H292 cells stimulated ± lithium.

Confluent H292 bronchial epithelial cells in serum-free basal medium were stimulated ± 20mM lithium chloride for 16 hours, fixed with 4% paraformaldehyde, permeabilised with Triton X-100, and stained using FITC (green) labelled anti-pan-β-catenin (PBC) monoclonal antibody. Nuclei were counterstained using 7-AAD (red). Increased yellow co-localisation of FITC and 7-AAD in response to lithium stimulation was observed, suggesting increased nuclear localisation of PBC. The isotype control was negative.

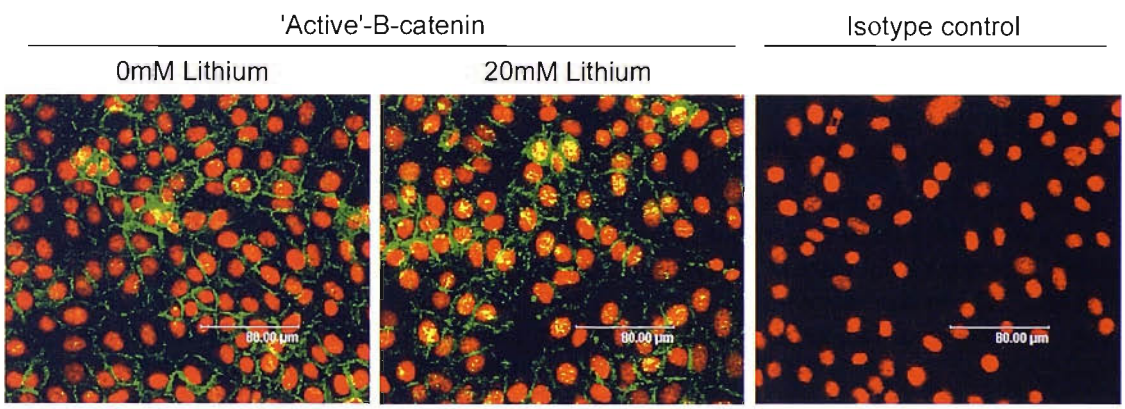

Figure 4.2: Confocal images of ABC expression in H292 cells stimulated ± lithium.

Confluent H292 bronchial epithelial cells in serum-free basal medium were stimulated ± 20mM lithium chloride for 16 hours, fixed in acetone, and stained using FITC (green) labelled anti-hypophosphorylated ('active') β-catenin (ABC) monoclonal antibody. Nuclei were counterstained using 7-AAD (red). Increased yellow co-localisation of FITC and 7-AAD in response to lithium stimulation was observed, suggesting increased nuclear localisation of ABC. The isotype control was negative.

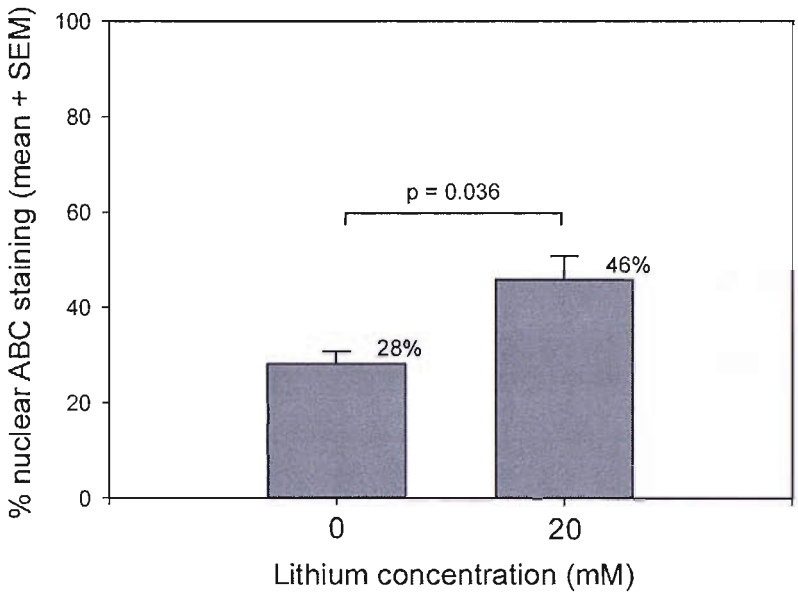

Figure 4.3: Percentage nuclear ABC staining in H292 cells stimulated ± lithium.

Taking random fields (n=3) from confocal images of hypophosphorylated ('active') β-catenin (ABC) expression in H292 cells stimulated ± 20mM lithium chloride for 16 hours (see Figure 4.2), semi-quantitative analysis of percentage nuclear staining by ABC was undertaken. Data are expressed as mean ± S.E.M and were analysed using the unpaired Student's T-test. Percentage nuclear ABC staining significantly increased from 28 ± 3% to 46 ± 5% in response to lithium stimulation.

collagen-coated 8-well Nunc Lab-Tek II glass chamber slides were seeded with 5 x 10^4 viable HBE cells per chamber in 500µl BEGM. Cells were incubated and culture medium changed every 48 hours. When confluent, BEGM was replaced with growth factor-free BEBM ± 20mM LiCl for 16 hours, prior to fixation and immunostaining for β-catenin. As previously observed (Section 3.2.3), the pattern of PBC expression was predominantly membranous with evidence of diffuse cytosolic staining and minimal nuclear localisation (Figure 4.4). Furthermore, no appreciable change in yellow co-localisation of FITC-labelled PBC and 7-AAD in response to lithium stimulation was seen. However, when stained with the ABC antibody, lithium stimulation enhanced the yellow co-localisation of FITC and 7-AAD, indicating a lithium-induced increase in nuclear localisation of transcriptionally active β-catenin (Figure 4.5). Semi-quantitative analysis of percentage nuclear staining by ABC on random fields of view (n=8) confirmed a significant increase from 30 ± 2% to 38 ± 3% in response to lithium stimulation (Figure 4.6).

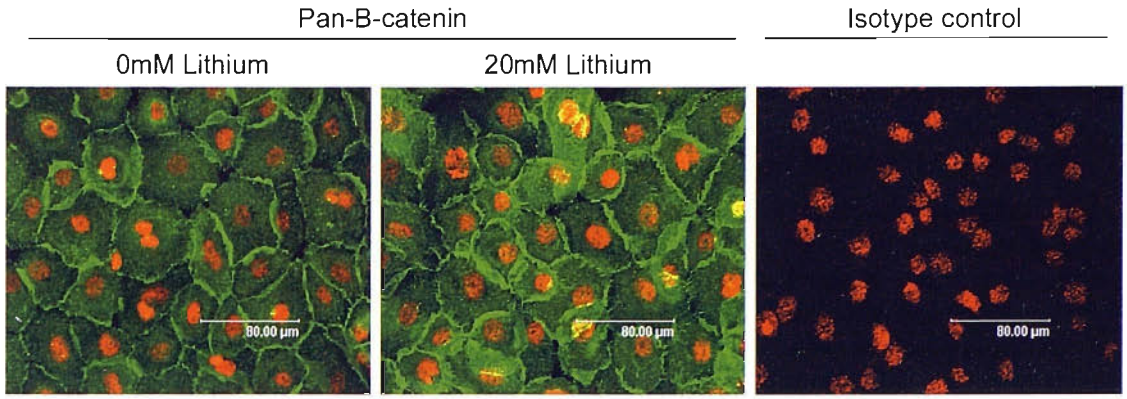

Figure 4.4: Confocal images of PBC expression in HBE cells stimulated ± lithium.

Confluent primary human bronchial epithelial (HBE) cells in serum-free basal medium, obtained from healthy volunteer subjects, were stimulated ± 20mM lithium chloride for 16 hours, fixed with 4% paraformaldehyde, permeabilised with Triton X-100, and stained using FITC (green) labelled anti-pan-β-catenin (PBC) monoclonal antibody. Nuclei were counterstained using 7-AAD (red). The pattern of PBC expression was predominantly membranous with evidence of diffuse cytosolic staining. No appreciable change in yellow co-localisation of FITC and 7-AAD in response to lithium stimulation were observed. The isotype control was negative.

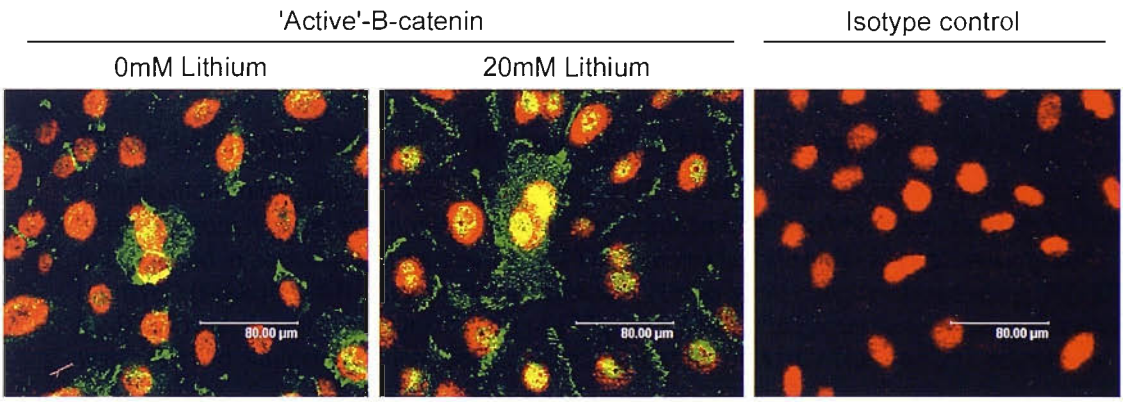

Figure 4.5: Confocal images of ABC expression in HBE cells stimulated ± lithium.

Confluent primary human bronchial epithelial (HBE) cells in serum-free basal medium, obtained from healthy volunteer subjects, were stimulated ± 20mM lithium chloride for 16 hours, fixed in acetone, and stained using FITC (green) labelled anti-hypophosphorylated ('active') β-catenin (ABC) monoclonal antibody. Nuclei were counterstained using 7-AAD (red). Increased yellow co-localisation of FITC and 7-AAD in response to lithium stimulation was observed, suggesting increased nuclear localisation of ABC. The isotype control was negative.

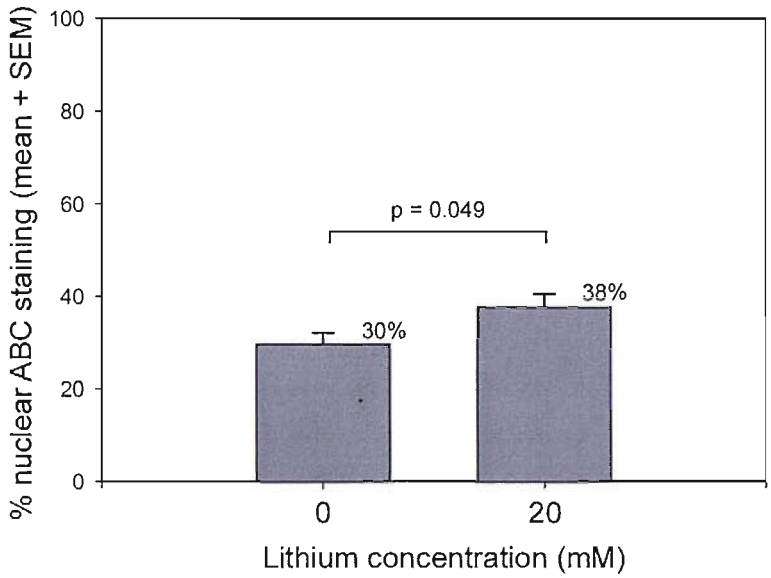

Figure 4.6: Percentage nuclear ABC staining in HBE cells stimulated ± lithium.

Taking random fields (n=8) from confocal images of hypophosphorylated ('active') β-catenin (ABC) expression in primary human bronchial epithelial (HBE) cells from healthy volunteer subjects stimulated ± 20mM lithium chloride for 16 hours (see Figure 4.5), semi-quantitative analysis of percentage nuclear staining by ABC was undertaken. Data are expressed as mean ± S.E.M and were analysed using the unpaired Student's T-test. Percentage nuclear ABC staining significantly increased from 30 ± 2% to 38 ± 3% in response to lithium stimulation.

4.2.2 Lithium induces activation of a Tcf/Lef-1 reporter in H292 cells

To investigate the Tcf/Lef-1 transcriptional response to stimulation with lithium, 6-well Nunc dishes were seeded with 5 x 10^5 H292 cells per well in 2ml standard RPMI 1640 medium, incubated for 24 hours, and then transiently transfected with TOPflash or FOPflash (Upstate Biotechnology, USA) as described in Section 2.15.6. Cells were incubated for 7 hours, before being placed in serum-free UltraCULTURE medium ± 20mM LiCl for 18 hours. Samples were then harvested and analysed as described in Section 2.15.7. When harvested, H292 cells were >80% confluent. The initial experiment (n=1) included lithium concentrations of 5 and 10mM, and showed a dose-response in Tcf/Lef-1 reporter activity with increasing lithium concentration (Figure 4.7). Additional experiments (n=5) confirmed that 20mM lithium induced a 4.5-fold increase in TOPflash reporter activity when compared to unstimulated controls (Figure 4.8).

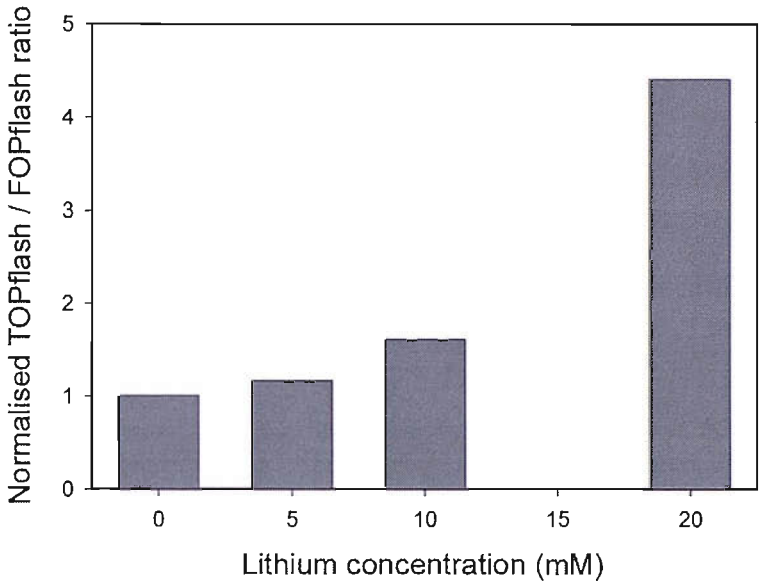

Figure 4.7: TOPflash activity in H292 cells stimulated ± lithium (dose-response).

H292 bronchial epithelial cells were transiently transfected with TOPflash or FOPflash reporters prior to stimulation with 0, 5, 10 or 20mM lithium chloride for 18 hours (n=1). Cells were >80% confluent. Data are expressed normalised to the unstimulated control, and show a dose-response with increasing lithium concentration.

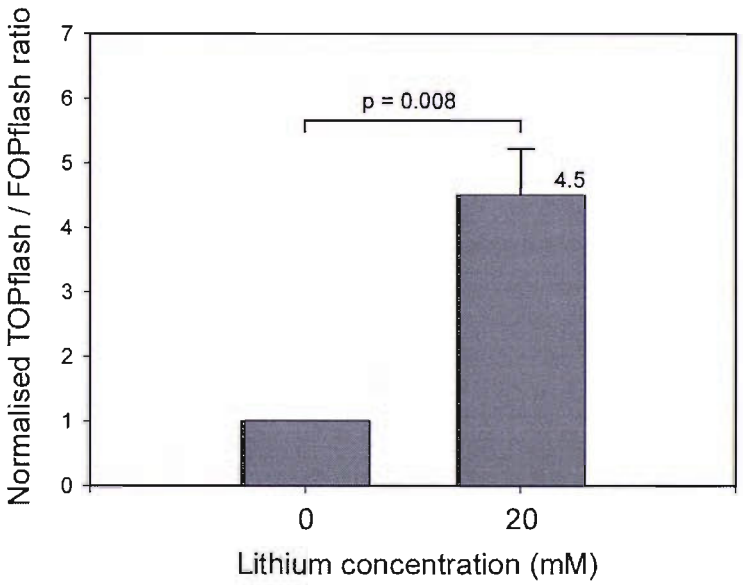

Figure 4.8: TOPflash reporter activity in H292 cells stimulated ± 20mM lithium.

H292 bronchial epithelial cells were transiently transfected with TOPflash or FOPflash reporters prior to stimulation ± 20mM lithium chloride for 18 hours (n=5). Cells were >80% confluent in all experiments. Data are expressed as mean ± S.E.M, normalised to the unstimulated control, and were analysed using the paired Student's T-test. 20mM lithium induced a 4.5-fold increase in TOPflash reporter activity.

4.2.3 Lithium does not alter *cyclin-D1*, *MMP-7* or *IL-8* gene expression in H292 cells

To identify lithium-induced changes in gene expression, H292 cells were seeded in 6-well Nunc dishes at 5 x 10^5 per well in 2ml standard RPMI 1640 medium, incubated for 32 hours, and placed in serum-free UltraCULTURE medium for 18 hours. Cells were then stimulated with fresh UltraCULTURE containing 0, 10 and 20mM LiCl for 1, 2, 4 and 8 hours. Cells were lysed with 1ml TRIzol Reagent per well before RNA extraction, DNase treatment (see Section 2.8), and reverse transcription to cDNA (see Section 2.11.2). Using primers for *cyclin-D1*, *MMP7* and *IL-8* (Table 4.1) designed and validated by Dr Rob Powell (University of Southampton), gene expression was investigated by qPCR (see Section 2.13). FAM probes were designed for *cyclin-D1* and *IL-8*, whereas the SYBR Green dye assay was used for *MMP7*. The PCR protocol began with a 95°C 'hot start' for 8 minutes, followed by 50 cycles of *denaturation*

Gene (Accession N°)	**Primer and FAM Probe sequences** (**F**orward and **R**everse)
Cyclin-D1 (NM_053056.1)	**F**: 5'-CCTCGGTGTCCTACTTCAAATGT-3' **R**: 5'-AAGACCTCCTCCTCGCACTT-3' **Probe**: 5'-TGTTCCTCGCAGACCTCCAGCATCCAG-3'
MMP7 (NM_002423.2)	**F**: 5'-CCGTGCTGTGTGCTGTGTG-3' **R**: 5'-CTTGAGATAGTCCTGAGCCTGTTC-3' SYBR Green dye assay
IL-8 (NM_000584)	**F**: 5'-AAGGAACCATCTCACTGTGTGTAAAC-3' **R**: 5'-TTAGCACTCCTTGGCAAAACTG-3' **Probe**: 5'-CTGCCAAGAGAGCCACGGCCAG-3'
18S rRNA	Commercially available primers and FAM probe Eurogentec, Seraing, Belgium

Table 4.1: Primers and FAM probes for *cyclin-D1*, *MMP7* and *IL-8* qPCR.

Forward (sense) and reverse (anti-sense) primers and FAM probes for quantitative PCR analysis of *cyclin-D1*, *MMP7* and *IL-8* gene expression were designed and validated by Dr Rob Powell (University of Southampton).

(95°C for 15 seconds) and *annealing/extension* (60°C for 60 seconds). When using the SYBR Green dye assay, SYBR melt curve analysis was performed in order to assess signal quality and identify the peak melt temperature (T_M), an indicator of amplicon size. All samples were measured in triplicate, and relative gene expression levels calculated using the $\Delta\Delta C_T$ method of quantification with commercially available 18S rRNA primer and FAM probe mix (Eurogentec, Belgium) as the normalising control.

Representative qPCR cycle graphs for samples in triplicate show good signal strength for *cyclin-D1* (Figure 4.9) and *IL-8* (Figure 4.10), with C_T values ranging from 22-26. Importantly, no signal was detected with the RT-minus controls, indicating that amplicons were derived from amplified RNA and not genomic or contaminating DNA. However, the representative qPCR cycle graph for *MMP7* shows relatively high C_T values that are within 6 cycles of those for the RT-minus control, indicating signal strength of such low intensity that it could not reliably be differentiated from

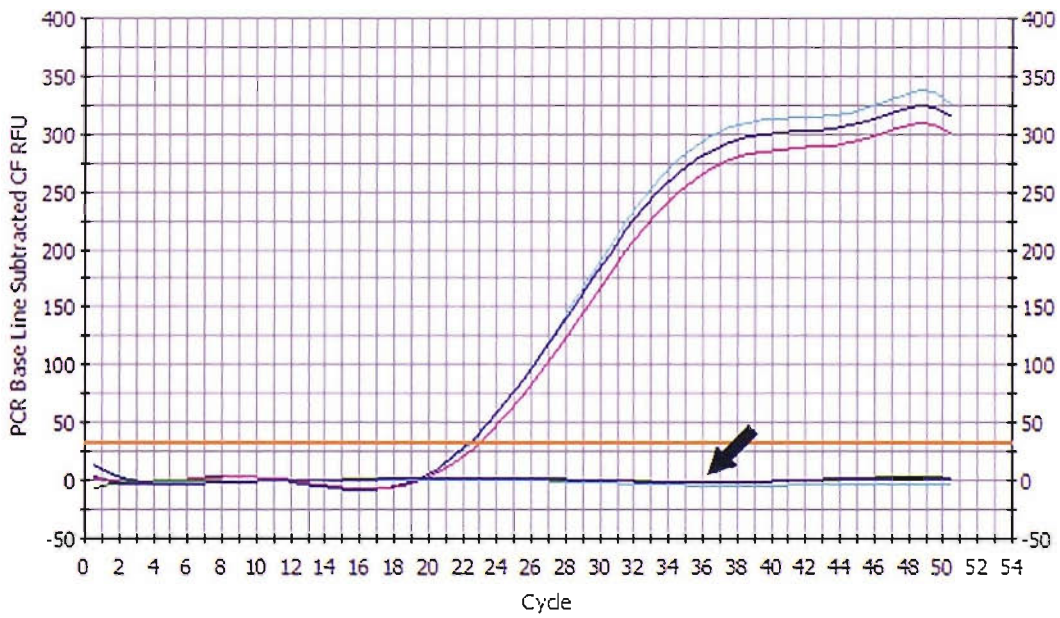

Figure 4.9: Representative qPCR cycle graph for *cyclin-D1* expression in H292 cells.

RNA from H292 cells stimulated with 0, 10 and 20mM lithium chloride for 1, 2, 4 and 8 hours was reverse transcribed and *cyclin-D1* gene expression investigated by qPCR (TaqMan). A representative PCR cycle graph for a sample in triplicate shows good signal strength, with C_T values of 22-23. No signal was detected with the RT-minus control (arrowed).

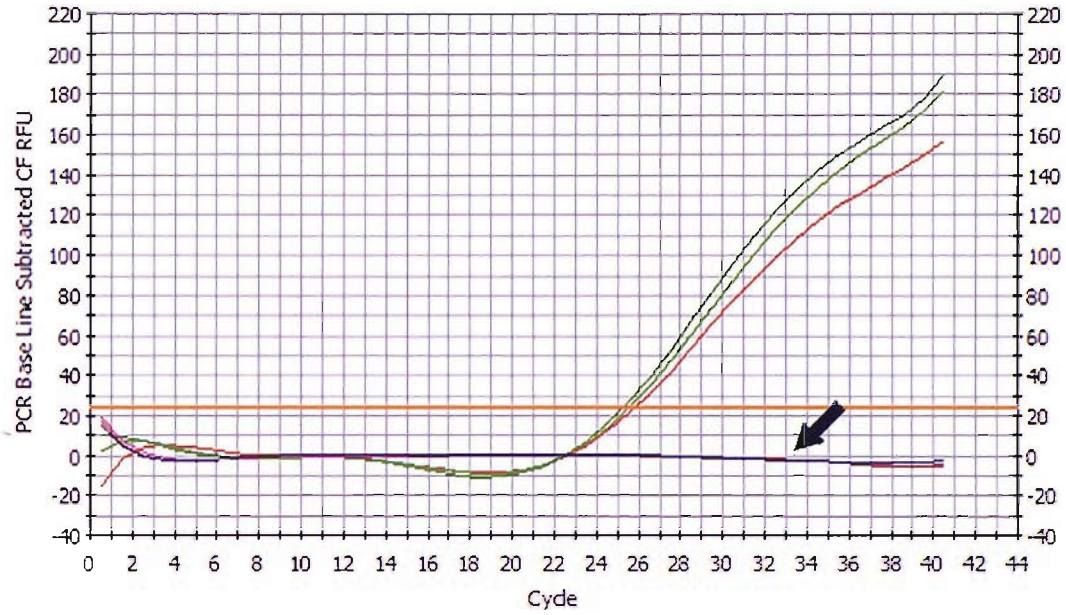

Figure 4.10: Representative qPCR cycle graph for *IL-8* expression in H292 cells.

RNA from H292 cells stimulated with 0, 10 and 20mM lithium chloride for 1, 2, 4 and 8 hours was reverse transcribed and *IL-8* gene expression investigated by qPCR (TaqMan). A representative PCR cycle graph for a sample in triplicate shows good signal strength, with C_T values of 25-26. No signal was detected with the RT-minus control (arrowed).

background noise (Figure 4.11). Since SYBR melt curve analysis of amplicons derived from SW480 cell (positive control) cDNA shows a single peak coinciding with the predicted peak melt temperature of 79°C (Figure 4.12), it was concluded that the primer set employed were accurate and efficient, and that H292 cells did not express significant levels of mRNA encoding MMP7 above RT-minus controls under the above conditions (n=3; Table 10.25). For comparison of *cyclin-D1* (n=4) or *IL-8* (n=4) gene expression in H292 cells stimulated with 0, 10 and 20mM lithium chloride for 1, 2, 4 and 8 hours, data are presented as mean $\Delta\Delta C_T$ value ± S.E.M, normalised to the unstimulated control at each time-point, and statistical significance assessed using the paired Student's T-test and one-way Analysis of Variance (ANOVA). No significant change in *cyclin-D1* (Figure 4.13) or *IL-8* (Figure 4.14) gene expression was observed.

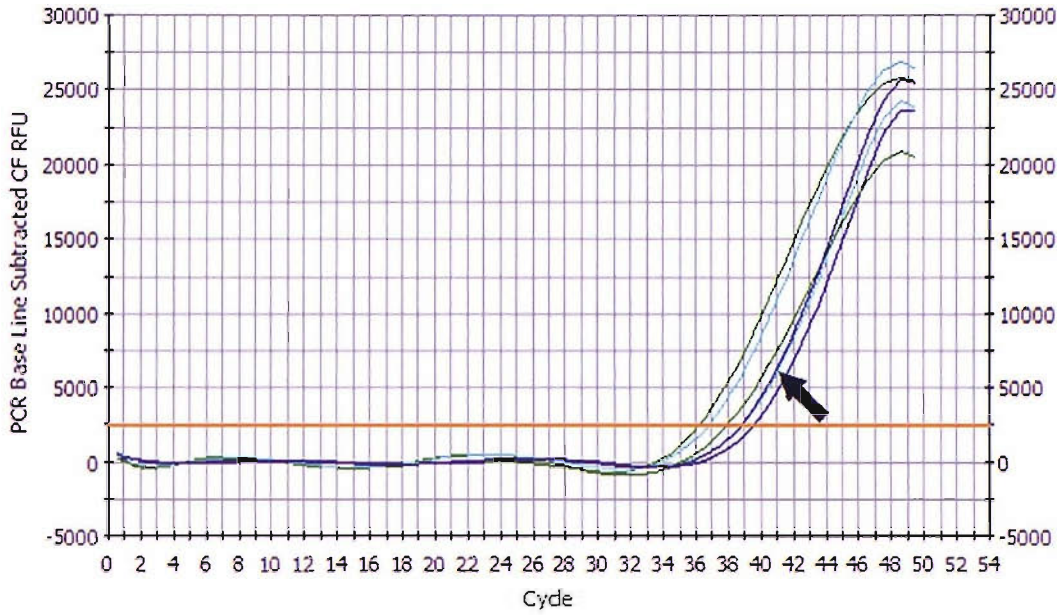

Figure 4.11: Representitive qPCR cycle graph for *MMP7* expression in H292 cells.

RNA from H292 cells stimulated with 0, 10 and 20mM lithium chloride for 1, 2, 4 and 8 hours was reverse transcribed, and *MMP7* gene expression investigated by quantitative RT-PCR (qPCR). A representative PCR cycle graph for a sample in triplicate shows high C_T values that are within 6 cycles of those for the RT-minus controls (arrowed), indicating signal strength of such low intensity that that is could not reliably be differentiated from background noise.

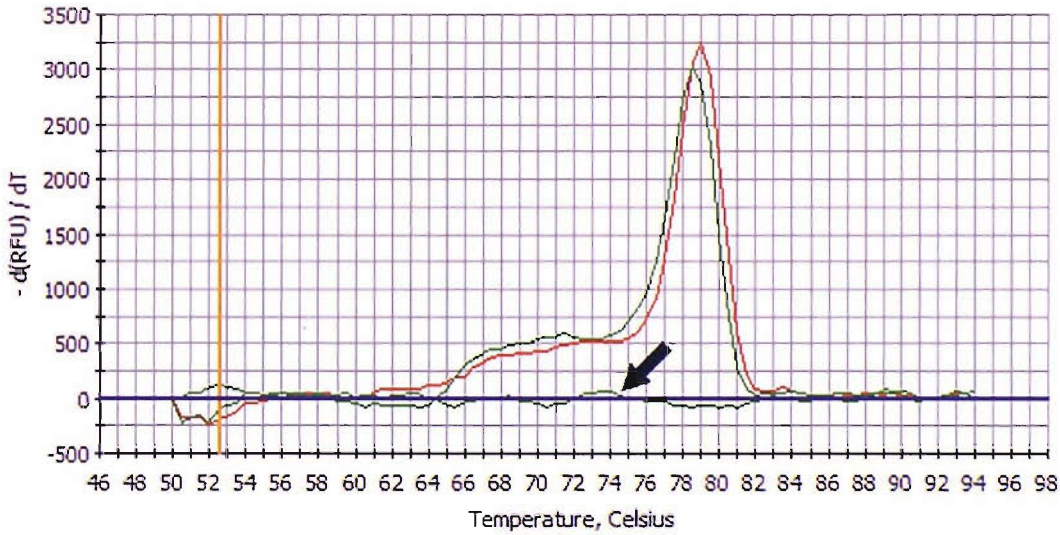

Figure 4.12: SYBR melt curve for amplicons of qPCR primers designed for *MMP7*.

Forward and reverse primers (Table 4.1) were designed for investigation of *MMP7* gene expression by qPCR. Using cDNA from SW480 cells, amplicons from a PCR reaction were checked using the SYBR melt curve technique. The predicted peak melt temperature of 79°C was observed, suggesting that the primer pair was specific for *MMP7*. No amplicons were detected with the RT-minus control (arrowed).

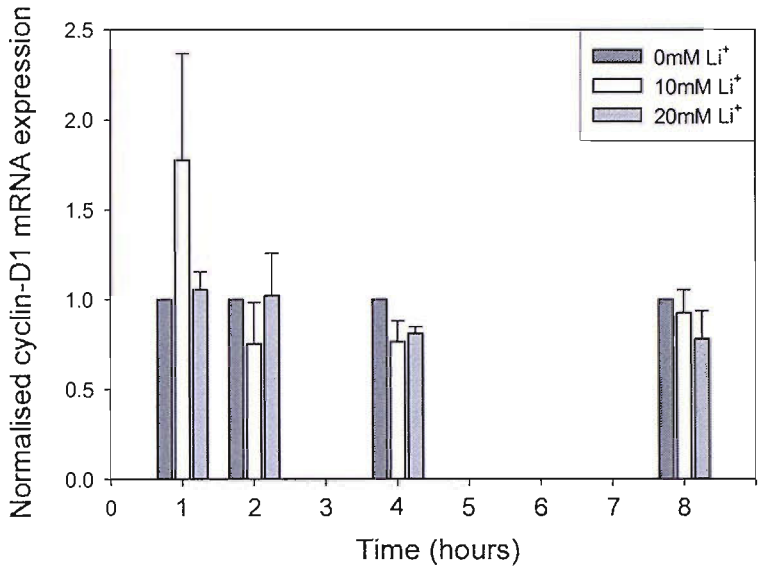

Figure 4.13: *Cyclin-D1* gene expression in H292 cells stimulated ± lithium.

RNA from H292 cells (n=4) stimulated with 0, 10 and 20mM lithium chloride for 1, 2, 4 and 8 hours was reverse transcribed, and *cyclin-D1* gene expression investigated by qPCR (TaqMan), using the primers and probe in Table 4.1 and 18S rRNA as a normalising control for calculating $\Delta\Delta C_T$ values. Cells were >80% confluent in all experiments. Data are expressed as mean ± S.E.M, normalised to the unstimulated control at each time-point, and were analysed using the paired Student's T-test and one-way ANOVA. No significant change in *cyclin-D1* gene expression was observed.

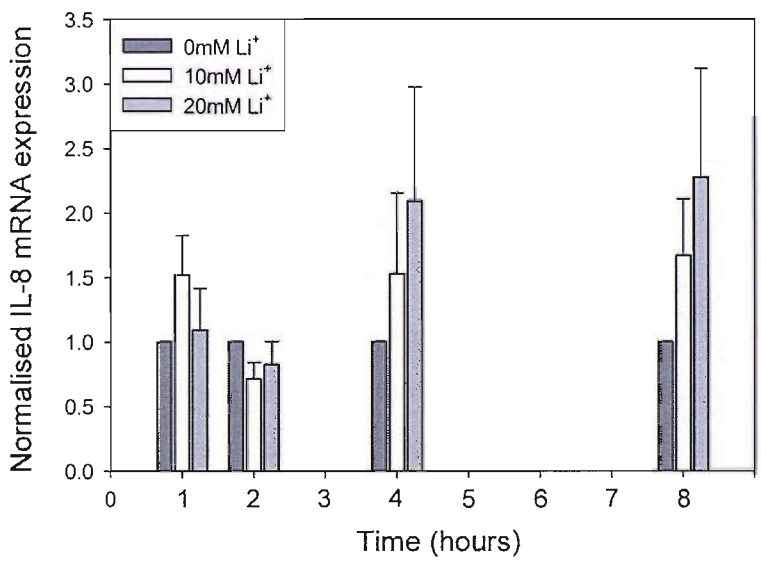

Figure 4.14: *IL-8* gene expression in H292 cells stimulated ± lithium.

RNA from H292 cells (n=4) stimulated with 0, 10 and 20mM lithium chloride for 1, 2, 4 and 8 hours was reverse transcribed, and *IL-8* gene expression investigated by qPCR (TaqMan) using 18S rRNA as a normalising control for calculating $\Delta\Delta C_T$ values. Cells were >80% confluent in all experiments. Data are expressed as mean ± S.E.M, normalised to the unstimulated control at each time-point, and were analysed using the paired Student's T-test and one-way ANOVA. No significant change in *IL-8* gene expression was observed.

4.3 Discussion

Lithium mimics class-1 Wnt activity by acting as a non-competitive inhibitor of Gsk-3β, and has been widely employed as an exogenous activator of Wnt/β-catenin signalling (Coghlan et al., 2000; Phiel and Klein, 2001). Importantly, I have shown that lithium can induce nuclear localisation of β-catenin in confluent H292 and primary HBE cells, suggesting lithium-induced inhibition of the Gsk-3β/Apc/axin destruction complex and activation of the canonical pathway. Again, this observation was made using a monoclonal antibody (ABC) that recognises the hypophosphorylated (non-phosphorylated T41 and S37) form of β-catenin, thought to represent the transcriptionally active fraction (Staal et al., 2002; van Noort et al., 2002). Furthermore, and consistent with my confocal data, I have also shown that lithium can activate the TOPflash reporter in H292 cells. To date, there has been one other published report involving transfection of lung cancer cells with a Tcf/Lef-1 reporter (Sunaga et al., 2001). This identified high constitutive activation of Tcf/Lef-1 transcription factors in one (A427 adenoncarcinoma cells) of fifteen lung cancer cell lines, associated with a point mutation at T41 in β-catenin. However, the study focused on the postulated link between Wnt pathway mutations and lung cancer pathogenesis, and did not attempt to *induce* activation of the putative canonical Wnt pathway in remaining cells (Sunaga et al., 2001).

In attempting to correlate lithium-induced TOPflash reporter activation with up-regulated gene expression in H292 cells, *cyclin-D1*, *MMP7* and *IL-8* were selected as candidates based on them having been identified as target genes of Tcf/Lef-1 transcription factors in other human cell types, and their involvement in cell proliferation, migration and stress responses (Brabletz et al., 1999; Crawford et al., 1999; Levy et al., 2002; Shtutman et al., 1999; Tetsu and McCormick, 1999). However, *MMP7* mRNA was not detected and no significant change in *cyclin-D1* or *IL-8* gene expression was observed in H292 cells stimulated with lithium at timepoints up to and including 8 hours. Unlike *cyclin-D1*, expression of *IL-8* mRNA did exhibit a *trend* towards a dose-response at 4 and 8 hours, and it is possible that lack of statistical significance reflected lack of power in this study (n=4). Nevertheless, the mean increase in *IL-8* expression above unstimulated control was

no greater than 2-fold, which for this gene would be a relatively small change, and the trend from 4 to 8 hours did not suggest a continued increase in *IL-8* expression had the time-course of the experiment been extended. Furthermore, lithium is a *non-selective* inhibitor of Gsk-3β with a number of other enzyme targets, including inositol monophosphatase and a family of structurally related phosphomonoesterases (Phiel and Klein, 2001). Thus, lithium-induced activation of *parallel* signalling pathways could account for changes in gene expression and might even oppose the influence of Tcf/Lef-1 transcription factors on expression of their target genes. However, an alternative explanation for the lack of correlation between lithium-induced TOPflash reporter activation and lithium-induced change in *cyclin-D1*, *MMP7* or *IL-8* expression is that these genes are *not* targets of Tcf/Lef-1 transcription factors in adult human bronchial epithelial cells. Despite this, my data still suggest that H292 and primary HBE cells have an intact canonical pathway downstream of Gsk-3β. Although these findings support my hypothesis, they do not provide evidence relating to factors *upstream* of the Gsk-3β/Apc/axin destruction complex, required for transducing a class-1 Wnt signal.

CHAPTER 5

THE RESPONSE OF ADULT HUMAN AIRWAY EPITHELIAL CELLS TO EXOGENOUS WNT-3A

5.1 Aims of the study

In chapter 4, my data suggested that adult human bronchial epithelial (HBE) cells have an intact canonical Wnt pathway downstream of Gsk-3β. However, these studies do not provide evidence relating to factors *upstream* of the Gsk-3β/Apc/axin destruction complex. Therefore, the aims of this chapter were to further test the hypotheses that ***adult HBE cells express key components of the Wnt/β-catenin signalling pathway***, focusing on elements *upstream* of Gsk-3β, ***and are capable of transducing a canonical Wnt signal in response to exogenous Wnt stimulation***.

Frizzleds function as cell surface receptors for Wnts and are required for Wnt signal transduction (Bhanot et al., 1996; Yang-Snyder et al., 1996). Therefore, RNase protection assays (RPA) were employed to investigate the expression of five out of the ten known human Frizzled (FZD) genes in total RNA samples from H292 and primary HBE cells. At the time of this study, Wnt-3a expressing L-cells (murine fibroblasts) were the best available source of biologically active class-1 Wnt. Therefore, using this physiologically relevant stimulus in a paracrine model, evidence of Wnt-3a induced nuclear localisation of hypophosphorylated (transcriptionally active) β-catenin in co-cultured H292 and primary HBE cells was sought by laser confocal microscopy. In addition, conditioned medium (CM) from L-cells was used to investigate Wnt-3a induced activation of Tcf/Lef-1 transcription factors in TOPflash-containing H292 cells. Finally, quantitative PCR (qPCR) was employed to assess Wnt-3a CM-induced change in expression of *cyclin-D1*, *MMP7* (*matrilysin*) and *IL-8*, candidate target genes for Tcf/Lef-1 transcription factors (Brabletz et al., 1999; Crawford et al., 1999; Levy et al., 2002; Shtutman et al., 1999; Tetsu and McCormick, 1999).

5.2 Methods and results

5.2.1 H292 and primary HBE cells express FZD and SFRP family members

For analysis of Frizzled (FZD) gene expression, RNase protection assays (RPA) were employed using a commercially available RiboQuant Human Frizzled (hFZD) Multi-Probe Template Set (BD Biosciences, Oxford, UK). In addition, this Multi-Probe Template Set allowed assessment of three out of the five known human secreted frizzled-related protein (SFRP) genes, encoding a family of proteins that function as Wnt antagonists by interfering with Wnt/Fzd interactions in the extracellular space (Wodarz and Nusse, 1998). Incidently, the Template Set also included a probe for Smoothened (SMOH) mRNA, encoding a seven transmembrane spanning (7TMS) protein that functions as part of the receptor complex for the sonic hedgehog (Shh) morphogen (Bellusci et al., 1996). 55cm^2 Nunc petri dishes were seeded with 3 x 10^6 H292 cells in 8ml standard RPMI 1640 medium. Cells were incubated for 32 hours, serum-starved for 18 hours in UltraCULTURE medium, and then lysed with 5.5ml TRIzol Reagent per petri dish, prior to RNA extraction and DNase treatment (see Section 2.8). RNase protection assays were undertaken (see Section 2.10) using MAXIscript T7 and RPA III Ribonuclease Protection Assay kits (Ambion, Huntingdon, UK). RPA products were resolved by 5% polyacrylamide gel electrophoresis (PAGE), and positive reaction products detected using a Phosphor Screen and a Storm 860 PhosphorImager (Molecular Dynamics, USA). FragmeNT Analysis software (Molecular Dynamics) was used to identify protected probe bands, based on size relative to full length reference probe bands, and quantify band intensity. Figure 5.1 shows a representative polyacrylamide gel with protected bands of predicted size seen for SFRP-1, FZD-2, -3, -5 and -6, and smoothened (SMOH), but not for SFRP-2, FRZB (SFRP-3) and FZD9. L32 ribosomal protein and GAPDH were used as internal controls. Importantly, bands are absent in the RNase-treated yeast tRNA negative control, indicating intact RNase integrity. The double band appearance of protected RNA is a common RPA artefact reflecting the fact that RNases recognise and cleave specific sequences. This observation was confirmed by four independent experiments, the summary of which is shown in Figure 5.2, with data expressed as mean band intensity ± the standard error of the mean (S.E.M.),

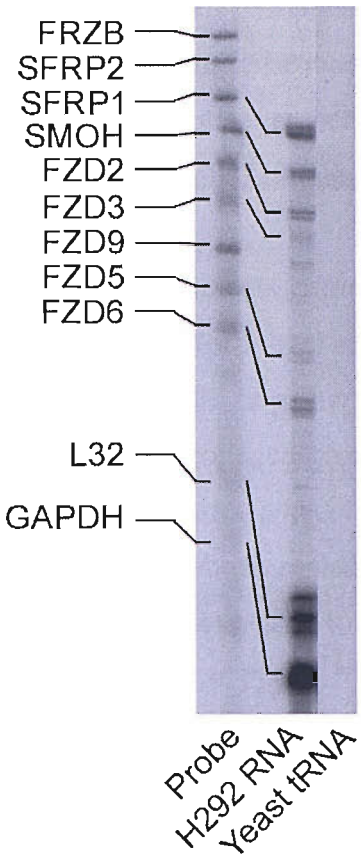

Figure 5.1: Expression of FZD and SFRP mRNA in H292 cells.

RNA was extracted from confluent H292 bronchial epithelial cells in serum-free basal medium. Frizzled (FZD) and secreted frizzled-related protein (SFRP) gene expression were investigated by RNase protection assay (RPA). A representative polyacrylamide gel is shown. Protected bands of predicted size were observed for SFRP-1, FZD-2, -3, -5 and -6, and smoothened (SMOH). mRNA encoding SFRP-2, FRZB (SFRP-3) and FZD9 was not detected. L32 ribosomal protein and GAPDH were used as internal controls. The yeast tRNA control was negative.

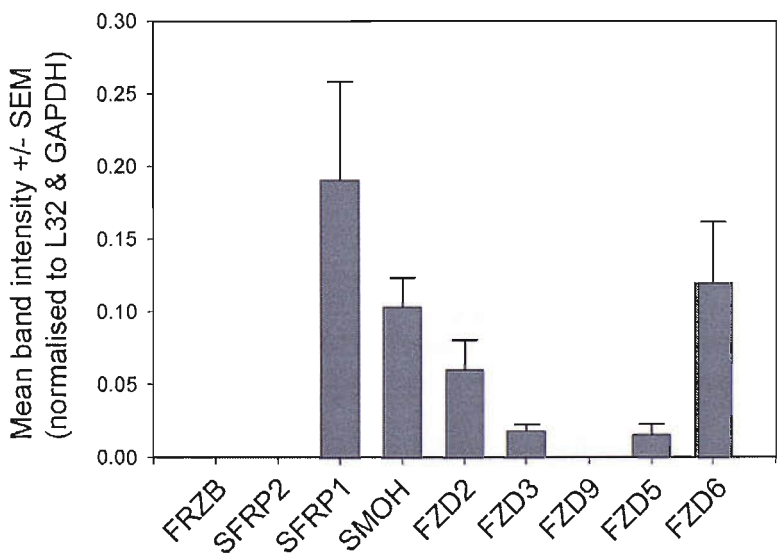

Figure 5.2: Expression of FZD and SFRP mRNA in H292 cells (summary data).

RNA was extracted from confluent H292 bronchial epithelial cells in serum-free basal medium (n=4). Frizzled (FZD) and secreted frizzled-related protein (SFRP) gene expression were investigated by RNase protection assay (RPA). Data are expressed as mean band intensity ± S.E.M, normalised to both L32 ribosomal protein and GAPDH internal control genes. H292 cells were found to express mRNA encoding SFRP-1, FZD-2 and -6, and smoothened (SMOH), with relatively low-level expression of FZD-3 and -5. mRNA encoding SFRP-2, FRZB (SFRP-3) and FZD9 mRNA was not detected.

normalised to both L32 ribosomal protein and GAPDH. These data do not allow direct comparisons to be made in the amount of expression *between* genes on the multi-probe template set, because this would require controlling for the number of ^{32}P nuclei in each probe, a function of probe length.

In parallel experiments, primary HBE cell cultures were established by seeding cells brushed from the proximal airways of four mild persistent asthmatic and four healthy volunteer subjects. At passage 2 (P2), 5 x 10^5 viable HBE cells from each subject were seeded on collagen-coated 55cm^2 Nunc petri dishes containing 8ml BEGM. Cells were incubated and culture medium changed every 48 hours. When near-confluent, BEGM was replaced with growth factor-free BEBM for 18 hours. Cells were then harvested, prior to RNA extraction, DNase treatment and analysis by RPA, as described above. Figure 5.3 shows a representative polyacrylamide gel from a healthy volunteer subject with protected bands of predicted size seen for SFRP-1, FZD-2, -5 and -6, and SMOH. For comparison of FZD and SFRP gene expression

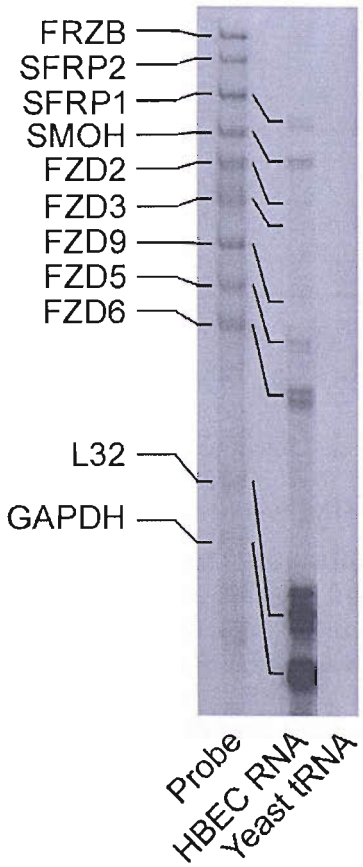

Figure 5.3: Expression of FZD and SFRP mRNA in HBE cells.

RNA was extracted from confluent primary human bronchial epithelial (HBE) cells in serum-free basal medium. Frizzled (FZD) and secreted frizzled-related protein (SFRP) gene expression were investigated by RNase protection assay (RPA). A representative polyacrylamide gel is shown. Protected bands of predicted size were observed for SFRP-1, FZD-2, -3, -9, -5 and -6, and smoothened (SMOH). mRNA encoding SFRP-2 and FRZB (SFRP-3) was not detected. L32 ribosomal protein and GAPDH were used as internal controls. The yeast tRNA control was negative.

between primary HBE from mild persistent asthmatic (n=4) and healthy volunteer subjects (n=4), and H292 cells (n=4), data are presented as median band intensity + interquartile range, normalised to both L32 ribosomal protein and GAPDH internal control genes, and statistical significance assessed using the Mann-Whitney U test. Compared with H292 cells, HBE cells from healthy volunteer subjects express equivalent amounts of mRNA encoding FZD-5 and -6, with relatively low-level expression of SFRP-1, FZD-2 and SMOH. Although not readily evident on the polyacrylamide gel, low levels of FZD-3 and -9 mRNA were also detected in HBE cells, the latter not expressed by H292 cells. Neither HBE nor H292 cells expressed SFRP-2 or FRZB (Figure 5.4). No significant difference in FZD and SFRP gene expression was observed between primary HBE cells from mild persistent asthmatic

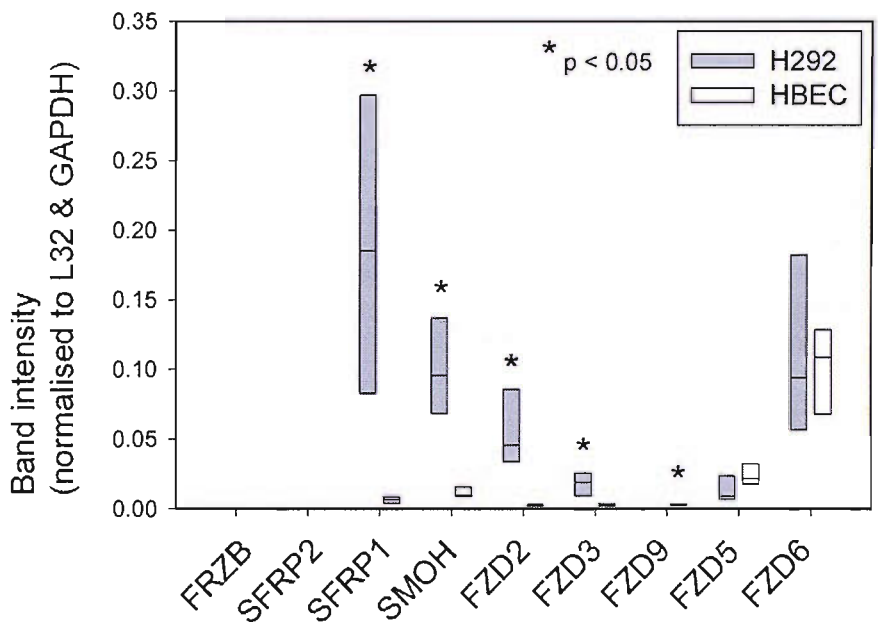

Figure 5.4: Expression of FZD and SFRP mRNA in H292 and HBE cells.

RNA was extracted from confluent primary human bronchial epithelial (HBE) cells in serum-free basal medium, obtained from healthy volunteer subjects (n=4). Frizzled (FZD) and secreted frizzled-related protein (SFRP) gene expression were investigated by RNase protection assay (RPA). Data are expressed as median band intensity and interquartile range, normalised to both L32 ribosomal protein and GAPDH internal control genes. Comparison was made with FZD and SFRP gene expression in H292 cells (data relating to Figure 5.2), and analysis made using the Mann-Whitney U test. Compared with H292 cells, HBE cells express equivalent levels of mRNA encoding FZD-5 and -6, with relatively low-level expression of SFRP1, SMOH, FZD-2 and -3. FZD9 mRNA was detected at low levels in HBE cells, but not detected in H292 cells. Neither SFRP-2 nor FRZB (SFRP-3) mRNA were detected in HBE or H292 cells.

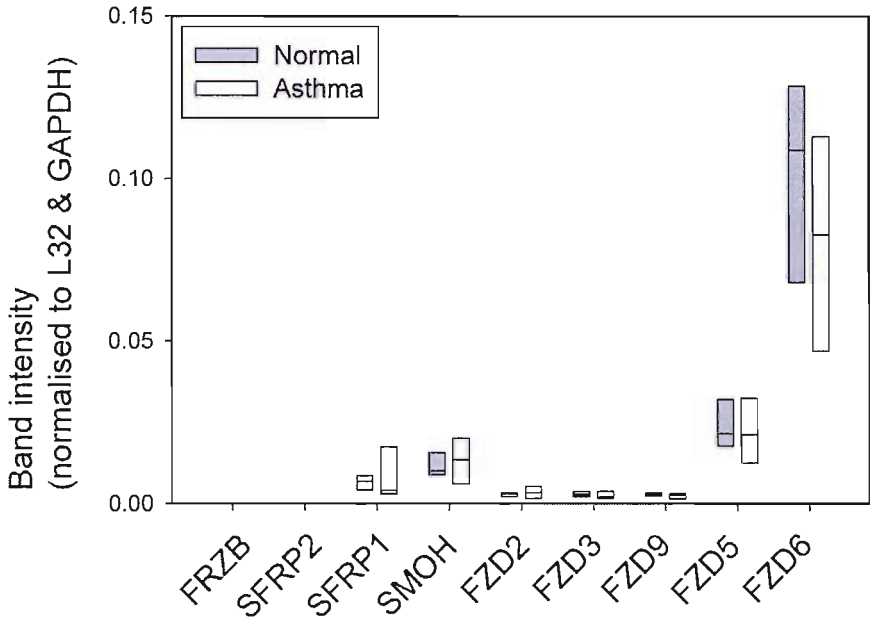

Figure 5.5: Expression of FZD and SFRP mRNA in normal and asthmatic HBE cells.

RNA was extracted from confluent primary human bronchial epithelial (HBE) cells in serum-free basal medium, obtained from volunteer subjects with mild persistent asthma (n=4). Frizzled (FZD) and secreted frizzled-related protein (SFRP) gene expression were investigated by RNase protection assay (RPA). Data are expressed as median band intensity and interquartile range, normalised to both L32 ribosomal protein and GAPDH internal control genes. Comparison was made with FZD and SFRP gene expression in HBE cells from normal volunteer subjects (n=4; data relating to Figure 5.4), and analysis made using the Mann-Whitney U test. No significant difference in FZD and SFRP gene expression was observed between the two groups.

and healthy volunteer subjects (Figure 5.5). Owing to the unavailability of specific antibodies, analysis of Fzd and Sfrp proteins was not possible at this time.

5.2.2 Wnt-3a expressing L-cells induce nuclear localisation of β-catenin in co-cultured H292 and primary HBE cells

To investigate the cellular expression and localisation of β-catenin in response to co-culture with Wnt-3a expressing L-cells (murine fibroblasts; ATCC), 8-well Nunc Lab-Tek II glass chamber slides were seeded with a mix of 1 x 10^4 H292 cells and 2 x 10^4 L Wnt-3a cells, or 2 x 10^4 parental (control) L-cells, per chamber in 400µl standard RPMI 1640 medium, and incubated for 48 hours. Cells were fixed and

immunostained using the hypophosphorylated ('active') β-catenin (ABC; clone 8E7; Upstate Biotechnology, USA) monoclonal antibody, and slides examined by laser confocal microscopy (see Section 2.16). In Figure 5.6, H292 cells (arrowed) are identified on the basis of their rounder nuclei, tendency to cluster, and classical cadherin expression (membranous staining for β-catenin), absent in L-cells. Co-culture with Wnt-3a expressing L-cells can be seen to enhance the yellow co-localisation of FITC-labelled ABC and 7-AAD in H292 cells, suggesting a Wnt-3a induced increase in nuclear localisation of hypophosphorylated (transcriptionally active) β-catenin. In addition, increased nuclear localisation of ABC was also observed in L-cells expressing Wnt-3a. Semi-quantitative analysis of percentage nuclear staining in H292 cells by ABC on random fields of view (n=6) confirmed a significant increase from 16 ± 3% to 40 ± 6% when co-cultured with Wnt-3a expressing L-cells (Figure 5.7).

In parallel experiments, primary HBE cell cultures were established from normal volunteer subjects. At passage 2 (P2), collagen-coated 8-well Nunc Lab-Tek II glass

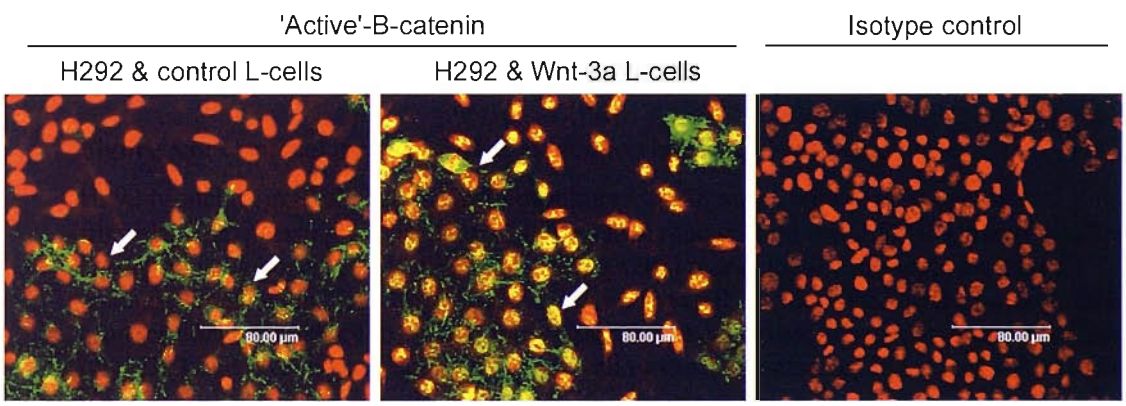

Figure 5.6: Confocal images of ABC expression in H292 / L-cell co-cultures.

H292 bronchial epithelial cells were co-cultured for 48 hours with L-cells (murine fibroblasts) expressing ± Wnt-3a, fixed in acetone, and stained using FITC (green) labelled anti-hypophosphorylated ('active') β-catenin (ABC) monoclonal antibody. Nuclei were counterstained using 7-AAD (red). H292 cells (arrowed) are identified on the basis of their rounder nuclei, tendency to cluster, and classical cadherin expression (membranous staining for ABC), not present in L-cells. Increased yellow co-localisation of FITC and 7-AAD was observed in H292 cells co-cultured with Wnt-3a expressing L-cells, suggesting increased nuclear localisation of ABC. Increased nuclear localisation of ABC was also observed in L-cells expressing Wnt-3a. The isotype control was negative.

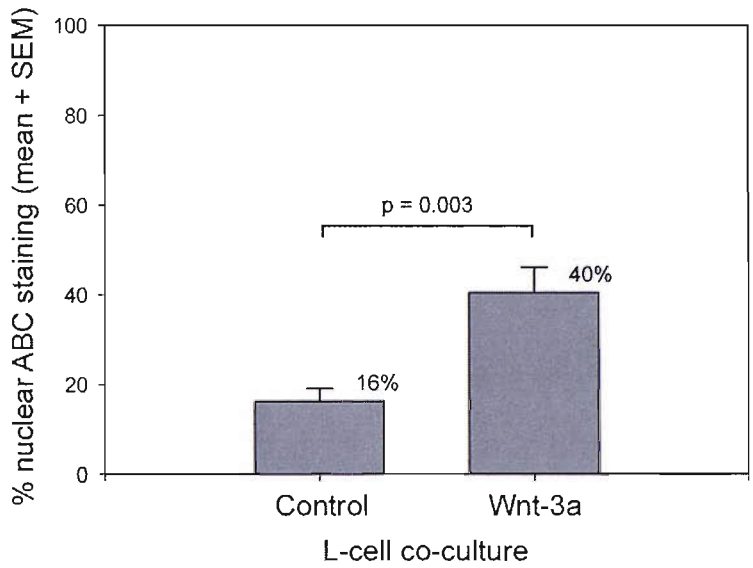

Figure 5.7: Percentage nuclear ABC staining in H292 cells co-cultured with L-cells.

Taking random fields (n=6) from confocal images of hypophosphorylated ('active') β-catenin (ABC) expression in H292 cells co-cultured for 48 hours with L-cells expressing ± Wnt-3a (see Figure 5.6), semi-quantitative analysis of percentage nuclear staining by ABC in H292 cells was undertaken. Data are expressed as mean ± S.E.M and were analysed using the unpaired Student's T-test. Percentage nuclear ABC staining significantly increased from 16 ± 3% to 40 ± 6% when H292 cells were co-cultured with Wnt-3a expressing L-cells.

chamber slides were seeded with a mix of 5 x 10^4 viable HBE cells and 5 x 10^4 L Wnt-3a cells, or 2 x 10^4 parental (control) L-cells, per chamber in 400µl BEBM. Cells were incubated for 48 hours, prior to fixation and immunostaining for transcriptionally active β-catenin. In Figure 5.8, FITC images are overlayed on phase-contrast images to allow morphological differentiation of the two cell types. Primary HBE cells (arrowed) are identified on the basis of their relatively large size, whereas L-cells tend to adopt a fibroblastic morphology. Co-culture with Wnt-3a expressing L-cells can be seen to enhance the intensity of FITC staining in the nuclei of HBE cells, suggesting a Wnt-3a induced increase in nuclear localisation of transcriptionally active β-catenin. Semi-quantitative analysis of percentage nuclear staining in primary HBE cells by ABC on random fields of view (n=6) confirmed a significant increase from 26 ± 5% to 52 ± 4% when co-cultured with Wnt-3a expressing L-cells (Figure 5.9).

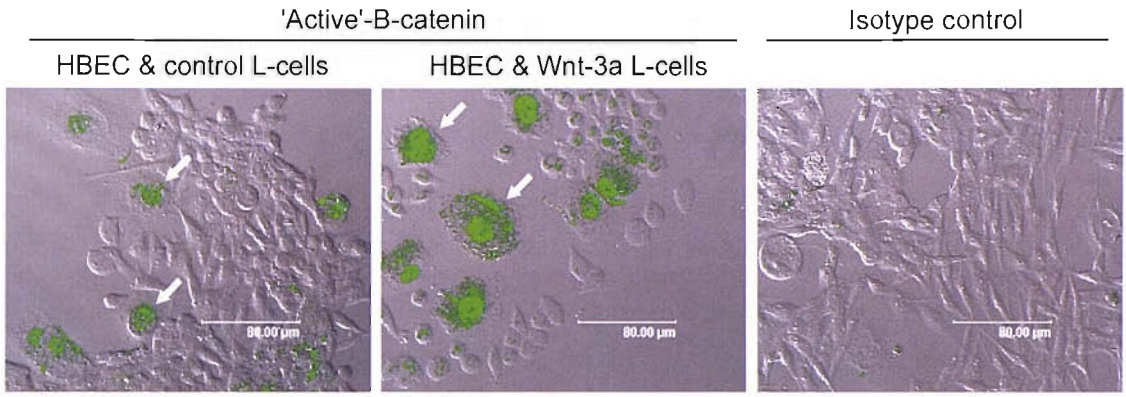

Figure 5.8: Confocal images of ABC expression in HBE cell / L-cell co-cultures.

Primary human bronchial epithelial (HBE) cells obtained from healthy volunteer subjects were co-cultured in serum-free medium for 48 hours with L-cells expressing ± Wnt-3a, fixed in acetone, and stained using FITC (green) labelled anti-hypophosphorylated ('active') β-catenin (ABC) monoclonal antibody. FITC images were overlayed on phase-contrast images to allow morphological differentiation of the two cell types. HBE cells (arrowed) are identified on the basis of their relatively large size, whereas L-cells tend to adopt a fibroblastic morphology. More intense nuclear FITC staining was observed in HBE cells co-cultured with Wnt-3a expressing L-cells, suggesting increased nuclear localisation of ABC. The isotype control was negative.

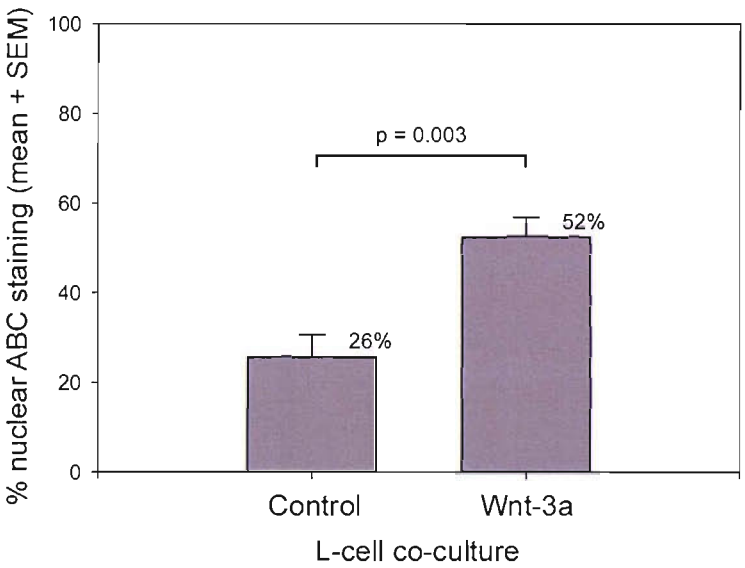

Figure 5.9: Percentage nuclear ABC staining in HBE cells co-cultured with L-cells.

Taking random fields (n=6) from confocal images of hypophosphorylated ('active') β-catenin (ABC) expression in primary human bronchial epithelial (HBE) cells from healthy volunteer subjects co-cultured for 48 hours with L-cells expressing ± Wnt-3a (see Figure 5.8), semi-quantitative analysis of percentage nuclear staining by ABC in HBE cells was undertaken. Data are expressed as mean ± S.E.M and were analysed using the unpaired Student's T-test. Percentage nuclear ABC staining significantly increased from 26 ± 5% to 52 ± 4% when HBE cells were co-cultured with Wnt-3a expressing L-cells.

5.2.3 Wnt-3a induces activation of a Tcf/Lef-1 reporter in H292 cells

To investigate the Tcf/Lef-1 transcriptional response to stimulation with conditioned medium (CM) from Wnt-3a expressing L-cells, 6-well Nunc dishes were seeded with 5 x 10^5 H292 cells per well in 2ml standard RPMI 1640 medium, incubated for 24 hours, and then transiently transfected with TOPflash or FOPflash (Upstate Biotechnology, USA) as described in Section 2.15.6. Cells were incubated for 7 hours, before being placed in 25% v/v CM from Wnt-3a expressing or control L-cells in serum-free UltraCULTURE for 18 hours. Samples were then harvested and analysed as described in Section 2.15.7. When harvested, H292 cells were >80% confluent. The initial experiment (n=1) included 1, 2, 4, 8 and 24 hour time-points, and showed the response in Tcf/Lef-1 reporter activity to be greatest at 18 hours when normalised to the control for that time-point (Figure 5.10). Additional experiments (n=4) confirmed that 18 hours stimulation with Wnt-3a CM induced a 1.4-fold increase in TOPflash reporter activity when compared to control CM (Figure 5.11).

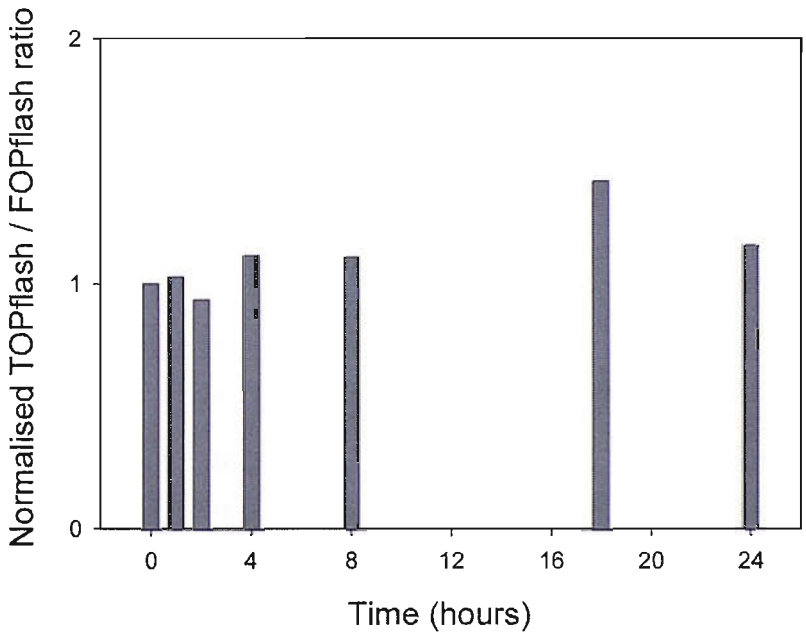

Figure 5.10: TOPflash activity in H292 cells stimulated ± Wnt-3a CM (time-response).

H292 bronchial epithelial cells were transiently transfected with TOPflash or FOPflash reporters prior to stimulation with 25% v/v conditioned medium (CM) from Wnt-3a expressing or control L-cells in serum-free medium for 1, 2, 4, 8, 18 and 24 hours (n=1). Cells were >80% confluent. Data are expressed normalised to the unstimulated control for each time-point. This initial experiment determined the selection of the 18 hour time-point for more detailed investigation (see Figure 5.11).

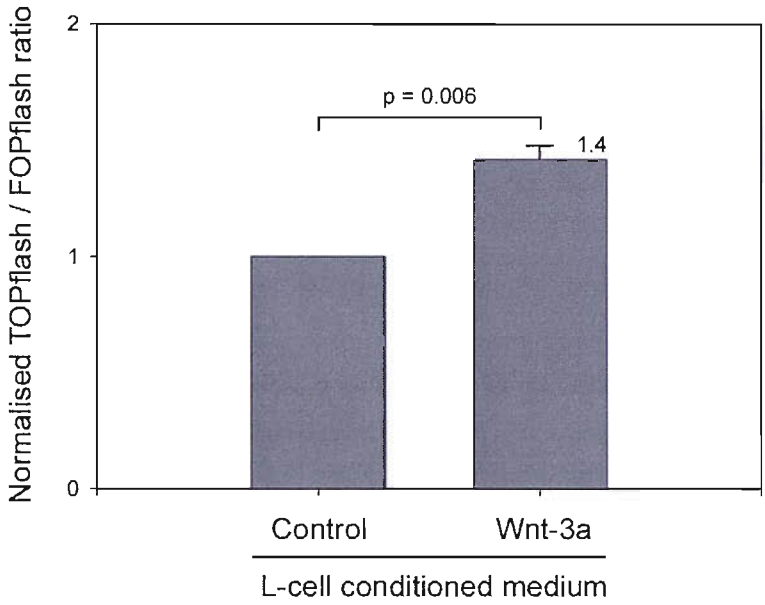

Figure 5.11: TOPflash reporter activity in H292 cells stimulated ± Wnt-3a CM.

H292 bronchial epithelial cells were transiently transfected with TOPflash or FOPflash reporters prior to stimulation with 25% v/v conditioned medium (CM) from Wnt-3a expressing or control L-cells in serum-free medium for 18 hours (n=4). Cells were >80% confluent. Data are expressed as mean ± S.E.M, normalised to the unstimulated control, and were analysed using the paired Student's T-test. Wnt-3a CM induced a 1.4-fold increase in TOPflash reporter activity.

5.2.4 Wnt-3a does not alter *cyclin-D1*, *MMP7* or *IL-8* gene expression in H292 cells

To identify changes in gene expression induced by conditioned medium from Wnt-3a expressing L-cells, H292 cells were seeded in 6-well Nunc dishes at 5 x 10^5 per well in 2ml standard RPMI 1640 medium, incubated for 32 hours, and then placed in serum-free UltraCULTURE medium for 18 hours. Cells were then stimulated for 1, 2, 4 and 8 hours with fresh UltraCULTURE containing 25% v/v CM from Wnt-3a expressing or control L-cells. Cells were lysed with 1ml TRIzol Reagent per well before RNA extraction, DNase treatment (see Section 2.8), and reverse transcription to cDNA (see Section 2.11.2). Samples were analysed by qPCR using primers for *cyclin-D1*, *MMP7* and *IL-8* (see Section 4.2.3). No significant change in *cyclin-D1* (Figure 5.12) or *IL-8* (Figure 5.13) gene expression was observed (n=4), and no significant levels of mRNA encoding MMP7 were detected above RT-minus controls (n=2; Table 10.26).

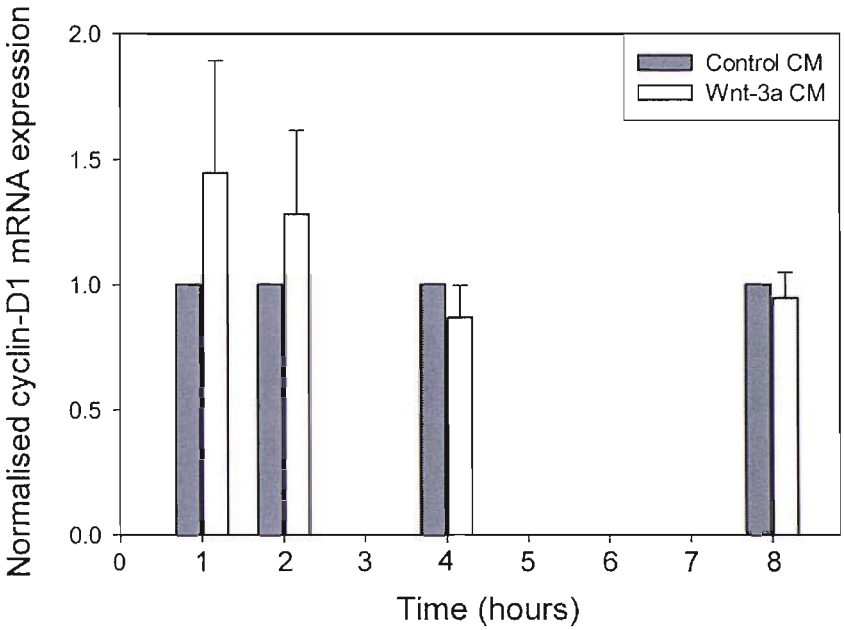

Figure 5.12: *Cyclin-D1* gene expression in H292 cells stimulated ± Wnt-3a CM.

RNA from H292 cells (n=4) stimulated ± 25% v/v Wnt-3a conditioned medium (CM) in Ultraculture for 1, 2, 4 and 8 hours was reverse transcribed, and *cyclin-D1* gene expression investigated by quantitative PCR (qPCR; TaqMan), using the primers and probe in Table 4.1 and 18S rRNA as a normalising control for calculating $\Delta\Delta C_T$ values. Cells were >80% confluent in all experiments. Data are expressed as mean ± S.E.M, normalised to the unstimulated control at each time-point, and were analysed using the paired Student's T-test and one-way ANOVA. No significant change in *cyclin-D1* gene expression was observed.

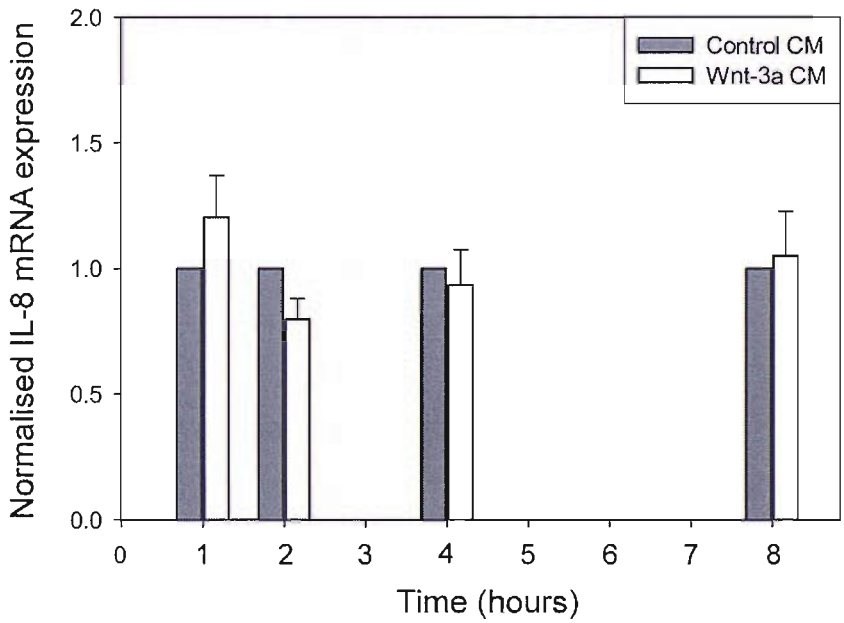

Figure 5.13: *IL-8* gene expression in H292 cells stimulated ± Wnt-3a CM.

Experiments (n=4) were performed as described in Figure 5.12, except that *IL-8* gene expression was investigated instead of *cyclin-D1*.

5.3 Discussion

Frizzleds function as cell surface receptors for Wnts and are required for Wnt signal transduction (Bhanot et al., 1996; Yang-Snyder et al., 1996). Of the ten known human FZD genes, all but FZD-9 have been detected in adult whole lung tissue by RT-PCR or northern blot analysis (Table 1.5). However, little is known about FZD gene expression in each of the more than forty cell types involved. Compared with H292 cells, I have shown that primary HBE cells express similar levels of FZD-5 and -6, with relatively low-level expression of FZD-2 and -3. Primary HBE cells also express low levels of FZD-9, not detected in H292 cells. Importantly, no significant difference in FZD gene expression was seen between HBE cells from mild persistent asthmatic and healthy volunteer subjects. Interestingly, human Fzd-5 has been shown to activate the Wnt/β-catenin pathway, whereas Fzd-3 and -6 appear to activate the non-canonical Wnt/Ca^{2+} pathway (Kuhl et al., 2000b) which can negatively regulate Tcf/Lef-1 transcriptional activity downstream of β-catenin (Golan et al., 2004; Kuhl et al., 2001). In addition, human Fzd-9 has been shown to directly bind Wg, the *Drosophila* homologue of Wnt-1, suggesting it might also be involved in canonical signalling (Wang et al., 1997). Thus, my data suggest that both H292 and primary HBE cells have the potential to respond to canonical *and* non-canonical Wnts, though the functional significance of the observed differences in FZD gene expression between these cells is unclear.

Intriguingly, of the nineteen known human WNT genes, nine have been shown to be expressed in adult whole lung tissue (Table 1.5), including Wnt-3a (Saitoh et al., 2001c), but the cell specific source of individual Wnts remains to be determined. If Frizzled receptors expressed by the bronchial epithelium are occupied *in vivo*, then likely sources of Wnts would include neighbouring (myo)fibroblasts within the epithelial-mesenchymal trophic unit (short-range paracrine signalling), and epithelial cells themselves (autocrine signalling). Indeed, *in vitro* studies have shown primary HBE cells from heavy smokers to express mRNA encoding Wnt-7A (Calvo et al., 2000), and expression of WNT-10B is reported to be up-regulated in primary adult human lung fibroblasts stimulated with the Th2 cytokine, IL-13 (Lee et al., 2001).

Secreted frizzled-related proteins (Sfrp) are a family that function as Wnt antagonists by interfering with Wnt/Fzd interactions in the extracellular space (Wodarz and Nusse, 1998). I have shown that H292 and primary HBE cells both express mRNA encoding Sfrp-1, with relatively low levels in the latter, and no significant difference between mild persistent asthmatic and healthy control groups. Interestingly, SFRP-1 gene expression is reportedly up-regulated in whole lung tissue from patients with pulmonary emphysema, although the cell source is uncertain (Imai and D'Armiento, 2000). Sfrp-1 was first identified in conditioned medium from human embryonic lung (M426) fibroblasts (Finch et al., 1997), and subsequently shown to induce apoptosis, in association with reduced intracellular levels of β-catenin, in human breast adenocarcinoma (MCF7) cells stimulated with TNF-α (Melkonyan et al., 1997). For this reason, SFRP-1 was initially termed secreted apoptosis-related protein-2 (SARP-2) (Melkonyan et al., 1997). Thus, my data suggest that primary HBE cells have the potential to modulate Wnt signals in both autocrine and paracrine modes, and might thereby influence cell fate within the epithelial-mesenchymal trophic unit (EMTU).

Members of the sonic hedgehog (Shh) and Wnt families are among a complex network of morphogens and growth factors within the EMTU that orchestrate the process of mammalian lung development (Warburton et al., 2005). Smoothened (SMOH) is a seven transmembrane spanning (7TMS) protein involved in signal transduction through interactions with the Shh receptor, Patched. Null mutations in transgenic mice indicate that the Shh/Patched/Smoothened pathway plays a fundamental role in the induction of epithelial proliferation and gene expression during branching morphogenesis (Warburton et al., 2000). I have shown that H292 and primary HBE cells both express mRNA encoding Smoothened, raising the possibility that these cells remain capable of transducing a Shh signal. Intruigingly, reactivation of this embryonic signalling pathway has been implicated in epithelial regeneration (Beachy et al., 2004), including that of the mammalian airway (Warburton et al., 2000; Watkins et al., 2003).

To test if adult HBE cells are capable of transducing a canonical Wnt signal, Wnt-3a expressing L-cells were employed as a source of biologically active class-1 Wnt. Importantly, and consistent with my RNase protection data, I have shown that Wnt-3a

expressing L-cells can induce nuclear localisation of hypophosphorylated (transcriptionally active) β-catenin in co-cultured H292 and primary HBE cells, suggesting Wnt-3a induced inhibition of the Gsk-3β/Apc/axin destruction complex and stabilisation of β-catenin (Cook et al., 1996; Liu et al., 2002; Miller et al., 1999; Staal et al., 2002). Increased nuclear localisation of ABC was also observed in Wnt-3a expressing L-cells themselves, consistent with known autocrine activation of the canonical Wnt pathway in this cell type (Shibamoto et al., 1998). Importantly, and consistent with my confocal data, I have also shown that conditioned medium (CM) from Wnt-3a expressing L-cells induced a 1.4-fold increase ($p=0.006$) in TOPflash reporter activity in confluent H292 cells. Although the magnitude of this response appears small, it should be remembered that TOPflash provides a measure of *mean* Tcf/Lef-1 transcriptional activity, and gives no indication of the *range* of activity across the population of transfected cells. Indeed, a *mean* 1.4-fold increase in TOPflash activity could be explained by Tcf/Lef-1 transcriptional activation in 30% of cells to levels comparable with those measured in response to 20mM lithium stimulation, i.e. 4.5-fold (see chapter 4). Thus, I provide good evidence that adult HBE cells express key components of the Wnt/β-catenin signalling pathway, from Frizzled receptors through to Tcf/Lef-1 transcription factors, and that these cells are capable of transducing a canonical Wnt signal. However, the increase in TOPflash reporter activity induced by Wnt-3a CM in was not associated with a significant change in *cyclin-D1*, *MMP7* or *IL-8* gene expression, suggesting that these are not targets of Tcf/Lef-1 transcription factors in this cell type.

CHAPTER 6

SIGNALLING BY β-CATENIN IN A MODEL OF REGENERATING ADULT HUMAN AIRWAY EPITHELIUM

6.1 Aims of the study

In chapter 5, my data suggested that adult human bronchial epithelial (HBE) cells are capable of transducing a canonical Wnt signal. However, the functional significance of the Wnt/β-catenin pathway in these cells is unclear. Transient nuclear localisation of β-catenin in human colorectal epithelial cells during the regenerative phase following radiation-induced injury (Hardy et al., 2002) and human endometrial cells during the mid/late-proliferative and early secretory phases of the menstrual cycle (Nei et al., 1999), strongly suggest a role for β-catenin signalling in epithelial regeneration. Therefore, the aims of this study were to test the hypothesis that ***regulation of the Wnt/β-catenin signalling pathway plays a role in bronchial epithelial repair.***

Reminiscent of *in vivo* events that occur during the process of epithelial restitution following injury, subconfluent cells in log-phase growth achieve confluence *in vitro* by migrating and proliferating (Leir et al., 2000). Thus, the influence of cell density on activation of Tcf/Lef-1 mediated transcription was investigated using subconfluent HBE cells (10-20% confluent) as a simple model of repairing bronchial epithelium, with relatively quiescent cells in near-confluent monolayer (>80% confluent) modelling intact epithelium. In addition, laser confocal microscopy was used to investigate the relationships between changes in cell density, nuclear localisation of hypophosphorylated (transcriptionally active) β-catenin and the percentage of cells expressing the nuclear antigen Ki67, a marker of cell proliferation expressed in late G1, S, G2 and M phases of the cell cycle (Brown and Gatter, 2002).

6.2 Methods and results

6.2.1 Reduced cell density induces activation of a Tcf/Lef-1 reporter in H292 cells

To investigate the Tcf/Lef-1 transcriptional response to changes in cell density *in vitro*, 6-well Nunc dishes were seeded with 5 x 10^4 (low-density) or 5 x 10^5 (high-density) H292 cells per well in 2ml standard RPMI 1640 medium, incubated for 24 hours, and then transiently transfected with TOPflash or FOPflash (Upstate Biotechnology, USA) as described in Section 2.15.6. Cells were incubated for 7 hours, before serum-starvation in UltraCULTURE medium for 18 hours. Samples were then harvested and analysed as described in Section 2.15.7. Figure 6.1 shows a comparison of Tcf/Lef-1 reporter activity between H292 cells at low- and high-cell density (n=6). Reduced cell density induced a 1.8-fold increase in TOPflash reporter activity when compared to cells at high-density.

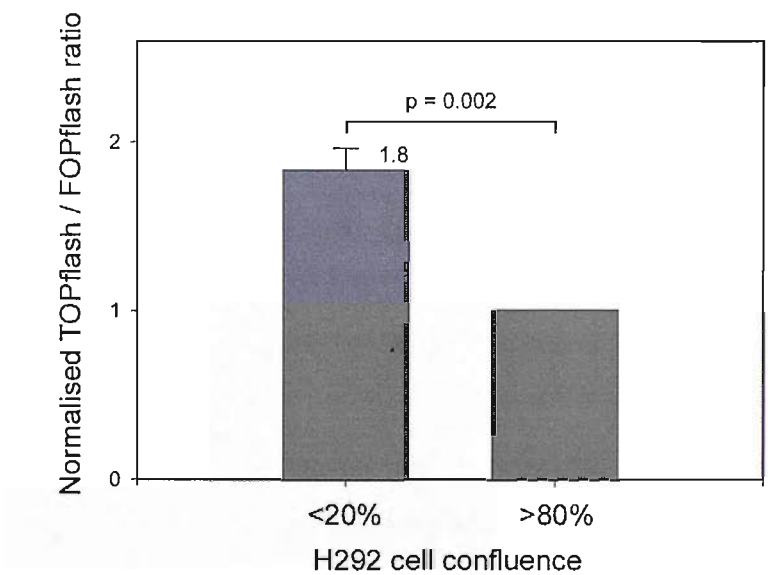

Figure 6.1: TOPflash reporter activity in H292 cells at low- and high-density.

H292 bronchial epithelial cells at low (10-20% confluent) and high (>80% confluent) cell density were transiently transfected with TOPflash or FOPflash reporters prior to culture in serum-free basal medium for 18 hours (n=6). Data are expressed as mean ± S.E.M, normalised to the reporter activity in cells at high-density, and were analysed using the paired Student's T-test. Reduced cell density induced a 1.8-fold increase in TOPflash reporter activity.

6.2.2 Reduced cell density induces nuclear localisation of β-catenin and up-regulates Ki67 expression in H292 and primary HBE cells

To investigate the cellular expression and localisation of β-catenin and Ki67 in response to changes in cell density *in vitro*, 8-well Nunc Lab-Tek II glass chamber slides were seeded with 1.5 x 10^4 (low-density) or 1.5 x 10^5 (high-density) H292 cells per chamber in 500μl standard RPMI 1640 medium. Cells were incubated for 54 hours with culture medium changed at 24 hours, and then placed in serum-free UltraCULTURE medium for 18 hours. Cells were fixed and immunostained using either hypophosphorylated ('active') β-catenin (ABC; clone 8E7; Upstate Biotechnology, USA) or Ki67 (clone MIB-1; DakoCytomation, Ely, UK) monoclonal antibodies, and slides examined by laser confocal microscopy (see Section 2.16). Increased yellow co-localisation of FITC-labelled ABC and 7-AAD was seen in H292 cells at low-density when compared with cells at high-density, indicating an increase in nuclear localisation of hypophosphorylated (transcriptionally active) β-catenin in low-density cells (Figure 6.2). Semi-quantitative analysis of percentage nuclear staining by ABC on random fields of view (n=4) confirmed a significant increase from 27 ± 3% to 51 ± 7% as cell density decreased (Figure 6.3). In H292

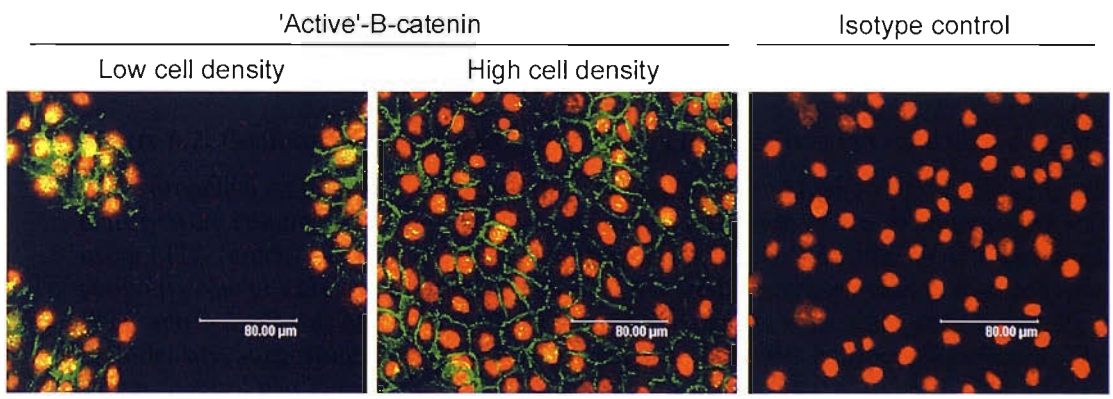

Figure 6.2: Confocal images of ABC expression in H292 cells at low- and high-density.

H292 bronchial epithelial cells at low (10-20% confluent) and high (>80% confluent) cell density were cultured in serum-free basal medium for 18 hours, fixed in acetone, and stained using FITC (green) labelled anti-hypophosphorylated ('active') β-catenin (ABC) monoclonal antibody. Nuclei were counterstained using 7-AAD (red). Increased yellow co-localisation of FITC and 7-AAD was observed in H292 cells at low-density when compared with cells at high-density, suggesting increased nuclear localisation of ABC in subconfluent cells. The isotype control was negative.

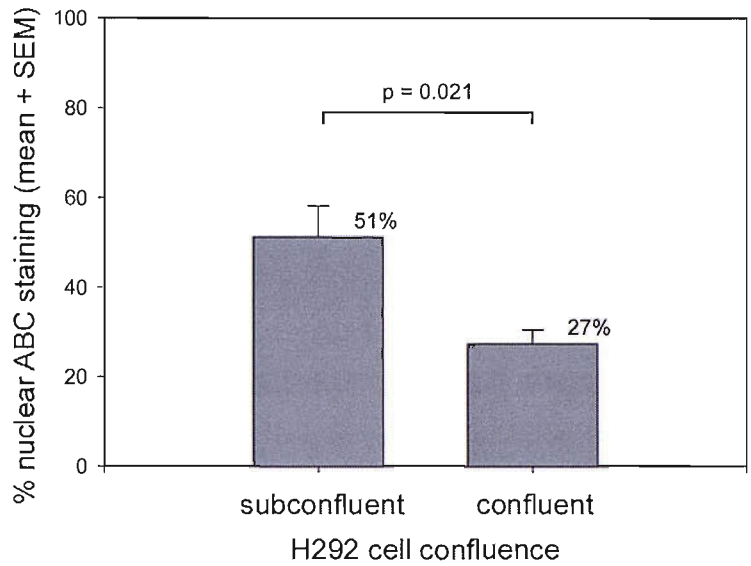

Figure 6.3: Percentage nuclear ABC staining in H292 cells at low- and high-density.

Taking random fields (n=4) from confocal images of hypophosphorylated ('active') β-catenin (ABC) expression in H292 cells at low (10-20% confluent) and high (>80% confluent) cell density (see Figure 6.2), semi-quantitative analysis of percentage nuclear staining by ABC was undertaken. Data are expressed as mean ± S.E.M and were analysed using the unpaired Student's T-test. Percentage nuclear ABC staining significantly increased from 27 ± 3% to 51 ± 7% as cell density decreased.

cells at low-density, yellow co-localisation of FITC-labelled Ki67 and 7-AAD was seen in almost every cell, indicating nuclear expression of Ki67 and very high mitotic index (Figure 6.4). However, in H292 cells at high-density, the proportion of nuclei expressing Ki67 decreased, suggesting a fall in the mitotic index and reduced cell proliferation as H292 cells reached confluence. Semi-quantitative analysis of the percentage of cells expressing Ki67 on random fields of view (n=3) confirmed a significant increase from 34 ± 14% to 99 ± 0% as cell density decreased (Figure 6.5).

In parallel experiments, primary HBE cell cultures were established by seeding cells brushed from the proximal airways of normal volunteer subjects. At passage 2 (P2), collagen-coated 8-well Nunc Lab-Tek II glass chamber slides were seeded with 5 x 10^4 viable HBE cells per chamber in 500μl BEGM. Cells were incubated and culture medium changed every 48 hours. When cells were subconfluent or confluent, BEGM was replaced with growth factor-free BEBM for 18 hours, prior to fixation and immunostaining for transcriptionally active β-catenin and Ki67. Increased yellow co-localisation of FITC-labelled ABC and 7-AAD was seen in primary HBE cells at

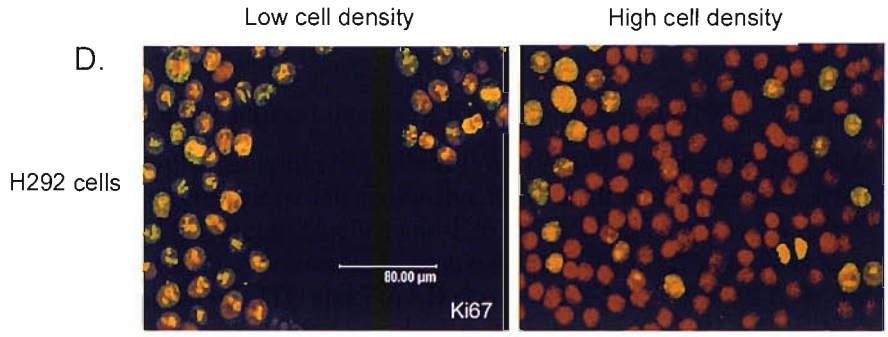

Figure 6.4: Confocal images of Ki67 expression in H292 cells at low- and high-density.

H292 bronchial epithelial cells at low (10-20% confluent) and high (>80% confluent) cell density were cultured in serum-free basal medium for 18 hours, fixed in acetone, and stained using FITC (green) labelled anti-Ki67 monoclonal antibody, a marker of cell proliferation. Nuclei were counterstained using 7-AAD (red). In H292 cells at low-density, yellow co-localisation of FITC and 7-AAD was observed in almost all cells, indicating nuclear expression of Ki67 and very high mitotic index. In H292 cells at high-density, the proportion of nuclei expressing Ki67 was reduced, indicating decreased proliferation as H292 cells reached confluence.

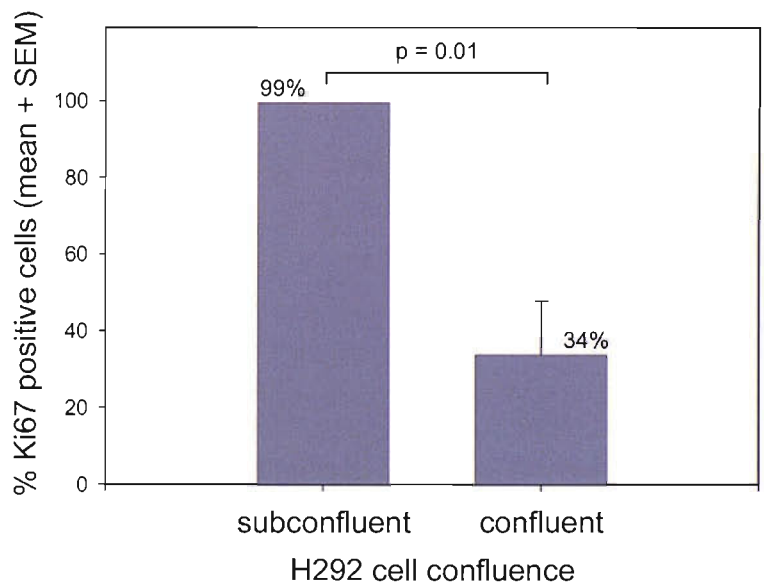

Figure 6.5: Percentage of H292 cells expressing Ki67 at low- and high-density.

Taking random fields (n=3) from confocal images of Ki67 expression in H292 cells at low (10-20% confluent) and high (>80% confluent) cell density (see Figure 6.1), quantitative analysis of the percentage of cells expressing Ki67 was undertaken. Data are expressed as mean ± S.E.M and were analysed using the unpaired Student's T-test. The percentage of H292 cells expressing Ki67 significantly decreased from 99 ± 0% to 34 ± 14% as cell density increased, indicating reduced proliferation as H292 cells reached confluence.

low-density when compared with cells at confluence, indicating an increase in nuclear localisation of transcriptionally active β-catenin in subconfluent cells (Figure 6.6). In addition, ABC was seen to redistribute into cell-cell membrane contacts in HBE cells at confluence. Semi-quantitative analysis of percentage nuclear staining by ABC on random fields of view (n=8) confirmed a significant increase from 24 ± 2% to 65 ± 5% as HBE cell density decreased (Figure 6.7). In primary HBE cells at low-density, yellow co-localisation of FITC-labelled Ki67 and 7-AAD was frequently observed, indicating nuclear expression of Ki67 (Figure 6.8). However, in HBE cells at high-density, the proportion of nuclei expressing Ki67 decreased. Semi-quantitative analysis of the percentage of cells expressing Ki67 on random fields of view (n=4) confirmed a significant increase from 26 ± 2% to 66 ± 3% as cell density decreased (Figure 6.9).

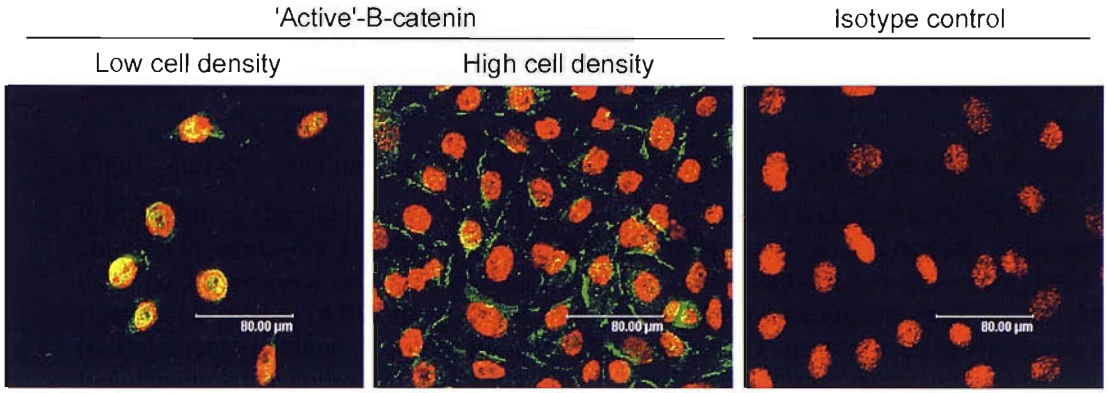

Figure 6.6: Confocal images of ABC expression in HBE cells at low- and high-density.

Primary human bronchial epithelial (HBE) cells from healthy volunteer subjects were cultured in serum-free basal medium for 18 hours at low and high cell density. Cells were then fixed in acetone, and stained using FITC (green) labelled anti-hypophosphorylated ('active') β-catenin (ABC) monoclonal antibody. Nuclei were counterstained using 7-AAD (red). Increased yellow co-localisation of FITC and 7-AAD was observed in HBE cells at low-density when compared with cells at high-density, suggesting increased nuclear localisation of ABC. In HBE cells at high cell density, ABC was also seen to redistribute into cell-cell membrane contacts. The isotype control was negative.

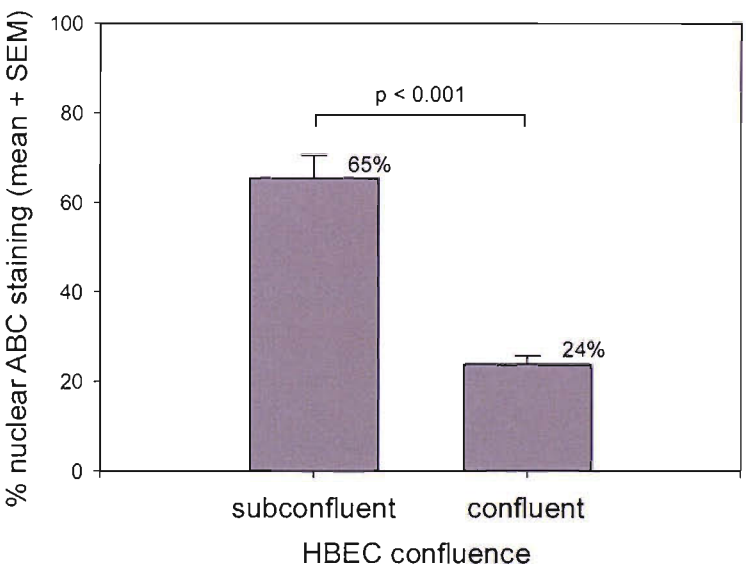

Figure 6.7: Percentage nuclear ABC staining in HBE cells at low- and high-density.

Taking random fields (n=8) from confocal images of hypophosphorylated ('active') β-catenin (ABC) expression in primary human bronchial epithelial (HBE) cells from healthy volunteer subjects at low- and high-density (see Figure 6.6), semi-quantitative analysis of percentage nuclear staining by ABC was undertaken. Data are expressed as mean ± S.E.M and were analysed using the unpaired Student's T-test. Percentage nuclear ABC staining significantly increased from 24 ± 2% to 65 ± 5% as cell density decreased.

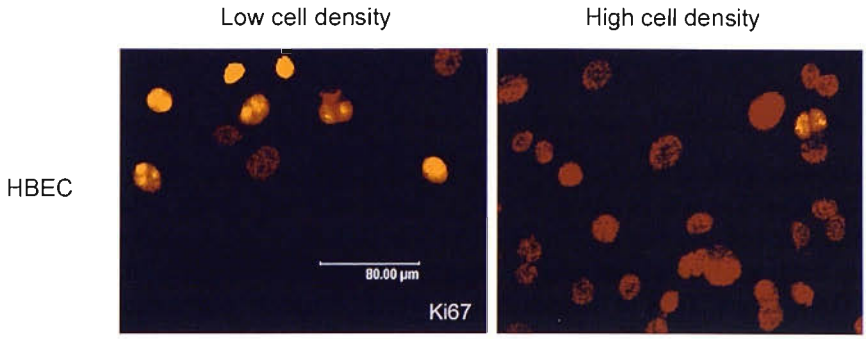

Figure 6.8: Confocal images of Ki67 expression in HBE cells at low- and high-density.

Primary human bronchial epithelial (HBE) cells from healthy volunteer subjects were cultured in serum-free basal medium for 18 hours at low and high cell density. Cells were then fixed in acetone, and stained using FITC (green) labelled anti-Ki67 monoclonal antibody, a marker of cell proliferation. Nuclei were counterstained using 7-AAD (red). In HBE cells at low-density, yellow co-localisation of FITC and 7-AAD was frequently observed, indicating nuclear expression of Ki67. However, the proportion of nuclei expressing Ki67 was reduced in HBE cells at high-density, indicating decreased proliferation as HBE cells reached confluence.

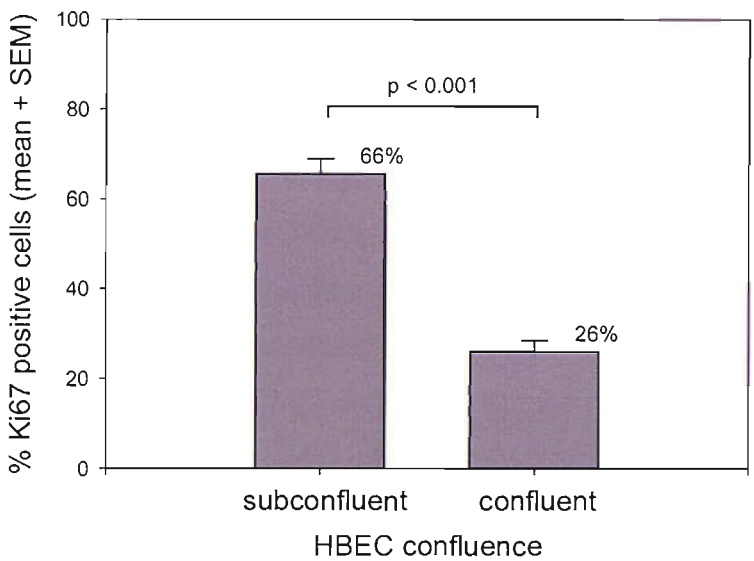

Figure 6.9: Percentage of HBE cells expressing Ki67 at low- and high-density.

Taking random fields (n=4) from confocal images of Ki67 expression in primary human bronchial epithelial (HBE) cells from healthy volunteer subjects at low- and high-density (see Figure 6.8), quantitative analysis of the percentage of cells expressing Ki67 was undertaken. Data are expressed as mean ± S.E.M and were analysed using the unpaired Student's T-test. The percentage of HBE cells expressing Ki67 significantly decreased from 66 ± 3% to 26 ± 2% as cell density increased, indicating reduced proliferation as HBE cells reached confluence.

6.3 Discussion

Subconfluent cells in log-phase growth achieve confluence by migrating and proliferating, and were therefore used as a simple model of repairing epithelium, with intact epithelium modelled by relatively quiescent cells in near-confluent monolayer. Under serum-free conditions to remove the influence of exogenous growth factors, I have shown that H292 cells at low-density (10-20% confluent) exhibit a 1.8-fold increase ($p=0.002$) in TOPflash reporter activity when compared with cells at high-density (>80% confluent). I have also shown that reduced H292 cell density induces nuclear localisation of transcriptionally active β-catenin, and that similar events occur in primary HBE cells. Taken together, these data suggest that β-catenin mediated Tcf/Lef-1 transcriptional activity is up-regulated in subconfluent HBE cells, and that this signalling pathway might play an important role in the 'repair' phenotype. Target genes identified in human colorectal cancer cells include those involved in cell migration (*MMP7*, *CD44*) (Crawford et al., 1999; Wielenga et al., 1999) and proliferation (*cyclin-D1*, *c-myc*) (He et al., 1998; Shtutman et al., 1999). However, experiments in chapters 4 and 5 suggested that *MMP7* and *cyclin-D1* were not targets of the canonical Wnt pathway in HBE cells. Despite this, a positive correlation was observed between β-catenin mediated Tcf/Lef-1 transcriptional activity and expression of Ki67 in these cells, raising the possibility that this signalling pathway might regulate epithelial proliferation via the expression of genes involved in cell cycle control, other than *cyclin-D1*. Such candidates would include *c-myc* (He et al., 1998) which, like *cyclin-D1*, permits G1/S phase progression by antagonising the cyclin dependent kinase (Cdk) inhibitor, $p21^{Waf1/Cip1}$, thereby allowing activation of the cyclin-E/Cdk-2 complex at the G1/S checkpoint (Steiner et al., 1995).

Density-dependent inhibition of growth is a well recognised feature of non-malignant and non-transformed cells that corresponds to the plateau phase of the *in vitro* growth curve, where the rate of proliferation falls at confluence until cells arrest at the G1/S checkpoint and become quiescent (G0 resting state). In contrast, malignant and transformed cells are characterised by partial or complete loss of this phenomenon, with dysregulated proliferation beyond confluence leading to very high cell density ± cell stratification. Although the mechanisms of density-dependent growth inhibition

remain controversial, one model of particular interest is that of *contact inhibition*, in which mitogenic signalling by growth factor receptors is somehow inhibited by the process of increased cell-cell adhesion. In this respect, attention has focused on the role played by adherens junctions, which comprise cadherin/β-catenin complexes linked to the actin cytoskeleton via α-catenin (Aberle et al., 1996; Ozawa et al., 1989). E-cadherin (uvomorulin) is the principal cadherin of epithelial cells, and binds to molecules on juxtaposed cells in a calcium-dependent and homophilic manner. Studies have shown that reduced or absent expression of E-cadherin &/or α-catenin is a frequent finding in carcinoma cells (Shiozaki et al., 1994), and that ectopic E-cadherin (St Croix et al., 1998; Stockinger et al., 2001) or α-catenin (Bullions et al., 1997) can induce growth suppression. In keeping with observations made by Dietrich *et al* in human keratinocytes (Dietrich et al., 2002), my data suggest a link between β-catenin mediated signalling and contact inhibition, since transcriptionally active β-catenin redistributes from the nuclear to membrane compartment probably binding to E-cadherin as the extent of cell-cell contact increases. These observations have led to a model of contact inhibition in which classical cadherins compete with Tcf/Lef-1 transcription factors for direct binding to the *armadillo*-like (*arm*) repeat domain of β-catenin, thereby modifying the kinetics of the uncomplexed, transcriptionally active pool (Huber and Weis, 2001; Stockinger et al., 2001; von Kries et al., 2000). Consistent with this hypothesis, Tcf/Lef-1 transcriptional activity can be reduced in SW480 cells by ectopic E-cadherin (Gottardi et al., 2001) or α-catenin (Giannini et al., 2000), and has been shown to correlate with epithelial cell growth (Orford et al., 1999; Zhu and Watt, 1999).

E-cadherin mediated intercellular adhesion is a highly dynamic process, and whether adherens junctions are up- or down-regulated will depend on the balance between their rates of assembly and disassembly. Evidence suggests that tyrosine phosphorylation of β-catenin by the epidermal growth factor (EGF) receptor (ErbB1) prevents it binding to α-catenin, thereby destabilising adherens junctions (Hoschuetzky et al., 1994; Shiozaki et al., 1995; Takahashi et al., 1997; Tsukatani et al., 1997). The rate of adherens junction assembly will reflect the extent of E-cadherin mediated contact between adjacent cells. In contrast, the rate of adherens junction disassembly will reflect the balance between activities of the EGF receptor and

members of the protein tyrosine phosphatase (PTP) family (Fuchs et al., 1996; Muller et al., 1999). In contrast to epithelial cells in log-phase growth, studies have shown that β-catenin is not phosphorylated on tyrosine residues when cells are confluent and quiescent, reflecting dominance of PTP over EGF receptor activity under these conditions (St Croix et al., 1998; Takahashi et al., 1997; Tsukatani et al., 1997). Furthermore, evidence suggests that extensive cadherin-mediated cell-cell adhesion can inhibit ligand-induced activation of the EGF receptor by preventing ErbB1 dimerization and tyrosine autophosphorylation (Takahashi and Suzuki, 1996), possibly through competition for actin binding sites (den Hartigh et al., 1992) &/or allosteric hindrance (Takahashi and Suzuki, 1996). This has led to the hypothesis of reciprocal and reversible control of intercellular adhesion and cell proliferation by two-way signalling between E-cadherin and the EGF receptor (Jawhari et al., 1999), and provides an alternative model of contact inhibition (Takahashi and Suzuki, 1996). Moreover, in addition to promoting G1/S phase progression downstream of the MEK/MAPK and PI3K pathways, the EGF receptor has also been shown to inhibit Gsk-3β and activate Tcf/Lef-1 mediated gene transcription (Cheon et al., 2004), providing an essential co-signal required for passage through the G1/S checkpoint (Graham and Asthagiri, 2004).

Finally, cell density related change in class-1 Wnt expression has not been described in the literature to date. However, there have been reports of up-regulated expression of secreted frizzled-related proteins-1 and -2 in quiescent cells at confluence, when compared with cells in log-phase growth (Huguet et al., 1995; Roth et al., 2000). These findings support a third model of density-dependent growth inhibition in which inhibition of the Gsk-3β/Apc/axin destruction complex and stabilisation of transcriptionally active β-catenin are promoted by *autocrine* canonical Wnt signals, but modulated by Wnt antagonists.

CHAPTER 7

FACTORS REGULATING β-CATENIN MEDIATED TCF/LEF-1 TRANSCRIPTIONAL ACTIVITY IN HUMAN AIRWAY EPITHELIAL CELLS

7.1 Aims of the study

In chapter 6, Tcf/Lef-1 mediated transcriptional activity was shown to be influenced by cell density, and correlated with changes in both nuclear β-catenin and cell proliferation in a simple model of bronchial epithelial repair. However, the mechanisms involved were unclear. Therefore, I decided to investigate the regulation of β-catenin signalling by factors relevant to both the epithelial injury/repair cycle and models of density-dependent growth inhibition by testing the following hypotheses:

1. ***Epidermal growth factor (EGF) receptor activation leads to increased Tcf/Lef-1 transcriptional activity.***
2. ***Loss of E-cadherin mediated cell-cell contact leads to an increase in β-catenin mediated transcription.***
3. ***Cell density regulates the expression of secreted frizzled-related proteins (SFRP) in bronchial epithelial cells.***

The EGF receptor (ErbB1) plays an important role in epithelial repair, promoting all phases of epithelial restitution, including cell migration, proliferation and differentiation (Davies et al., 1999). EGF is secreted by goblet cells into the airway epithelial lining fluid, and disruption of tight junctions as a consequence of epithelial injury allows autocrine activation of the EGF receptor, expressed along the basolateral cell membrane (Davies et al., 1999). Thus, evidence of EGF-induced activation of Tcf/Lef-1 transcription factors and nuclear localisation of β-catenin was sought in H292 cells using the TOPflash reporter and laser confocal microscopy. Since epithelial injury involves the loss of E-cadherin mediated intercellular junctions, changes in β-catenin mediated transcriptional activity were also assessed using calcium- and magnesium-free medium to disrupt calcium-dependent cadherin-mediated cell-cell contacts. Finally, SFRP expression was investigated in H292 cells

at low (10-20% confluent) and high (>80% confluent) density using RNase protection assays.

7.2 Methods and results

7.2.1 EGF receptor activation induces activation of a Tcf/Lef-1 reporter in H292 cells at *high* cell density in association with reduced membranous localisation of β-catenin

To investigate Tcf/Lef-1 transcriptional activity, 6-well Nunc dishes were seeded with 5 x 10^5 (high-density) H292 cells per well in 2ml standard RPMI 1640 medium, incubated for 24 hours, and then transiently transfected with TOPflash or FOPflash (Upstate Biotechnology, USA) as described in Section 2.15.6. Cells were incubated for 7 hours, ready for experimentation. To investigate the influence of EGF receptor activation on Tcf/Lef-1 transcriptional activity, cells were serum-starved for 18 hours in UltraCULTURE medium, before being placed in UltraCULTURE ± 20ng/ml recombinant EGF (Peprotech, London, UK) ± 1μM tyrphostin (AG1478; Biomol, Hamburg, Germany), a selective inhibitor of the EGF receptor (Puddicombe et al., 2000). Samples were then harvested at 15, 30 and 45 minutes, and 1, 2, 4, 8 and 24 hours, and analysed as described in Section 2.15.7. Importantly, access to the EGF receptor was not restricted, because H292 cells do not express tight junctions (Winton et al., 1998). No significant change in TOPflash reporter activity was observed at 15, 30 and 45 minutes, and 1, 2, 4 and 8 hours in *high*-density H292 cells (n=7) in response to EGF stimulation (Figure 7.1). However, Tcf/Lef-1 reporter activation was observed when independent experiments (n=4) were performed at 24 hours (Figure 7.2); EGF induced a 1.3-fold increase in TOPflash activity above unstimulated control (p=0.004) that was completely abolished by addition of AG1478, indicating dependence on EGF receptor activation. Furthermore, AG1478 induced a fall in reporter activity that was significantly below that of the unstimulated control (p=0.002). To investigate whether the influence of the EGF receptor on Tcf/Lef-1 transcriptional activity was a cell-density related phenomenon, this experiment was repeated with H292 cells at *low*-density (seeded at 5 x 10^4 cells per well) and comparison made with unstimulated cells at high-density (n=4). As previously shown

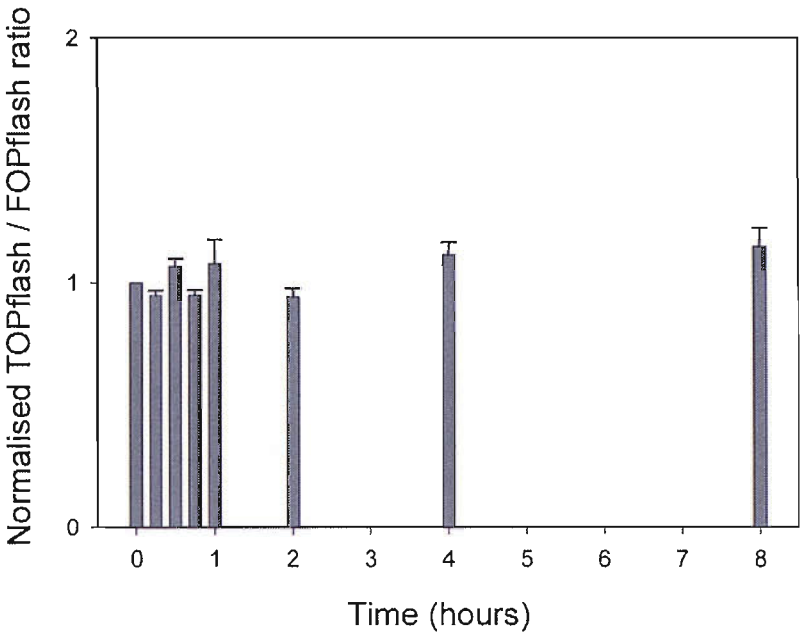

Figure 7.1: TOPflash reporter activity in H292 cells stimulated ± EGF (time-response). H292 bronchial epithelial cells were transiently transfected with TOPflash or FOPflash reporters prior to stimulation ± 20ng/ml EGF (epidermal growth factor) for 15, 30 and 45 minutes, and 1, 2, 4 and 8 hours (n=7). Cells were >80% confluent in all experiments. Data are expressed as mean ± S.E.M, normalised to the unstimulated control for each time-point, and were analysed using the paired Student's T-test and one-way ANOVA. No significant change in Tcf/Lef-1 reporter activity was observed in response to EGF stimulation.

in chapter 6, unstimulated H292 cells at low-density exhibited a 1.7-fold increase in TOPflash activity when compared with cells at high-density (Figure 7.3). Under conditions of low cell density, EGF stimulation induced a small increase in Tcf/Lef-1 mediated signalling that failed to reach statistical significance. Although AG1478 suppressed this small effect, it did not reduce the higher basal level of reporter activity in low-density cells to the lower basal level observed in unstimulated cells at high-density.

To investigate the cellular expression and localisation of β-catenin in response to EGF in cells at high-density, 8-well Nunc Lab-Tek II glass chamber slides were seeded with 10^5 H292 cells per chamber in 500µl standard RPMI 1640 medium. Cells were incubated for 30 hours, placed in serum-free UltraCULTURE for 16 hours, and then stimulated with fresh UltraCULTURE ± 20ng/ml EGF for 24 hours. Cells were fixed and immunostained using the hypophosphorylated ('active') β-catenin (ABC;

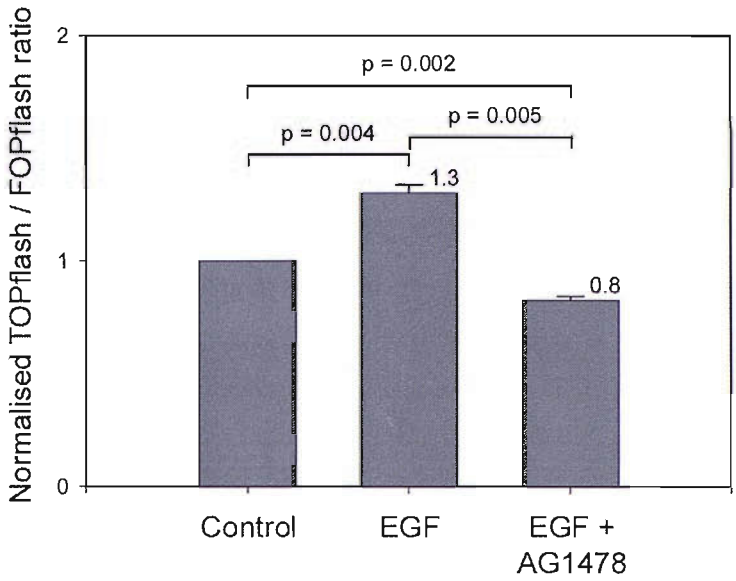

Figure 7.2: TOPflash reporter activity in high-density H292 cells stimulated ± EGF.

H292 bronchial epithelial cells were transiently transfected with TOPflash or FOPflash reporters prior to stimulation ± 20ng/ml EGF (epidermal growth factor) ± 1μM AG1478 (tyrphostin) for 24 hours (n=4). Cells were >80% confluent in all experiments. Data are expressed as mean ± S.E.M, normalised to the unstimulated control, and were analysed using the paired Student's T-test. EGF induced a 1.3-fold increase in Tcf/Lef-1 reporter activity (p=0.004) that was completely abolished by addition of AG1478, a selective inhibitor of the EGF receptor. Furthermore, AG1478 induced a fall in reporter activity that was significantly below baseline.

clone 8E7; Upstate Biotechnology, USA) monoclonal antibody, and slides examined by laser confocal microscopy (see Section 2.16). No discernable change in yellow co-localisation of FITC-labelled ABC and 7-AAD in response to EGF stimulation was seen (Figure 7.4). Semi-quantitative analysis of percentage nuclear staining by ABC on random fields of view (n=8) confirmed this observation; although a small increase in percentage nuclear ABC staining was observed in response EGF stimulation at this time-point, it failed to reach statistical significance (Figure 7.5).

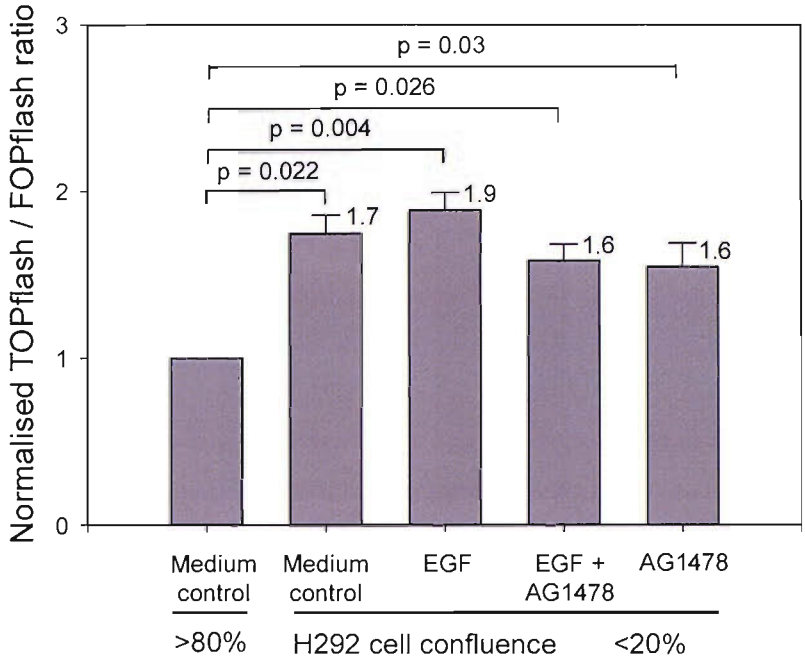

Figure 7.3: TOPflash reporter activity in low-density H292 cells stimulated ± EGF.

H292 bronchial epithelial cells were transiently transfected with TOPflash or FOPflash reporters prior to stimulation ± 20ng/ml EGF (epidermal growth factor) ± 1μM AG1478 (tyrphostin) for 24 hours (n=4). In all experiments, low-density cells were 10-20% confluent, and comparison was made with unstimulated cells at high-density (>80% confluent). Data are expressed as mean ± S.E.M, normalised to the unstimulated high-density control, and were analysed using the paired Student's T-test. EGF failed to induce a significant change in Tcf/Lef-1 reporter activity in low-density cells. Furthermore, AG1478 did not decrease reporter activity to levels observed in cells at high-density.

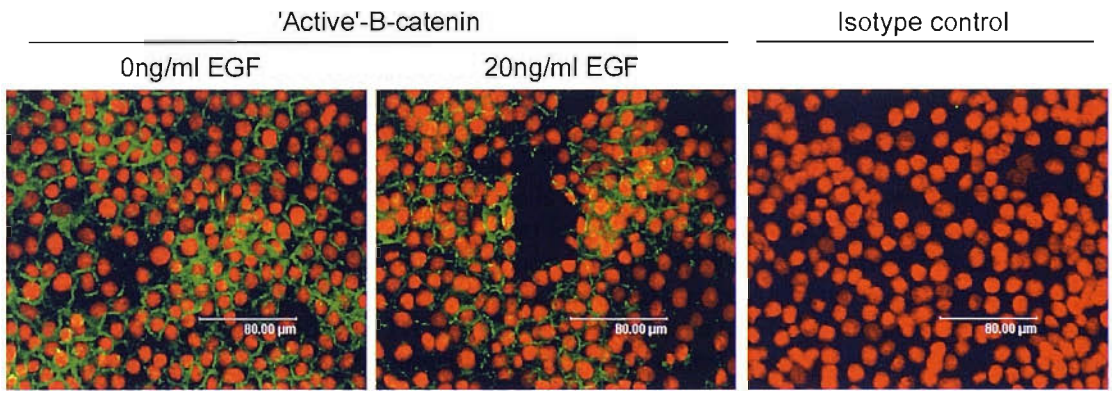

Figure 7.4: Confocal images of ABC expression in H292 cells stimulated ± EGF.

Confluent H292 bronchial epithelial cells in serum-free basal medium were stimulated ± 20ng/ml EGF (epidermal growth factor) for 24 hours, fixed in acetone, and stained using FITC (green) labelled anti-hypophosphorylated ('active') β-catenin (ABC) monoclonal antibody. Nuclei were counterstained using 7-AAD (red). Although no discernable change in yellow co-localisation of FITC and 7-AAD in response to EGF stimulation was seen, reduced membranous staining was observed. The isotype control was negative.

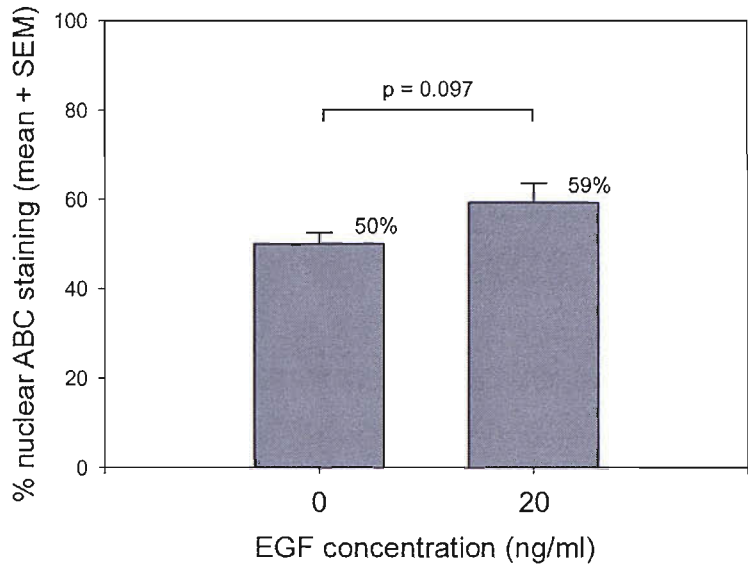

Figure 7.5: Percentage nuclear ABC staining in H292 cells stimulated ± EGF.

Taking random fields (n=8) from confocal images of hypophosphorylated ('active') β-catenin (ABC) expression in confluent H292 cells stimulated ± 20ng/ml EGF (epidermal growth factor) for 24 hours (see Figure 7.2), semi-quantitative analysis of percentage nuclear staining by ABC was undertaken. Data are expressed as mean ± S.E.M and were analysed using the unpaired Student's T-test. No significant change in percentage nuclear ABC staining was observed in response EGF stimulation at this time-point.

7.2.2 Tcf/Lef-1 reporter activity is not increased following disruption of cell-cell junctions by low Ca^{2+} medium in H292 cells at high cell density

To demonstrate the effect of Ca^{2+}- and Mg^{2+}-free medium on cadherin-mediated cell-cell contacts, the cellular expression and localisation of E-cadherin and β-catenin was investigated by laser confocal microscopy. 8-well Nunc Lab-Tek II glass chamber slides were seeded with 10^5 H292 cells per chamber in 500µl standard RPMI 1640 medium. Cells were incubated for 30 hours, placed in serum-free LHC-9 medium (Invitrogen, Paisley, UK) supplemented with 0.424mM calcium chloride ($CaCl_2$) and 0.407mM magnesium sulphate (Mg_2SO_4) for 16 hours, then stimulated with fresh LHC-9 medium ± 0.424mM $CaCl_2$ and 0.407mM Mg_2SO_4 for 24 hours. Cells were fixed and immunostained using either E-cadherin (clone HECD-1; R&D Systems, Abingdon, UK) or pan-β-catenin (PBC; clone 14; BD Biosciences, Oxford, UK) monoclonal antibodies, and slides examined by laser confocal microscopy (see Section 2.16). Ca^{2+}- and Mg^{2+}-free medium induced disruption of calcium-dependent

cadherin-mediated cell-cell junctions, resulting in the rounding of cells and internalisation of E-cadherin and β-catenin away from cell membranes (Figure 7.6).

To investigate Tcf/Lef-1 transcriptional activity in this Ca^{2+} switch model, 6-well Nunc dishes were seeded with 5 x 10^4 (low-density) or 5 x 10^5 (high-density) H292 cells per well and transiently transfected with TOPflash or FOPflash, as described in Section 7.2.1. When ready for experimentation, cells were placed in LHC-9 medium ± 0.424mM $CaCl_2$ plus 0.407mM Mg_2SO_4 ± 20mM lithium chloride for 24 hours, prior to harvesting. Three independent experiments were performed, and samples analysed as described in Section 7.2.1. In H292 cells at high-density, switch to Ca^{2+}- and Mg^{2+}-free medium failed to increase Tcf/Lef-1 reporter activity to levels observed in cells at low-density, but induced a small decrease in TOPflash activity (Figure 7.7). Importantly, Ca^{2+}- and Mg^{2+}-free medium did not alter the response of H292 cells to stimulation with lithium, used as a positive control (Figure 7.8).

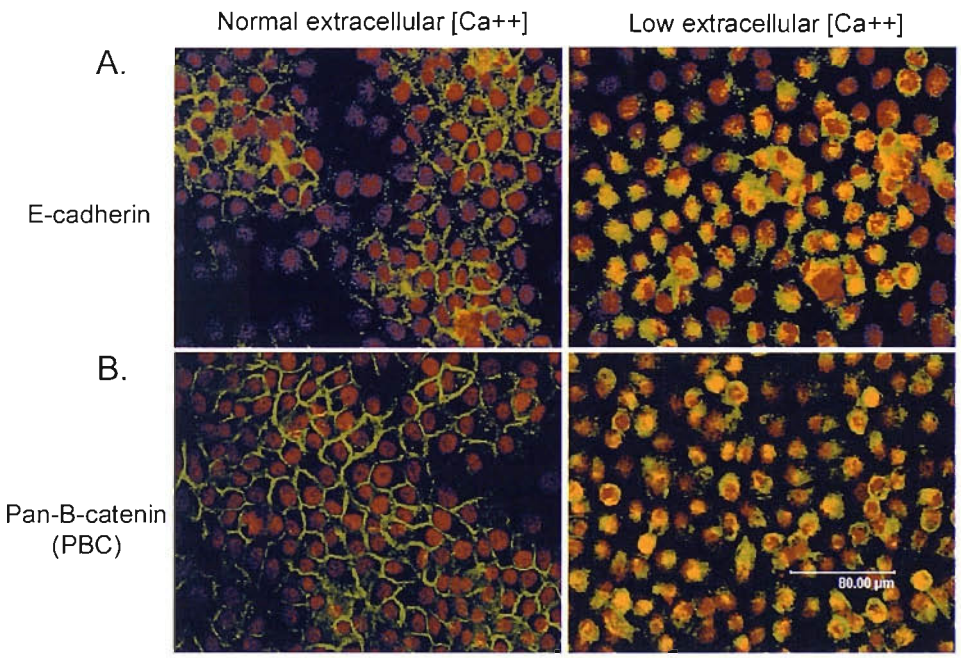

Figure 7.6: Confocal images of E-cadherin & PBC in H292 cells ± low Ca^{2+} medium.

Confluent H292 bronchial epithelial cells were stimulated ± Ca^{2+}- and Mg^{2+}-free medium for 24 hours, fixed in acetone, and stained using FITC (green) labelled anti-E-cadherin or anti-pan-β-catenin (PBC) monoclonal antibodies. Nuclei were counterstained using 7-AAD (red). Ca^{2+}- and Mg^{2+}-free medium induced disruption of calcium-dependent cadherin-mediated cell-cell junctions, resulting in cell rounding and internalisation of E-cadherin and β-catenin away from cell membranes.

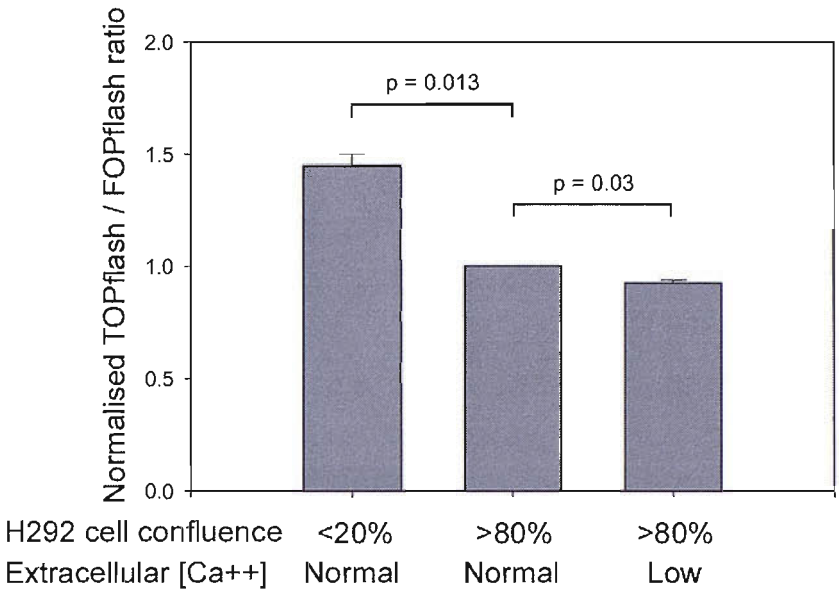

Figure 7.7: TOPflash reporter activity in H292 cells stimulated ± low Ca^{2+} medium.

H292 bronchial epithelial cells were transiently transfected with TOPflash or FOPflash reporters prior to stimulation ± Ca^{2+}- and Mg^{2+}-free medium for 24 hours (n=3). In all experiments, high-density cells were >80% confluent, and comparison was made with low-density cells (10-20% confluent). Data are expressed as mean ± S.E.M, normalised to high-density cells in calcium-containing medium, and were analysed using the paired Student's T-test. In H292 cells at high-density, switch to Ca^{2+}- and Mg^{2+}-free medium failed to increase Tcf/Lef-1 reporter activity to levels observed in cells at low-density, but induced a small but significant decrease in reporter activity (p=0.03). As a positive control, Ca^{2+}- and Mg^{2+}-free medium did not alter the response of H292 cells to stimulation with lithium.

7.2.3 Increased cell density up-regulates FZD6 gene expression in H292 cells

To assess the influence of cell density on secreted frizzled-related protein (SFRP) gene expression, RNase protection assays (RPA) were employed using the commercially available RiboQuant Human Frizzled (FZD) Multi-Probe Template Set (BD Biosciences, Oxford, UK). 6-well Nunc dishes were seeded with 5 x 10^4 (low-density) or 5 x 10^5 (high-density) H292 cells per well in 2ml per well standard RPMI 1640 medium. Cells were incubated for 32 hours, serum-starved for 18 hours in UltraCULTURE medium, and then lysed with TRIzol Reagent (1ml and 200µl per well for high- and low-density cells, respectively), prior to RNA extraction, DNase treatment and analysis by RPA, as described in Section 5.2.1. Figure 7.9 shows a representative polyacrylamide gel using RNA from H292 cells at low (lane 2) and high (lane 3) density. As previously observed in Section 5.2.1, protected bands of predicted size were seen for SFRP-1, FZD-2, -3, -5 and -6, and smoothened (SMOH),

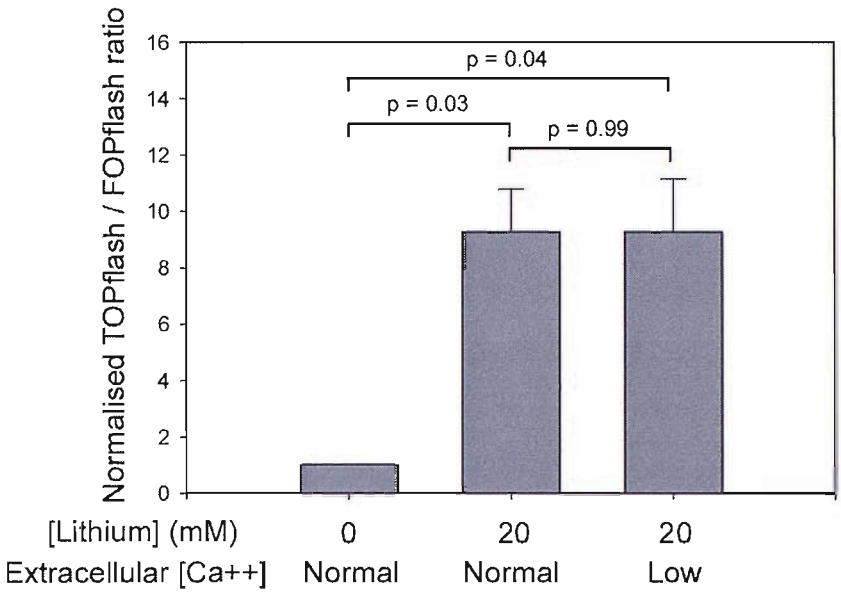

Figure 7.8: TOPflash activity in H292 cells stimulated ± low Ca^{2+} medium ± 20mM lithium.

H292 cells were transiently transfected with TOPflash or FOPflash reporters prior to stimulation ± Ca^{2+}- and Mg^{2+}-free medium ± 20mM lithium chloride for 24 hours (n=3). In all experiments, cells were >80% confluent. Data are expressed as mean ± S.E.M, normalised to unstimulated cells in calcium-containing medium, and were analysed using the paired Student's T-test. 20mM lithium induced a 9.2-fold increase in TOPflash reporter activity. This response was not altered by Ca^{2+}- and Mg^{2+}-free medium.

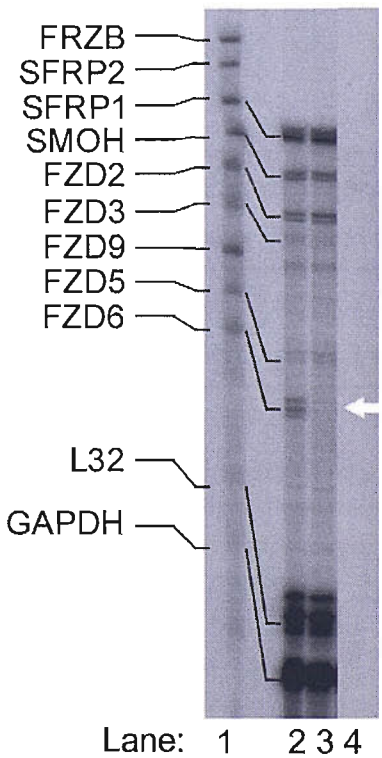

Figure 7.9: Expression of FZD and SFRP mRNA in H292 cells at low- and high-density.

RNA was extracted from H292 bronchial epithelial cells at low (10-20% confluent) and high (>80% confluent) density in serum-free basal medium. Frizzled (FZD) and secreted frizzled-related protein (SFRP) gene expression were investigated by RNase protection assay (RPA). A representative polyacrylamide gel is shown for cells at low (lane 2) and high (lane 3) density. Protected bands of predicted size were observed for SFRP-1, FZD-2, -3, -5 and -6, and smoothened (SMOH). Importantly, a cell density related change in FZD6 gene expression was observed (arrowed), with up-regulation in cells at high-density. L32 ribosomal protein and GAPDH were used as internal controls. The yeast tRNA control (lane 4) was negative.

but were absent for SFRP-2, FRZB (SFRP-3) and FZD9. No difference in expression of SFRP-1 was seen between H292 cells at low- and high-density. However, a cell density related change in FZD6 gene expression was detected (arrowed), with up-regulated expression in high-density cells.

Using DNase-treated RNA from H292 cells at low- and high-density, reverse transcribed to cDNA, the influence of cell density on FZD6 gene expression was further investigated by quantitative PCR (qPCR) using primers for FZD6 (Table 7.1) designed and validated by Dr Rob Powell (University of Southampton), and the SYBR Green dye assay (see Section 2.13). SYBR melt curve analysis of amplicons showed a single peak coinciding with the predicted peak melt temperature of 86°C, suggesting that the primer pair was specific for FZD6 (Figure 7.10). No amplicons were detected with the RT-minus control (pale blue line). Representative qPCR cycle graphs for samples in triplicate show good signal strength for FZD6 (Figure 7.11), with C_T values of 24-25. Importantly, no signal was detected with the RT-minus control, indicating that amplicons were derived from amplified RNA and not genomic or contaminating DNA. When compared with H292 cells low-density (n=5), FZD6 gene expression was up-regulated as cells approached confluence (Figure 7.12).

Gene (Accession N°)	**Primer sequences** (**F**orward and **R**everse)
FZD6 (NM_003506.2)	**F**: 5'-AGAGGTGAAAGCGGACGGA-3' **R**: 5'-AGAGAGTCTGGAGATGGATGCT-3'

Table 7.1: Primers for FZD6 qPCR.

Forward (sense) and reverse (anti-sense) primers for quantitative PCR analysis of FZD6 gene expression were designed and validated by Dr Rob Powell (University of Southampton).

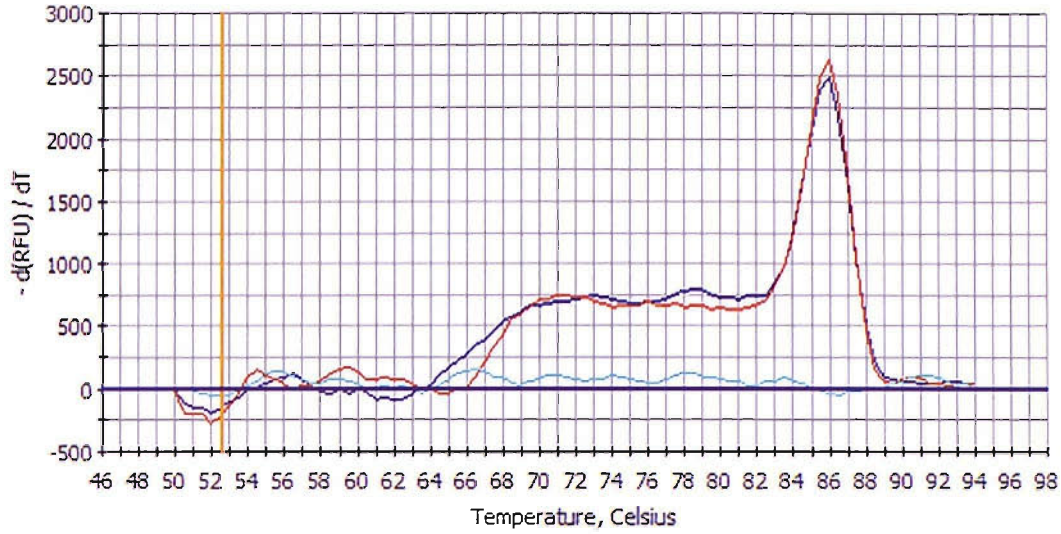

Figure 7.10: SYBR melt curve for amplicons of qPCR primers designed for FZD6.

Forward and reverse primers (Table 7.1) were designed for investigation of FZD6 gene expression by quantitative PCR (qPCR). Amplicon size was checked using the SYBR melt curve technique. The predicted peak melt temperature of 86°C was observed, suggesting that the primer pair was specific for FZD6. No amplicons were detected with the RT-minus control (pale blue line).

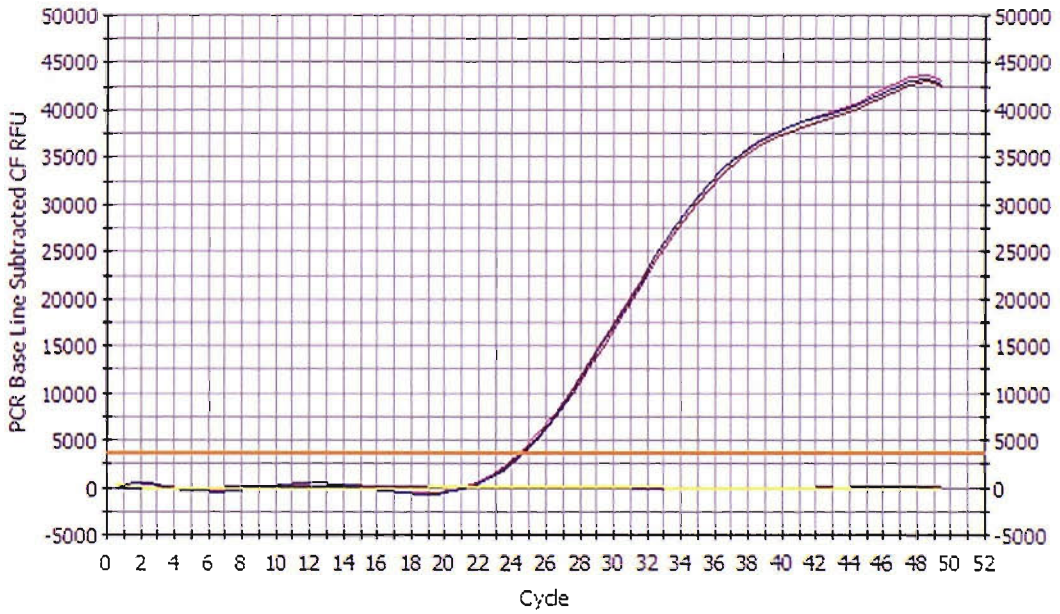

Figure 7.11: Representitive qPCR cycle graph for FZD6 expression in H292 cells.

RNA from H292 cells in serum-free basal medium at low (10-20% confluent) and high (>80% confluent) density was reverse transcribed, and FZD6 gene expression investigated by quantitative PCR (qPCR). A representative cycle graph for a sample in triplicate shows good signal strength, with C_T values of 24-25. No signal was detected with the RT-minus control.

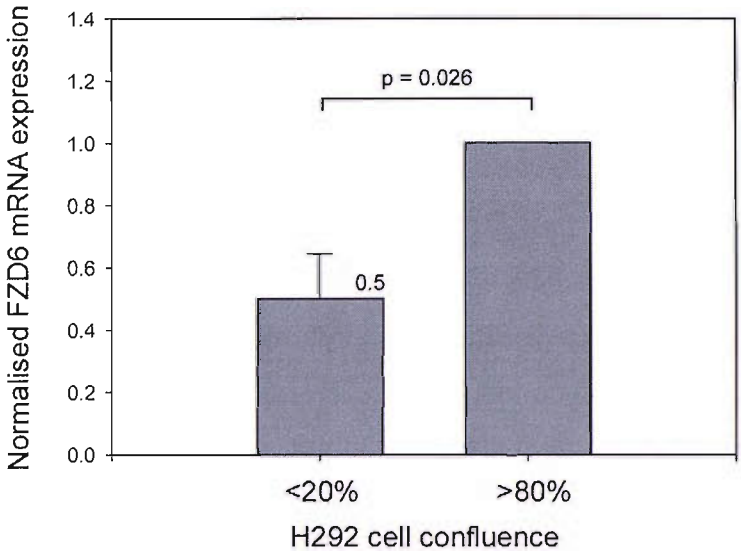

Figure 7.12: FZD6 gene expression in H292 cells at low- and high-density.

RNA extracted from H292 cells (n=5) at low (10-20% confluent) and high (>80% confluent) density in serum-free basal medium was reverse transcribed, and FZD6 gene expression investigated by quantitative PCR (qPCR), using the primers in Table 7.1 and 18S rRNA as a normalising control for calculating $\Delta\Delta C_T$ values. Data are expressed as mean ± S.E.M, normalised to high-density cells, and were analysed using the paired Student's T-test. FZD6 gene expression was up-regulated in cells at high-density.

7.3 Discussion

I have shown that exogenous EGF induced a 1.3-fold increase (p=0.004) in TOPflash reporter activity in H292 cells at *high*-density and that this response was completely abolished by the addition of AG1478, indicating that Tcf/Lef-1 driven gene transcription can be activated downstream of the EGF receptor. Furthermore, AG1478 induced a fall in TOPflash activity that was significantly below that of the unstimulated control, suggesting that EGF receptor activation contributes to the basal Tcf/Lef-1 transcriptional activity observed in H292 cells at *high*-density. However, under conditions of *low* cell density, EGF did not significantly alter TOPflash activity, and AG1478 failed to reduce Tcf/Lef-1 mediated signalling to the lower basal level observed in cells at *high*-density. These data suggest that the increase in Tcf/Lef-1 transcriptional activity observed in H292 cells at *low*-density is not the result of EGF receptor activation, but due to other factors related to changes in cell density.

Consistent with my data, recent reports have also implicated the EGF receptor as an activator of Tcf/Lef-1 mediated gene transcription (Cheon et al., 2004). This involved inhibition of Gsk-3β (Cheon et al., 2004), and is thought to provide an essential co-signal required for passage through the G1/S checkpoint (Graham and Asthagiri, 2004). However, my confocal data failed to demonstrate a significant increase in the nuclear localisation of transcriptionally active β-catenin in response to EGF stimulation in near-confluent H292 cells. Although this could reflect a lack of statistical power, it might equally support the view that EGF receptor-induced activation of Tcf/Lef-1 driven gene transcription can also occur *independently* of the Gsk-3β/Apc/axin destruction complex (Lu and Hunter, 2004). Indeed, my confocal images did show a reduction in membranous ABC staining, suggesting that the EGF receptor might *indirectly* influence canonical Wnt signalling by liberating transcriptionally active β-catenin from the membrane compartment through destabilisation and down-regulation of adherens junctions (Al Moustafa et al., 2002; Eger et al., 2000; Hoschuetzky et al., 1994; Muller et al., 1999; Shiozaki et al., 1995; Takahashi et al., 1997; Tsukatani et al., 1997), thus altering the competition between classical cadherins and Tcf/Lef-1 transcription factors for direct binding to β-catenin (Gottardi et al., 2001; Lu and Hunter, 2004; Stockinger et al., 2001). Furthermore, a mechanism related to changes in cell-cell contact such as this might also account for the relatively high basal level of Tcf/Lef-1 transcriptional activity observed in cells at *low*-density, as well as for the failure of exogenous EGF to induce a TOPflash response in H292 cells under these same conditions. However, despite the effective disruption of E-cadherin-mediated cell-cell contacts in H292 cells at *high*-density using Ca^{2+}- and Mg^{2+}-free medium, attempts to recapitulate the increase in Tcf/Lef-1 transcriptional activity observed in cells at *low*-density proved unsuccessful. Although the lack of response might be explained by an inhibitory influence of Ca^{2+}- and Mg^{2+}-free medium on canonical Wnt signalling, this calcium-switch model has reportedly led to the activation of a Tcf/Lef-1 reporter in other cell systems (Chakrabarty et al., 2003), and the effect of lithium was not altered when used as a positive control in my experiments. These data suggest that the increased activation state of β-catenin in my low-density model of repairing epithelium is not the result of

reduced E-cadherin mediated cell-cell contact, but due to density related changes in non-cadherin-mediated cell-cell contact &/or signalling by secreted mediators.

The view that EGF receptor signalling might influence Tcf/Lef-1 mediated transcription through an *indirect* mechanism that is independent of the Gsk-3β/Apc/axin destruction complex is also suggested by the observed delay in response to EGF, with no significant change in TOPflash activity seen during the initial 8 hours of stimulation. In this respect, other growth factors have been shown to down-regulate the expression of class-5a WNT genes (Huguet et al., 1995; Olson and Papkoff, 1994). Furthermore, class-5a Wnts can block Tcf/Lef-1 mediated transcription downstream of β-catenin by activating the non-canonical Wnt/Ca^{2+} pathway (Kuhl et al., 2001). Evidence suggests that this involves the activation of NEMO-like kinase (NLK), downstream of Ca^{2+}-calmodulin-dependent protein kinase II (CamKII) and TGFβ activated kinase-1 (TAK-1), leading to the phosphorylation of Tcf/Lef-1 transcription factors, thereby inhibiting there interaction with β-catenin (Ishitani et al., 1999; Kuhl et al., 2001). Thus, EGF receptor activation might increase Tcf/Lef-1 transcriptional activity through negative regulation of the Wnt/Ca^{2+} pathway. Moreover, reports of a correlation between epithelial cell-density and WNT-5A gene expression (Olson and Papkoff, 1994) also suggest a mechanism in which Wnt-5a inhibits Tcf/Lef-1 mediated transcription via the Wnt/Ca^{2+} pathway as cells achieve confluence. Consistent with this model, I have shown that the decrease in Tcf/Lef-1 transcriptional activity observed in H292 cells at high-density correlates with the up-regulated expression of FZD6. This gene encodes a receptor that has been implicated in Wnt/Ca^{2+} signal transduction (Golan et al., 2004; Kuhl et al., 2000b), and might therefore be antagonistic to signalling by β-catenin. Thus, canonical *and* non-canonical Wnt signalling pathways may both be involved in modulating the activation state of β-catenin in my model of bronchial epithelial repair.

CHAPTER 8

IN VIVO LOCALISATION OF β-CATENIN IN ADULT HUMAN AIRWAY EPITHELIUM

8.1 Aims of the study

I have shown that adult human bronchial epithelial (HBE) cells express key components of the Wnt/β-catenin signalling pathway and are capable of transducing a class-1 Wnt signal. I have also observed activation of the canonical Wnt pathway in subconfluent cells used as a simple model of repairing bronchial epithelium, and shown that Tcf/Lef-1 transcriptional activity can be modulated by the EGF receptor, known to play an important role in epithelial restitution. However, human bronchial epithelium is not an undifferentiated monolayer, but is a pseudostratified structure with basal and columnar cell layers, the latter comprising ciliated and mucous-secreting goblet cells. Thus, caution must be applied when extrapolating *in vitro* observations into the *in vivo* situation. Therefore, postulating that ***reactivation of the canonical Wnt signalling pathway plays a role in human bronchial epithelial regeneration following injury***, the aims of this study were to seek *in vivo* evidence of nuclear localisation of β-catenin in regions of damaged bronchial epithelium, using endobronchial biopsies obtained from volunteer subjects by fibreoptic bronchoscopy. In addition, comparisons were made with a more complex *in vitro* model of bronchial epithelial regeneration in which confluent primary HBE cells stratify and differentiate at the air-liquid interface (ALI) (Bernacki et al., 1999).

8.2 Methods and results

8.2.1 Evidence for *in vivo* localisation of β-catenin to the nuclei of bronchial epithelial cells is lacking

To investigate the cellular expression and localisation of β-catenin *in vivo*, endobronchial biopsies obtained at fibreoptic bronchoscopy from normal (n=5),

moderate persistent asthmatic (n=4) and chronic bronchitic (current smokers; n=7) volunteer subjects were processed in glycolmethacrylate (GMA), and 2μm thick tissue sections cut. Sections were stained using the pan-β-catenin (PBC; clone 14; BD Biosciences, Oxford, UK) monoclonal antibody and streptavidin/biotin/3.3'-diaminobenzidine (SAB-DAB) detection system (BioGenex, Wokingham, UK) as described in Section 2.17, and examined by light microscopy. Normal (n=1) and cancerous (n=1) colonic tissue from anonymised bowel resection specimens were used as a positive control for nuclear staining with the PBC antibody. The hypophosphorylated ('active') β-catenin (ABC; clone 8E7; Upstate Biotechnology, USA) monoclonal antibody was not used in this survey, because attempts at titration failed to attain significant staining in the positive control. PBC staining was almost entirely membranous within the crypts of normal colon, but localised to the nuclei of colon cancer cells (Figure 8.1). Importantly, staining was absent in the isotype

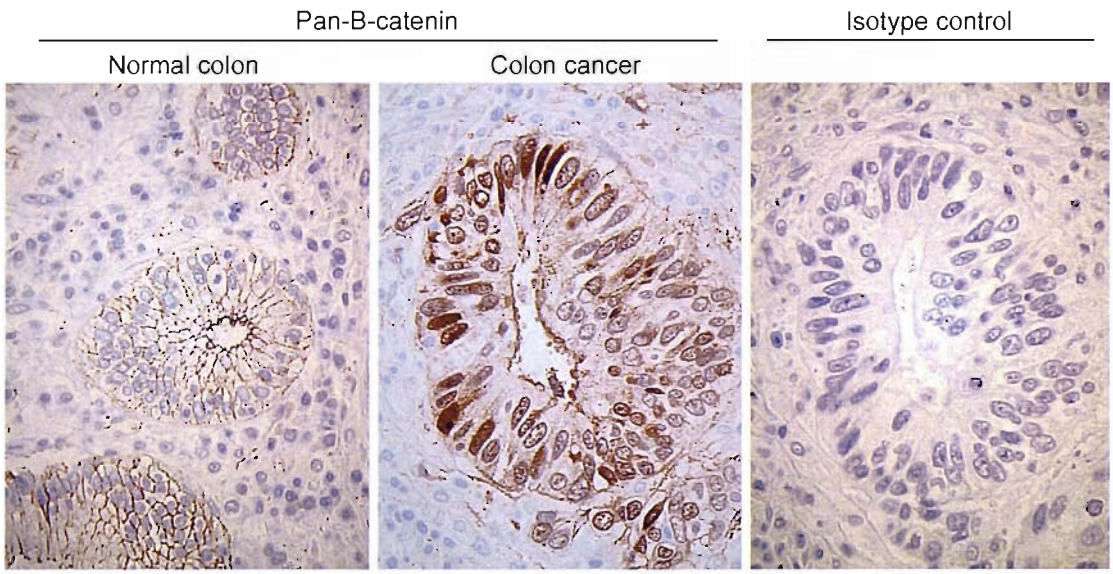

Figure 8.1: β-catenin expression in normal and cancerous human colon.

2μm thick tissue sections of normal (n=1) and cancerous (n=1) colonic tissue, processed in glycolmethacrylate (GMA), were stained using anti-pan-β-catenin (PBC) monoclonal antibody and the streptavidin/biotin/3,3'-diaminobenzidine (SAB-DAB) detection system. In normal colon, expression of PBC (brown stain) was almost entirely membranous in epithelial cells within the crypts. In contrast, PBC localised to the nuclei of colon cancer cells. The isotype control was negative (x40 objective).

control. Figure 8.2 shows representative sections of endobronchial biopsies from normal, moderate persistent asthmatic and chronic bronchitic volunteer subjects. In all three groups, the pattern of PBC expression within the bronchial epithelium was predominantly membranous in both basal and columnar cell layers. In asthmatic epithelium, PBC also localised to squamous-type cells overlying basal cells in regions

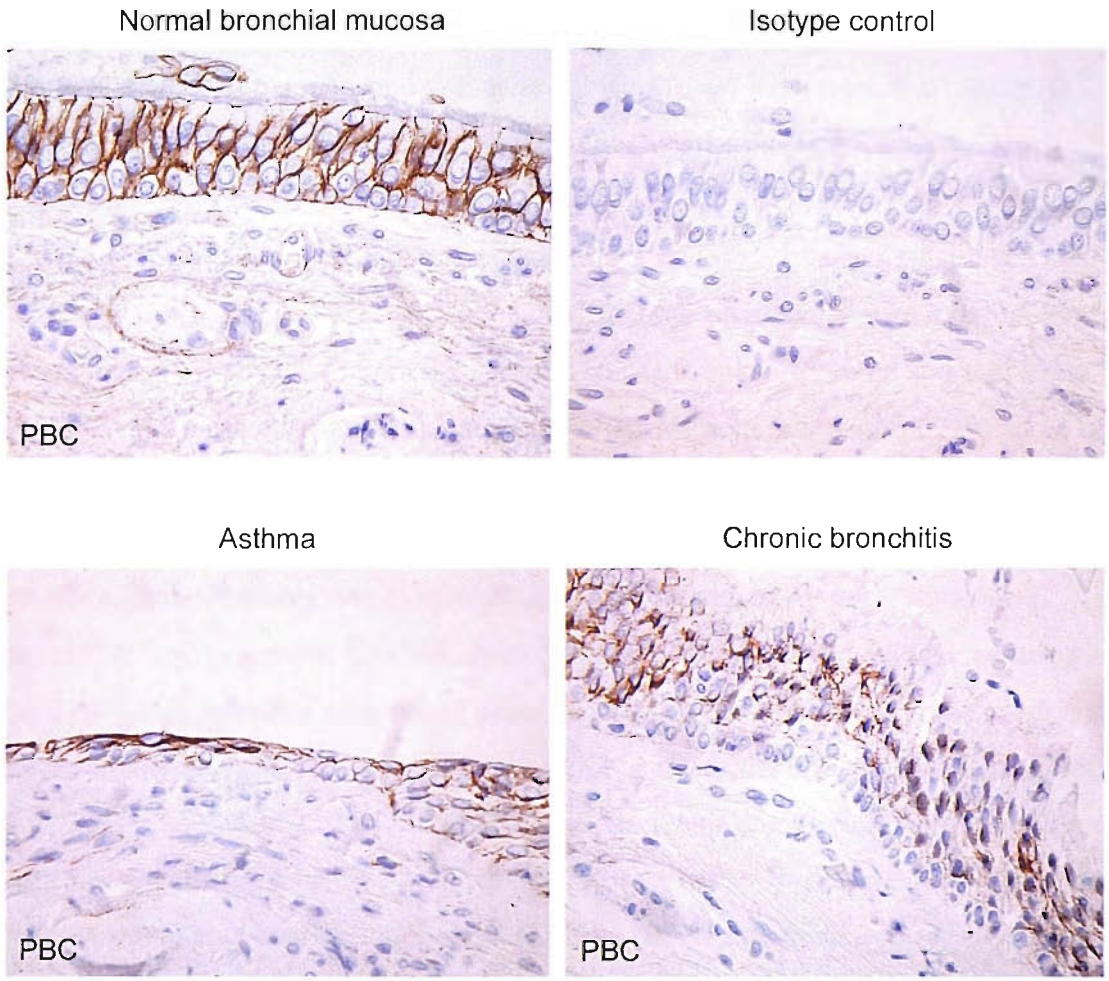

Figure 8.2: β-catenin expression in human bronchial mucosa.

Endobronchial biopsies from normal (n=5), moderate persistent asthmatic (n=4) and chronic bronchitic (current smokers; n=7) volunteer subjects were processed in glycolmethacrylate (GMA), and 2μm thick tissue sections were stained using anti-pan-β-catenin (PBC) monoclonal antibody and the streptavidin/biotin/3,3'-diaminobenzidine (SAB-DAB) detection system. In all three groups, the pattern of PBC expression (brown stain) within the bronchial epithelium was predominantly membranous in both basal and columnar cell layers. In asthmatic epithelium, PBC also localised to squamous-type cells overlying basal cells in regions of columnar cell loss. Of particular interest was the apparent localisation of PBC to the nuclei of occasional epithelial cells in all 3 groups, especially in one small region of chronic bronchitic epithelium (image shown). However, it was not possible to confidently exclude this as an artefactual appearance. The isotype control was negative (x40 objective).

of columnar cell loss. Of particular interest was the apparent localisation of PBC to the nuclei of occasional epithelial cells in all 3 groups, especially in one small region of chronic bronchitic epithelium (image shown). However, lack of resolution meant that it was not possible to confidently exclude these as artefactual appearances.

8.2.2 Evidence for *in vitro* localisation of β-catenin to the nuclei of stratified primary HBE cells at the air-liquid interface is lacking

Primary HBE cells from normal volunteer subjects (n=3) were seeded at passage 2 (P2) onto the collagen-coated inserts (apical chamber) of 24-well Costar transwell plates (Corning Costar, High Wycombe, UK) at 1 x 10^5 viable HBE cells per well in 150µl BEGM; the basal chamber contained 500µl BEGM. Cells were incubated and culture medium changed every 48 hours. When 100% confluent, cells were brought to the air-liquid interface by removing medium from the apical chamber and replacing BEGM in the basal chamber with 300µl/well ALI medium (see Section 2.7). ALI medium was replaced daily, with care taken to remove any medium from the apical chamber that had leaked across the transwell. On days 7, 14 and 21 at the air-liquid interface, the epithelium was carefully cut from the insert on its polycarbonate membrane, and processed in GMA. 2µm thick sections were then cut, stained using the SAB-DAB detection system and examined by light microscopy, as described above. However, both PBC and ABC monoclonal antibodies were used. At all three timepoints, the pattern of PBC and ABC expression was predominantly membranous, with staining most intense in the apical cell layer from day 14 (Figure 8.3). Again, it was not possible to confidently localise PBC or ABC to cell nuclei.

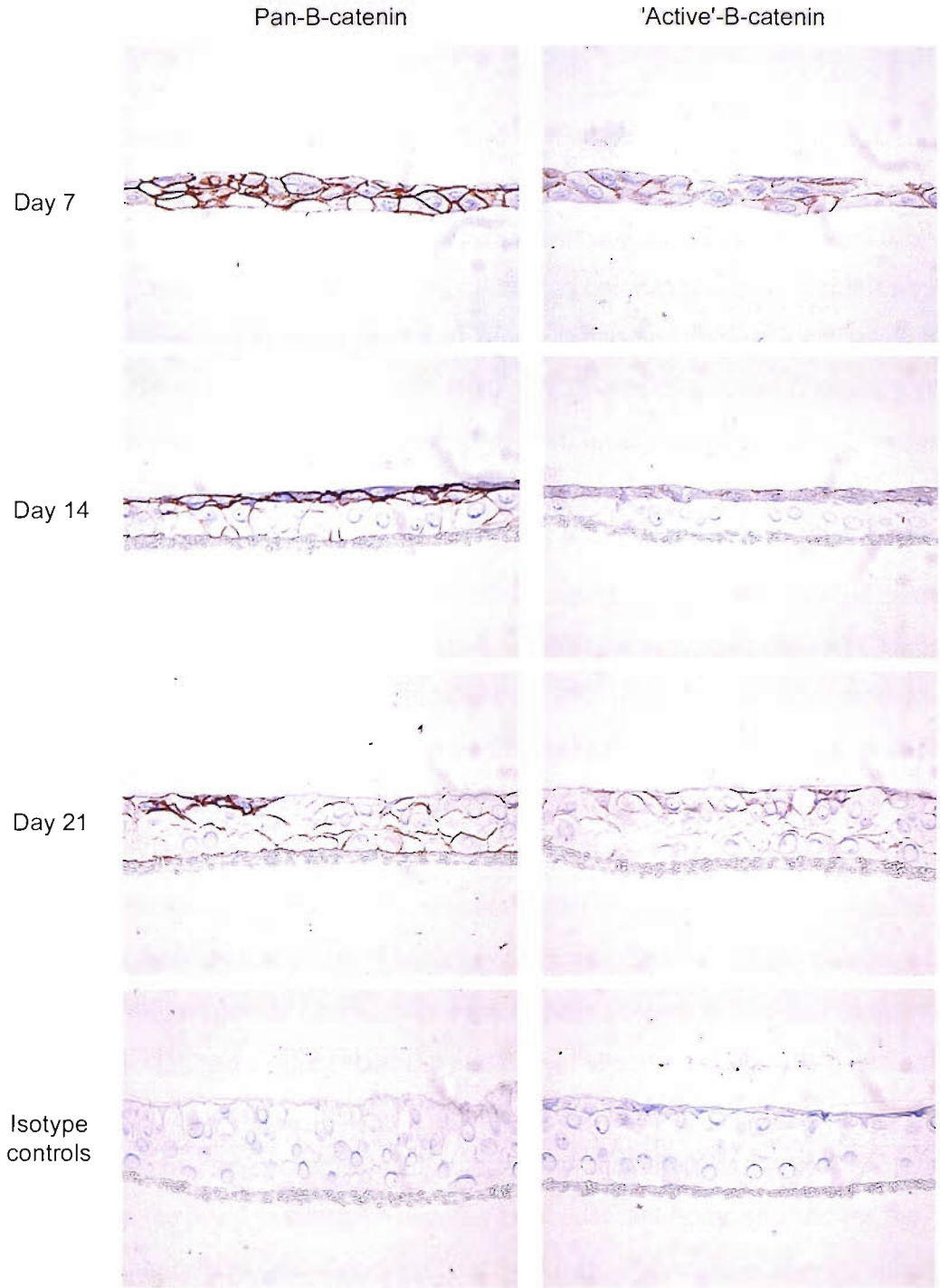

Figure 8.3: β-catenin expression in ALI-cultures.

Primary human bronchial epithelial (HBE) cells, obtained from healthy volunteer subjects (n=3), were grown to confluence and encouraged to stratify by culture at an air-liquid interface (ALI). On days 7, 14 and 21, ALI-cultures were processed in glycolmethacrylate (GMA), and 2μm thick tissue sections were stained using anti-pan-β-catenin (PBC) or anti-hypophosphorylated ('active') β-catenin (ABC) monoclonal antibodies and the streptavidin/biotin/3,3'-diaminobenzidine (SAB-DAB) detection system. At all three timepoints, the pattern of PBC and ABC expression (brown stain) was predominantly membranous. From day 14, expression of PBC and ABC was most intense within the apical cell layer. It was not possible to confidently localise PBC or ABC expression to the nuclei of cells. The isotype controls were negative (x40 objective).

8.3 Discussion

Human bronchial epithelium is not an undifferentiated monolayer, but is a pseudostratified structure with basal and columnar cell layers. Therefore, *in vivo* evidence of nuclear localisation of β-catenin was sought in endobronchial biopsies from volunteer subjects. Since almost all human colorectal cancers exhibit high constitutive activation of the canonical Wnt pathway and nuclear localisation of β-catenin (Miyoshi et al., 1992; Morin et al., 1997), cancerous colonic tissue was used as a positive control. In normal colon, β-catenin localised almost entirely to the membranes of epithelial cells within the crypts, consistent with its involvement in the formation of cadherin-mediated intercellular adherens junctions (Aberle et al., 1996; Ozawa et al., 1989). In contrast, β-catenin localised to the nuclei of colon cancer cells, likely reflecting a mutation in the adenomatous polyposis coli (APC) gene (Miyoshi et al., 1992). Indeed, approximately 85% of all human colorectal cancers contain loss-of-function APC mutations (Miyoshi et al., 1992), with many of the remaining 15% containing point mutations in the N-terminal region of β-catenin (β-cateninΔN) (Morin et al., 1997). Interestingly, despite processing and storage of GMA-embedded samples at -20°C, nuclear epitopes remained preserved for the pan-β-catenin antibody (clone 14). This is in contrast to the loss of PBC staining observed when SW480 colorectal cancer cells were fixed in acetone at this same temperature (see chapter 3), and suggests that the masking of specific epitopes on β-catenin in the nuclear compartment reported by Munné *et al* (Munne et al., 1999) may not simply be the result of freezing *per se*. Also of interest was the failure to attain significant staining in the positive control when using the ABC antibody, specific for the hypophosphorylated (transcriptionally active) form of β-catenin. Having subsequently stained primary HBE cells in ALI-culture, it seems unlikely that the initial lack of staining for ABC in cancerous colonic tissue was the result of GMA processing, and raises the possibility that the positive control was one of the 15% or so of human colon cancers to contain a point mutation in the N-terminal region of β-catenin, not recognised by this antibody.

Using the PBC antibody, the expression and cellular localisation of β-catenin was next investigated in GMA-embedded endobronchial biopsies. Since injury to the

bronchial epithelium is a feature that is recognised in chronic inflammatory disorders of the airways (Holgate et al., 1999; O'Donnell et al., 2004; Richter et al., 2002), biopsies from volunteer subjects with moderate persistent asthma and smoking-related chronic bronchitis were included in the survey. In asthma, the bronchial epithelium appears to be abnormally susceptible to oxidant-induced apoptosis (Bucchieri et al., 2002), with selective shedding of columnar cells and failure to proliferate as part of the normal repair response (Demoly et al., 1994). As a consequence, the asthmatic epithelium is persistently stressed and activated, releasing cytokines and growth factors that drive both chronic airways inflammation and airway wall remodelling (Holgate et al., 1999). In contrast, the epithelium in chronic bronchitis shows signs of *increased* cell proliferation (Demoly et al., 1994), with goblet cell and squamous metaplasia contributing to the response of these cells to persistent cigarette smoke-induced injury (O'Donnell et al., 2004). In all three groups, the pattern of β-catenin expression was predominantly membranous in both basal and columnar cell layers, similar to findings in normal colon. However, even when using the oil immersion lens, lack of spatial resolution meant that is was not possible to confidently confirm the apparent localisation of β-catenin to the nuclei of cells within the bronchial epithelium, not least because of their small size when compared to the relatively large nuclei of colon cancer cells.

A second major limitation of this study is that nuclear localisation of β-catenin is likely to be a *transient* event and my biopsy samples were a few millimetres in size. In other words, it is possible that increased nuclear localisation of β-catenin is an event of such infrequency that it was not captured in my survey. This is illustrated by the observed transient nuclear localisation of β-catenin in human colorectal epithelial cells during the regenerative phase following radiation-induced injury, strongly suggesting a role for the canonical Wnt pathway in colonic epithelial repair (Hardy et al., 2002). Yet, this *in vivo* evidence is likely to have been missed had only normal colonic epithelium been studied, and this might have remained the case had only *small* samples of diseased epithelium been included. Thus, despite the apparent lack of spatial resolution, it is possible that immunohistochemical analysis might still allow the unambiguous *in vivo* detection of β-catenin within bronchial epithelial cell nuclei. For this reason, evidence of transient nuclear localisation was sought in a

more complex *in vitro* model of bronchial epithelial regeneration in which confluent primary HBE cells stratify and differentiate at the air-liquid interface, with mucous-secreting goblet cells typically present from day 7, and ciliated cells evident from day 14. (Bernacki et al., 1999). However, the pattern of β-catenin staining was again predominantly membranous, and lack of spatial resolution remained a fundamental problem. This was particularly the case on day 14 when appearances were reminiscent of the asthmatic epithelium, with squamous-type cells overlying basal cells in regions of columnar cell loss. Since GMA autofluoresces, it was not possible to improve resolution using laser confocal microscopy.

CHAPTER 9

FINAL DISCUSSION AND FUTURE DIRECTIONS

Bronchial epithelial repair plays an important role in the pathogenesis of chronic inflammatory disorders of the airways, such as asthma (Holgate et al., 1999) and smoking-related chronic bronchitis (O'Donnell et al., 2004;Richter et al., 2002). Therefore, investigating the processes that regulate epithelial repair could provide new insights into these conditions. With recent reports that epithelial regeneration involves the reactivation of embryonic morphogenetic pathways (Hardy et al., 2002;Watkins et al., 2003), I chose to investigate signalling by Wnt/β-catenin in adult human bronchial epithelial (HBE) cells.

Frizzleds function as cell surface receptors for Wnts (Bhanot et al., 1996;Kuhl et al., 2000b;Wang et al., 1997;Yang-Snyder et al., 1996), and Tcf/Lef-1 transcription factors are required for canonical Wnt signal transduction (Molenaar et al., 1996;van Noort and Clevers, 2002). I have shown that HBE cells express these key components of the Wnt/β-catenin pathway, with mRNA encoding frizzled-5, Tcf-4 and -3, and low-level expression of FZD9, TCF-1 and LEF-1. In addition to detecting splice variants of the TCF-4 and LEF-1 transcripts, I have also demonstrated the expression of Tcf-4 protein. Using stably transfected murine fibroblasts as a source of biologically active Wnt-3a, I went on to provide evidence that adult HBE cells are capable of transducing a canonical Wnt signal, showing activation of a Tcf/Lef-1 reporter and nuclear localisation of transcriptionally active β-catenin. I next used subconfluent cells in log-phase growth as a simple model of repairing epithelium, and observed up-regulated β-catenin mediated Tcf/Lef-1 transcriptional activity in the 'repair' phenotype, reminiscent of the transient nuclear localisation of β-catenin reported in human colorectal epithelial cells during the regenerative phase following radiation-induced injury (Hardy et al., 2002). Mechanistically, I found no evidence to indicate that increased β-catenin signalling in subconfluent cells was the consequence of epidermal growth factor (EGF) receptor activation or loss of E-cadherin mediated cell-cell contact. However, I did observe up-regulated expression of FZD6 in cells at

high-density. This gene encodes a receptor that has been implicated in Wnt/Ca^{2+} signal transduction (Golan et al., 2004;Kuhl et al., 2000b), and might therefore be antagonistic to signalling by β-catenin (Ishitani et al., 1999;Kuhl et al., 2001). Thus, I would postulate that frizzled-6 negatively regulates Tcf/Lef-1 mediated transcription via the Wnt/Ca^{2+} pathway as cells achieve confluence. To investigate this mechanism further, TOPflash containing H292 cells at *low*-density could be transfected with a FZD6 construct for gain-of-function (GOF) studies designed to test the hypothesis that up-regulated expression of FZD6 leads to a decrease in Tcf/Lef-1 transcriptional activity. To circumvent the possible need for Wnts to activate ectopic frizzled-6, an inducible β_2-adrenergic/frizzled-6 chimeric receptor may be required (Liu et al., 1999). In contrast, loss-of-function studies would ask the question: does down-regulation of FZD6 or inhibition of the Wnt/Ca^{2+} pathway lead to an increase in Tcf/Lef-1 mediated transcription in H292 cells at *high*-density? FZD6 expression could be down-regulated by small interfering RNA (siRNA) (Golan et al., 2004). Alternatively, Wnt/Ca^{2+} signalling could be blocked using inhibitors of heterotrimeric G-proteins (pertussis toxin), phospholipase C (U-37122), inositol monophosphate (L-690,330) or the inositol-1,4,5-trisphosphate (IP_3) receptor (Xestospongin) (Kuhl, 2004). Downstream changes in Wnt/Ca^{2+} pathway activity could be confirmed using assays such as that for Ca^{2+}-calmodulin-dependent protein kinase II (CamKII) (Kuhl et al., 2001).

The functional relevance of up-regulated signalling by β-catenin in subconfluent HBE cells remains unclear. Cells achieve confluence through migration and proliferation (Leir et al., 2000), recognised as sequential steps in airway epithelial repair (Dupuit et al., 2000;Shimizu et al., 1994). Therefore, it seems reasonable to postulate a role for this pathway in the regulation of one or both of these phenotypes. Thus, with disrupted cell-cell contact, β-catenin might provide key signals involved in cell fate determination at the G1/S checkpoint, required for epithelial restitution. In this respect, an integrated response would result from convergence with other motility and mitogenic signalling pathways, including those downstream of the EGF receptor (Davies et al., 1999). Indeed, evidence suggests that β-catenin provides important co-signals required for both EGF receptor induced cell motility (Muller et al., 2002) and G1/S phase progression (Graham and Asthagiri, 2004). Since suppression of Tcf/Lef-1 mediated transcription induces both cell cycle arrest (Mariadason et al., 2001;Tetsu

and McCormick, 1999) and increased apoptotic susceptibility (Chen et al., 2001), co-signals provided by β-catenin might include those required for cell survival when cell-cell contact is lost as a consequence of epithelial injury (Orford et al., 1999). In this context, negative regulation of Tcf/Lef-1 transcriptional activity by frizzled-6 via the Wnt/Ca2+ pathway might provide a mechanism for density-dependent inhibition of growth *in vitro*, and also prevent the dysregulated migration and proliferation of cells that characterize neoplastic change, *in vivo*. Although I did not identify *cyclin-D1* and *MMP7* as targets of Tcf/Lef-1 transcription factors in HBE cells, I did observe a positive correlation between β-catenin mediated signalling and epithelial cell proliferation. To elucidate the functional relevance of this pathway, further studies could include microarray analysis to identify target genes up-regulated by *purified* Wnt-3a (Willert et al., 2002;Willert et al., 2003). Candidates would then have their promoter regions interrogated for evidence of putative Tcf/Lef-1 binding sites in an attempt to discriminate between primary and secondary targets. Using assays for proliferation, migration and oxidant-induced apoptosis in HBE cells at low-density, GOF studies would involve stimulation with purified Wnt-3a, whilst LOF studies could be achieved by using a dominant-negative Tcf-4 construct (Yun et al., 2005), or siRNA-mediated knockdown of β-catenin or Tcf-4 (Sun et al., 2006;Yun et al., 2005). Given current difficulties transfecting primary HBE cells with a Tcf/Lef-1 reporter, electrophoretic mobility shift assays could be used to confirm the presence of β-catenin/Tcf DNA complex formation as a marker of increased β-catenin mediated Tcf/Lef-1 transcriptional activity (Mei et al., 2000a;Mei et al., 2000b).

Although signalling by β-catenin was not influenced by activation of the EGF receptor in subconfluent HBE cells, I did observe increased Tcf/Lef-1 transcriptional activity in cells at confluence. Again, the functional relevance of this is uncertain, but it is tempting to speculate that such co-operative signalling in the context of a confluent monolayer might play an important role in epithelial stratification &/or differentiation. Indeed, evidence suggests that EGF receptor activation can induce the up-regulated expression of MUC5AC (Mata et al., 2005;Shao et al., 2004) and is required for goblet cell differentiation in the *in vitro* model of the stratified bronchial epithelium at the air-liquid interface (ALI) (Atherton et al., 2003). Furthermore, goblet cell hyperplasia is a feature of β-catenin over-expression in transgenic mice (Mucenski et al., 2005). Thus, future experiments could investigate the processes of

epithelial stratification and goblet cell differentiation in ALI-cultures using laser confocal microscopy to co-localise transcriptionally active β-catenin to cell nuclei, and siRNA technology to knockdown β-catenin or Tcf-4 in LOF studies (Platz et al., 2005). However, such methods are likely to be technically difficult.

My simple model of repairing epithelium took no account of potential signals from mesenchymal and inflammatory cells or extracellular matrix proteins within the microenvironment of the airway. Postulating that nuclear localisation of transcriptionally active β-catenin is a transient phenomenon involved in the regulation of bronchial epithelial restitution, stratification and goblet cell differentiation, obtaining *in vivo* evidence of signalling from biopsy samples of *normal* airway is probably unlikely for the reasons discussed in chapter 8. To investigate the regenerative process *in vivo*, one approach would be to use a xenograft model in which human bronchial epithelial cells repopulate denuded rat tracheae grafted in nude mice (Dupuit et al., 2000;Engelhardt et al., 1992). Alternatively, *ex vivo* bronchial explants from resected lung specimens could be used to investigate the response of the fully differentiated epithelium to wounding (Resau et al., 1987). In either case, confident identification of nuclear β-catenin would probably require laser confocal microscopy, and would therefore need an alternative method of tissue processing to glycolmethacrylate (GMA), such as that employed by Weichselbaum *et al* (Weichselbaum et al., 2005). My hypothesis would also predict nuclear localisation of transcriptionally active β-catenin as being a more frequent event in diseases of the airway characterised by increased bronchial epithelial injury and repair, and epithelial remodelling with goblet cell hyperplasia and mucous hypersecretion. Such diseases would include asthma, smoking-related chronic bronchitis and cystic fibrosis (Groneberg et al., 2002;O'Donnell et al., 2004;Richter et al., 2002). Indeed, WNT-10B is reported to be up-regulated in primary adult human lung fibroblasts stimulated with the Th2 cytokine, IL-13 (Lee et al., 2001), WNT-7A has been shown to be expressed in primary HBE cells from heavy smokers, and Lef-1 has been implicated in postnatal submucosal gland development in cystic fibrosis (Duan et al., 1998;Duan et al., 1999). Therefore, further studies would include a more detailed survey of these airways, ideally from resected lung specimens.

My research has focused on the epithelium of proximal airways. However, recent reports suggest that signalling by β-catenin may be of greater relevance to the regeneration and remodelling of distal airways, where gas exchange normally occurs. In the context of alveolar injury from pneumonia (Eberhart and Argani, 2001), primary tumour growth (Nakatani et al., 2002) or idiopathic pulmonary fibrosis (Chilosi et al., 2003) in man, or acute lung injury in mice (Douglas et al., 2005), nuclear β-catenin has been observed in reactive type II pneumocytes, and shown to co-localise with the up-regulated expression of cyclin-D1 and MMP7 (matrilysin) (Chilosi et al., 2003). Consistent with these findings, transgenic mouse models have shown that conditional knockout of β-catenin in the pulmonary epithelium results in the failure of distal airway formation during lung development (Mucenski et al., 2003), whilst over-expression leads to type II pneumocyte hyperplasia with cells also present in conducting airways (Mucenski et al., 2005). Taken together, these observations suggest an important role for Wnt/β-catenin signalling in regulating the type II pneumocyte population, putative adult stem cells of distal airway epithelium (Mason et al., 1997;Otto, 2002). Therefore, further studies could investigate disease-related differences in WNT, FZD, SFRP and DKK gene expression to test the hypothesis that *altered* Wnt signalling contributes to the pathogenesis of *distal* airways disease. Indeed, SFRP-1 has been identified as a gene up-regulated in emphysematous human lung (Imai and D'Armiento, 2000) as well as murine lung exposed to cigarette smoke (Imai and D'Armiento, 2002). Although the cellular source of this Wnt antagonist remains unclear, evidence suggests that it can increase the susceptibility of small airway epithelial cells (SAEC) to oxidant-induced apoptosis in association with reduced cellular levels of β-catenin (Imai and D'Armiento, 2002;Mercer et al., 2002). These findings suggest a model in which Wnt/β-catenin signalling in type II pneumocytes is reduced by SFRP-1, leading to the impaired regeneration of distal airway epithelium in response to cigarette-smoke induced injury, thereby increasing susceptibility for the development of emphysema. To test this hypothesis, the effect of cigarette-smoke exposure could be investigated in transgenic mice (Mucenski et al., 2003) in which doxycycline-inducible deletion of β-catenin in airway epithelial cells is initiated postnatally, following complete lung development.

Finally, the above models of proximal and distal airways disease offer candidate targets for therapeutic intervention. If abnormally increased signalling by β-catenin was to play an important role in the pathogenesis of cystic fibrosis, idiopathic pulmonary fibrosis, acute lung injury or primary bronchogenic carcinoma, then secreted Wnt antagonists such as members of the Sfrp or Dkk family might prove to be effective therapeutic biologicals. In addition, antagonists of frizzled receptors involved in Wnt/β-catenin signalling, or agonsts of frizzled receptors that are part of the Wnt/Ca^{2+} pathway, might provide alternative therapeutic options. In contrast, drugs having the opposite mechanisms of action could potentially be of value if abnormally reduced signalling by β-catenin were to play an important role in the susceptibility of the airway epithelium to oxidant-induced apoptosis, as postulated for emphysema and asthma. An advantage of treating lung disease is the availability of inhaled delivery systems to help minimise potential adverse reactions in other organ systems.

10.1 cDNA sequences encoding TCF/LEF-1

The coding sequences (CDS) and *untranslated regions (UTR)* are shown along with intron-exon boundaries, and **forward and reverse primer** positions.

10.1.1 cDNA sequence encoding LEF-1

```
   1  aagatctaaaaacggacatctccaccgtgggtggctccttttttcttttttcttttttttccc
  61  acccttcaggaagtggacgtttcgttatcttctgatccttgcaccttcttttggggaaac
 121  ggggcccttctgcccagatcccctctcttttctcggaaaacaaactactaagtcggcatc
 181  cggggtaactacagtggagagggtttccgcggagacgcgccgccggaccctcctctgcac
 241  tttggggaggcgtgctccctccagaaccggcgttctccgcgcgcaaatcccggcgacgcg
 301  gggtcgcggggtggccgccggggcagcctcgtctagcgcgccgccgcagacgccccccgg
 361  agtcgccagctaccgcagccctcgccgcccagtgcccttcggcctcggggcgggcgcctg
 421  cgtcggtctccgcgaagcgggaaagcgcggcggccgccgggattcgggcgccgcggcagc
 481  tgctccggctgccggccggcggccccgcgctcgcccgccccgcttccgcccgctgtcctg
 541  ctgcacgaacccttccaactctcctttcctcccccacccttgagttacccctctgtcttt
 601  cctgctgttgcgcgggtgctcccacagcggagcggagattacagagccgccgggatgccc
 661  caactctccggaggaggtggcggcggcgggggggacccggaactctgcgccacggacgag
 721  atgatccccttcaaggacgagggcgatcctcagaaggaaaagatcttcgccgagatcagt
 781  catcccgaagaggaaggcgatttagctgacatcaagtcttccttggtgaacgagtctgaa
 841  atcatcccggccagcaacggacacgaggtggccagacaagcacaaacctctcaggagccc
 901  taccacgacaaggccagagaacaccccgatgacggaaagcatccagatggaggcctctac
 961  aacaagggaccctcctactcgagttattccgggtacataatgatgccaaatatgaataac
1021  gacccatacatgtcaaatggatctctttctcc[acccatcccgagaacatcaaataa]agtg
1081  cccgtggtgcagccatcccatgcggtccatcctctcacccccctcatcacttacagtgac
1141  gagcacttttctccaggatcacacccgtcacacatcccatcagatgtcaactccaaacaa
1201  ggcatgtccagacatcctccagctcctgatatccctacttttatcccttgtctccgggt
1261  ggtgttggacagatcaccccacctcttggctggcaaggtcagcctgtatatcccatcacg
1321  ggtggattcaggcaaccctacccatcctcactgtcagtcgacacttccatgtccaggttt
1381  tcccatca[tatgattcccggtcctcctgg]tccccacacaactggcatccctcatccagct
1441  attgtaacacctcaggtcaaacaggaacatccccacactgacagtgacctaatgcacgtg
1501  aagcctcagcatgaacagagaaaggagcaggagccaaaaagacctcacattaagaagcct
1561  ctgaatgcttttatgttatacatgaaagaaatgagagcgaatgtcgttgctgagtgtact
1621  ctaaaagaaagtgcagctatcaaccagattcttggcagaaggtggcatgccctctcccgt
1681  gaagagcaggctaaatattatgaattagcacggaaagaaagacagctacatatgcagctt
1741  tatccaggctggtctgcaagagacaattatggtaagaaaaagaagaggaagagagagaaa
1801  ctacaggaatctgcatcaggtacaggtccaagaatgacagctgcctacatctgaaacatg
1861  gtggaaaacgaagctcattcccaacgtgcaaagccaaggcagcgaccccaggacctcttc
1921  tggagatggaagcttgttgaaaacccagactgtctccacggcctgcccagtcgacgccaa
1981  aggaacactgacatcaattttaccctgaggtcactgctagagacgctgatccataaagac
2041  aatcactgccaacccctctttcgtctactgcaagagccaagttccaaaataaagcataaa
2101  aaggtttttaaaaggaaatgtaaaagcacatgagaatgctagcaggctgtggggcagct
2161  gagcagcttttctcccccatatctgcgtgcacttcccagagcatcttgcatccaaacct
2221  gtaacctttcggcaaggacggtaacttggctgcatttgcctgtcatgcgcaactggagcc
2281  agcaaccagctatccatcagcaccccagtggaggagttcatggaagagttccctctttgt
2341  ttctgcttcatttttctttctttttctttctcctaaagcttttatttaacagtgcaaaag
2401  gatcgtttttttttgctttttaaacttgaatttttttaatttacacttttagttttaa
2461  ttttcttgtatattttgctagctatgagcttttaaataaaattgaaagttctggaaaagt
```

```
2521  ttgaaataatgacataaaaagaagccttcttttttctgagacagcttgtctggtaagtggc
2581  ttctctgtgaattgcctgtaacacatagtggcttctccgcccttgtaaggtgttcagtag
2641  agctaaataaatgtaatagccaaaccccactctgttggtagcaattggcagccctatttc
2701  agtttatttttttcttctgttttcttcttttcttttttttaaacagtaaaccttaacagatg
2761  cgttcagcagactggtttgcagtgaattttcatttctttccttatcacccccttgttgta
2821  aaaagcccagcacttgaattgttattactttaaatgttctgtatttgtatctgtttttat
2881  tagccaattagtgggatttttatgccagttgttaaaatgagcattgatgtacccatttttt
2941  aaaaaagcaagcacagcctttgcccaaaactgtcatcctaacgtttgtcattccagtttg
3001  agttaatgtgctgagcatttttttaaaagaagctttgtaataaaacatttttaaaaattg
3061  tcatttaaaaaaaaaaaaaaaaaa
```

10.1.2 cDNA sequence encoding TCF-1

```
   1 gcccaggtgactgactaatccgccgccttcaggagacagaattggccaaggcctgaaggc
  61 cccggagtgcaccagcggcatgtacaaagagaccgtctactccgccttcaatctgctcat
 121 gcattacccacccccctcgggagcagggcagcacccccagccgcagcccccgctgcacaa
 181 ggccaatcagcccccccacggtgtccccccaactctctctctacgaacatttcaacagccc
 241 acatcccacccctgcacctgcggacatcagccagaagcaagttcacaggcctctgcagac
 301 ccctgacctctctggcttctactccctgacctcaggcagcatggggcagctcccccacac
 361 tgtgagctggttcacccacccatccttgatgctaggttctggtgtacctggtcacccagc
 421 agccatcccccacccggccattgtgcccccctcagggaagcaggagctgcagcccttcga
 481 ccgcaacctgaagacacaagcagagtccaaggcagagaaggaggccaagaagccaaccat
 541 caagaagcccctcaatgccttcatgctgtacatgaaggagatgagagccaaggtcattgc
 601 agagtgcaca<u>cttaaggagagcgctgccatcaac</u>cagatcctgggccgcaggtggcacgc
 661 gctgtcgcgagaagagcaggccaagtactatgagctggcccgcaaggagaggcagctgca
 721 catgcagctatacccaggctggtcagcgcgggacaactacgggaagaagaagaggcggtc
 781 gagggaaaagcaccaagaatccaccacagaccctggctcgcctaagaaatgccgtgctcg
 841 ctttggcctcaaccagcagacg<u>gattggtgtggtccgtgcagataa</u>ctctcttcactatt
 901 cctaggaggaaaaagaaatgcattcggtacttacccggagaaggccgctgccccagcccc
 961 gttccttccgatgacagtgctctaggctgccccgggtccccagctccccaggactcaccc
1021 tcataccatctgctgccccgcttccccacagaactgcttactagccctgcggagccggca
1081 cctacatccccaggtctctccactgctctcagcctcccaaccccagggcccccacaggcc
1141 ccccgcagcaccctgcagagcacacaggtacagcaacaggaatctcagagacaggtggcc
1201 tagcaggcacaggacacctggccgcctccaggagcctacccctgaaagtgacagagacc
1261 cagatctcatggaaactggccaggggtcctgttaacgtcatctcagggtccagaccctga
1321 agatttcagaggctgcaggacttctgcctgaacctggggtcatcgattcaaactgctcca
1381 agtggtgggaatcagatctgtcttgatgtgtcatctaattaagggaatcccttgtaccta
1441 tggctgcctgcatctattctttgtaccatctgtcttgccagccagaagcctctgcctccc
1501 tagcttttctgctataggtcagagatgggctgaactgagcctagctaccttctctaccca
1561 tctcccccatcccccactgccacaccctcccccattcagacacttcatggaccaagaatga
1621 gctggtttgtcaaacaacatgtgagcatggtcacaagcacaaagctcaagatgacagctc
1681 ttctaaggaaatggagaagctctgtttataaaaacaaaaacaaaaccagctgctactcat
1741 aagttggaccagaggaagccccttactatgatctcaggagcttgcaagaagcaggaaggg
1801 gaatggaataggttaagtttaggcctatcaacctaagcaacagaaataatctgacactac
1861 cttatcaggcaaattggggagggagggtgtatctagctctagttcaaattatttggaag
1921 tgttccctgagaaacccaccagcctaagaagctctggccccaggcttgtcactagcagct
1981 gcagtcaacagttcaaagaagtcatggcccaaatccagtgtgcacccctccccattcaca
2041 gagccttttcacaattccatttccagttcatctatggcagtccagccagctcctgggca
2101 gcttgagagggcaaacccaaaacctcatgacagccagagcctgtctttcagcattcagtc
2161 cgcctggccggctccagtttccccatggggctgcgggacagaggaccattacaactagat
2221 caaggagcccagaaaacctccagtagtggacaacaggttttcaccatagcctacgttaac
2281 ccatttttgagccaagcttcaaccctcagccttgaaaaacaagtctttaatttaattttt
2341 gtttttgcctaaatccaaagaaaaagggctgccgggccaggcgcggtggctcacgcctg
2401 taatcccagcactttggcaggccgaggcaggtggatcacctgacgtcagtagtttgagac
2461 cagcctggccaacatggtgaaaccctgtatctactaaaaatacaaaaattagccggacgt
2521 ggtggtgcgcgcatgtaatcccagctactcgggaggctgaggcggaagaatcacttgaac
2581 ccgggaggcggaggttccagtgagccgagatggcgctattgcactccagtctgggtaaca
2641 gggagactgcatctcaaaaaaaaaaaaaaaaaaaaaaaaaggctgtccatgtattcacac
```

2701 acccctcaaaaaaagcctttagttcctactttagccactggtttctcagaatccaaagat
2761 cacatattctagtgtaacactgcaagaagtcttgagaaaaagattattgtagtgttcaaa
2821 atatttttgtattgttaatgcatcatcatagaaaaacttttaaacatgagaataaagata
2881 ctttttactgggtttgtttttcaaagcctgaaaaaaa

10.1.3 cDNA sequence encoding TCF-3

1 gcgccgggccgggccgggcagggcgcgggcggctaggggctccgagagcggcggccccgg
61 cccgcggcccccaccatgccccagctcggcggcgggggcggcggcggcggcggcagcg
121 ggggaggcggcggctccagcgccggggcggccggcggaggggacgacctcggggcgaacg
181 acgagctgatcccccttccaggacgaggggggcgaggagcaggagccgagcagcgatagcg
241 cctcggcgcagcgggacctagacgaggtcaagtcgtccctggtcaacgagtcggagaacc
301 agagcagcagctcggactcggaggcggagaggcgcccgcagcccgtccgggacactttcc
361 agaagccgcgggactatttcgccgaagtgagaa**ggcctcaggacagcgcgttctttta**aag
421 gacccccgtaccctgggtacccccttcctgatgatcccggacctgagcagcccgtacctct
481 ccaacggacccctgtctcccggaggagcgcgcacctacctgcagatgaaatggcccctcc
541 tcgatgtcccctccagcgccacagtcaaggacacgaggtcaccatctccagcacacttgt
601 ctaataaagttcctgtcgttcagcacccgcatcacatgcatccgctgactcccctcatca
661 cctacagcaatgaccacttctcccccggctcccctcccacccacctctccccagagatcg
721 atccaaagacaggaatcccccggcccccctcacccatccgagctgtcaccgtattacccac
781 tctctcccggagctgtcggacaaatcccccacccccctcggctggctcgtcccacagcaag
841 gccagcccatgtactccttcctcccggtggcttccggcacccttaccccgccctcgcc**a**
901 tgaacgcctcgatgtccagcctggtctccagtcggttctctcctcacatggtggctcctg
961 cccaccctggcctgcccacctcagggatcccccacccctgccatcgtctcccccatcgtca
1021 agcaggaaccggcacccccagcctgagccctgcagtgagcgtgaaatcaccagtcaccg
1081 tgaaaaaggaggaggaaaagaagccccacgtgaagaagcctctgaatgccttcatgttgt
1141 atatgaaggagatgagggccaaggtggtggctgagtgcaccctgaaggaaagtgcagcca
1201 ttaaccagatccttggaagaaagtggcacaacctgtctcgagaagaacaggccaagtact
1261 acgagctggcccggaaggagcggcagcttcactcgcagctctacccaacctggtcagccc
1321 gggacaactatggtaagaaaaagaagaggaagagagaaaagcagctgtcccagacacagt
1381 cacagcagcaagtccaggaggcagagggtgccctggcctccaagagcaagaagccatgtg
1441 ttcagtacctgccccccgagaagccctgtgacagccctgcctcctcccacgggagcatgc
1501 tggactccccggccactccctctgcagctttggcctcaccagctgcccctgctgccaccc
1561 attcggagcaagcccagcccctctccctcaccaccaaaccagaaacccgggcccagctgg
1621 ctctccactctgccgccttcctgtcggctaaggctgcagcctcctcctctgggcagatgg
1681 gcagccagcctcccctcctgtcccggcccctcccccttgggtccatgcccacagctctgc
1741 tggcctctccccgtccttccccgccacgctccatgcccaccaggccctcccggtgctac
1801 aggcccagcctctttccctggtcaccaagtctgcccactaa*gctcccccgacccctgca*
1861 ggctgtcacatgactcattgagtagtaatgattcagaagaaaaagaaaaaggagacttta
1921 ttggtcaatatttgaccactctggactgttctgtaaagtggctggtaacaacagcacttt
1981 acagtttgtagatgtaaccagtagctgatcttaaggctttttaaaaaacaaaacaaaac
2041 aacaaaaaaaaatctttataagaaagagaactgaaaagtagcgtgctattcgtcctgtag
2101 gtgctgtggtggatggacctgggcagagggcacttctctctcttacctctcttgcacttt
2161 ctgtctcctgtctctttctcgcccctgccgcctgccccagcttccccgactccatctgcag
2221 ctctgccattgtgacatttcctgttacccagcccaagttttcatcgtctgctcaataccg
2281 tgggttcttcttcgtcctctgtcctctgcccagtgtgaggccatcaccatgtgagaagac
2341 atcttggcctgatttgctgccaccagcgtcccctccctcagtgggcccgaactcgccagc
2401 cccagctttcagtggagaaagcggtcctctgaaatggtttcctcccaacccccgcattta
2461 aagggactcaaggtgcctgccacttcctcagcgaagaagtctgtgttcctccccgtcctt
2521 gccagtggcgatcatcccttcacaatcccagagtggcaggcgggaccagccccatggtct
2581 ggctcctgtcacctgggtccgtgccagcacaatctgccaaagttctagagaccctgttcc
2641 cttccccatcacctcacatgcttcttctgtgtgtatttcttttgtttttatggttttg
2701 gagcaatttaaactcccagttgtttatttcacaaaagaaaataaaattgcagttgcaag
2761 aaaaaaaaaaaaaaaaaaa

10.1.4 cDNA sequence encoding TCF-4 (Vega gene TCFL2-003)

```
   1  ggttttttttttttaccccccttttttatttattatttttttgcacattgagcggatcct
  61  tgggaacgagagaaaaaagaaacccaaactcacgcgtgcagaagatctcccccccttcc
 121  cctcccctcctccctctttcccctccccaggagaaaaagacccccaagcagaaaaaagt
 181  tcaccttggactcgtctttttcttgcaatatttttgggggggcaaaactttgaggggct
 241  gatttttttggctttttcttcctccttcatttttcttccaaaattgctgctggtgggtga
 301  aaaaaaaatgccgcagctgaacggcggtggaggggatgacctaggcgccaacgacgaact
 361  gatttccttcaaagacgagggcgaacaggaggagaagagctccgaaaactcctcggcaga
 421  gagggatttagctgatgtcaaatcgtctctagtcaatgaatcagaaacgaatcaaaacag
 481  ctcctccgattccgaggcggaaagacggcctccgcctcgctccgaaagtttccgagacaa
 541  atcccgggaaagtttggaagaagcggccaagaggcaagatggagggctctttaaggggcc
 601  accgtatcccggctacccttcatcatgatccccgacctgacgagcccctacctccccaa
 661  cggatcgctctcgcccaccgcccgaacCTatctccagatgaaatggccactgcttgatgt
 721  ccaggcagggagcctccagagtagacaagccctcaaggatgcccggtccccatcaccggc
 781  acacattgtctctaacaaagtgccagtggtgcagcaccctcaccatgtccacccctcac
 841  gcctcttatcacgtacagcaatgaacacttcacgccgggaaacccacctccacacttacc
 901  agccgacgtagaccccaaaacaggaatcccacggcctccgcaccctccagatatatcccc
 961  gtattacccactatcgcctggcaccgtaggacaaatcccccatccgctaggatggttagt
1021  accacagcaaggtcaaccagtgtacccaatcacgacaggaggattcagacacccctaccc
1081  cacagctctgaccgtcaatgcttccgtgtccaggttcctccccatatggtcccaccaca
1141  tcatacgctacacacgacgggcattccgcatccggccatagtcacaccaacagtcaaaca
1201  ggaatcgtcccagagtgatgtcggctcactccatagttcaaagcatcaggactccaaaaa
1261  ggaagaagaaaagaagaagccccacataaagaaacctcttaatgcattcatgttgtatat
1321  gaaggaaatgagagcaaaggtcgtagctgagtgcacgttgaaagaaagcgcggccatcaa
1381  ccagatccttgggcggaggtggcatgcactgtccagagaagagcaagcgaaatactacga
1441  gctggcccggaaggagcgacagcttcatatgcaactgtaccccggctggtccgcgcggga
1501  taactatggaaagaagaagaagaggaaaagggacaagcagccgggagagaccaatgaaca
1561  cagcgaatgtttcctaaatccttgcctttcacttcctccgattacagacctcagcgctcc
1621  taagaaatgccgagcgcgctttggccttgatcaacagaataactggtgcggcccttgcag
1681  gagaaaaaaaaagtgcgttcgctacatacaaggtgaaggcagctgcctcagcccaccctc
1741  ttcagatggaagcttactagattcgcctcccccctccccgaacctgctaggctcccctcc
1801  ccgagacgccaagtcacagactgagcagacccagcctctgtcgctgtccctgaagcccga
1861  ccccctggcccacctgtccatgatgcctccgccacccgccctcctgctcgctgaggccac
1921  ccacaaggcctccgccctctgtcccaacggggccctggacctgcccccagccgctttgca
1981  gcctgccgccccctcctcatcaattgcacagccgtcgacttcttggttacattcccacag
2041  ctccctggccgggacccagccccagccgctgtcgctcgtcaccaagtctttagaatagct
2101  ttagcgtcgtgaaccccgctgctttgtttatggttttgtttcacttttcttaatttgccc
2161  cccacccccaccttgaaaggttttgttttgtactctcttaattttgtgccatgtggctac
2221  attagttgatgtttatcgagttcattggtcaatatttgacccattcttatttcaatttct
2281  ccttttaaatatgtagatgagagaagaacctcatgattggtaccaaaatttttatcaaca
2341  gctgtttaaagtctttgtagcgtttaaaaaatatatatatatacataactgttatgtagt
2401  tcggatagcttagttttaaaagactgattaaaaaacaaaaaaaa
```

NB. Vega gene TCFL2-003 corresponds to the lower TCF-4 band (777 bp) in Figures 3.2 and 3.3. The upper TCF-4 band (846 bp) has an additional 69 bp inserted at **CT**, corresponding to exon 4 in Vega genes TCFL2-002 and TCFL2-004; this sequence is:

CTCCATTTTC AGTCCGGCAG CACACATTAC TCTGCGTACA AAACGATTGA
ACACCAGATT GCAGTTCAG

10.2 TOPflash data

In all TOPflash experiments, samples were in duplicate and the Firefly luciferase control was 0.000.

Table 10.1: Data for Figure 3.13.

TOPflash reporter activity in H292 and SW480 cells at baseline.

	Sample 1		Sample 2		Sample 1		Sample 2		
H292	TOP	Renilla	TOP	Renilla	FOP	Renilla	FOP	Renilla	Renilla control
N=1	40.81	11.53	41.33	12.14	26.69	17.93	32.33	23.15	1.446
N=2	1.264	6.206	1.419	6.567	3.140	13.25	3.255	11.96	2.159
N=3	161.7	120.5	210.3	125.9	87.42	126.5	100.2	129.6	5.445
N=4	405.4	180.7	457.7	205.9	323.7	267.6	323.4	264.9	5.590
N=5	1246	254.6	1437	286.2	1023	405.4	1113	438.3	2.736
N=6	723.2	138.9	794.5	148.4	438.8	187.5	437.2	194.3	2.780

	Sample 1		Sample 2		Sample 1		Sample 2		
SW480	TOP	Renilla	TOP	Renilla	FOP	Renilla	FOP	Renilla	Renilla control
N=1	1391	12.75	1397	12.61	88.66	15.02	92.47	14.69	0.463
N=2	4858	16.22	4811	15.29	414.7	24.04	358.5	19.44	0.532
N=3	4769	10.63	5388	11.58	407.3	14.82	413.4	15.52	0.394

Table 10.2: Data for Figure 4.7.

TOPflash activity in H292 cells stimulated ± lithium (dose-response).

		Sample 1		Sample 2		Sample 1		Sample 2		
	[LiCl] mM	TOP	Renilla	TOP	Renilla	FOP	Renilla	FOP	Renilla	Renilla control
N=1	0	59.32	43.94	59.77	46.68	147.2	72.99	147.3	78.84	2.912
	5	129.8	58.97	126.7	61.83	262.6	101.0	277.0	99.75	2.912
	10	255.0	66.96	253.6	67.96	315.0	91.04	306.8	91.15	2.912
	20	677.2	64.80	687.0	63.08	370.6	105.9	332.1	92.61	2.912

Table 10.3: Data for Figure 4.8.

TOPflash reporter activity in H292 cells stimulated ± 20mM lithium.

		Sample 1		Sample 2		Sample 1		Sample 2		
	[LiCl] mM	TOP	Renilla	TOP	Renilla	FOP	Renilla	FOP	Renilla	Renilla control
N=1	0	33.49	25.64	30.11	29.21	128.5	114.8	120.0	112.4	2.912
	20	510.0	28.06	646.0	32.14	299.2	123.1	304.7	118.5	2.912
N=2	0	59.32	43.94	59.77	46.68	147.2	72.99	147.3	78.84	2.912
	20	677.2	64.80	687.0	63.08	370.6	105.9	332.1	92.61	2.912
N=3	0	71.52	50.16	70.22	49.41	129.2	47.46	130.4	47.68	2.912
	20	780.0	81.76	792.6	86.43	538.8	81.03	483.8	72.02	2.912
N=4	0	46.36	25.27	42.01	24.18	165.4	45.49	159.4	42.20	2.912
	20	349.9	30.25	321.4	31.90	275.6	51.09	278.1	48.80	2.912
N=5	0	42.89	38.04	38.06	35.38	175.0	45.39	170.1	46.92	2.912
	20	350.8	49.22	402.8	53.55	333.9	59.14	349.0	61.83	2.912

Table 10.4: Data for Figure 5.10.

TOPflash activity in H292 cells stimulated ± Wnt-3a CM (time-response).

		Sample 1		Sample 2		Sample 1		Sample 2		
Time	CM	TOP	Renilla	TOP	Renilla	FOP	Renilla	FOP	Renilla	Renilla control
1h	Wnt-3a	342.7	95.51	368.0	106.6	216.2	131.2	216.3	132.6	1.4315
	Control	347.8	98.48	378.8	106.3	222.5	130.7	224.8	133.1	1.4315
2h	Wnt-3a	302.1	92.03	332.7	102.5	248.5	129.8	223.6	130.9	1.4315
	Control	322.9	93.62	321.9	99.77	225.2	127.0	213.5	126.7	1.4315
4h	Wnt-3a	346.9	89.00	322.0	85.26	211.6	113.4	210.9	116.3	1.4315
	Control	412.0	111.0	425.4	116.1	272.0	138.4	281.5	143.2	1.4315
8h	Wnt-3a	313.8	67.01	334.5	69.44	187.9	89.52	198.0	91.17	1.4315
	Control	261.8	61.33	289.0	69.61	181.0	87.45	185.7	87.37	1.4315
16h	Wnt-3a	144.9	106.6	145.2	108.3	79.54	117.5	95.93	124.5	5.092
	Control	117.5	121.3	129.0	127.5	98.04	130.8	101.9	131.4	5.092
24h	Wnt-3a	68.93	36.07	74.55	40.07	37.50	46.06	39.87	51.21	1.4315
	Control	64.18	40.69	72.23	43.81	41.56	51.49	40.51	53.20	1.4315

Table 10.5: Data for Figure 5.11.

TOPflash reporter activity in H292 cells stimulated ± Wnt-3a CM.

		Sample 1		Sample 2		Sample 1		Sample 2		
	CM	TOP	Renilla	TOP	Renilla	FOP	Renilla	FOP	Renilla	Renilla control
N=1	Wnt-3a	144.9	106.6	145.2	108.3	79.54	117.5	95.93	124.5	5.092
	Control	117.5	121.3	129.0	127.5	98.04	130.8	101.9	131.4	5.092
N=2	Wnt-3a	26.35	16.99	29.28	17.73	23.52	23.63	26.48	27.12	2.912
	Control	39.15	15.44	36.11	19.64	19.24	21.22	15.92	20.76	2.912
N=3	Wnt-3a	1.327	5.789	1.470	5.471	2.724	13.59	2.890	13.24	2.160
	Control	2.080	5.579	1.962	4.307	2.557	9.034	2.841	11.02	2.160

		Sample 1		Sample 2		Sample 1		Sample 2		
	CM	TOP	Renilla	TOP	Renilla	FOP	Renilla	FOP	Renilla	Renilla control
N=4	Wnt-3a	179.2	134.4	193.3	151.2	81.77	133.7	76.33	135.9	5.445
	Control	225.3	122.5	223.8	125.2	75.66	122.5	81.58	126.8	5.445

Table 10.6: Data for Figure 6.1.

TOPflash reporter activity in H292 cells at low- and high-density.

		Sample 1		Sample 2		Sample 1		Sample 2		
	Cell density	TOP	Renilla	TOP	Renilla	FOP	Renilla	FOP	Renilla	Renilla control
N=1	Low	157.2	22.01	181.3	25.04	240.7	30.13	239.0	28.79	2.912
	High	71.52	50.16	70.22	49.41	129.2	47.46	130.4	47.68	2.912
N=2	Low	62.28	20.58	77.27	24.29	133.1	32.05	148.3	39.50	2.912
	High	43.86	80.97	40.96	76.70	121.9	84.41	110.2	77.61	2.912
N=3	Low	223.3	14.28	262.6	17.66	628.5	31.22	639.7	32.90	2.912
	High	235.4	95.01	226.6	97.91	638.0	106.2	580.9	97.43	2.912
N=4	Low	228.1	16.99	260.8	19.08	666.6	32.45	608.5	32.99	2.912
	High	70.09	31.18	80.42	35.21	333.9	47.13	323.1	46.20	2.912
N=5	Low	234.6	20.12	231.3	20.21	515.1	33.73	497.2	36.64	2.912
	High	266.0	73.52	299.5	83.96	627.3	88.89	643.0	90.59	2.912
N=6	Low	257.8	48.83	363.1	66.79	254.0	112.3	287.2	134.7	2.912
	High	405.4	180.7	457.7	205.9	323.7	267.6	323.4	264.9	2.912

Table 10.7: Data for Figure 7.1.

TOPflash reporter activity in H292 cells stimulated ± EGF (time-response).

N=1		Sample 1		Sample 2		Sample 1		Sample 2		
Time	[EGF] ng/ml	TOP	Renilla	TOP	Renilla	FOP	Renilla	FOP	Renilla	Renilla control
15m	20	40.47	36.36	39.56	39.81	129.0	63.27	128.2	60.35	2.912
	0	39.84	33.34	41.10	40.75	90.65	51.15	113.0	50.86	2.912
30m	20	38.77	30.18	47.23	37.51	110.4	43.67	125.9	53.99	2.912
	0	37.61	35.06	40.02	42.74	104.9	47.64	128.6	58.61	2.912
45m	20	64.08	47.27	54.36	45.48	146.3	54.04	151.6	56.07	2.912
	0	50.35	39.36	52.09	40.66	155.4	57.02	128.6	50.39	2.912
1h	20	58.75	39.58	61.26	40.39	130.6	48.68	141.5	54.34	2.912
	0	50.88	36.57	49.71	41.99	131.2	48.99	151.1	49.80	2.912
2h	20	71.26	41.45	75.35	46.14	204.2	65.90	209.5	67.63	2.912
	0	54.91	42.73	55.36	45.34	139.6	55.37	133.1	56.63	2.912
4h	20	91.99	40.65	94.75	42.62	223.8	56.80	206.9	56.93	2.912
	0	49.75	40.35	52.18	41.81	142.4	55.63	130.7	51.53	2.912
8h	20	85.54	38.17	88.87	43.23	141.2	45.67	142.9	46.39	2.912
	0	32.33	30.66	49.13	47.03	131.4	54.26	136.2	57.42	2.912

N=2		Sample 1		Sample 2		Sample 1		Sample 2		
Time	[EGF] ng/ml	TOP	Renilla	TOP	Renilla	FOP	Renilla	FOP	Renilla	Renilla control
15m	20	77.44	50.05	72.80	54.32	352.3	89.74	340.9	103.8	2.912
	0	70.14	46.52	69.44	50.32	357.0	95.19	333.8	91.87	2.912
30m	20	74.29	51.35	82.17	58.34	338.4	88.74	335.5	90.45	2.912
	0	72.96	51.43	73.48	52.55	354.7	92.94	403.3	97.60	2.912
45m	20	86.89	58.54	73.96	53.94	396.1	98.73	378.6	87.55	2.912
	0	77.59	42.54	65.04	50.30	390.7	94.34	335.9	71.66	2.912

N=2		Sample 1		Sample 2		Sample 1		Sample 2		
Time	[EGF] ng/ml	TOP	Renilla	TOP	Renilla	FOP	Renilla	FOP	Renilla	Renilla control
1h	20	81.53	44.19	70.29	47.59	366.2	81.86	357.8	80.44	2.912
	0	61.61	46.59	58.79	50.03	388.2	85.19	362.7	76.25	2.912
2h	20	151.7	63.69	146.1	66.10	643.8	100.8	637.2	118.4	2.912
	0	91.06	52.31	89.83	59.54	447.8	102.0	409.0	104.8	2.912
4h	20	153.7	49.13	164.1	55.65	596.7	87.44	564.3	86.34	2.912
	0	92.20	55.86	79.04	58.57	387.3	84.16	368.0	86.39	2.912
8h	20	121.6	28.44	123.5	29.53	129.2	28.21	120.0	25.78	2.912
	0	63.86	27.18	57.33	25.78	54.39	23.43	55.50	23.38	2.912

N=3		Sample 1		Sample 2		Sample 1		Sample 2		
Time	[EGF] ng/ml	TOP	Renilla	TOP	Renilla	FOP	Renilla	FOP	Renilla	Renilla control
15m	20	74.15	33.92	65.81	33.04	75.26	33.41	64.49	29.43	2.912
	0	80.38	35.02	75.01	43.41	72.88	33.59	63.05	29.18	2.912
30m	20	86.48	37.67	88.80	37.42	79.93	35.58	64.88	30.32	2.912
	0	82.74	39.89	76.15	37.78	72.43	35.38	75.71	31.83	2.912
45m	20	87.00	34.62	89.62	36.88	86.71	31.59	88.33	35.33	2.912
	0	93.80	35.58	89.18	38.27	77.01	33.00	81.73	35.55	2.912
1h	20	107.3	37.24	103.6	37.64	105.9	38.49	87.95	35.65	2.912
	0	84.66	34.65	86.38	35.29	85.32	33.48	94.25	30.38	2.912
2h	20	129.5	33.15	113.2	32.67	176.2	37.99	156.8	39.68	2.912
	0	81.35	30.83	80.77	35.67	106.4	37.18	93.35	35.56	2.912
4h	20	122.6	28.21	130.0	31.05	154.7	29.32	144.5	30.23	2.912
	0	84.06	32.55	72.24	29.75	107.4	33.02	99.95	31.13	2.912
8h	20	111.0	71.21	102.8	79.82	279.2	111.3	262.1	103.2	2.912
	0	62.34	72.32	57.48	73.19	149.2	89.11	158.4	106.8	2.912

N=4		Sample 1		Sample 2		Sample 1		Sample 2		
Time	[EGF] ng/ml	TOP	Renilla	TOP	Renilla	FOP	Renilla	FOP	Renilla	Renilla control
15m	20	74.58	66.11	74.57	75.32	176.8	105.0	187.8	115.0	2.912
	0	69.75	69.77	74.70	87.82	151.0	109.5	168.2	112.1	2.912
30m	20	65.90	73.12	67.69	78.17	166.8	101.4	145.5	101.5	2.912
	0	67.79	77.33	64.76	80.55	160.7	107.6	153.4	110.7	2.912
45m	20	85.61	79.16	91.49	77.53	176.1	91.82	187.6	108.3	2.912
	0	74.37	73.60	90.69	81.84	154.9	99.62	153.2	98.77	2.912
1h	20	108.7	40.67	108.1	42.75	217.0	50.62	166.1	44.82	2.912
	0	110.5	51.91	85.96	40.33	176.0	46.42	190.7	48.40	2.912
2h	20	115.3	83.37	119.6	81.83	282.0	119.4	299.8	108.8	2.912
	0	90.41	82.10	88.02	87.11	172.0	97.17	183.2	114.3	2.912
4h	20	121.5	75.79	130.2	82.97	289.9	106.6	298.8	113.6	2.912
	0	82.45	79.01	74.71	86.23	183.5	105.1	201.2	109.8	2.912
8h	20	106.2	35.59	118.4	36.29	223.5	42.65	221.2	39.67	2.912
	0	65.97	35.66	57.70	32.77	151.7	42.67	149.7	42.39	2.912

N=5		Sample 1		Sample 2		Sample 1		Sample 2		
Time	[EGF] ng/ml	TOP	Renilla	TOP	Renilla	FOP	Renilla	FOP	Renilla	Renilla control
15m	20	98.75	36.26	89.45	37.44	193.1	44.98	191.1	47.33	2.912
	0	88.28	34.71	82.00	36.96	135.3	41.70	171.9	44.77	2.912
30m	20	91.42	37.91	77.92	38.21	145.8	44.15	186.0	47.67	2.912
	0	76.34	38.52	83.97	40.45	145.2	43.95	149.7	42.42	2.912
45m	20	114.3	37.77	113.5	43.77	232.6	46.88	226.8	50.47	2.912
	0	95.17	39.89	102.4	44.13	213.0	51.53	209.7	52.00	2.912

N=5		Sample 1		Sample 2		Sample 1		Sample 2		
Time	[EGF] ng/ml	TOP	Renilla	TOP	Renilla	FOP	Renilla	FOP	Renilla	Renilla control
1h	20	160.4	56.91	148.2	56.47	353.1	94.47	294.0	85.04	2.912
	0	147.2	47.50	134.5	46.43	335.9	88.42	309.1	88.13	2.912
2h	20	136.0	39.61	146.8	44.95	323.4	51.70	286.8	47.42	2.912
	0	102.5	43.04	111.2	44.04	240.1	57.62	200.1	48.81	2.912
4h	20	146.2	35.06	140.1	36.07	295.4	41.78	264.4	38.17	2.912
	0	83.80	35.78	81.09	35.12	165.1	42.23	169.6	41.93	2.912
8h	20	166.7	45.08	170.2	49.00	329.2	66.67	293.6	59.66	2.912
	0	79.20	42.83	80.05	43.82	170.3	62.35	161.8	61.23	2.912

N=6		Sample 1		Sample 2		Sample 1		Sample 2		
Time	[EGF] ng/ml	TOP	Renilla	TOP	Renilla	FOP	Renilla	FOP	Renilla	Renilla control
15m	20	130.0	48.74	132.3	54.96	265.6	76.12	240.8	76.48	2.912
	0	136.0	41.96	151.4	48.04	278.7	71.38	287.1	76.32	2.912
30m	20	165.6	41.81	153.5	47.18	315.0	70.77	291.9	75.13	2.912
	0	157.2	41.74	151.7	44.72	304.6	65.67	276.7	60.72	2.912
45m	20	126.7	60.52	125.6	60.33	291.2	90.70	261.3	85.42	2.912
	0	131.0	58.61	128.4	58.17	329.4	104.8	286.7	89.83	2.912
1h	20	171.9	61.38	179.5	72.80	532.1	113.1	528.7	118.2	2.912
	0	130.2	54.88	159.0	64.86	393.9	113.2	403.0	113.1	2.912
2h	20	178.3	55.57	157.1	54.08	377.4	85.96	346.4	80.06	2.912
	0	129.7	42.61	119.2	51.58	263.4	85.56	282.2	88.36	2.912
4h	20	195.7	40.81	200.7	49.73	403.4	67.99	369.4	61.94	2.912
	0	129.1	38.88	129.5	49.28	268.7	64.31	238.2	65.34	2.912
8h	20	191.6	36.63	165.4	36.65	474.2	72.92	442.8	65.88	2.912
	0	100.6	38.47	102.1	37.30	237.1	68.69	237.2	61.39	2.912

N=7		Sample 1		Sample 2		Sample 1		Sample 2		
Time	[EGF] ng/ml	TOP	Renilla	TOP	Renilla	FOP	Renilla	FOP	Renilla	Renilla control
15m	20	-	-	-	-	-	-	-	-	-
	0	-	-	-	-	-	-	-	-	-
30m	20	127.8	49.04	129.5	49.27	324.5	78.25	279.3	71.50	2.912
	0	133.2	45.33	124.6	43.59	334.9	78.65	317.2	76.32	2.912
45m	20	-	-	-	-	-	-	-	-	-
	0	-	-	-	-	-	-	-	-	-
1h	20	72.38	69.44	59.27	77.63	125.9	56.01	130.8	61.37	2.912
	0	77.66	75.66	82.79	75.13	105.6	60.51	117.1	64.94	2.912
2h	20	-	-	-	-	-	-	-	-	-
	0	-	-	-	-	-	-	-	-	-
4h	20	204.4	46.58	227.7	48.40	577.7	85.22	559.0	76.43	2.912
	0	130.3	49.18	124.4	53.36	368.7	89.18	353.6	90.23	2.912
8h	20	93.13	62.46	95.56	66.62	142.4	55.73	134.6	53.10	2.912
	0	50.70	67.99	45.13	56.48	85.32	50.73	71.35	44.89	2.912

Table 10.8: Data for Figure 7.2.

TOPflash reporter activity in high-density H292 cells stimulated ± EGF.

			Sample 1		Sample 2		Sample 1		Sample 2		
	EGF	AG1478	TOP	Renilla	TOP	Renilla	FOP	Renilla	FOP	Renilla	Renilla control
N=1	+	-	59.09	59.99	65.03	65.09	136.0	65.19	129.6	63.27	2.912
	+	+	7.062	23.53	6.649	22.89	21.03	21.27	22.52	24.56	2.912
	-	-	15.21	32.93	17.27	37.54	44.08	35.82	40.12	33.43	2.912
N=2	+	-	98.96	62.67	113.5	66.55	260.3	70.50	236.9	65.23	2.912
	+	+	23.91	29.97	20.03	28.26	96.79	32.96	99.32	34.37	2.912
	-	-	39.98	52.03	40.53	50.54	144.2	60.69	135.3	58.10	2.912
N=3	+	-	200.5	39.48	159.0	31.42	555.9	52.75	541.8	51.94	2.912
	+	+	36.06	20.32	29.43	16.65	115.1	20.87	128.5	20.47	2.912
	-	-	53.33	25.90	86.19	34.25	264.9	40.02	256.2	39.94	2.912
N=4	+	-	110.5	25.24	112.3	25.74	354.9	51.63	345.9	50.50	2.912
	+	+	-	-	-	-	-	-	-	-	-
	-	-	45.36	20.45	45.04	20.27	203.8	45.80	181.4	43.30	2.912
N=4	+	-	-	-	-	-	-	-	-	-	-
	+	+	0.453	5.855	0.478	6.183	5.518	7.476	5.402	6.643	2.912
	-	-	0.707	4.778	1.230	5.332	9.024	5.314	8.528	5.378	2.912

Table 10.9: Data for Figure 7.3.

TOPflash reporter activity in low-density H292 cells stimulated ± EGF.

			Sample 1		Sample 2		Sample 1		Sample 2		
	EGF	AG1478	TOP	Renilla	TOP	Renilla	FOP	Renilla	FOP	Renilla	Renilla control
N=1	+	-	44.98	10.12	48.21	10.76	83.69	13.12	75.93	13.18	1.151
	+	+	17.79	6.648	19.44	6.934	38.06	9.967	37.69	7.798	1.151
	-	+	21.31	7.274	19.23	7.568	38.95	7.985	39.10	9.806	1.151
	-	-	27.17	8.767	31.63	10.45	51.35	11.82	59.38	11.99	1.151
HD	-	-	15.21	32.93	17.27	37.54	44.08	35.82	40.12	33.43	2.912
N=2	+	-	130.4	10.65	137.5	11.92	225.5	11.97	207.4	12.8	1.151
	+	+	48.84	7.081	47.43	7.469	108.1	7.888	113.2	7.921	1.151
	-	+	37.35	6.382	45.40	8.536	112.2	8.452	101.3	7.738	1.151
	-	-	61.92	9.207	60.24	10.37	158.8	11.76	146.7	12.61	1.151
HD	-	-	39.98	52.03	40.53	50.54	144.2	60.69	135.3	58.10	2.912
N=3	+	-	241.5	8.548	268.3	10.35	532.4	13.10	594.7	14.30	1.151
	+	+	-	-	-	-	-	-	-	-	-
	-	+	92.19	6.481	110.0	9.349	274.0	9.194	266.9	9.969	1.151
	-	-	133.9	9.724	147.8	10.73	296.9	12.55	308.6	17.13	1.151
HD	-	-	53.33	25.90	86.19	34.25	264.9	40.02	256.2	39.94	2.912
N=4	+	-	117.9	8.511	135.7	9.812	64.12	9.275	66.79	9.093	0.971
	+	+	53.62	6.402	52.05	8.138	27.30	6.490	29.62	8.423	0.971
	-	+	51.56	7.132	64.17	7.555	27.54	8.251	32.66	9.020	0.971
	-	-	-	-	-	-	-	-	-	-	-
HD	-	-	30.30	27.08	33.05	27.13	32.20	31.76	34.99	38.00	2.509

HD (high cell density).

Table 10.10: Data for Figure 7.7.

TOPflash reporter activity in H292 cells stimulated ± low Ca2+ medium.

			Sample 1		Sample 2		Sample 1		Sample 2		
	Cell density	[Calcium]	TOP	Renilla	TOP	Renilla	FOP	Renilla	FOP	Renilla	Renilla control
N=1	L	N	468.7	99.30	557.4	107.7	322.4	111.1	366.7	123.3	0.307
	H	N	136.9	366.5	140.8	356.4	121.4	387.3	110.9	367.6	0.224
	H	L	126.2	458.7	121.8	437.6	106.0	441.8	108.4	450.3	0.224
N=2	L	N	701.8	125.0	759.4	138.7	524.1	130.6	556.6	136.8	0.469
	H	N	545.5	1098	466.2	1005	584.0	1062	560.2	1100	0.434
	H	L	346.1	1209	424.5	1385	451.3	1322	535.8	1534	0.434
N=3	L	N	1065	161.7	1129	158.9	624.6	164.0	616.9	169.3	1.179
	H	N	559.9	1211	608.8	1371	414.5	1166	461.8	1226	0.467
	H	L	586.7	1633	615.9	1793	459.5	1391	476.5	1582	0.467

H (high); L (low); N (normal).

Table 10.11: Data for Figure 7.8.

TOPflash reporter activity in H292 cells stimulated ± low Ca2+ medium ± 20mM lithium.

			Sample 1		Sample 2		Sample 1		Sample 2		
	[Lithium] mM	[Calcium]	TOP	Renilla	TOP	Renilla	FOP	Renilla	FOP	Renilla	Renilla control
N=1	0	N	136.9	366.5	140.8	356.4	121.4	387.3	110.9	367.6	0.224
	20	N	3743	323.7	3420	308.4	309.2	335.3	313.8	378.5	0.224
	20	L	2431	338.7	2391	354.5	179.6	350.7	172.7	363.0	0.224
N=2	0	N	545.5	1098	466.2	1005	584.0	1062	560.2	1100	0.434
	20	N	7609	371.3	7642	415.4	826.3	435.1	810.5	416.5	0.434
	20	L	8894	758.9	9696	849.6	1019	833.4	1020	928.5	0.434
N=3	0	N	559.9	1211	608.8	1371	414.5	1166	461.8	1226	0.467
	20	N	6401	989.2	7140	1074	755.3	926.8	863.8	971.1	0.467
	20	L	5995	1186	6315	1242	764.8	1031	829.4	1097	0.467

L (low); N (normal).

10.3 Image analysis data: percentage nuclear ABC staining

Table 10.12: Data for Figure 4.3.

Percentage nuclear ABC staining in H292 cells stimulated ± lithium.

	[LiCl] mM	Percentage nuclear ABC staining
N=1	0	29.5
	20	55.4
N=2	0	22.8
	20	38.5
N=3	0	31.8
	20	43.4

Table 10.13: Data for Figure 4.6.

Percentage nuclear ABC staining in HBE cells stimulated ± lithium.

	[LiCl] mM	Percentage nuclear ABC staining
N=1	0	23.2
	20	36.2
N=2	0	38.5
	20	38.6
N=3	0	21.8
	20	29.8
N=4	0	37.3
	20	35.3
N=5	0	22.7
	20	54.0
N=6	0	33.3
	20	29.4
N=7	0	25.6
	20	43.3
N=8	0	34.4
	20	34.9

Table 10.14: Data for Figure 5.7.

Percentage nuclear ABC staining in H292 cells co-cultured with L-cells.

	L-cells	Percentage nuclear ABC staining
N=1	Control	14.0
	Wnt-3a	29.3
N=2	Control	7.8
	Wnt-3a	59.2

	L-cells	Percentage nuclear ABC staining
N=3	Control	16.8
	Wnt-3a	44.6
N=4	Control	13.8
	Wnt-3a	21.4
N=5	Control	15.0
	Wnt-3a	38.4
N=6	Control	29.5
	Wnt-3a	50.0

Table 10.15: Data for Figure 5.9.

Percentage nuclear ABC staining in HBE cells co-cultured with L-cells.

	L-cells	Percentage nuclear ABC staining
N=1	Control	10.3
	Wnt-3a	35.3
N=2	Control	23.6
	Wnt-3a	48.6
N=3	Control	32.3
	Wnt-3a	53.8
N=4	Control	17.8
	Wnt-3a	68.3
N=5	Control	45.7
	Wnt-3a	50.8
N=6	Control	24.3
	Wnt-3a	57.4

Table 10.16: Data for Figure 6.3.

Percentage nuclear ABC staining in H292 cells at low- and high-density.

	Cell density	Percentage nuclear ABC staining
N=1	Low	47.4
	High	27.7
N=2	Low	35.1
	High	24.4
N=3	Low	68.7
	High	35.8
N=4	Low	53.1
	High	20.9

Table 10.17: Data for Figure 6.7.

Percentage nuclear ABC staining in HBE cells at low- and high-density.

	Cell density	Percentage nuclear ABC staining
N=1	Low	61.0
	High	25.1
N=2	Low	55.4
	High	10.9
N=3	Low	72.6
	High	24.0
N=4	Low	36.7
	High	30.3
N=5	Low	68.8
	High	27.0
N=6	Low	73.7
	High	21.7
N=7	Low	83.3
	High	24.3

	Cell density	Percentage nuclear ABC staining
N=8	Low	71.3
	High	26.6

Table 10.18: Data for Figure 7.5.

Percentage nuclear ABC staining in H292 cells stimulated ± EGF.

	[EGF] ng/ml	Percentage nuclear ABC staining
N=1	0	43.9
	20	54.1
N=2	0	42.7
	20	45.9
N=3	0	43.9
	20	47.8
N=4	0	52.2
	20	44.2
N=5	0	53.7
	20	74.0
N=6	0	44.7
	20	66.4
N=7	0	53.7
	20	74.5
N=8	0	64.0
	20	65.0

10.4 Image analysis data: percentage of cells expressing Ki67

Table 10.19: Data for Figure 6.5.

Percentage of H292 cells expressing Ki67 at low- and high-density.

	Cell density	Percentage Ki67 expression
N=1	Low	99.3
	High	61.8
N=2	Low	99.3
	High	21.7
N=3	Low	99.3
	High	17.0

Table 10.20: Data for Figure 6.9.

Percentage of HBE cells expressing Ki67 at low- and high-density.

	Cell density	Percentage Ki67 expression
N=1	Low	59.2
	High	24.8
N=2	Low	61.8
	High	20.8
N=3	Low	74.6
	High	26.0
N=4	Low	66.7
	High	32.6

10.5 Quantitative PCR (qPCR; TaqMan) data

Outliers were excluded from the analysis.

Table 10.21: Data for Figure 4.13.

Cyclin-D1 gene expression in H292 cells stimulated ± lithium.

			Cyclin-D1 C_T values			18S C_T values		
	Time	[LiCl] mM	Sample 1	Sample 2	Sample 3	Sample 1	Sample 2	Sample 3
N=1	1h	0	25.6	24.2	24.9	13.5	12.0	12.1
		10	23.9	24.0	24.7	11.1	12.4	12.2
		20	25.4	25.2	24.9	12.0	12.4	12.2
	2h	0	25.0	25.1	25.2	12.1	11.9	13.4
		10	24.5	23.6	24.4	11.3	11.6	11.6
		20	24.1	23.7	24.2	11.6	11.6	11.8
	4h	0	23.9	24.4	23.9	11.6	11.8	11.6
		10	24.4	23.7	24.3	11.6	11.3	12.0
		20	24.3	24.5	24.1	11.8	11.6	11.8
	8h	0	23.7	23.7	23.0	11.3	11.2	11.5
		10	24.2	24.8	24.6	11.6	11.7	11.8
		20	30.3	24.6	25.2	11.4	11.5	11.7
N=2	1h	0	25.7	24.8	25.1	15.2	11.9	12.9
		10	24.3	24.6	24.7	11.5	13.3	13.7
		20	24.7	24.5	24.0	11.8	11.6	12.9
	2h	0	24.2	24.1	24.6	12.4	12.5	12.9
		10	24.2	23.8	23.9	12.0	11.4	12.0
		20	23.7	23.8	23.8	12.0	11.8	11.9

			Cyclin-D1 C_T values			18S C_T values		
	Time	[LiCl] mM	Sample 1	Sample 2	Sample 3	Sample 1	Sample 2	Sample 3
N=2	4h	0	23.2	23.4	23.3	12.1	12.2	12.2
		10	23.3	23.3	23.3	12.0	14.3	12.1
		20	23.5	22.9	23.6	11.8	11.7	11.7
	8h	0	23.5	23.3	23.2	11.9	12.0	12.2
		10	22.9	23.0	22.8	11.7	12.0	11.8
		20	22.7	22.9	23.4	11.4	11.7	12.2
N=3	1h	0	28.7	25.3	25.1	14.7	12.8	12.7
		10	25.3	25.9	25.6	12.3	11.6	12.2
		20	25.0	24.8	25.1	12.7	12.3	12.4
	2h	0	24.3	24.2	26.6	12.5	11.7	13.8
		10	25.9	25.2	25.7	12.9	12.1	12.4
		20	24.2	24.1	24.1	12.2	12.0	12.6
	4h	0	23.6	23.7	23.6	12.2	12.3	11.7
		10	24.8	24.6	25.3	12.1	12.3	11.9
		20	23.5	23.7	23.7	11.8	11.2	12.0
	8h	0	24.9	24.9	24.9	11.3	12.1	12.2
		10	25.0	25.6	25.7	11.9	12.4	12.0
		20	25.0	24.8	25.6	12.1	11.9	12.3
N=4	1h	0	29.4	28.0	28.4	21.5	17.1	16.9
		10	28.2	28.6	28.3	17.1	17.4	17.8
		20	27.6	28.1	26.5	16.7	16.8	15.1
	2h	0	28.1	27.4	28.6	17.8	17.1	18.9
		10	27.3	27.0	27.3	16.6	15.0	15.8
		20	26.3	26.9	26.9	15.0	15.8	16.0

			Cyclin-D1 C_T values			18S C_T values		
	Time	[LiCl] mM	Sample 1	Sample 2	Sample 3	Sample 1	Sample 2	Sample 3
N=4	4h	0	27.1	27.3	27.2	16.9	16.9	16.6
		10	27.4	27.3	27.4	16.7	16.8	16.2
		20	27.0	26.7	27.3	17.1	16.1	15.9
	8h	0	27.1	27.4	27.5	16.6	16.6	16.4
		10	26.6	26.6	26.6	15.9	16.0	15.9
		20	27.0	27.5	28.2	15.8	15.6	16.5

Table 10.22: Data for Figure 4.14.

IL-8 gene expression in H292 cells stimulated ± lithium.

			IL-8 C_T values			18S C_T values		
	Time	[LiCl] mM	Sample 1	Sample 2	Sample 3	Sample 1	Sample 2	Sample 3
N=1	1h	0	24.3	24.1	23.8	13.5	12.0	12.1
		10	24.2	24.4	24.6	11.1	12.4	12.2
		20	25.4	25.6	24.9	12.0	12.4	12.2
	2h	0	25.3	24.9	25.1	12.1	11.9	13.4
		10	25.2	24.4	24.5	11.3	11.6	11.6
		20	24.8	24.7	24.9	11.6	11.6	11.8
	4h	0	25.3	24.9	24.9	11.6	11.8	11.6
		10	24.3	24.4	24.7	11.6	11.3	12.0
		20	24.5	24.6	24.0	11.8	11.6	11.8
	8h	0	24.5	24.6	24.8	11.3	11.2	11.5
		10	23.9	23.8	24.0	11.6	11.7	11.8
		20	23.6	23.5	23.8	11.4	11.5	11.7

			IL-8 C_T values			18S C_T values		
	Time	[LiCl] mM	Sample 1	Sample 2	Sample 3	Sample 1	Sample 2	Sample 3
N=2	1h	0	25.7	25.4	25.8	15.2	11.9	12.9
		10	25.1	26.0	25.6	11.5	13.3	13.7
		20	25.5	25.6	25.3	11.8	11.6	12.9
	2h	0	25.7	25.6	26.0	12.4	12.5	12.9
		10	25.0	25.3	25.0	12.0	11.4	12.0
		20	25.0	25.1	25.3	12.0	11.8	11.9
	4h	0	26.6	26.7	26.5	12.1	12.2	12.2
		10	24.6	24.7	25.0	12.0	14.3	12.1
		20	24.0	24.1	24.0	11.8	11.7	11.7
	8h	0	26.7	26.7	26.5	11.9	12.0	12.2
		10	25.1	25.6	25.3	11.7	12.0	11.8
		20	25.0	24.9	25.2	11.4	11.7	12.2
N=3	1h	0	29.5	29.0	29.1	14.7	12.8	12.7
		10	27.9	28.4	28.6	12.3	11.6	12.2
		20	28.5	28.7	28.4	12.7	12.3	12.4
	2h	0	28.3	28.0	28.9	12.5	11.7	13.8
		10	29.0	29.4	28.9	12.9	12.1	12.4
		20	27.7	27.7	28.2	12.2	12.0	12.6
	4h	0	27.9	28.0	28.2	12.2	12.3	11.7
		10	28.1	28.3	28.2	12.1	12.3	11.9
		20	26.6	26.3	26.6	11.8	11.2	12.0
	8h	0	29.9	30.0	29.8	11.3	12.1	12.2
		10	29.4	28.9	29.1	11.9	12.4	12.0
		20	28.0	28.0	28.2	12.1	11.9	12.3

			IL-8 C_T values			18S C_T values		
	Time	[LiCl] mM	Sample 1	Sample 2	Sample 3	Sample 1	Sample 2	Sample 3
N=4	1h	0	29.8	29.0	29.5	21.5	17.1	16.9
		10	29.1	29.0	29.1	17.1	17.4	17.8
		20	28.6	28.1	28.0	16.7	16.8	15.1
	2h	0	29.0	28.9	29.2	17.8	17.1	18.9
		10	28.4	28.4	28.7	16.6	15.0	15.8
		20	28.8	28.9	29.1	15.0	15.8	16.0
	4h	0	27.4	27.5	27.1	16.9	16.9	16.9
		10	28.0	28.4	28.4	16.7	16.8	16.2
		20	30.3	29.9	30.5	17.1	16.1	15.9
	8h	0	27.9	27.9	27.7	16.6	16.6	16.4
		10	29.0	28.7	28.5	15.9	16.0	15.9
		20	33.9	29.9	30.3	15.8	15.6	16.5

Table 10.23: Data for Figure 5.12.

Cyclin-D1 gene expression in H292 cells stimulated ± Wnt-3a CM.

			Cyclin-D1 C_T values			18S C_T values		
	Time	CM	Sample 1	Sample 2	Sample 3	Sample 1	Sample 2	Sample 3
N=1	1h	Wnt-3a	24.6	24.4	24.6	12.7	12.3	11.1
		Control	24.2	24.3	24.5	11.1	12.0	11.4
	2h	Wnt-3a	24.1	23.8	23.8	11.7	11.5	11.0
		Control	24.2	24.4	25.1	11.7	11.3	12.5
	4h	Wnt-3a	23.9	23.8	24.0	12.1	11.3	11.9
		Control	23.7	23.5	24.0	11.9	11.1	11.8
	8h	Wnt-3a	24.2	23.9	23.6	11.9	11.5	11.3
		Control	24.0	24.2	24.9	11.5	11.7	12.2

			Cyclin-D1 C_T values			18S C_T values		
	Time	CM	Sample 1	Sample 2	Sample 3	Sample 1	Sample 2	Sample 3
N=2	1h	Wnt-3a	-	-	-	-	-	-
		Control	-	-	-	-	-	-
	2h	Wnt-3a	23.2	23.0	23.0	12.2	12.0	11.2
		Control	22.7	22.9	23.7	12.0	11.8	12.6
	4h	Wnt-3a	22.1	22.0	22.1	12.3	11.8	11.9
		Control	21.9	22.0	22.1	11.6	11.8	11.9
	8h	Wnt-3a	22.2	22.2	21.9	12.1	12.2	11.6
		Control	21.9	22.0	22.6	12.0	12.0	12.7
N=3	1h	Wnt-3a	26.1	25.2	25.1	13.1	12.4	12.3
		Control	27.0	26.3	26.5	12.6	12.5	12.6
	2h	Wnt-3a	24.6	24.8	24.7	12.2	12.0	12.0
		Control	25.5	25.0	26.3	12.0	11.4	12.4
	4h	Wnt-3a	24.2	24.2	23.9	12.6	12.2	12.3
		Control	23.1	23.1	23.0	12.1	12.3	12.4
	8h	Wnt-3a	23.8	23.7	23.5	12.7	12.2	12.0
		Control	23.0	23.1	23.4	11.6	11.9	12.7
N=4	1h	Wnt-3a	27.8	27.0	27.1	17.0	15.9	15.9
		Control	27.4	27.5	27.6	16.3	16.3	16.9
	2h	Wnt-3a	-	-	-	-	-	-
		Control	-	-	-	-	-	-
	4h	Wnt-3a	25.3	25.2	24.9	15.8	-	15.6
		Control	26.0	25.9	25.9	17.0	16.8	16.5
	8h	Wnt-3a	-	-	-	-	-	-
		Control	-	-	-	-	-	-

Table 10.24: Data for Figure 5.13.

IL-8 gene expression in H292 cells stimulated ± Wnt-3a CM.

			IL-8 C_T values			18S C_T values		
	Time	CM	Sample 1	Sample 2	Sample 3	Sample 1	Sample 2	Sample 3
N=1	1h	Wnt-3a	24.5	24.3	25.1	12.7	12.3	11.1
		Control	24.6	24.5	24.6	11.1	12.0	11.4
	2h	Wnt-3a	24.9	24.6	24.6	11.7	11.5	11.0
		Control	24.8	24.9	25.6	11.7	11.3	12.5
	4h	Wnt-3a	25.5	24.9	25.1	12.1	11.3	11.9
		Control	25.3	25.2	25.3	11.9	11.1	11.8
	8h	Wnt-3a	24.7	24.6	24.4	11.9	11.5	11.3
		Control	25.1	25.2	25.6	11.5	11.7	12.2
N=2	1h	Wnt-3a	-	-	-	-	-	-
		Control	-	-	-	-	-	-
	2h	Wnt-3a	24.2	24.3	24.4	12.2	12.0	11.2
		Control	23.9	24.3	24.6	12.0	11.8	12.6
	4h	Wnt-3a	25.4	25.4	25.3	12.3	11.8	11.9
		Control	25.5	25.1	25.3	11.6	11.8	11.9
	8h	Wnt-3a	25.2	25.2	25.0	12.1	12.2	11.6
		Control	24.9	25.0	25.9	12.0	12.0	12.7
N=3	1h	Wnt-3a	28.0	27.8	27.7	13.1	12.4	12.3
		Control	28.1	28.1	28.4	12.6	12.5	12.6
	2h	Wnt-3a	28.2	28.8	28.0	12.2	12.0	12.0
		Control	27.6	27.6	31.8	12.0	11.4	12.4
	4h	Wnt-3a	28.1	27.9	28.1	12.6	12.2	12.3
		Control	27.4	27.6	27.8	12.1	12.3	12.4
	8h	Wnt-3a	28.6	28.1	28.0	12.7	12.2	12.0
		Control	27.6	27.7	28.1	11.6	11.9	12.7

			IL-8 C_T values			18S C_T values		
	Time	CM	Sample 1	Sample 2	Sample 3	Sample 1	Sample 2	Sample 3
N=4	1h	Wnt-3a	27.4	27.1	27.1	17.0	15.9	15.9
		Control	27.6	27.7	27.5	16.3	16.3	16.9
	2h	Wnt-3a	-	-	-	-	-	-
		Control	-	-	-	-	-	-
	4h	Wnt-3a	27.9	27.8	27.9	15.8	-	15.6
		Control	28.4	28.3	28.0	17.0	16.8	16.5
	8h	Wnt-3a	-	-	-	-	-	-
		Control	-	-	-	-	-	-

Table 10.25: Data for Figure 7.12.

FZD6 gene expression in H292 cells at low- and high-density.

		FZD6 C_T values			18S C_T values		
	Cell density	Sample 1	Sample 2	Sample 3	Sample 1	Sample 2	Sample 3
N=1	High	27.0	26.9	27.1	12.0	11.6	12.0
	Low	28.9	28.6	29.7	12.4	12.6	12.5
N=2	High	25.8	26.1	26.2	12.1	11.9	12.1
	Low	26.4	26.5	26.3	12.4	12.3	12.4
N=3	High	29.7	29.3	30.5	12.7	12.3	11.7
	Low	31.7	32.3	33.2	12.4	12.3	12.6
N=4	High	27.0	26.8	27.5	16.7	16.0	16.1
	Low	28.7	28.3	28.1	16.0	15.2	15.6
N=5	High	24.2	24.5	24.4	11.8	12.0	11.5
	Low	25.4	25.0	23.8	11.7	11.9	12.5

Table 10.26: *MMP7* gene expression data in H292 cells stimulated ± lithium.

			MMP7 C_T values			18S C_T values		
	Time	[LiCl] mM	Sample 1	Sample 2	Sample 3	Sample 1	Sample 2	Sample 3
N=1	1h	0	43.1	44.2	39.0	14.7	12.8	12.7
		10	42.6	45.5	45.8	12.3	11.6	12.2
		20	45.8	39.5	46.2	12.7	12.3	12.4
	2h	0	39.5	42.0	41.8	12.5	11.7	13.8
		10	-	-	-	-	-	-
		20	>50.0	47.1	46.7	12.2	12.0	12.6
	4h	0	46.1	>50.0	44.8	12.2	12.3	11.7
		10	43.7	44.2	36.8	12.1	12.3	11.9
		20	44.8	44.9	40.9	11.8	11.2	12.0
	8h	0	41.1	44.9	42.4	11.3	12.1	12.2
		10	-	-	-	-	-	-
		20	45.3	42.1	45.4	12.1	11.9	12.3
	RT-minus control		>50.0	44.0	44.8	-	-	-
	UHQ water control		>50.0	>50.0	>50.0	-	-	-
N=2	1h	0	44.7	42.1	41.7	13.5	12.0	12.1
		10	42.2	39.8	41.2	11.1	12.4	12.2
		20	42.1	43.8	42.2	12.0	12.4	12.2
	2h	0	40.4	41.9	40.5	12.1	11.9	13.4
		10	37.5	39.9	40.4	11.3	11.6	11.6
		20	40.4	39.3	40.8	11.6	11.6	11.8
	4h	0	40.5	38.8	42.1	11.6	11.8	11.6
		10	39.3	39.7	47.5	11.6	11.3	12.0
		20	45.2	37.6	41.6	11.8	11.6	11.8

			MMP7 C_T values			18S C_T values		
	Time	[LiCl] mM	Sample 1	Sample 2	Sample 3	Sample 1	Sample 2	Sample 3
N=2	8h	0	40.9	39.6	38.6	11.3	11.2	11.5
		10	40.3	>50.0	38.0	11.6	11.7	11.8
		20	>50.0	39.0	38.8	11.4	11.5	11.7
	RT-minus control		38.8	38.1	39.8	-	-	-
	UHQ water control		>50.0	>50.0	>50.0	-	-	-
N=3	1h	0	36.4	40.7	34.3	14.7	12.8	12.7
		10	37.6	38.3	37.5	12.3	11.6	12.2
		20	37.3	33.8	35.9	12.7	12.3	12.4
	2h	0	34.7	35.1	36.1	12.5	11.7	13.8
		10	35.5	34.5	35.4	12.9	12.1	12.4
		20	38.9	34.2	36.3	12.2	12.0	12.6
	4h	0	36.9	35.1	33.7	12.2	12.3	11.7
		10	34.7	35.0	31.3	12.1	12.3	11.9
		20	34.0	35.2	36.3	11.8	11.2	12.0
	8h	0	37.1	36.8	34.3	11.3	12.1	12.2
		10	35.9	36.3	36.3	11.9	12.4	12.0
		20	40.4	34.6	36.5	12.1	11.9	12.3
	RT-minus control		40.3	>50.0	-	-	-	-
	UHQ water control		>50.0	>50.0	-	-	-	-

Table 10.27: *MMP7* gene expression in H292 cells stimulated ± Wnt-3a CM.

			MMP7 C_T values			18S C_T values		
	Time	CM	Sample 1	Sample 2	Sample 3	Sample 1	Sample 2	Sample 3
N=1	1h	Wnt-3a	39.1	40.0	42.9	12.7	12.3	11.1
		Control	37.8	39.0	39.0	11.1	12.0	11.4
	2h	Wnt-3a	39.9	>50.0	37.3	11.7	11.5	11.0
		Control	37.0	39.5	40.6	11.7	11.3	12.5
	4h	Wnt-3a	38.0	48.2	>50.0	12.1	11.3	11.9
		Control	40.7	38.7	41.4	11.9	11.1	11.8
	8h	Wnt-3a	41.3	41.3	37.8	11.9	11.5	11.3
		Control	45.3	40.2	40.0	11.5	11.7	12.2
	RT-minus control		38.8	38.1	39.8	-	-	-
	UHQ water control		>50.0	>50.0	>50.0	-	-	-
N=2	1h	Wnt-3a	38.3	38.6	34.7	13.1	12.4	12.3
		Control	34.9	36.0	35.9	12.6	12.5	12.6
	2h	Wnt-3a	34.3	37.0	34.6	12.2	12.0	12.0
		Control	35.4	37.4	36.2	12.0	11.4	12.4
	4h	Wnt-3a	35.4	32.7	34.9	12.6	12.2	12.3
		Control	36.4	36.1	33.4	12.1	12.3	12.4
	8h	Wnt-3a	34.7	35.1	33.9	12.7	12.2	12.0
		Control	35.0	35.4	37.0	11.6	11.9	12.7
	RT-minus control		40.3	>50.0	-	-	-	-
	UHQ water control		>50.0	>50.0	-	-	-	-

10.6 RNase protection assay (RPA) data

Table 10.28: Data for Figures 5.2, 5.4 and 5.5.

		Band intensity		
	Gene	H292 cells	Normal HBE cells	Asthmatic HBEC
N=1	FRZB	0	0	0
	SFRP2	0	0	0
	SFRP1	72878.453	111015.701	25347.504
	SMOH	136148.997	228229.860	41466.073
	FZD2	55145.430	34575.079	9304.866
	FZD3	11679.268	37651.036	8155.047
	FZD9	0	20562.686	3110.359
	FZD5	16443.352	204892.293	48247.913
	FZD6	253096.747	1416281.776	229856.164
	L32	1283909.502	9766567.767	4099363.840
	GAPDH	4173264.294	13631002.280	9659953.281
N=2	FRZB	0	0	0
	SFRP2	0	0	0
	SFRP1	433494.607	9658.019	5017.559
	SMOH	218247.787	13722.324	43841.141
	FZD2	92634.842	4171.279	10837.884
	FZD3	45944.149	2874.296	5591.600
	FZD9	0	4245.764	7250.883
	FZD5	9032.628	26867.462	57526.662
	FZD6	104808.490	66696.649	250925.142
	L32	1184537.299	1074712.957	1614889.264
	GAPDH	3656484.837	2865257.366	3702256.502

		Band intensity		
	Gene	H292 cells	Normal HBE cells	Asthmatic HBEC
N=3	FRZB	0	0	0
	SFRP2	0	0	0
	SFRP1	251679.325	6097.512	5065.837
	SMOH	131756.349	26826.963	6283.968
	FZD2	76806.635	4218.530	2075.642
	FZD3	24633.752	12192.843	2264.428
	FZD9	0	10833.537	3200.237
	FZD5	19054.582	121772.774	23253.469
	FZD6	106586.602	410149.800	76050.543
	L32	1238109.739	2105661.640	991002.914
	GAPDH	4681124.596	5872112.335	2462719.782
N=4	FRZB	0	0	0
	SFRP2	0	0	0
	SFRP1	665417.565	13438.473	90201.878
	SMOH	287968.107	20689.475	60963.573
	FZD2	226274.857	6522.814	16618.757
	FZD3	47429.425	3944.470	15043.035
	FZD9	0	5635.498	8537.308
	FZD5	70506.423	46818.650	116627.191
	FZD6	445925.734	175589.215	340513.566
	L32	1060318.013	1306079.671	2147345.610
	GAPDH	8793180.388	3386272.239	4861968.186

LIST OF REFERENCES

1. Aberle, H., H.Schwartz, and R.Kemler. 1996. Cadherin-catenin complex: protein interactions and their implications for cadherin function. *J Cell Biochem.* 61:514-523.

2. Al Moustafa, A.E., L.Yen, N.Benlimame, and M.A.Alaoui-Jamali. 2002. Regulation of E-cadherin/catenin complex patterns by epidermal growth factor receptor modulation in human lung cancer cells. *Lung Cancer* 37:49-56.

3. Atherton, H.C., G.Jones, and H.Danahay. 2003. IL-13-induced changes in the goblet cell density of human bronchial epithelial cell cultures: MAP kinase and phosphatidylinositol 3-kinase regulation. *Am. J Physiol Lung Cell Mol. Physiol* 285:L730-L739.

4. Barker, N., G.Huls, V.Korinek, and H.Clevers. 1999. Restricted high level expression of Tcf-4 protein in intestinal and mammary gland epithelium. *Am. J Pathol.* 154:29-35.

5. Beachy, P.A., S.S.Karhadkar, and D.M.Berman. 2004. Tissue repair and stem cell renewal in carcinogenesis. *Nature* 432:324-331.

6. Behrens, J., B.A.Jerchow, M.Wurtele, J.Grimm, C.Asbrand, R.Wirtz, M.Kuhl, D.Wedlich, and W.Birchmeier. 1998. Functional interaction of an axin homolog, conductin, with beta- catenin, APC, and GSK3beta. *Science* 280:596-599.

7. Behrens, J., J.P.von Kries, M.Kuhl, L.Bruhn, D.Wedlich, R.Grosschedl, and W.Birchmeier. 1996. Functional interaction of beta-catenin with the transcription factor LEF-1. *Nature* 382:638-642.

8. Bellusci, S., R.Henderson, G.Winnier, T.Oikawa, and B.L.Hogan. 1996. Evidence from normal expression and targeted misexpression that bone

morphogenetic protein (Bmp-4) plays a role in mouse embryonic lung morphogenesis. *Development* 122:1693-1702.

9. Bernacki, S.H., A.L.Nelson, L.Abdullah, J.K.Sheehan, A.Harris, C.W.Davis, and S.H.Randell. 1999. Mucin gene expression during differentiation of human airway epithelia in vitro. Muc4 and muc5b are strongly induced. *Am. J. Respir. Cell Mol. Biol.* 20:595-604.

10. Bhanot, P., M.Brink, C.H.Samos, J.C.Hsieh, Y.Wang, J.P.Macke, D.Andrew, J.Nathans, and R.Nusse. 1996. A new member of the frizzled family from Drosophila functions as a Wingless receptor. *Nature* 382:225-230.

11. Booth, C. and C.S.Potten. 2000. Gut instincts: thoughts on intestinal epithelial stem cells. *J Clin Invest* 105:1493-1499.

12. Bournat, J.C., A.M.Brown, and A.P.Soler. 2000. Wnt-1 dependent activation of the survival factor NF-kappaB in PC12 cells. *J Neurosci. Res* 61:21-32.

13. Boutros, M., N.Paricio, D.I.Strutt, and M.Mlodzik. 1998. Dishevelled activates JNK and discriminates between JNK pathways in planar polarity and wingless signaling. *Cell* 94:109-118.

14. Brabletz, T., A.Jung, S.Dag, F.Hlubek, and T.Kirchner. 1999. beta-catenin regulates the expression of the matrix metalloproteinase-7 in human colorectal cancer. *Am. J Pathol.* 155:1033-1038.

15. Brandon, C., L.M.Eisenberg, and C.A.Eisenberg. 2000. WNT signaling modulates the diversification of hematopoietic cells. *Blood* 96:4132-4141.

16. Brantjes, H., J.Roose, W.M.van De, and H.Clevers. 2001. All Tcf HMG box transcription factors interact with Groucho-related co-repressors. *Nucleic Acids Res.* 29:1410-1419.

17. Bremnes, R.M., R.Veve, F.R.Hirsch, and W.A.Franklin. 2002. The E-cadherin cell-cell adhesion complex and lung cancer invasion, metastasis, and prognosis. *Lung Cancer* 36:115-124.

18. Brown, D.C. and K.C.Gatter. 2002. Ki67 protein: the immaculate deception? *Histopathology* 40:2-11.

19. Brown, S.D., R.C.Twells, P.J.Hey, R.D.Cox, E.R.Levy, A.R.Soderman, M.L.Metzker, C.T.Caskey, J.A.Todd, and J.F.Hess. 1998. Isolation and characterization of LRP6, a novel member of the low density lipoprotein receptor gene family. *Biochem. Biophys. Res Commun.* 248:879-888.

20. Bucchieri, F., S.M.Puddicombe, J.L.Lordan, A.Richter, D.Buchanan, S.J.Wilson, J.Ward, G.Zummo, P.H.Howarth, R.Djukanovic, S.T.Holgate, and D.E.Davies. 2002. Asthmatic bronchial epithelium is more susceptible to oxidant-induced apoptosis. *Am. J. Respir. Cell Mol. Biol.* 27:179-185.

21. Bullions, L.C., D.A.Notterman, L.S.Chung, and A.J.Levine. 1997. Expression of wild-type alpha-catenin protein in cells with a mutant alpha-catenin gene restores both growth regulation and tumor suppressor activities. *Mol. Cell Biol.* 17:4501-4508.

22. Bullock,G.R., A.M.Campbell, M.J.Warhol, H.A.B.Multhaupt, and J.Bousquet. Expression of E-cadherin and a-, b- and g-catenin is associated with epithelial shedding in human lung and nose. J Allergy Clin Immunol 101. 1998.
Ref Type: Abstract

23. Calvo, R., J.West, W.Franklin, P.Erickson, L.Bemis, E.Li, B.Helfrich, P.Bunn, J.Roche, E.Brambilla, R.Rosell, R.M.Gemmill, and H.A.Drabkin. 2000. Altered HOX and WNT7A expression in human lung cancer. *Proc. Natl. Acad. Sci. U. S. A* 97:12776-12781.

24. Carayol, N., A.Campbell, I.Vachier, B.Mainprice, J.Bousquet, P.Godard, and P.Chanez. 2002a. Modulation of cadherin and catenins expression by tumor

necrosis factor- alpha and dexamethasone in human bronchial epithelial cells. *Am J Respir Cell Mol. Biol.* 26:341-347.

25. Carayol,N., I.Vachier, A.M.Campbell, P.Godard, J.Bousquet, and P.Chanez. Dexamethasone induce beta-catenin signaling pathway in human bronchial epithelial cells. ATS 98th International Conference . 2002b.

Ref Type: Abstract

26. Cavallo, R.A., R.T.Cox, M.M.Moline, J.Roose, G.A.Polevoy, H.Clevers, M.Peifer, and A.Bejsovec. 1998. Drosophila Tcf and Groucho interact to repress Wingless signalling activity. *Nature* 395:604-608.

27. Chakrabarty, S., V.Radjendirane, H.Appelman, and J.Varani. 2003. Extracellular calcium and calcium sensing receptor function in human colon carcinomas: promotion of E-cadherin expression and suppression of beta-catenin/TCF activation. *Cancer Res.* 63:67-71.

28. Chen, R.H., W.V.Ding, and F.McCormick. 2000. Wnt signaling to beta-catenin involves two interactive components. Glycogen synthase kinase-3beta inhibition and activation of protein kinase C. *J Biol. Chem.* 275:17894-17899.

29. Chen, S., D.C.Guttridge, Z.You, Z.Zhang, A.Fribley, M.W.Mayo, J.Kitajewski, and C.Y.Wang. 2001. Wnt-1 signaling inhibits apoptosis by activating beta-catenin/T cell factor-mediated transcription. *J Cell Biol.* 152:87-96.

30. Cheon, S.S., A.Y.Cheah, S.Turley, P.Nadesan, R.Poon, H.Clevers, and B.A.Alman. 2002. beta-Catenin stabilization dysregulates mesenchymal cell proliferation, motility, and invasiveness and causes aggressive fibromatosis and hyperplastic cutaneous wounds. *Proc. Natl. Acad. Sci. U. S. A* 99:6973-6978.

31. Cheon, S.S., P.Nadesan, R.Poon, and B.A.Alman. 2004. Growth factors regulate beta-catenin-mediated TCF-dependent transcriptional activation in

fibroblasts during the proliferative phase of wound healing. *Exp. Cell Res.* 293:267-274.

32. Chilosi, M., V.Poletti, A.Zamo, M.Lestani, L.Montagna, P.Piccoli, S.Pedron, M.Bertaso, A.Scarpa, B.Murer, A.Cancellieri, R.Maestro, G.Semenzato, and C.Doglioni. 2003. Aberrant Wnt/beta-catenin pathway activation in idiopathic pulmonary fibrosis. *Am. J. Pathol.* 162:1495-1502.

33. Christian, J.L. 2000. BMP, Wnt and Hedgehog signals: how far can they go? *Curr. Opin. Cell Biol.* 12:244-249.

34. Christian, J.L., J.A.McMahon, A.P.McMahon, and R.T.Moon. 1991. Xwnt-8, a Xenopus Wnt-1/int-1-related gene responsive to mesoderm- inducing growth factors, may play a role in ventral mesodermal patterning during embryogenesis. *Development* 111:1045-1055.

35. Chuang, P.T. and A.P.McMahon. 2003. Branching morphogenesis of the lung: new molecular insights into an old problem. *Trends Cell Biol.* 13:86-91.

36. Clark, C.C., I.Cohen, I.Eichstetter, L.A.Cannizzaro, J.D.McPherson, J.J.Wasmuth, and R.V.Iozzo. 1993. Molecular cloning of the human proto-oncogene Wnt-5A and mapping of the gene (WNT5A) to chromosome 3p14-p21. *Genomics* 18:249-260.

37. Cockcroft, D.W., D.N.Killian, J.J.Mellon, and F.E.Hargreave. 1977. Bronchial reactivity to inhaled histamine: a method and clinical survey. *Clin Allergy* 7:235-243.

38. Coghlan, M.P., A.A.Culbert, D.A.Cross, S.L.Corcoran, J.W.Yates, N.J.Pearce, O.L.Rausch, G.J.Murphy, P.S.Carter, C.L.Roxbee, D.Mills, M.J.Brown, D.Haigh, R.W.Ward, D.G.Smith, K.J.Murray, A.D.Reith, and J.C.Holder. 2000. Selective small molecule inhibitors of glycogen synthase kinase-3 modulate glycogen metabolism and gene transcription. *Chem. Biol.* 7:793-803.

39. Cook, D., M.J.Fry, K.Hughes, R.Sumathipala, J.R.Woodgett, and T.C.Dale. 1996. Wingless inactivates glycogen synthase kinase-3 via an intracellular signalling pathway which involves a protein kinase C. *EMBO J* 15:4526-4536.

40. Cooper, C.A., V.J.Bubb, N.Smithson, R.L.Carter, S.Gledhill, D.Lamb, A.H.Wyllie, and F.A.Carey. 1996. Loss of heterozygosity at 5q21 in non-small cell lung cancer: a frequent event but without evidence of apc mutation. *J Pathol.* 180:33-37.

41. Crawford, H.C., B.Fingleton, M.D.Gustavson, N.Kurpios, R.A.Wagenaar, J.A.Hassell, and L.M.Matrisian. 2001. The PEA3 subfamily of Ets transcription factors synergizes with beta- catenin-LEF-1 to activate matrilysin transcription in intestinal tumors. *Mol. Cell Biol.* 21:1370-1383.

42. Crawford, H.C., B.M.Fingleton, L.A.Rudolph-Owen, K.J.Goss, B.Rubinfeld, P.Polakis, and L.M.Matrisian. 1999. The metalloproteinase matrilysin is a target of beta-catenin transactivation in intestinal tumors. *Oncogene* 18:2883-2891.

43. Cui, Y., J.D.Brown, R.T.Moon, and J.L.Christian. 1995. Xwnt-8b: a maternally expressed Xenopus Wnt gene with a potential role in establishing the dorsoventral axis. *Development* 121:2177-2186.

44. D'Armiento, J., S.S.Dalal, Y.Okada, R.A.Berg, and K.Chada. 1992. Collagenase expression in the lungs of transgenic mice causes pulmonary emphysema. *Cell* 71:955-961.

45. Dale, T.C. 1998. Signal transduction by the Wnt family of ligands. *Biochem. J* 329 (Pt 2):209-223.

46. DasGupta, R. and E.Fuchs. 1999. Multiple roles for activated LEF/TCF transcription complexes during hair follicle development and differentiation. *Development* 126:4557-4568.

47. Davies, D.E., R.Polosa, S.M.Puddicombe, A.Richter, and S.T.Holgate. 1999. The epidermal growth factor receptor and its ligand family: their potential role in repair and remodelling in asthma. *Allergy* 54:771-783.

48. Delcommenne, M., C.Tan, V.Gray, L.Rue, J.Woodgett, and S.Dedhar. 1998. Phosphoinositide-3-OH kinase-dependent regulation of glycogen synthase kinase 3 and protein kinase B/AKT by the integrin-linked kinase. *Proc. Natl. Acad. Sci. U. S. A* 95:11211-11216.

49. Demoly, P., J.Simony-Lafontaine, P.Chanez, J.L.Pujol, N.Lequeux, F.B.Michel, and J.Bousquet. 1994. Cell proliferation in the bronchial mucosa of asthmatics and chronic bronchitics. *Am. J. Respir. Crit Care Med.* 150:214-217.

50. den Hartigh, J.C., van Bergen en Henegouwen PM, A.J.Verkleij, and J.Boonstra. 1992. The EGF receptor is an actin-binding protein. *J Cell Biol.* 119:349-355.

51. Dietrich, C., J.Scherwat, D.Faust, and F.Oesch. 2002. Subcellular localization of beta-catenin is regulated by cell density. *Biochem. Biophys. Res. Commun.* 292:195-199.

52. Ding, V.W., R.H.Chen, and F.McCormick. 2000. Differential regulation of glycogen synthase kinase 3beta by insulin and Wnt signaling. *J Biol. Chem.* 275:32475-32481.

53. Dong, Y., H.Drissi, M.Chen, D.Chen, M.J.Zuscik, E.M.Schwarz, and R.J.O'Keefe. 2005. Wnt-mediated regulation of chondrocyte maturation: modulation by TGF-beta. *J Cell Biochem.* 95:1057-1068.

54. Dong, Y., W.Lathrop, D.Weaver, Q.Qiu, J.Cini, D.Bertolini, and D.Chen. 1998. Molecular cloning and characterization of LR3, a novel LDL receptor family protein with mitogenic activity. *Biochem. Biophys. Res Commun.* 251:784-790.

55. Douglas, I.S., D.Diaz, V, R.A.Winn, and N.F.Voelkel. 2005. Beta-Catenin in the Fibroproliferative Response to Acute Lung Injury. *Am. J Respir. Cell Mol. Biol.*

56. Du, S.J., S.M.Purcell, J.L.Christian, L.L.McGrew, and R.T.Moon. 1995. Identification of distinct classes and functional domains of Wnts through expression of wild-type and chimeric proteins in Xenopus embryos. *Mol. Cell Biol.* 15:2625-2634.

57. Duan, D., A.Sehgal, J.Yao, and J.F.Engelhardt. 1998. Lef1 transcription factor expression defines airway progenitor cell targets for in utero gene therapy of submucosal gland in cystic fibrosis. *Am J Respir Cell Mol. Biol.* 18:750-758.

58. Duan, D., Y.Yue, W.Zhou, B.Labed, T.C.Ritchie, R.Grosschedl, and J.F.Engelhardt. 1999. Submucosal gland development in the airway is controlled by lymphoid enhancer binding factor 1 (LEF1). *Development* 126:4441-4453.

59. Dupuit, F., D.Gaillard, J.Hinnrasky, E.Mongodin, S.de Bentzmann, E.Copreni, and E.Puchelle. 2000. Differentiated and functional human airway epithelium regeneration in tracheal xenografts. *Am. J Physiol Lung Cell Mol. Physiol* 278:L165-L176.

60. Duval, A., S.Rolland, E.Tubacher, H.Bui, G.Thomas, and R.Hamelin. 2000. The human T-cell transcription factor-4 gene: structure, extensive characterization of alternative splicings, and mutational analysis in colorectal cancer cell lines. *Cancer Res.* 60:3872-3879.

61. Eberhart, C.G. and P.Argani. 2001. Wnt signaling in human development: beta-catenin nuclear translocation in fetal lung, kidney, placenta, capillaries, adrenal, and cartilage. *Pediatr. Dev. Pathol.* 4:351-357.

62. Eger, A., A.Stockinger, B.Schaffhauser, H.Beug, and R.Foisner. 2000. Epithelial mesenchymal transition by c-Fos estrogen receptor activation

involves nuclear translocation of beta-catenin and upregulation of beta-catenin/lymphoid enhancer binding factor-1 transcriptional activity. *J Cell Biol.* 148:173-188.

63. Engelhardt, J.F., H.Schlossberg, J.R.Yankaskas, and L.Dudus. 1995. Progenitor cells of the adult human airway involved in submucosal gland development. *Development* 121:2031-2046.

64. Engelhardt, J.F., J.R.Yankaskas, and J.M.Wilson. 1992. In vivo retroviral gene transfer into human bronchial epithelia of xenografts. *J Clin Invest* 90:2598-2607.

65. Fagotto, F., N.Funayama, U.Gluck, and B.M.Gumbiner. 1996. Binding to cadherins antagonizes the signaling activity of beta-catenin during axis formation in Xenopus. *J Cell Biol.* 132:1105-1114.

66. Fagotto, F., U.Gluck, and B.M.Gumbiner. 1998. Nuclear localization signal-independent and importin/karyopherin- independent nuclear import of beta-catenin. *Curr. Biol.* 8:181-190.

67. Fang, X., S.X.Yu, Y.Lu, R.C.Bast, Jr., J.R.Woodgett, and G.B.Mills. 2000. Phosphorylation and inactivation of glycogen synthase kinase 3 by protein kinase A. *Proc. Natl. Acad. Sci. U. S. A* 97:11960-11965.

68. Fear, M.W., D.P.Kelsell, N.K.Spurr, and M.R.Barnes. 2000. Wnt-16a, a novel Wnt-16 isoform, which shows differential expression in adult human tissues. *Biochem. Biophys. Res Commun.* 278:814-820.

69. Fedi, P., A.Bafico, S.A.Nieto, W.H.Burgess, T.Miki, D.P.Bottaro, M.H.Kraus, and S.A.Aaronson. 1999. Isolation and biochemical characterization of the human Dkk-1 homologue, a novel inhibitor of mammalian Wnt signaling. *J Biol. Chem.* 274:19465-19472.

70. Finch, P.W., X.He, M.J.Kelley, A.Uren, R.P.Schaudies, N.C.Popescu, S.Rudikoff, S.A.Aaronson, H.E.Varmus, and J.S.Rubin. 1997. Purification

and molecular cloning of a secreted, Frizzled-related antagonist of Wnt action. *Proc. Natl. Acad. Sci. U. S. A* 94:6770-6775.

71. Freemantle, S.J., H.B.Portland, K.Ewings, F.Dmitrovsky, K.DiPetrillo, M.J.Spinella, and E.Dmitrovsky. 2002. Characterization and tissue-specific expression of human GSK-3-binding proteins FRAT1 and FRAT2. *Gene* 291:17-27.

72. Fuchs, M., T.Muller, M.M.Lerch, and A.Ullrich. 1996. Association of human protein-tyrosine phosphatase kappa with members of the armadillo family. *J Biol. Chem.* 271:16712-16719.

73. Funayama, N., F.Fagotto, P.McCrea, and B.M.Gumbiner. 1995. Embryonic axis induction by the armadillo repeat domain of beta- catenin: evidence for intracellular signaling. *J Cell Biol.* 128:959-968.

74. Gat, U., R.DasGupta, L.Degenstein, and E.Fuchs. 1998. De Novo hair follicle morphogenesis and hair tumors in mice expressing a truncated beta-catenin in skin. *Cell* 95:605-614.

75. Gazit, A., A.Yaniv, A.Bafico, T.Pramila, M.Igarashi, J.Kitajewski, and S.A.Aaronson. 1999. Human frizzled 1 interacts with transforming Wnts to transduce a TCF dependent transcriptional response. *Oncogene* 18:5959-5966.

76. Giannini, A.L., M.Vivanco, and R.M.Kypta. 2000. alpha-catenin inhibits beta-catenin signaling by preventing formation of a beta-catenin*T-cell factor*DNA complex. *J Biol. Chem.* 275:21883-21888.

77. Golan, T., A.Yaniv, A.Bafico, G.Liu, and A.Gazit. 2004. The human Frizzled 6 (HFz6) acts as a negative regulator of the canonical Wnt. beta-catenin signaling cascade. *J Biol. Chem.* 279:14879-14888.

78. Gottardi, C.J., E.Wong, and B.M.Gumbiner. 2001. E-cadherin suppresses cellular transformation by inhibiting beta- catenin signaling in an adhesion-independent manner. *J Cell Biol.* 153:1049-1060.

79. Gounari, F., S.Signoretti, R.Bronson, L.Klein, W.R.Sellers, J.Kum, A.Siermann, M.M.Taketo, H.V.Boehmer, and K.Khazaie. 2002. Stabilization of beta-catenin induces lesions reminiscent of prostatic intraepithelial neoplasia, but terminal squamous transdifferentiation of other secretory epithelia. *Oncogene* 21:4099-4107.

80. Graham, N.A. and A.R.Asthagiri. 2004. Epidermal growth factor-mediated T-cell factor/lymphoid enhancer factor transcriptional activity is essential but not sufficient for cell cycle progression in nontransformed mammary epithelial cells. *J. Biol. Chem.* 279:23517-23524.

81. Groneberg, D.A., P.R.Eynott, T.Oates, S.Lim, R.Wu, I.Carlstedt, A.G.Nicholson, and K.F.Chung. 2002. Expression of MUC5AC and MUC5B mucins in normal and cystic fibrosis lung. *Respir. Med.* 96:81-86.

82. Hadjiargyrou, M., F.Lombardo, S.Zhao, W.Ahrens, J.Joo, H.Ahn, M.Jurman, D.W.White, and C.T.Rubin. 2002. Transcriptional profiling of bone regeneration: Insight into the molecular complexity of wound repair. *J Biol. Chem.*

83. Hardiman, G., R.A.Kastelein, and J.F.Bazan. 1997. Isolation, characterization and chromosomal localization of human WNT10B. *Cytogenet. Cell Genet.* 77:278-282.

84. Hardy, R.G., R.M.Brown, S.J.Miller, C.Tselepis, D.G.Morton, J.A.Jankowski, and D.S.Sanders. 2002. Transient P-cadherin expression in radiation proctitis; a model of mucosal injury and repair. *J. Pathol.* 197:194-200.

85. He, T.C., T.A.Chan, B.Vogelstein, and K.W.Kinzler. 1999. PPARdelta is an APC-regulated target of nonsteroidal anti-inflammatory drugs. *Cell* 99:335-345.

86. He, T.C., A.B.Sparks, C.Rago, H.Hermeking, L.Zawel, L.T.da Costa, P.J.Morin, B.Vogelstein, and K.W.Kinzler. 1998. Identification of c-MYC as a target of the APC pathway. *Science* 281:1509-1512.

87. He, X., J.P.Saint-Jeannet, Y.Wang, J.Nathans, I.Dawid, and H.Varmus. 1997. A member of the Frizzled protein family mediating axis induction by Wnt-5A. *Science* 275:1652-1654.

88. Hecht, A. and R.Kemler. 2000. Curbing the nuclear activities of beta-catenin. Control over Wnt target gene expression. *EMBO Rep.* 1:24-28.

89. Hey, P.J., R.C.Twells, M.S.Phillips, N.Yusuke, S.D.Brown, Y.Kawaguchi, R.Cox, X.Guochun, V.Dugan, H.Hammond, M.L.Metzker, J.A.Todd, and J.F.Hess. 1998. Cloning of a novel member of the low-density lipoprotein receptor family. *Gene* 216:103-111.

90. Hinck, L., W.J.Nelson, and J.Papkoff. 1994. Wnt-1 modulates cell-cell adhesion in mammalian cells by stabilizing beta-catenin binding to the cell adhesion protein cadherin. *J Cell Biol.* 124:729-741.

91. Hino, S., T.Michiue, M.Asashima, and A.Kikuchi. 2003. Casein kinase I epsilon enhances the binding of Dvl-1 to Frat-1 and is essential for Wnt-3a-induced accumulation of beta-catenin. *J Biol. Chem.* 278:14066-14073.

92. Hoang, B., M.Moos, Jr., S.Vukicevic, and F.P.Luyten. 1996. Primary structure and tissue distribution of FRZB, a novel protein related to Drosophila frizzled, suggest a role in skeletal morphogenesis. *J Biol. Chem.* 271:26131-26137.

93. Holgate, S.T., P.M.Lackie, D.E.Davies, W.R.Roche, and A.F.Walls. 1999. The bronchial epithelium as a key regulator of airway inflammation and remodelling in asthma. *Clin. Exp. Allergy* 29 Suppl 2:90-95.

94. Holmen, S.L., A.Salic, C.R.Zylstra, M.W.Kirschner, and B.O.Williams. 2002. A novel set of wnt-frizzled fusion proteins identifies receptor components that activate beta -catenin-dependent signaling. *J Biol. Chem.*

95. Hommura, F., K.Furuuchi, K.Yamazaki, S.Ogura, I.Kinoshita, M.Shimizu, T.Moriuchi, H.Katoh, M.Nishimura, and H.Dosaka-Akita. 2002. Increased expression of beta-catenin predicts better prognosis in nonsmall cell lung carcinomas. *Cancer* 94:752-758.

96. Hoschuetzky, H., H.Aberle, and R.Kemler. 1994. Beta-catenin mediates the interaction of the cadherin-catenin complex with epidermal growth factor receptor. *J Cell Biol.* 127:1375-1380.

97. Hovanes, K., T.W.Li, J.E.Munguia, T.Truong, T.Milovanovic, M.J.Lawrence, R.F.Holcombe, and M.L.Waterman. 2001. Beta-catenin-sensitive isoforms of lymphoid enhancer factor-1 are selectively expressed in colon cancer. *Nat. Genet.* 28:53-57.

98. Huber, A.H. and W.I.Weis. 2001. The structure of the beta-catenin/E-cadherin complex and the molecular basis of diverse ligand recognition by beta-catenin. *Cell* 105:391-402.

99. Huelsken, J., R.Vogel, B.Erdmann, G.Cotsarelis, and W.Birchmeier. 2001. beta-Catenin controls hair follicle morphogenesis and stem cell differentiation in the skin. *Cell* 105:533-545.

100. Huguet, E.L., K.Smith, R.Bicknell, and A.L.Harris. 1995. Regulation of Wnt5a mRNA expression in human mammary epithelial cells by cell shape, confluence, and hepatocyte growth factor. *J Biol. Chem.* 270:12851-12856.

101. Ikegawa, S., Y.Kumano, K.Okui, T.Fujiwara, E.Takahashi, and Y.Nakamura. 1996. Isolation, characterization and chromosomal assignment of the human WNT7A gene. *Cytogenet. Cell Genet.* 74:149-152.

102. Imai, K. and J.D'Armiento. 2000. Activation of an embryonic gene product in pulmonary emphysema : identification of the secreted frizzled-related protein. *Chest* 117:229S.

103. Imai, K. and J.D'Armiento. 2002. Differential gene expression of sFRP-1 and apoptosis in pulmonary emphysema. *Chest* 121:7S.

104. Imai, K., S.S.Dalal, E.S.Chen, R.Downey, L.L.Schulman, M.Ginsburg, and J.D'Armiento. 2001. Human collagenase (matrix metalloproteinase-1) expression in the lungs of patients with emphysema. *Am J Respir Crit Care Med* 163:786-791.

105. Iozzo, R.V., I.Eichstetter, and K.G.Danielson. 1995. Aberrant expression of the growth factor Wnt-5A in human malignancy. *Cancer Res* 55:3495-3499.

106. Ishitani, T., J.Ninomiya-Tsuji, S.Nagai, M.Nishita, M.Meneghini, N.Barker, M.Waterman, B.Bowerman, H.Clevers, H.Shibuya, and K.Matsumoto. 1999. The TAK1-NLK-MAPK-related pathway antagonizes signalling between beta- catenin and transcription factor TCF. *Nature* 399:798-802.

107. Jawhari, A.U., M.J.Farthing, and M.Pignatelli. 1999. The E-cadherin/epidermal growth factor receptor interaction: a hypothesis of reciprocal and reversible control of intercellular adhesion and cell proliferation. *J Pathol.* 187:155-157.

108. Jho, E.H., T.Zhang, C.Domon, C.K.Joo, J.N.Freund, and F.Costantini. 2002. Wnt/beta-catenin/Tcf signaling induces the transcription of Axin2, a negative regulator of the signaling pathway. *Mol. Cell Biol.* 22:1172-1183.

109. Jones, S.E., C.Jomary, J.Grist, H.J.Stewart, and M.J.Neal. 2000a. Altered expression of secreted frizzled-related protein-2 in retinitis pigmentosa retinas. *Invest Ophthalmol. Vis. Sci.* 41:1297-1301.

110. Jones, S.E., C.Jomary, J.Grist, H.J.Stewart, and M.J.Neal. 2000b. Modulated expression of secreted frizzled-related proteins in human retinal degeneration. *Neuroreport* 11:3963-3967.

111. Jue, S.F., R.S.Bradley, J.A.Rudnicki, H.E.Varmus, and A.M.Brown. 1992. The mouse Wnt-1 gene can act via a paracrine mechanism in transformation of mammary epithelial cells. *Mol. Cell Biol.* 12:321-328.

112. Katoh, M. 2001a. Frequent up-regulation of WNT2 in primary gastric cancer and colorectal cancer. *Int. J Oncol.* 19:1003-1007.

113. Katoh, M. 2001b. Molecular cloning and characterization of human WNT3. *Int. J. Oncol.* 19:977-982.

114. Katoh, M., M.Hirai, T.Sugimura, and M.Terada. 1996. Cloning, expression and chromosomal localization of Wnt-13, a novel member of the Wnt gene family. *Oncogene* 13:873-876.

115. Kim, K., Z.Lu, and E.D.Hay. 2002. DIRECT EVIDENCE FOR A ROLE OF beta-CATENIN/LEF-1 SIGNALING PATHWAY IN INDUCTION OF EMT. *Cell Biol. Int.* 26:463-476.

116. Kirikoshi, H., N.Sagara, J.Koike, K.Tanaka, H.Sekihara, M.Hirai, and M.Katoh. 1999. Molecular cloning and characterization of human Frizzled-4 on chromosome 11q14-q21. *Biochem. Biophys. Res Commun.* 264:955-961.

117. Kirikoshi, H., H.Sekihara, and M.Katoh. 2001a. Molecular cloning and characterization of human WNT11. *Int. J Mol. Med* 8:651-656.

118. Kirikoshi, H., H.Sekihara, and M.Katoh. 2001b. Molecular cloning and characterization of human WNT7B. *Int. J. Oncol.* 19:779-783.

119. Kirikoshi, H., H.Sekihara, and M.Katoh. 2001c. Molecular cloning and characterization of WNT14B, a novel member of the WNT gene family. *Int. J Oncol.* 19:947-952.

120. Kirikoshi, H., H.Sekihara, and M.Katoh. 2001d. WNT10A and WNT6, clustered in human chromosome 2q35 region with head-to- tail manner, are

strongly coexpressed in SW480 cells. *Biochem. Biophys. Res Commun.* 283:798-805.

121. Koike, J., A.Takagi, T.Miwa, M.Hirai, M.Terada, and M.Katoh. 1999. Molecular cloning of Frizzled-10, a novel member of the Frizzled gene family. *Biochem. Biophys. Res Commun.* 262:39-43.

122. Korinek, V., N.Barker, P.Moerer, E.van Donselaar, G.Huls, P.J.Peters, and H.Clevers. 1998. Depletion of epithelial stem-cell compartments in the small intestine of mice lacking Tcf-4. *Nat. Genet.* 19:379-383.

123. Korinek, V., N.Barker, P.J.Morin, D.van Wichen, R.de Weger, K.W.Kinzler, B.Vogelstein, and H.Clevers. 1997. Constitutive transcriptional activation by a beta-catenin-Tcf complex in APC-/- colon carcinoma. *Science* 275:1784-1787.

124. Kratochwil, K., M.Dull, I.Farinas, J.Galceran, and R.Grosschedl. 1996. Lef1 expression is activated by BMP-4 and regulates inductive tissue interactions in tooth and hair development. *Genes Dev.* 10:1382-1394.

125. Krupnik, V.E., J.D.Sharp, C.Jiang, K.Robison, T.W.Chickering, L.Amaravadi, D.E.Brown, D.Guyot, G.Mays, K.Leiby, B.Chang, T.Duong, A.D.Goodearl, D.P.Gearing, S.Y.Sokol, and S.A.McCarthy. 1999. Functional and structural diversity of the human Dickkopf gene family. *Gene* 238:301-313.

Kuhl, M. 2004. The Wnt/Calcium pathway: biochemical mediators, tools and future requirements. *Frontiers of Bioscience* 9: 967-974.

126. Kuhl, M., K.Geis, L.C.Sheldahl, T.Pukrop, R.T.Moon, and D.Wedlich. 2001. Antagonistic regulation of convergent extension movements in Xenopus by Wnt/beta-catenin and Wnt/Ca(2+) signaling. *Mech. Dev.* 106:61-76.

127. Kuhl, M., L.C.Sheldahl, C.C.Malbon, and R.T.Moon. 2000a. Ca(2+)/calmodulin-dependent protein kinase II is stimulated by Wnt and

Frizzled homologs and promotes ventral cell fates in Xenopus. *J Biol. Chem.* 275:12701-12711.

128. Kuhl, M., L.C.Sheldahl, M.Park, J.R.Miller, and R.T.Moon. 2000b. The Wnt/Ca2+ pathway: a new vertebrate Wnt signaling pathway takes shape. *Trends Genet.* 16:279-283.

129. Kuhl, M. and D.Wedlich. 1996. Xenopus cadherins: sorting out types and functions in embryogenesis. *Dev. Dyn.* 207:121-134.

130. Labbe, E., A.Letamendia, and L.Attisano. 2000. Association of Smads with lymphoid enhancer binding factor 1/T cell- specific factor mediates cooperative signaling by the transforming growth factor-beta and wnt pathways. *Proc. Natl. Acad. Sci. U. S. A* 97:8358-8363.

131. Labus, M.B., C.M.Stirk, W.D.Thompson, and W.T.Melvin. 1998. Expression of Wnt genes in early wound healing. *Wound. Repair Regen.* 6:58-64.

132. Lako, M., T.Strachan, P.Bullen, D.I.Wilson, S.C.Robson, and S.Lindsay. 1998. Isolation, characterisation and embryonic expression of WNT11, a gene which maps to 11q13.5 and has possible roles in the development of skeleton, kidney and lung. *Gene* 219:101-110.

133. Landesman, Y. and S.Y.Sokol. 1997. Xwnt-2b is a novel axis-inducing Xenopus Wnt, which is expressed in embryonic brain. *Mech. Dev.* 63:199-209.

134. Lau, K.F., C.C.Miller, B.H.Anderton, and P.C.Shaw. 1999. Expression analysis of glycogen synthase kinase-3 in human tissues. *J Pept. Res* 54:85-91.

135. Lee, J.H., N.Kaminski, G.Dolganov, G.Grunig, L.Koth, C.Solomon, D.J.Erle, and D.Sheppard. 2001. Interleukin-13 induces dramatically different transcriptional programs in three human airway cell types. *Am. J. Respir. Cell Mol. Biol.* 25:474-485.

136. Lee, J.S., A.Ishimoto, and S.Yanagawa. 1999. Characterization of mouse dishevelled (Dvl) proteins in Wnt/Wingless signaling pathway. *J Biol. Chem.* 274:21464-21470.

137. Leir, S.H., J.E.Baker, S.T.Holgate, and P.M.Lackie. 2000. Increased CD44 expression in human bronchial epithelial repair after damage or plating at low cell densities. *Am. J Physiol Lung Cell Mol. Physiol* 278:L1129-L1137.

138. Letamendia, A., E.Labbe, and L.Attisano. 2001. Transcriptional regulation by Smads: crosstalk between the TGF-beta and Wnt pathways. *J Bone Joint Surg. Am.* 83-A Suppl 1:S31-S39.

139. Levay-Young, B.K. and M.Navre. 1992. Growth and developmental regulation of wnt-2 (irp) gene in mesenchymal cells of fetal lung. *Am. J Physiol* 262:L672-L683.

140. Levy, L., C.Neuveut, C.A.Renard, P.Charneau, S.Branchereau, F.Gauthier, J.T.Van Nhieu, D.Cherqui, A.F.Petit-Bertron, D.Mathieu, and M.A.Buendia. 2002. Transcriptional activation of interleukin-8 by beta-catenin-Tcf4. *J. Biol. Chem.* 277:42386-42393.

141. Li, H., R.Pamukcu, and W.J.Thompson. 2002a. beta-Catenin signaling: therapeutic strategies in oncology. *Cancer Biol. Ther.* 1:621-625.

142. Li, L., J.Mao, L.Sun, W.Liu, and D.Wu. 2002b. Second cysteine-rich domain of Dickkopf-2 activates canonical Wnt signaling pathway via LRP-6 independently of dishevelled. *J Biol. Chem.* 277:5977-5981.

143. Li, L., H.Yuan, C.D.Weaver, J.Mao, G.H.Farr, III, D.J.Sussman, J.Jonkers, D.Kimelman, and D.Wu. 1999. Axin and Frat1 interact with dvl and GSK, bridging Dvl to GSK in Wnt- mediated regulation of LEF-1. *EMBO J* 18:4233-4240.

144. Liu, C., Y.Li, M.Semenov, C.Han, G.H.Baeg, Y.Tan, Z.Zhang, X.Lin, and X.He. 2002. Control of beta-catenin phosphorylation/degradation by a dual-kinase mechanism. *Cell* 108:837-847.

145. Liu, G., A.Bafico, V.K.Harris, and S.A.Aaronson. 2003. A novel mechanism for Wnt activation of canonical signaling through the LRP6 receptor. *Mol. Cell Biol.* 23:5825-5835.

146. Liu, X., T.Liu, D.C.Slusarski, J.Yang-Snyder, C.C.Malbon, R.T.Moon, and H.Wang. 1999. Activation of a frizzled-2/beta-adrenergic receptor chimera promotes Wnt signaling and differentiation of mouse F9 teratocarcinoma cells via Galphao and Galphat. *Proc. Natl. Acad. Sci. U. S. A* 96:14383-14388.

147. Lu, Z. and T.Hunter. 2004. Wnt-independent beta-catenin transactivation in tumor development. *Cell Cycle* 3:571-573.

148. Lustig, B., B.Jerchow, M.Sachs, S.Weiler, T.Pietsch, U.Karsten, W.M.van De, H.Clevers, P.M.Schlag, W.Birchmeier, and J.Behrens. 2002. Negative feedback loop of Wnt signaling through upregulation of conductin/axin2 in colorectal and liver tumors. *Mol. Cell Biol.* 22:1184-1193.

149. Mann, B., M.Gelos, A.Siedow, M.L.Hanski, A.Gratchev, M.Ilyas, W.F.Bodmer, M.P.Moyer, E.O.Riecken, H.J.Buhr, and C.Hanski. 1999. Target genes of beta-catenin-T cell-factor/lymphoid-enhancer-factor signaling in human colorectal carcinomas. *Proc. Natl. Acad. Sci. U. S. A* 96:1603-1608.

150. Mao, J., J.Wang, B.Liu, W.Pan, G.H.Farr, III, C.Flynn, H.Yuan, S.Takada, D.Kimelman, L.Li, and D.Wu. 2001. Low-density lipoprotein receptor-related protein-5 binds to Axin and regulates the canonical Wnt signaling pathway. *Mol. Cell* 7:801-809.

151. Marchenko, G.N., N.D.Marchenko, J.Leng, and A.Y.Strongin. 2002. Promoter characterization of the novel human matrix metalloproteinase- 26 gene:

regulation by the T-cell factor-4 implies specific expression of the gene in cancer cells of epithelial origin. *Biochem. J* 363:253-262.

152. Mariadason, J.M., M.Bordonaro, F.Aslam, L.Shi, M.Kuraguchi, A.Velcich, and L.H.Augenlicht. 2001. Down-regulation of beta-catenin TCF signaling is linked to colonic epithelial cell differentiation. *Cancer Res* 61:3465-3471.

153. Mason, R.J., M.C.Williams, H.L.Moses, S.Mohla, and M.A.Berberich. 1997. Stem cells in lung development, disease, and therapy. *Am. J Respir. Cell Mol. Biol.* 16:355-363.

154. Mata, M., B.Sarria, A.Buenestado, J.Cortijo, M.Cerda, and E.J.Morcillo. 2005. Phosphodiesterase 4 inhibition decreases MUC5AC expression induced by epidermal growth factor in human airway epithelial cells. *Thorax* 60:144-152.

155. McCrea, P.D., C.W.Turck, and B.Gumbiner. 1991. A homolog of the armadillo protein in Drosophila (plakoglobin) associated with E-cadherin. *Science* 254:1359-1361.

156. McMahon, A.P. and R.T.Moon. 1989. Ectopic expression of the proto-oncogene int-1 in Xenopus embryos leads to duplication of the embryonic axis. *Cell* 58:1075-1084.

157. Mei, J.M., N.G.Hord, D.F.Winterstein, S.P.Donald, and J.M.Phang. 2000a. Differential formation of beta-catenin/lymphoid enhancer factor-1 DNA binding complex induced by nitric oxide in mouse colonic epithelial cells differing in adenomatous polyposis coli (Apc) genotype. *Cancer Res* 60:3379-3383.

158. Mei, J.M., N.G.Hord, D.F.Winterstein, S.P.Donald, and J.M.Phang. 2000b. Expression of prostaglandin endoperoxide H synthase-2 induced by nitric oxide in conditionally immortalized murine colonic epithelial cells. *FASEB J* 14:1188-1201.

159. Melkonyan, H.S., W.C.Chang, J.P.Shapiro, M.Mahadevappa, P.A.Fitzpatrick, M.C.Kiefer, L.D.Tomei, and S.R.Umansky. 1997. SARPs: a family of secreted apoptosis-related proteins. *Proc. Natl. Acad. Sci. U. S. A* 94:13636-13641.

160. Mercer,B., K.Imai, and J.D'Armiento. Regulation of matrix metalloproteinases (MMPs) by secreted Frizzled related protein-1 (sFRP1). ATS 98th International Conference . 2002.

Ref Type: Abstract

161. Merrill, B.J., U.Gat, R.DasGupta, and E.Fuchs. 2001. Tcf3 and Lef1 regulate lineage differentiation of multipotent stem cells in skin. *Genes Dev.* 15:1688-1705.

162. Midgley, C.A., S.White, R.Howitt, V.Save, M.G.Dunlop, P.A.Hall, D.P.Lane, A.H.Wyllie, and V.J.Bubb. 1997. APC expression in normal human tissues. *J Pathol.* 181:426-433.

163. Miller, J.R., A.M.Hocking, J.D.Brown, and R.T.Moon. 1999. Mechanism and function of signal transduction by the Wnt/beta-catenin and Wnt/Ca2+ pathways. *Oncogene* 18:7860-7872.

164. Miwa, N., M.Furuse, S.Tsukita, N.Niikawa, Y.Nakamura, and Y.Furukawa. 2001. Involvement of claudin-1 in the beta-catenin/Tcf signaling pathway and its frequent upregulation in human colorectal cancers. *Oncol. Res* 12:469-476.

165. Miyoshi, Y., H.Nagase, H.Ando, A.Horii, S.Ichii, S.Nakatsuru, T.Aoki, Y.Miki, T.Mori, and Y.Nakamura. 1992. Somatic mutations of the APC gene in colorectal tumors: mutation cluster region in the APC gene. *Hum. Mol. Genet.* 1:229-233.

166. Molenaar, M., W.M.van De, M.Oosterwegel, J.Peterson-Maduro, S.Godsave, V.Korinek, J.Roose, O.Destree, and H.Clevers. 1996. XTcf-3 transcription

factor mediates beta-catenin-induced axis formation in Xenopus embryos. *Cell* 86:391-399.

167. Moon, R.T., J.D.Brown, and M.Torres. 1997. WNTs modulate cell fate and behavior during vertebrate development. *Trends Genet.* 13:157-162.

168. Moon, R.T., R.M.Campbell, J.L.Christian, L.L.McGrew, J.Shih, and S.Fraser. 1993. Xwnt-5A: a maternal Wnt that affects morphogenetic movements after overexpression in embryos of Xenopus laevis. *Development* 119:97-111.

169. Morali, O.G., V.Delmas, R.Moore, C.Jeanney, J.P.Thiery, and L.Larue. 2001. IGF-II induces rapid beta-catenin relocation to the nucleus during epithelium to mesenchyme transition. *Oncogene* 20:4942-4950.

170. Morin, P.J. 1999. beta-catenin signaling and cancer. *Bioessays* 21:1021-1030.

171. Morin, P.J., A.B.Sparks, V.Korinek, N.Barker, H.Clevers, B.Vogelstein, and K.W.Kinzler. 1997. Activation of beta-catenin-Tcf signaling in colon cancer by mutations in beta-catenin or APC. *Science* 275:1787-1790.

172. Mucenski, M.L., J.M.Nation, A.R.Thitoff, V.Besnard, Y.Xu, S.E.Wert, N.Harada, M.M.Taketo, M.T.Stahlman, and J.A.Whitsett. 2005. Beta-catenin regulates differentiation of respiratory epithelial cells in vivo. *Am. J Physiol Lung Cell Mol. Physiol* 289:L971-L979.

173. Mucenski, M.L., S.E.Wert, J.M.Nation, D.E.Loudy, J.Huelsken, W.Birchmeier, E.E.Morrisey, and J.A.Whitsett. 2003. beta-Catenin is required for specification of proximal/distal cell fate during lung morphogenesis. *J Biol. Chem.* 278:40231-40238.

174. Mudher, A. and S.Lovestone. 2002. Alzheimer's disease-do tauists and baptists finally shake hands? *Trends Neurosci.* 25:22-26.

175. Muller, T., G.Bain, X.Wang, and J.Papkoff. 2002. Regulation of epithelial cell migration and tumor formation by beta-catenin signaling. *Exp. Cell Res.* 280:119-133.

176. Muller, T., A.Choidas, E.Reichmann, and A.Ullrich. 1999. Phosphorylation and free pool of beta-catenin are regulated by tyrosine kinases and tyrosine phosphatases during epithelial cell migration. *J Biol. Chem.* 274:10173-10183.

177. Munemitsu, S., I.Albert, B.Souza, B.Rubinfeld, and P.Polakis. 1995. Regulation of intracellular beta-catenin levels by the adenomatous polyposis coli (APC) tumor-suppressor protein. *Proc. Natl. Acad. Sci. U. S. A* 92:3046-3050.

178. Munne, A., M.Fabre, M.L.Marinoso, M.Gallen, and F.X.Real. 1999. Nuclear beta-catenin in colorectal tumors: to freeze or not to freeze? Colon Cancer Team at IMAS. *J Histochem. Cytochem.* 47:1089-1094.

179. Murakami, T., S.Toda, M.Fujimoto, M.Ohtsuki, H.R.Byers, T.Etoh, and H.Nakagawa. 2001. Constitutive activation of Wnt/beta-catenin signaling pathway in migration-active melanoma cells: role of LEF-1 in melanoma with increased metastatic potential. *Biochem. Biophys. Res Commun.* 288:8-15.

180. Naishiro, Y., T.Yamada, A.S.Takaoka, R.Hayashi, F.Hasegawa, K.Imai, and S.Hirohashi. 2001. Restoration of epithelial cell polarity in a colorectal cancer cell line by suppression of beta-catenin/T-cell factor 4-mediated gene transactivation. *Cancer Res* 61:2751-2758.

181. Nakatani, Y., K.Masudo, Y.Miyagi, Y.Inayama, N.Kawano, Y.Tanaka, K.Kato, T.Ito, H.Kitamura, Y.Nagashima, S.Yamanaka, N.Nakamura, J.Sano, N.Ogawa, N.Ishiwa, K.Notohara, M.Resl, and E.J.Mark. 2002. Aberrant Nuclear Localization and Gene Mutation of beta-catenin in Low- Grade Adenocarcinoma of Fetal Lung Type: Up-Regulation of the Wnt Signaling Pathway May Be a Common Denominator for the Development of Tumors that Form Morules. *Mod. Pathol.* 15:617-624.

182. Nei, H., T.Saito, H.Yamasaki, H.Mizumoto, E.Ito, and R.Kudo. 1999. Nuclear localization of beta-catenin in normal and carcinogenic endometrium. *Mol. Carcinog.* 25:207-218.

183. Nelson, W.J. and R.Nusse. 2004. Convergence of Wnt, beta-catenin, and cadherin pathways. *Science* 303:1483-1487.

184. Nishita, M., M.K.Hashimoto, S.Ogata, M.N.Laurent, N.Ueno, H.Shibuya, and K.W.Cho. 2000. Interaction between Wnt and TGF-beta signalling pathways during formation of Spemann's organizer. *Nature* 403:781-785.

185. Novak, A., S.C.Hsu, C.Leung-Hagesteijn, G.Radeva, J.Papkoff, R.Montesano, C.Roskelley, R.Grosschedl, and S.Dedhar. 1998. Cell adhesion and the integrin-linked kinase regulate the LEF-1 and beta-catenin signaling pathways. *Proc. Natl. Acad. Sci. U. S. A* 95:4374-4379.

186. Nozaki, I., T.Tsuji, O.Iijima, Y.Ohmura, A.Andou, M.Miyazaki, N.Shimizu, and M.Namba. 2001. Reduced expression of REIC/Dkk-3 gene in non-small cell lung cancer. *Int. J Oncol.* 19:117-121.

187. Nusse, R. 1999. WNT targets. Repression and activation. *Trends Genet.* 15:1-3.

188. Nusse, R., A.Brown, J.Papkoff, P.Scambler, G.Shackleford, A.McMahon, R.Moon, and H.Varmus. 1991. A new nomenclature for int-1 and related genes: the Wnt gene family. *Cell* 64:231.

189. Nusse, R. and H.E.Varmus. 1982. Many tumors induced by the mouse mammary tumor virus contain a provirus integrated in the same region of the host genome. *Cell* 31:99-109.

190. Nusse, R. and H.E.Varmus. 1992. Wnt genes. *Cell* 69:1073-1087.

191. O'Donnell, R.A., A.Richter, J.Ward, G.Angco, A.Mehta, K.Rousseau, D.M.Swallow, S.T.Holgate, R.Djukanovic, D.E.Davies, and S.J.Wilson. 2004.

Expression of ErbB receptors and mucins in the airways of long term current smokers. *Thorax* 59:1032-1040.

192. Olson, D.J. and D.M.Gibo. 1998. Antisense wnt-5a mimics wnt-1-mediated C57MG mammary epithelial cell transformation. *Exp Cell Res* 241:134-141.

193. Olson, D.J. and J.Papkoff. 1994. Regulated expression of Wnt family members during proliferation of C57mg mammary cells. *Cell Growth Differ.* 5:197-206.

194. Oosterwegel, M., W.M.van De, J.Timmerman, A.Kruisbeek, O.Destree, F.Meijlink, and H.Clevers. 1993. Differential expression of the HMG box factors TCF-1 and LEF-1 during murine embryogenesis. *Development* 118:439-448.

195. Orford, K., C.Crockett, J.P.Jensen, A.M.Weissman, and S.W.Byers. 1997. Serine phosphorylation-regulated ubiquitination and degradation of beta-catenin. *J Biol. Chem.* 272:24735-24738.

196. Orford, K., C.C.Orford, and S.W.Byers. 1999. Exogenous expression of beta-catenin regulates contact inhibition, anchorage-independent growth, anoikis, and radiation-induced cell cycle arrest. *J Cell Biol.* 146:855-868.

197. Otto, W.R. 2002. Lung epithelial stem cells. *J Pathol.* 197:527-535.

198. Ozawa, M., H.Baribault, and R.Kemler. 1989. The cytoplasmic domain of the cell adhesion molecule uvomorulin associates with three independent proteins structurally related in different species. *EMBO J* 8:1711-1717.

199. Papkoff, J. 1989. Inducible overexpression and secretion of int-1 protein. *Mol. Cell Biol.* 9:3377-3384.

200. Papkoff, J. and M.Aikawa. 1998. WNT-1 and HGF regulate GSK3 beta activity and beta-catenin signaling in mammary epithelial cells. *Biochem. Biophys. Res Commun.* 247:851-858.

201. Papkoff, J., A.M.Brown, and H.E.Varmus. 1987. The int-1 proto-oncogene products are glycoproteins that appear to enter the secretory pathway. *Mol. Cell Biol.* 7:3978-3984.

202. Papkoff, J. and B.Schryver. 1990. Secreted int-1 protein is associated with the cell surface. *Mol. Cell Biol.* 10:2723-2730.

203. Perl, A.K. and J.A.Whitsett. 1999. Molecular mechanisms controlling lung morphogenesis. *Clin. Genet.* 56:14-27.

204. Phiel, C.J. and P.S.Klein. 2001. Molecular targets of lithium action. *Annu. Rev. Pharmacol. Toxicol.* 41:789-813.

205. Pirinen, R.T., P.Hirvikoski, R.T.Johansson, S.Hollmen, and V.M.Kosma. 2001. Reduced expression of alpha-catenin, beta-catenin, and gamma-catenin is associated with high cell proliferative activity and poor differentiation in non-small cell lung cancer. *J Clin. Pathol.* 54:391-395.

206. Pizzuti, A., F.Amati, G.Calabrese, A.Mari, A.Colosimo, V.Silani, L.Giardino, A.Ratti, D.Penso, L.Calza, G.Palka, G.Scarlato, G.Novelli, and B.Dallapiccola. 1996. cDNA characterization and chromosomal mapping of two human homologues of the Drosophila dishevelled polarity gene. *Hum. Mol. Genet.* 5:953-958.

207. Platz, J., O.Pinkenburg, C.Beisswenger, A.Puchner, T.Damm, and R.Bals. 2005. Application of small interfering RNA (siRNA) for modulation of airway epithelial gene expression. *Oligonucleotides.* 15:132-138.

208. Playford, M.P., D.Bicknell, W.F.Bodmer, and V.M.Macaulay. 2000. Insulin-like growth factor 1 regulates the location, stability, and transcriptional activity of beta-catenin. *Proc. Natl. Acad. Sci. U. S. A* 97:12103-12108.

209. Polakis, P. 2002. Casein kinase 1: a Wnt'er of disconnect. *Curr. Biol.* 12:R499-R501.

210. Puddicombe, S.M., R.Polosa, A.Richter, M.T.Krishna, P.H.Howarth, S.T.Holgate, and D.E.Davies. 2000. Involvement of the epidermal growth factor receptor in epithelial repair in asthma. *FASEB J.* 14:1362-1374.

211. Resau, J.H., J.R.Cottrell, K.A.Elligett, and E.A.Hudson. 1987. Cell injury and regeneration of human epithelium in organ culture. *Cell Biol. Toxicol.* 3:441-458.

212. Richter, A., R.A.O'Donnell, R.M.Powell, M.W.Sanders, S.T.Holgate, R.Djukanovic, and D.E.Davies. 2002. Autocrine ligands for the epidermal growth factor receptor mediate interleukin-8 release from bronchial epithelial cells in response to cigarette smoke. *Am. J. Respir. Cell Mol. Biol.* 27:85-90.

213. Riggleman, B., P.Schedl, and E.Wieschaus. 1990. Spatial expression of the Drosophila segment polarity gene armadillo is posttranscriptionally regulated by wingless. *Cell* 63:549-560.

214. Rijsewijk, F., M.Schuermann, E.Wagenaar, P.Parren, D.Weigel, and R.Nusse. 1987. The Drosophila homolog of the mouse mammary oncogene int-1 is identical to the segment polarity gene wingless. *Cell* 50:649-657.

215. Ritchie, T.C., W.Zhou, E.McKinstry, M.Hosch, Y.Zhang, I.Nathke, and J.F.Engelhardt. 2001. Developmental expression of catenins and associated proteins during submucosal gland morphogenesis in the airway. *Exp Lung Res* 27:121-141.

216. Rockman, S.P., S.A.Currie, M.Ciavarella, E.Vincan, C.Dow, R.J.Thomas, and W.A.Phillips. 2001. Id2 is a target of the beta-catenin/T cell factor pathway in colon carcinoma. *J Biol. Chem.* 276:45113-45119.

217. Roose, J., G.Huls, M.van Beest, P.Moerer, H.K.van der, R.Goldschmeding, T.Logtenberg, and H.Clevers. 1999. Synergy between tumor suppressor APC and the beta-catenin-Tcf4 target Tcf1. *Science* 285:1923-1926.

218. Roth, W., C.Wild-Bode, M.Platten, C.Grimmel, H.S.Melkonyan, J.Dichgans, and M.Weller. 2000. Secreted Frizzled-related proteins inhibit motility and promote growth of human malignant glioma cells. *Oncogene* 19:4210-4220.

219. Sagara, N., G.Toda, M.Hirai, M.Terada, and M.Katoh. 1998. Molecular cloning, differential expression, and chromosomal localization of human frizzled-1, frizzled-2, and frizzled-7. *Biochem. Biophys. Res Commun.* 252:117-122.

220. Saitoh, T., M.Hirai, and M.Katoh. 2001a. Molecular cloning and characterization of human Frizzled-5 gene on chromosome 2q33.3-q34 region. *Int. J Oncol.* 19:105-110.

221. Saitoh, T., M.Hirai, and M.Katoh. 2001b. Molecular cloning and characterization of human Frizzled-8 gene on chromosome 10p11.2. *Int. J Oncol.* 18:991-996.

222. Saitoh, T., M.Hirai, and M.Katoh. 2001c. Molecular cloning and characterization of WNT3A and WNT14 clustered in human chromosome 1q42 region. *Biochem. Biophys. Res. Commun.* 284:1168-1175.

223. Saitoh, T. and M.Katoh. 2001a. Molecular cloning and characterization of human WNT5B on chromosome 12p13.3 region. *Int. J Oncol.* 19:347-351.

224. Saitoh, T. and M.Katoh. 2001b. Molecular cloning and characterization of human WNT8A. *Int. J Oncol.* 19:123-127.

225. Saitoh, T., T.Mine, and M.Katoh. 2002. Up-regulation of WNT8B mRNA in human gastric cancer. *Int. J Oncol.* 20:343-348.

226. Saitoh, T., J.Moriwaki, J.Koike, A.Takagi, T.Miwa, K.Shiokawa, and M.Katoh. 2001d. Molecular cloning and characterization of FRAT2, encoding a positive regulator of the WNT signaling pathway. *Biochem. Biophys. Res Commun.* 281:815-820.

227. Sala, C.F., E.Formenti, G.C.Terstappen, and A.Caricasole. 2000. Identification, gene structure, and expression of human frizzled-3 (FZD3). *Biochem. Biophys. Res. Commun.* 273:27-34.

228. Schumann, H., J.Holtz, H.R.Zerkowski, and M.Hatzfeld. 2000. Expression of secreted frizzled related proteins 3 and 4 in human ventricular myocardium correlates with apoptosis related gene expression. *Cardiovasc. Res* 45:720-728.

229. Sehgal, R.N., B.M.Gumbiner, and L.F.Reichardt. 1997. Antagonism of cell adhesion by an alpha-catenin mutant, and of the Wnt- signaling pathway by alpha-catenin in Xenopus embryos. *J Cell Biol.* 139:1033-1046.

230. Semenov, M.V. and M.Snyder. 1997. Human dishevelled genes constitute a DHR-containing multigene family. *Genomics* 42:302-310.

231. Semenov, M.V., K.Tamai, B.K.Brott, M.Kuhl, S.Sokol, and X.He. 2001. Head inducer Dickkopf-1 is a ligand for Wnt coreceptor LRP6. *Curr. Biol.* 11:951-961.

232. Sen, M., M.Chamorro, J.Reifert, M.Corr, and D.A.Carson. 2001. Blockade of Wnt-5A/frizzled 5 signaling inhibits rheumatoid synoviocyte activation. *Arthritis Rheum.* 44:772-781.

233. Sen, M., K.Lauterbach, H.El Gabalawy, G.S.Firestein, M.Corr, and D.A.Carson. 2000. Expression and function of wingless and frizzled homologs in rheumatoid arthritis. *Proc. Natl. Acad. Sci. U. S. A* 97:2791-2796.

234. Shannon, J.M. and B.A.Hyatt. 2004. Epithelial-mesenchymal interactions in the developing lung. *Annu. Rev. Physiol* 66:625-645.

235. Shao, M.X., T.Nakanaga, and J.A.Nadel. 2004. Cigarette smoke induces MUC5AC mucin overproduction via tumor necrosis factor-alpha-converting

enzyme in human airway epithelial (NCI-H292) cells. *Am. J Physiol Lung Cell Mol. Physiol* 287:L420-L427.

236. Sheldahl, L.C., M.Park, C.C.Malbon, and R.T.Moon. 1999. Protein kinase C is differentially stimulated by Wnt and Frizzled homologs in a G-protein-dependent manner. *Curr. Biol.* 9:695-698.

237. Shibamoto, S., K.Higano, R.Takada, F.Ito, M.Takeichi, and S.Takada. 1998. Cytoskeletal reorganization by soluble Wnt-3a protein signalling. *Genes Cells* 3:659-670.

238. Shigemitsu, K., Y.Sekido, N.Usami, S.Mori, M.Sato, Y.Horio, Y.Hasegawa, S.A.Bader, A.F.Gazdar, J.D.Minna, T.Hida, H.Yoshioka, M.Imaizumi, Y.Ueda, M.Takahashi, and K.Shimokata. 2001. Genetic alteration of the beta-catenin gene (CTNNB1) in human lung cancer and malignant mesothelioma and identification of a new 3p21.3 homozygous deletion. *Oncogene* 20:4249-4257.

239. Shimizu, H., M.A.Julius, M.Giarre, Z.Zheng, A.M.Brown, and J.Kitajewski. 1997. Transformation by Wnt family proteins correlates with regulation of beta-catenin. *Cell Growth Differ.* 8:1349-1358.

240. Shimizu, T., M.Nishihara, S.Kawaguchi, and Y.Sakakura. 1994. Expression of phenotypic markers during regeneration of rat tracheal epithelium following mechanical injury. *Am. J Respir. Cell Mol. Biol.* 11:85-94.

241. Shiozaki, H., K.Iihara, H.Oka, T.Kadowaki, S.Matsui, J.Gofuku, M.Inoue, A.Nagafuchi, S.Tsukita, and T.Mori. 1994. Immunohistochemical detection of alpha-catenin expression in human cancers. *Am. J Pathol.* 144:667-674.

242. Shiozaki, H., T.Kadowaki, Y.Doki, M.Inoue, S.Tamura, H.Oka, T.Iwazawa, S.Matsui, K.Shimaya, M.Takeichi, and . 1995. Effect of epidermal growth factor on cadherin-mediated adhesion in a human oesophageal cancer cell line. *Br. J Cancer* 71:250-258.

243. Shtutman, M., J.Zhurinsky, I.Simcha, C.Albanese, M.D'Amico, R.Pestell, and A.Ben Ze'ev. 1999. The cyclin D1 gene is a target of the beta-catenin/LEF-1 pathway. *Proc. Natl. Acad. Sci. U. S. A* 96:5522-5527.

244. Shulman, J.M., N.Perrimon, and J.D.Axelrod. 1998. Frizzled signaling and the developmental control of cell polarity. *Trends Genet.* 14:452-458.

245. Siegfried, E., E.L.Wilder, and N.Perrimon. 1994. Components of wingless signalling in Drosophila. *Nature* 367:76-80.

246. Slusarski, D.C., V.G.Corces, and R.T.Moon. 1997a. Interaction of Wnt and a Frizzled homologue triggers G-protein-linked phosphatidylinositol signalling. *Nature* 390:410-413.

247. Slusarski, D.C., J.Yang-Snyder, W.B.Busa, and R.T.Moon. 1997b. Modulation of embryonic intracellular Ca2+ signaling by Wnt-5A. *Dev. Biol.* 182:114-120.

248. St Croix, B., C.Sheehan, J.W.Rak, V.A.Florenes, J.M.Slingerland, and R.S.Kerbel. 1998. E-Cadherin-dependent growth suppression is mediated by the cyclin-dependent kinase inhibitor p27(KIP1). *J Cell Biol.* 142:557-571.

249. Staal, F.J., M.M.Noort, G.J.Strous, and H.C.Clevers. 2002. Wnt signals are transmitted through N-terminally dephosphorylated beta-catenin. *EMBO Rep.* 3:63-68.

250. Steiner, P., A.Philipp, J.Lukas, D.Godden-Kent, M.Pagano, S.Mittnacht, J.Bartek, and M.Eilers. 1995. Identification of a Myc-dependent step during the formation of active G1 cyclin-cdk complexes. *EMBO J* 14:4814-4826.

251. Stockinger, A., A.Eger, J.Wolf, H.Beug, and R.Foisner. 2001. E-cadherin regulates cell growth by modulating proliferation-dependent beta-catenin transcriptional activity. *J. Cell Biol.* 154:1185-1196.

252. Sun, P., H.Xiong, T.H.Kim, B.Ren, and Z.Zhang. 2006. Positive Inter-Regulation between beta-Catenin/T Cell Factor-4 Signaling and Endothelin-1 Signaling Potentiates Proliferation and Survival of Prostate Cancer Cells. *Mol. Pharmacol.* 69:520-531.

253. Sunaga, N., T.Kohno, F.T.Kolligs, E.R.Fearon, R.Saito, and J.Yokota. 2001. Constitutive activation of the Wnt signaling pathway by CTNNB1 (beta-catenin) mutations in a subset of human lung adenocarcinoma. *Genes Chromosomes. Cancer* 30:316-321.

254. Surendran, K., S.P.McCaul, and T.C.Simon. 2002. A role for Wnt-4 in renal fibrosis. *Am J Physiol Renal Physiol* 282:F431-F441.

255. Tago, K., T.Nakamura, M.Nishita, J.Hyodo, S.Nagai, Y.Murata, S.Adachi, S.Ohwada, Y.Morishita, H.Shibuya, and T.Akiyama. 2000. Inhibition of Wnt signaling by ICAT, a novel beta-catenin-interacting protein. *Genes Dev.* 14:1741-1749.

256. Taipale, J. and P.A.Beachy. 2001. The Hedgehog and Wnt signalling pathways in cancer. *Nature* 411:349-354.

257. Takahashi, K. and K.Suzuki. 1996. Density-dependent inhibition of growth involves prevention of EGF receptor activation by E-cadherin-mediated cell-cell adhesion. *Exp. Cell Res.* 226:214-222.

258. Takahashi, K., K.Suzuki, and Y.Tsukatani. 1997. Induction of tyrosine phosphorylation and association of beta-catenin with EGF receptor upon tryptic digestion of quiescent cells at confluence. *Oncogene* 15:71-78.

259. Takemaru, K.I. and R.T.Moon. 2000. The transcriptional coactivator CBP interacts with beta-catenin to activate gene expression. *J Cell Biol.* 149:249-254.

260. Tamai, K., M.Semenov, Y.Kato, R.Spokony, C.Liu, Y.Katsuyama, F.Hess, J.P.Saint-Jeannet, and X.He. 2000. LDL-receptor-related proteins in Wnt signal transduction. *Nature* 407:530-535.

261. Tebar, M., O.Destree, W.J.de Vree, and A.A.Have-Opbroek. 2001. Expression of Tcf/Lef and sFrp and localization of beta-catenin in the developing mouse lung. *Mech. Dev.* 109:437-440.

262. Tetsu, O. and F.McCormick. 1999. Beta-catenin regulates expression of cyclin D1 in colon carcinoma cells. *Nature* 398:422-426.

263. Theisen, H., J.Purcell, M.Bennett, D.Kansagara, A.Syed, and J.L.Marsh. 1994. dishevelled is required during wingless signaling to establish both cell polarity and cell identity. *Development* 120:347-360.

264. Thompson, C.B. 1995. Apoptosis in the pathogenesis and treatment of disease. *Science* 267:1456-1462.

265. Tokuhara, M., M.Hirai, Y.Atomi, M.Terada, and M.Katoh. 1998. Molecular cloning of human Frizzled-6. *Biochem. Biophys. Res. Commun.* 243:622-627.

266. Torres, M.A., J.A.Yang-Snyder, S.M.Purcell, A.A.DeMarais, L.L.McGrew, and R.T.Moon. 1996. Activities of the Wnt-1 class of secreted signaling factors are antagonized by the Wnt-5A class and by a dominant negative cadherin in early Xenopus development. *J Cell Biol.* 133:1123-1137.

267. Tsuji, T., M.Miyazaki, M.Sakaguchi, Y.Inoue, and M.Namba. 2000. A REIC gene shows down-regulation in human immortalized cells and human tumor-derived cell lines. *Biochem. Biophys. Res Commun.* 268:20-24.

268. Tsuji, T., I.Nozaki, M.Miyazaki, M.Sakaguchi, H.Pu, Y.Hamazaki, O.Iijima, and M.Namba. 2001. Antiproliferative activity of REIC/Dkk-3 and its significant down- regulation in non-small-cell lung carcinomas. *Biochem. Biophys. Res Commun.* 289:257-263.

269. Tsukatani, Y., K.Suzuki, and K.Takahashi. 1997. Loss of density-dependent growth inhibition and dissociation of alpha- catenin from E-cadherin. *J Cell Physiol* 173:54-63.

270. Ueda, M., R.M.Gemmill, J.West, R.Winn, M.Sugita, N.Tanaka, M.Ueki, and H.A.Drabkin. 2001. Mutations of the beta- and gamma-catenin genes are uncommon in human lung, breast, kidney, cervical and ovarian carcinomas. *Br. J. Cancer* 85:64-68.

271. van Noort, M. and H.Clevers. 2002. TCF transcription factors, mediators of Wnt-signaling in development and cancer. *Dev. Biol.* 244:1-8.

272. van Noort, M., J.Meeldijk, Z.R.van der, O.Destree, and H.Clevers. 2002. Wnt signaling controls the phosphorylation status of beta-catenin. *J Biol. Chem.* 277:17901-17905.

273. Vinson, C.R. and P.N.Adler. 1987. Directional non-cell autonomy and the transmission of polarity information by the frizzled gene of Drosophila. *Nature* 329:549-551.

274. Virmani, A.K., A.Rathi, U.G.Sathyanarayana, A.Padar, C.X.Huang, H.T.Cunnigham, A.J.Farinas, S.Milchgrub, D.M.Euhus, M.Gilcrease, J.Herman, J.D.Minna, and A.F.Gazdar. 2001. Aberrant methylation of the adenomatous polyposis coli (APC) gene promoter 1A in breast and lung carcinomas. *Clin. Cancer Res* 7:1998-2004.

275. von Kries, J.P., G.Winbeck, C.Asbrand, T.Schwarz-Romond, N.Sochnikova, A.Dell'Oro, J.Behrens, and W.Birchmeier. 2000. Hot spots in beta-catenin for interactions with LEF-1, conductin and APC. *Nat. Struct. Biol.* 7:800-807.

276. Wada, M., C.W.Miller, J.Yokota, E.Lee, H.Mizoguchi, and H.P.Koeffler. 1997. Molecular analysis of the adenomatous polyposis coli gene in sarcomas, hematological malignancies and noncolonic, neoplastic tissues. *J Mol. Med* 75:139-144.

277. Wagenaar, R.A., H.C.Crawford, and L.M.Matrisian. 2001. Stabilized beta-catenin immortalizes colonic epithelial cells. *Cancer Res* 61:2097-2104.

278. Wainwright, B.J., P.J.Scambler, P.Stanier, E.K.Watson, G.Bell, C.Wicking, X.Estivill, M.Courtney, A.Boue, P.S.Pedersen, and . 1988. Isolation of a human gene with protein sequence similarity to human and murine int-1 and the Drosophila segment polarity mutant wingless. *EMBO J* 7:1743-1748.

279. Wang, Y.K., C.H.Samos, R.Peoples, L.A.Perez-Jurado, R.Nusse, and U.Francke. 1997. A novel human homologue of the Drosophila frizzled wnt receptor gene binds wingless protein and is in the Williams syndrome deletion at 7q11.23. *Hum. Mol. Genet.* 6:465-472.

280. Warburton, D., S.Bellusci, S.De Langhe, P.M.Del Moral, V.Fleury, A.Mailleux, D.Tefft, M.Unbekandt, K.Wang, and W.Shi. 2005. Molecular mechanisms of early lung specification and branching morphogenesis. *Pediatr. Res.* 57:26R-37R.

281. Warburton, D., M.Schwarz, D.Tefft, G.Flores-Delgado, K.D.Anderson, and W.V.Cardoso. 2000. The molecular basis of lung morphogenesis. *Mech. Dev.* 92:55-81.

282. Watkins, D.N., D.M.Berman, S.G.Burkholder, B.Wang, P.A.Beachy, and S.B.Baylin. 2003. Hedgehog signalling within airway epithelial progenitors and in small-cell lung cancer. *Nature* 422:313-317.

283. Wehrli, M., S.T.Dougan, K.Caldwell, L.O'Keefe, S.Schwartz, D.Vaizel-Ohayon, E.Schejter, A.Tomlinson, and S.DiNardo. 2000. arrow encodes an LDL-receptor-related protein essential for Wingless signalling. *Nature* 407:527-530.

284. Weichselbaum, M., M.P.Sparrow, E.J.Hamilton, P.J.Thompson, and D.A.Knight. 2005. A confocal microscopic study of solitary pulmonary neuroendocrine cells in human airway epithelium. *Respir. Res.* 6:115.

285. Weidenfeld, J., W.Shu, L.Zhang, S.E.Millar, and E.E.Morrisey. 2002. The WNT7b Promoter Is Regulated by TTF-1, GATA6, and Foxa2 in Lung Epithelium. *J Biol. Chem.* 277:21061-21070.

286. Wielenga, V.J., R.Smits, V.Korinek, L.Smit, M.Kielman, R.Fodde, H.Clevers, and S.T.Pals. 1999. Expression of CD44 in Apc and Tcf mutant mice implies regulation by the WNT pathway. *Am. J. Pathol.* 154:515-523.

287. Willert, J., M.Epping, J.Pollack, P.Brown, and R.Nusse. 2002. A Transcriptional Response to Wnt protein in human embryonic carcinoma cells. *BMC. Dev. Biol.* 2:8.

288. Willert, K., J.D.Brown, E.Danenberg, A.W.Duncan, I.L.Weissman, T.Reya, J.R.Yates, III, and R.Nusse. 2003. Wnt proteins are lipid-modified and can act as stem cell growth factors. *Nature* 423:448-452.

289. Wilson, S., A.Rydstrom, T.Trimborn, K.Willert, R.Nusse, T.M.Jessell, and T.Edlund. 2001. The status of Wnt signalling regulates neural and epidermal fates in the chick embryo. *Nature* 411:325-330.

290. Winton, H.L., H.Wan, M.B.Cannell, D.C.Gruenert, P.J.Thompson, D.R.Garrod, G.A.Stewart, and C.Robinson. 1998. Cell lines of pulmonary and non-pulmonary origin as tools to study the effects of house dust mite proteinases on the regulation of epithelial permeability. *Clin. Exp. Allergy* 28:1273-1285.

291. Wodarz, A. and R.Nusse. 1998. Mechanisms of Wnt signaling in development. *Annu. Rev. Cell Dev. Biol.* 14:59-88.

292. Wolda, S.L. and R.T.Moon. 1992. Cloning and developmental expression in Xenopus laevis of seven additional members of the Wnt family. *Oncogene* 7:1941-1947.

293. Wong, G.T., B.J.Gavin, and A.P.McMahon. 1994. Differential transformation of mammary epithelial cells by Wnt genes. *Mol. Cell Biol.* 14:6278-6286.

294. Wright, M., M.Aikawa, W.Szeto, and J.Papkoff. 1999. Identification of a Wnt-responsive signal transduction pathway in primary endothelial cells. *Biochem. Biophys. Res Commun.* 263:384-388.

295. Wu, W., A.Glinka, H.Delius, and C.Niehrs. 2000. Mutual antagonism between dickkopf1 and dickkopf2 regulates Wnt/beta- catenin signalling. *Curr. Biol.* 10:1611-1614.

296. Yamanaka, H., T.Moriguchi, N.Masuyama, M.Kusakabe, H.Hanafusa, R.Takada, S.Takada, and E.Nishida. 2002. JNK functions in the non-canonical Wnt pathway to regulate convergent extension movements in vertebrates. *EMBO Rep.* 3:69-75.

297. Yan, D., M.Wiesmann, M.Rohan, V.Chan, A.B.Jefferson, L.Guo, D.Sakamoto, R.H.Caothien, J.H.Fuller, C.Reinhard, P.D.Garcia, F.M.Randazzo, J.Escobedo, W.J.Fantl, and L.T.Williams. 2001. Elevated expression of axin2 and hnkd mRNA provides evidence that Wnt/beta - catenin signaling is activated in human colon tumors. *Proc. Natl. Acad. Sci. U. S. A* 98:14973-14978.

298. Yang-Snyder, J., J.R.Miller, J.D.Brown, C.J.Lai, and R.T.Moon. 1996. A frizzled homolog functions in a vertebrate Wnt signaling pathway. *Curr. Biol.* 6:1302-1306.

299. Yuan, H., J.Mao, L.Li, and D.Wu. 1999. Suppression of glycogen synthase kinase activity is not sufficient for leukemia enhancer factor-1 activation. *J Biol. Chem.* 274:30419-30423.

300. Yun, M.S., S.E.Kim, S.H.Jeon, J.S.Lee, and K.Y.Choi. 2005. Both ERK and Wnt/beta-catenin pathways are involved in Wnt3a-induced proliferation. *J Cell Sci.* 118:313-322.

301. Zakin, L.D., S.Mazan, M.Maury, N.Martin, J.L.Guenet, and P.Brulet. 1998. Structure and expression of Wnt13, a novel mouse Wnt2 related gene. *Mech. Dev.* 73:107-116.

302. Zhang, T., T.Otevrel, Z.Gao, Z.Gao, S.M.Ehrlich, J.Z.Fields, and B.M.Boman. 2001. Evidence that APC regulates survivin expression: a possible mechanism contributing to the stem cell origin of colon cancer. *Cancer Res* 61:8664-8667.

303. Zhao, Z., C.C.Lee, A.Baldini, and C.T.Caskey. 1995. A human homologue of the Drosophila polarity gene frizzled has been identified and mapped to 17q21.1. *Genomics* 27:370-373.

304. Zhu, A.J. and F.M.Watt. 1999. beta-catenin signalling modulates proliferative potential of human epidermal keratinocytes independently of intercellular adhesion. *Development* 126:2285-2298.

305. Zorn, A.M. 2001. Wnt signalling: Antagonistic Dickkopfs. *Curr. Biol.* 11:R592-R595.